This is an extra page for printing a blank page to include the Chinese abstraction!!!

Beamspace-Time Interference Cancelling RAKE Receiver for Sectored CDMA Systems

Student : Teng-Cheng Tsai   Advisor : Dr. Ta-Sung Lee

Institute of Communication Engineering

National Chiao Tung University

Abstract

In the cellular code division multiple access (CDMA) communication systems, each user communicate via the same radio channel such that interference increases with the number of subscribers. Traditional RAKE receivers cannot handle the multiple access interference (MAI) well, and this prompts the use of extra spatial degree of freedom (antenna array) and extra information of MAI (multiuser detection). Cell sectorization also has been widely used for improving system capacity. However, it causes extra computational load due to handoff. Through the dynamic sector synthesis by selecting of diversity beamformer, this allows to balance the traffic loading across sectors and to manage handoff overhead. In this thesis, we will discuss the performance of space-time 2-D RAKE receivers. In despite of the superior performance of the space-time joint processor, it needs more complex computations and the real-time processing is hard to achieve when the joint degree of freedom is large. To remedy this, we make use of the concept of reduced-dimension beamspace-time processing. The beamspace-time processing scheme involves two processors, a set of adaptive beamformers and a set of adaptive correlators. The beamformers are constructed to provide effective suppression of unwanted interference and reception of signals from a prescribed working sector. And the correlators are constructed to suppress the in-sector strong MAI and to receive the diversity paths from prescribed time region. Finally, the output data obtained by these processors are maximum ratio combined to capture the signal multipath components coherently. In particular, both two processors can be realized in the form of generalized sidelobe canceller (GSC) with the aid of channel estimation, and partially adaptivity is incorporated for reduce complexity processing and improved convergence.

Acknowledgement

I would like to express the deepest gratitude to my advisor, Professor Ta-Sung Lee, for his enthusiastic guidance and great patience. He brought me to the field of communication and array signal processing. His knowledge, experience and commitment have benefited me tremendously over these years. I also thank the members of my committee for their valuable comments and feedback.

I would also like to thank Chung Shan Institute of Science and Technology (CSIST) for providing the financial support for my research. Thank also goes to my former and present student colleagues of Communication Signal Processing Laboratory (CSP Lab.) for their inspiring discussions. Good luck to those of you still beavering away at school.

Finally, I want to thank my wife for taking care of my family. I dedicate this thesis to my wife Shu-Chin who spent so many lonely moments due to my work during these year, as well as to my lonely son and daughter.

Contents

List of Figures

List of Tables

Abbreviations

- AOA: angle of arrival

- AWGN: additive white Gaussian noise

- BC: beamformer-correlator pair

- BER: bit error rate

- CBT-RAKE: conventional beamspace 2-D RAKE receiver

- CSV: composite signature vector

- CST-RAKE: conventional space-time 2-D RAKE receiver

- DOA: direction of arrival

- DS/CDMA: direct-sequence code division multiple access

- EVD: eigenvalue decomposition

- FA: fully adaptive

- FDMA: frequency division multiple access

- GSC: generalized sidelobe canceller

- ILS: iterative least square

- LCMV: linearly constrained minimum variance

- LMS: least mean square

- MAI: multiple access interference
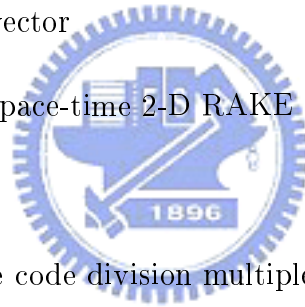
- MB: multi-beam technique

- MBT-RAKE: MMSE beamspace 2-D RAKE receiver

- MST-RAKE: MMSE space-time 2-D RAKE receiver

- MF: matched filter

- MIMO: multiple-input multiple-output

- ML: maximum likelihood

- MMSE: minimum mean square error

- MMSE-MUD: MMSE multiuser receiver

- MOE: minimum output energy

- MRC: maximum ratio combiner

- MSINR: maximum signal-to-interference-plus-noise ratio

- MSC: mobile switching center

- MSE: mean square error

- MST-RAKE: MMSE space-time 2-D RAKE receiver

- MUD: multiuser detection

- MVDR: minimum variance distortionless response

- NBI: narrowband interference

- NLMS: normalized least mean squares

- NSR: narrowband interference power to signal power ratio

- PA: partially adaptive

- PAST: projection approximation subspace tracking
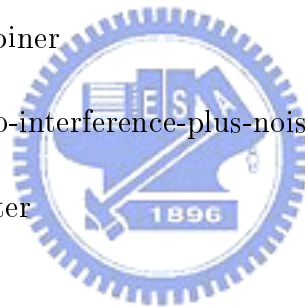
- PC: principal component

- PCS: personal computational system

- PIC: parallel interference canceller

- Post-BT: post-despread beamspace 2-D RAKE receiver

- Post-ST: post-despread antenna-space 2-D RAKE receiver

- Pre-BT: pre-despread beamspace 2-D RAKE receiver

- Pre-ST: pre-despread antenna-space 2-D RAKE receiver

- PSTN: public switching telephone network

- RLS: run least squares

- RZ-ID: reduced-size input data

- RZ-BM: reduced-size blocking matrix

- SIC: successive interference canceller

- SINR: signal-to-interference-plus-noise ratio

- SIMO: single-input multiple-output

- SISO: single-input single-output

- SOI: signal of interest

- SNR: signal-to-noise ratio

- ST: space-time

- ST-PC: space-time principal component receiver

- STSV: space-time signature vector

- SVD: singular value decomposition

- TDMA: time division multiple access

- ULA: uniformly linear array

- ZF: zero-forcing

- ZF-MUD: zero-forcing (the same as decorrelating) multiuser receiver

Symbols and Variables

- σ_k: amplitude of transmitted signal of user k

- σ_n^2: additive white noise power

- $\alpha_{k,l}$: lth path of kth user's complex fading gain

- α: forgetting factor of PASTd algorithm

- $\tau_{k,l}$: lth path of kth user's propagation delay

- Θ_s: active sector angle formed by selected active antennas

- θ_m: direction of arrival of mth beam

- η_k: multiuser efficiency user k

- $\bar{\eta}_k$: asymptotic efficiency of user k

- $\tilde{\eta}_k$: near-far resistance of user k

- η_v: quantity of temporal pseudo noise term

- η_g: quantity of spatial pseudo noise term

- $\bar{\eta}_k$: asymptotic efficiency of user k

- $\tilde{\eta}_k$: near-far resistance

- λ_i: ith eigenvalue of matrix

- λ_{ls}: exponential weighting factor of RLS

- λ_d: Lagrangian multiplier

- $\rho_{(k,l),(k',l')}$: crosscorrelation of code between kth user's lth path and k'th user's l'th path

- μ: stepsize of LMS algorithm

- $\bar{\mu}$: stepsize of NLMS

- $\mathbf{\Pi}^{\perp}_{\mathbf{C}_1}$: projection onto range $\Re\{\mathbf{C}_1\}^{\perp}$

- $\mathbf{a}(\theta_m)$: look angle steering vectors

- $a_{kl,d}$: dth element of $\mathbf{a}_{k,l}$

- $\mathbf{A}$: received amplitude matrix over processing window

- $\bar{\mathbf{A}}$: received amplitude matrix over one bit duration

- $\mathbf{a}_{k,l}$: array response of kth user's lth path

- $\mathbf{B}_c$: temporal blocking matrix of GSC structure

- $\mathbf{B}_a$: spatial blocking matrix of GSC structure

- $\bar{\mathbf{B}}_a$: spatial blocking matrix of GSC structure for Post-ST

- $b_k(i)$: ith bit symbol of kth user

- $\mathbf{b}(i)$: transmitted bits vector

- $\bar{\mathbf{b}}(i)$: transmitted bits vector without $b_1(i)$

- $c_k(t)$: spreading waveform of kth user

- $c_k[n]$: nth chip-sampled data of kth user's spreading waveform

- $\mathbf{c}_{k,l}$: spreading code sequence of $l$path of kth user

- $\mathbf{c}^{(+)}_{k,l}$: augmented signature vector associated with next symbol

- $\mathbf{c}_{k,l}^{(-)}$: augmented vector associated with previous symbol

- $\mathbf{C}_k$: multipath signature matrix of user k

- $\mathbf{d}_s(i)$: signal vector of desired user

- D: number of base station antenna

- e_k: transmitted bit energy of user k

- $\mathbf{F}$: channel fading coefficients matrix over processing window

- $\bar{\mathbf{F}}$: channel fading coefficients matrix over one bit duration

- $\tilde{\mathbf{F}}$: space-time channel fading coefficient matrix over processing window

- $\tilde{\mathbf{F}}_{(d)}$: channel fading coefficient matrix at dth antenna over processing window

- $\mathbf{f}_a$: multipath fading parameter vector

- $\mathbf{f}_{Capon}$: optimized parameter vector in Capon's MOE criterion

- $\mathbf{f}$: a generic weight vector of maximum ratio combiner

- $\mathbf{G}$: despreading weight matrix

- $\mathbf{g}_l$: weight vector of correlator at lth finger

- $\mathbf{g}_{l,m}$: adaptive correlator weights of mth beam at lth finger

- $h_k(t)$: kth user's channel impulse response

- $\mathbf{h}_k$: effective temporal composite signature vector (CSV) of user k

- $\tilde{\mathbf{h}}_k$: effective space-time CSV of user k

- $\mathbf{h}_{c-ST}$: concatenated Pre-ST CSV

- $\mathbf{h}_{c-SM}$: concatenated Post-ST CSV

- $\mathbf{H}_{ST}$: Pre-ST signature matrix

- $\mathbf{H}_{BT}$: Pre-BT signature matrix

- $\mathbf{H}_{SM}$: Post-ST signature matrix

- $\mathbf{H}_{BM}$: Post-BT signature matrix

- $\mathbf{i}(i)$: interference data vector

- $\mathbf{i}_{c-ST}$: concatenated Pre-ST interference vector

- $\mathbf{i}_{c-SM}$: concatenated Post-ST interference vector

- $\mathbf{I}$: identity matrix

- $\mathbf{I}(i)$: space-time chip-sampled interference matrix

- I: number of bits of processing window

- $\mathbf{k}(n)$: adaptive gain vector of RLS

- K_0: a constant in ML function

- K: number of active users in a cell

- L: number of resolvable multipaths

- M: number of diversity to cover the working sector

- N: processing gain or spreading factor

- N_s: simulation samples per Monte-Carlo run

- N_p: pilot symbols per Monte-Carlo run

- $n(t)$: additive white Gaussian noise (AWGN) process

- $\mathbf{n}$: chip-sampled noise data vector

- $\mathbf{n}_{ST}$: chip-sampled space-time noise data vector

- $n_{(d)}(t)$: white Gaussian noise signal at dth antenna element
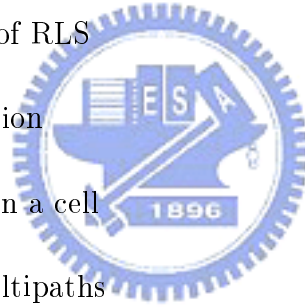
- $\mathbf{n}_{(\mathbf{d})}(i)$: chip-sampled noise vector at dth antenna over processing window

- $\bar{\mathbf{n}}_{(d)}(i)$: chip-sampled noise vector at dth antenna over ith bit duration

- $\mathbf{N}(i)$: space-time Gaussian noise matrix

- $\mathbf{O}$: zero matrix

- $p(t)$: chip pulse waveform

- P_1^c: probability of bit error of user 1 for RAKE receiver

- P_1^d: probability of bit error of user 1 for decorrelating receiver

- P_1^m: probability of bit error of user 1 for MMSE receiver

- P_k: probability of bit error of user k

- $\mathbf{H}_I$: matrix which column is composed by composite signature vector of interferers

- $\mathbf{P}_{\mathbf{y}_{ST}}(i)$: inverse of covariance in RLS

- $\mathbf{R}_{\{.\}}$: correlation matrix of data vector

- $\mathbf{R}_x$: correlation matrix of chip-sampled input data at single antenna element

- $r_k(t)$: received signal contributed by user k

- $\hat{\mathbf{r}}_{st}$: estimation of composite signature vector of Pre-ST receiver

- $\hat{\mathbf{r}}_{sm}$: estimation of composite signature vector of Post-ST receiver

- $\hat{\mathbf{r}}_{bt}$: estimation of composite signature vector of Pre-BT receiver

- $\hat{\mathbf{r}}_{bm}$: estimation of composite signature vector of Post-BT receiver

- $\mathbf{s}$: a generic temporal weight vector of single-user receiver

- $\mathbf{s}_z$: temporal weight vector of decorrelating receiver

- $\mathbf{s}_{moe}$: temporal weight vector of MOE receiver

- $\tilde{\mathbf{s}}_d$: weight vector of GSC with min/max algorithm at dth antenna

- $\mathbf{s}_l$: a generic temporal weight vector of lth path

- $\mathbf{s}_{l,m}$: correlator weights of mth beam at lth finger

- $\mathbf{S}_I$: interference subspace

- $\mathbf{S}$: sampled signature matrix over processing window

- $\bar{\mathbf{S}}(i)$: sampled signature matrix over ith bit duration

- $\tilde{\mathbf{S}}$: space-time signature matrix over processing window

- T: bit interval

- T_c: chip interval

- T_D: delay spread

- $\mathbf{T}$: matrix of linear transformation

- $\mathbf{T}_{ST_{MMSE}}$: weight matrix of optimal ST MMSE multiuser receiver

- $\mathbf{T}_{ST_{DEC}}$: weight matrix of optimal ST decorrelating multiuser receiver

- $\mathbf{U}$: reduced-dimension transformation

- $\mathbf{v}_{l,m}$: adaptive beamforming weights of mth beam at lth finger

- $\mathbf{w}$: a generic beamforming vector

- $\mathbf{w}_m$: beamforming weight of mth beam

- $\mathbf{W}_B$: beamforming weight matrix

- $\mathbf{W}_l$: beamforming weight matrix of lth finger

- $\mathbf{W}_d$: weight matrix of a set of correlator bank at dth antenna element

- $\mathbf{w}_{l,m}$: beamforming weight vector of mth beam at lth finger for Pre-ST data

- $\bar{\mathbf{w}}_{l,m}$: beamforming weights of mth beam at lth finger for Post-ST data

- $x(t)$: received signal at antenna

- $\tilde{x}_{ST}(t)$: received signal with antenna array

- $\mathbf{x}(i)$: chip-sampled data vector over processing window

- $\bar{\mathbf{x}}(i)$: chip-sampled vector over ith bit duration

- $x_{(d)}(t)$: received signal at dth antenna element

- $\mathbf{x}_{(\mathbf{d})}(i)$: chip-sampled data vector at dth antenna over processing window

- $\bar{\mathbf{x}}_{(d)}(i)$: chip-sampled data vector at dth antenna over ith bit duration

- $\tilde{\mathbf{x}}_l(\mathrm{i})$: post-despread ST data vector for lth finger

- $\mathbf{x}_{ST}$: received ST chip-sampled data vector

- $\mathbf{x}_{c-ST}$: concatenated Pre-ST data vector

- $\mathbf{x}_{c-SM}$: concatenated Post-ST data vector

- $\mathbf{X}(i)$: space-time chip-sampled data matrix

- $\mathbf{X}_{SM}$: generic Post-ST data matrix

- $\mathbf{y}(i)$: matched filtered outputs of input data vector

- $\mathbf{y}_{c-BT}$: generic concatenated Pre-BT data vector

- $\mathbf{y}_{c-BM}$: generic concatenated Post-BT data vector

- $\mathbf{y}_{l,m}$: Pre-BT data vector associated with lth vector

- y_{SU}: linear filtered output for single-user detection

- $\mathbf{y}_{ST}$: space-time matched filtered output data vector

- $\tilde{\mathbf{y}}_{ST}$: space-time matched filtered output without channel knowledge

- $\mathbf{Y}_{BM}$: generic Post-BT data matrix

- $\mathbf{Y}_{BT}$: generic Pre-BT data matrix

- $\mathbf{Y}_l$: Pre-BT data matrix associated with lth finger

- $z_{l,m}$: beamformer-correlator pair filtered outputs of mth beam at lth finger

- $\mathbf{z}$: concatenated beamformer-correlator pair filtered outputs

- $z_o(i)$: filtered output of maximum ratio combiner

Mathematical Notations

- $\delta(t)$: Dirac's delta function

- $\mathbf{v}[n]$: nth entry of $\mathbf{v}$

- $\mathbf{M}_k$: matrix striking out kth column and kth raw of matrix $\mathbf{M}$

- $\mathbf{M}[i,j]$: $(i,j)th$ entry of matrix $\mathbf{M}$

- $\nabla(\cdot)$: gradient operation

- $\mathcal{R}\{\cdot\}$: fetch the real part of operand

- $\Re\{\cdot\}$: range of subspace

- diag$\{\mathbf{v}\}$: diagonal matrix whose main diagonal is given by $\mathbf{v}$

- $\|\cdot\|$: Euclidean norm

- $|\cdot|$: absolute value operator

- $E\{\cdot\}$: expectation

- $\{\cdot\}^*$: complex conjugate

- $\{\cdot\}^T$: transpose

- $\{\cdot\}^H$: complex conjugate transpose

- $\{\cdot\}^+$: pseudo inverse

- $\text{rank}\,\{\cdot\}$: rank

- $\text{sign}\,\{\cdot\}$: take the sign value of operand

- $Q(x)$: Gaussian tail probability or error function

- $\Omega(\cdot)$: maximum likelihood function

- $\mathcal{N}(\mathbf{m}, \mathbf{C})$: multivariate Gaussian density with mean $\mathbf{m}$ and covariance $\mathbf{C}$

- $\text{tr}\,\{\cdot\}$: trace

- $\text{vec}\,\{\cdot\}$: vector obtained by concatenating column by comlumn of a matrix

Chapter 1

Introduction

The ability to communicate with people on the move has evolved remarkably since Guglielmo Marconi first demonstrated radio's ability to provide continuous contact with ships sailing the English Channel in 1897. Since then new wireless communications methods and services have been enthusiastically adopted by people throughout the world. Particularly during the past ten years, the mobile radio communications industries have grown by orders of magnitude, fueled by digital and radio frequency (RF) circuit fabrication improvements. Digital switching techniques have facilitated the large scale deployment of affordable, easy to use radio communication networks. The cellular radio communication networks have risen to offer universal network access while freeing users of locations and time restrictions. However, there are a lot of problems needed to be solved in modern communication environment. These include a complex multipath time-varying propagation channel, limited availability of radio spectrum, limited energy-storage capability of batteries in portable units, the demand for higher data rates, better communication quality, fewer dropped calls, and so on [1]. Among those demands discussed above, with the rapid growing of subscribers, engineers are facing the most demanding technological challenge: the need to increase the spectrum efficiency of wireless networks.

1.1 Cellular Radio Network Systems

A basic cellular system consists of three parts: a mobile unit, a base station, and a mobile switching center (MSC), with connections to link the three subsystems. When a mobile user initiates a telephone call, the mobile unit communicates with the base station at the center of a cell site via radio air interface. The messages are relayed through a backbone network to the MSC, which is the central coordinating element for all cell sites, and it interfaces with public switching telephone network (PSTN), controls call processing, and handles billing activities, etc. Cellular wireless systems rely on an intelligent allocation and reuse of channels throughout a coverage region. Each cellular base station is allocated a group of radio channels to be used within a small geographic area (cell). Base stations in adjacent cells are assigned different channel groups. By limiting the coverage area to within the boundaries of a cell, the same group of channels may be reused in different cells which are separated from one another by distances large enough to keep interference level within tolerable limits. The cellular concept and spectrum reuse are the key techniques for solving the problem of spectral congestion and user capacity. It offers higher capacity by using smaller and smaller cells. On the other hand, spectrum reuse implies that in a given coverage area there are multiple users that access the same set of channel resources. The mutual interference due to these multiple users is called the multiple access interference (MAI) and is the major limiting factor for spectrum efficiency. Moreover, because of the nature of wireless environments, multipath propagation results in signal fading and intersymbol interference (ISI), and this further deteriorates the quality of signals at the receiver.

1.2 Code Division Multiple Access

The most recent multiple access technology is code division multiple access (CDMA) based on direct sequence spread spectrum communications. Unlike frequency division multiple access (FDMA) and time division multiple access (TDMA), CDMA users occupy the entire bandwidth all the time. Users are distinguished from each other through the spreading codes assigned to them. The spreading code acts as a signature for the user and allows

the user's receiver to extract the desired signal from the MAI. Thus, the codes must be sufficiently uncorrelated, i.e., they must have good crosscorrelation properties to reduce interference. Wideband CDMA technology is being proposed for third-generation wireless personal communications [2]-[6]. Third generation systems will improve the technology and services provided by second generation systems. Furthermore, a lot of flexibility is being provided to allow for the evolution of technology. One of the special attributes of the proposals for wideband CDMA is the provision for advanced receivers. The novel aspects of wideband CDMA allow for the implementation of multiuser detections and smart antenna schemes. These features of advanced receivers may be employed in multirate third generation systems to perform interference rejection and improve system performance. More extensive discussions of multiple access technologies can be found in [1, 7]. The three popular multiple access techniques are illustrated in Figure 1.1.

The advantages of CDMA are primarily a result of the spread spectrum technology [8]. Spread spectrum provides resistance to frequency selective fading due to multipath through spectral diversity, and robustness to MAI. The variance of the signal-to-noise ratio (SNR) at the receiver is lower for CDMA than for narrowband FDMA when operating in frequency-selective fading channels. This applies to most practical CDMA systems where the signal bandwidth is significantly larger than the channel coherence bandwidth. CDMA is less susceptible to degradation due to ISI than TDMA is. One of the principal factors that influence the increase in the system capacity in CDMA systems is universal frequency reuse, which means that the same spectrum can be used in all cells, i.e., the reuse factor is 1. This also eliminates the need for frequency planning. The higher the reuse factor, the lower the system capacity. A typical reuse factor used in TDMA and FDMA cellular systems is 3-7. Furthermore, the impact of co-channel interference (CCI), which results from other cells using the same frequency, is greater for TDMA and FDMA systems than for CDMA systems with accurate power control. Power control in TDMA and FDMA systems helps reduce interference. However, power control is a more serious problem in CDMA systems. In the absence of fast and accurate power control, the near-far problem can cause much stronger signals received from users closer to the basestation to jam weaker signals received from mobiles at the edge of the cell. Another distinguished feature of CDMA is that it allows

for the exploitation of multipath energy with a RAKE receiver. The RAKE receiver provides a means of constructive combining of multipath. Distinguishing multipath components is possible because the coherence bandwidth of the channel is smaller than the signal bandwidth or, equivalently, the delays of the multipaths are larger than the chip duration. To improve the system capacity, CDMA may take advantages of the low voice-activity of normal speech. Human beings speak only about 30% ∼ 40% of the time during a conversation and listen for the rest of the time. If transmission is blocked during periods of silence, then interference can be reduced, thus increasing overall capacity. When a user moves from one cell to a neighboring cell, the signal must also move from one basestation to another via handoff. The RAKE receiver can be used to monitor the signal powers from two basestations carrying the same user's information. The gradual transition to another serving basestation is carried out through a process known as soft handoff. Soft handoff usually leads to fewer dropped calls and a more consistent coverage area [9]. Another attribute of CDMA is its soft capacity limit, which results in "soft blocking" of calls and a graceful degradation in performance. As well known, TDMA and FDMA place a hard limit on the number of users in a cell, resulting in "hard blocking". With CDMA, however, there is a graceful degradation in voice quality when the number of users exceeds a certain limit.

1.3 Space-Time Processing

The reasoning behind the use of space-time processing techniques is the optimization of the cellular spectral efficiency of the network. This is realized by implementing more than one antenna element to optimally transmit and receive signals by using both temporal and spatial signal processing techniques in the transceiver. Well known techniques such as antenna sectorization, diversity combining and adaptive beamforming (spatial and temporal signal processing in a broader sense) are considered to be examples of space-time processing. In fact, all antenna array systems can be considered to be space-time processors. More advanced space-time processors include space-time 2-D RAKE receivers, space-time equalizers and space-time multiuser detectors, etc. The main purpose of using multi-element antenna array in wireless links is to promise a significant increase in system capacity. For example,

in a system equipped with smart antennas, user terminals can transmit and receive with a smaller gain, resulting in a lower system level interference and thus equivalently larger capacity. On the other hand, exploitation of both the spatial and temporal domains at the same time allows for a much larger dimension to work with when performing signal reconstruction and interference cancellation. This certainly guarantees a better output SINR performance compared to either space-only or time-only processing. Recent theoretical results indicate that a point-to-point link utilizing D transmitting and receiving antennas can achieve an information theoretic capacity as high as D times that of a single antenna link [10]. This is called the multi-input, multi-output (MIMO) spatial multiplexing, and is considered the utmost exploitation of communications channel resources. In summary, space-time processing can improve network capacity, coverage and quality by reducing MAI while enhancing diversity and array gain. As a result, it has been an international research trend in the area of wireless communications to exploit the possibility of incorporating the "smart antenna", which is the most known name of space-time processing techniques.

Space-only and time-only signal processing techniques have been actively studied by numerous researchers over the past 20 years. Space-only processing with antenna array focuses mainly on distinguishing signatures of different user signals in the space domain, i.e., angles of arrival (AOA). Hence, it is very effective in suppressing strong narrowband interference (NBI) or MAI impinging on the antenna array from different directions other than the desired signal's. Moreover, antenna array combining (beamforming) further provides array gain and diversity gain to compensate for the loss of SNR due to fading. Space-only processing can also possibly reduce ISI. However, it is not practical since real channels with rich multipaths will require too many antenna elements. On the other hand, time-only processing with a single antenna and temporal processing units, e.g., RAKE receivers and Viterbi equalizers, focus on equalizing ISI in the time domain by using the temporal signature of the user signal, i.e., the channel impulse response. Even though time-only processing with over-sampling makes it possible to reduce MAI, the temporal channels for signal and interference will be similar in a practical channel with a small excess bandwidth, and MAI reduction leads to excessive noise enhancement. Therefore, temporal processing offers only a small leverage for suppressing MAI. In a cellular wireless system with both ISI and MAI, space-only or

time-only processing cannot handle both types of interference at the same time due to their fundamental limitation. The merge of space and time processing, i.e., space-time processing, provides a way to simultaneously exploit spatial and temporal structures, and suppress both ISI and MAI simultaneously. The desired signal and MAI, even in complex multipath environments, almost always arrive at the antenna array with distinct spatial and temporal signatures, thus allowing the receiver to exploit these differences to reduce MAI. Likewise, the space-time transmitter can use spatial selectivity to deliver signals to the desired mobile while minimizing interference for other mobiles. The space-time processing can be employed in a cascade space-only and time-only fashion and vice versa, or space-time joint fashion as shown in Figure 1.2 and Figure 1.3. The great potential of space-time signal processing will surely speed up the goal of providing affordable and ubiquitous wireless communication services in the near future.

1.4   Background and Literatures Review

There exist two main approaches to the demodulation of CDMA signals at the receiver. Single-user receivers basically estimate the signal of the desired user without caring the interferers' information. In contrast, multiuser detectors include all the users in the signal model [11]. The conventional RAKE receiver is a typical single-user CDMA receiver, which performs simply a matched filter operation. Because the crosscorrelations among the spreading sequences (or signatures) for different transmissions are nonzero, a nearby interference can disrupt reception of highly attenuated desired signal. The RAKE receiver was proven to be sensitive to the near-far problem [12].

Multiuser detection techniques provide alternatives to the conventional detector, by exploiting various levels of knowledge about the interfering signals to achieve near-far resistance [13]. The optimum multiuser detector attains the performance of the single user case by assuming the knowledge of the signature waveform, timing and received amplitude of each of the users. It is a nonlinear detector with superior performance to the conventional detector, but is exponentially complex in the number of users. Several suboptimal detectors have been proposed which require less knowledge of the interfering signals and/or have lower complex-

6

ity, but still maintain near-far resistance. An example is the decorrelating detector [13]-[14], which performs a linear transformation on the outputs of the matched filter, cancelling out the effect of MAI for each user. When the interfering users are weak compared to background noise level, the performance of the decorrelating detector may become worse than a conventional receiver. Linear minimum mean square error (MMSE) detectors solve this problem by incorporating the knowledge of the users' energies [15]. These detectors perform as decorrelating detector in the presence of strong multiple access interference, and act as conventional detector, when the background noise dominates. The chief advantage of the MMSE detectors, however, is in their ability to be easily implemented in an adaptive fashion. This eliminates the need for the knowledge of the signature waveforms of the interfering users. A training signal has to be retransmitted, every time there is a severe change in the received signal, which can become cumbersome in rapidly changing environments.

Blind or self recovering procedures for estimating the system parameters are possible by exploiting the characteristics of communication signals. Blind subspace methods show good performance [16]-[17], but the required singular value decomposition (SVD) of large matrices leads to a heavy computational load. On the contrary, blind adaptive multiuser detectors [18, 19] significantly reduce the computational burden. A scheme that was presented in [18] with constrained minimum output energy (MOE) exploits knowledge of the desired user's spreading code to operate in a blind manner. The MOE detectors minimize the receivers' output energy subject to one or more linear signal preserving constraints. The MOE method was extended to multipath environments by adding more constraints [19]. Under ideal conditions, it converges to the MMSE detector without requiring training signals. However, the MOE detectors are sensitive to mismatch in the signal preserving constraints. Robust implementations for that case are attempted in [20] by forcing the receiver response to the delayed copies of the signal to zero. With these additional constraints, MOE techniques are applicable, but have inferior performance since they treat part of the user signal as interference. Another robust implementation is to add an identity matrix so as to deemphasize an algorithm to errors known as diagonal loading in array processing [21, 22]. Recently however, constrained optimization solutions were developed to combine all multipath components of the signal of interest and jointly minimize MAI while maximizing the signal component at

7

the receiver's output [23]. The performance of this min/max approach tends to be close to that of the optimal MMSE receiver at high SNR in the presence of multipath [23]. However, the complexity is higher due to the use of the eigenvalue decomposition. In [24], a modified generalized sidelobe canceller (GSC) is employed to construct a bank of adaptive correlators, which is used to collect the multipath components and suppress MAI. A robust adaptive algorithm is also developed to reduce the computational burden.

Enormous increase in traffic throughput is promised by the use of antenna arrays in wireless radio frequency [25]. Optimal maximum likelihood space-time multiuser detection was suggested for flat-fading channels in [26, 27] and for multipath fading in [28]. Because optimum detectors' implementation is prohibitively complex for a large number of users, linear space-time multiuser detectors with lower complexity have been explored in [14, 29]. A space-time single-user receiver that exploits both the temporal and spatial structures of the desired signal to coherently combine the multipath energy is referred to as the space-time 2-D RAKE receivers [30]-[32]. The pioneering work for blind space-time 2-D RAKE receiver proposed in [30] exploits the distinctive structures of the pre-despread and post-despread spatial correlation matrices to estimate the spatial channels at different fingers of the signal of interest (SOI) via principal component (PC) eigenvalue decomposition. Beamforming is then performed at different fingers, followed by a RAKE combining. In [31], the PC based scheme is extended to perform space-time joint channel estimation and post-combining. The receivers in [30]-[32] work with the outputs of a bank of fixed correlators, and are thus post-despread receivers. They are simple to implement, but do not fully exploit the temporal degree of freedom available to handle strong MAI. As an alternative, a receiver which works directly with the chip sampled data is called a pre-despread receiver, and can be regarded as an adaptive matched filter that performs despreading and MAI suppression simultaneously [33]. A popular blind pre-despread receivers is the MOE receivers [18]. Temporal MOE detectors achieve good performance in multipath environments where the delay spread is limited to a portion of the symbol intervals by exploiting knowledge of the desired user's signature vector. Equivalent space-time MOE detectors require the information about the space-time signature vector, which depends on the temporal spreading code, the spatial array response vector, and the multipath channel. We can assume that the multipath delay

spread is limited to a few chip intervals, however AOA generally vary over a wide range and antenna calibration may be difficult to obtain, hence the space-time channel properties are difficult to characterize. In [34], a comprehensive treatment of constraints strategies under the assumption, with knowledge of the temporal code vector but no knowledge of the spatial response, is developed using fixed and optimized constraints based on temporal MOE detectors in [34]. Another space-time MOE detector is presented in [24], which utilizes a set of adaptive modified GSC beamformers steered to different look direction to encompass a working sector. These adaptive GSC beamformers perform adaptive nulling for strong MAI from outside the sector. The outputs of these beamformers are processed by a bank of adaptive correlators, which can be regarded as a set of linearly constrained minimum variance (LCMV) combiners in the time domain. A modified GSC in the temporal domain is employed again to collect the multipath components and suppress the in-sector MAI. The space-time MOE detector is blind in that the construction of adaptive beamformers and correlators does not require any training. The only information required is the desired user's signature vector, timing and a rough estimate of the AOA of the desired signal for the working sector selection. The adaptive beamformers and correlators can also be jointly constructed in the form of beamformer-correlator pairs to collect the multipath signals in a prescribed angular sector and time duration, and to suppress MAI and NBI [35]. This is done by performing adaptive nulling on a set of LCMV space-time processors steered to different look directions and delays. To avoid signal cancellation incurred with the mismatch of space-time signatures, a modified GSC is employed. The space-time receivers in [24, 35] performs "beamspace" beamforming in which array data are first pre-processed by a set of diversity beamformers encompassing an angular sector. This has two main advantages. First, with sectorization, the capacity of the system can be potentially increased. Second, MAI and NBI from outside the sector can be suppressed adaptively, leading to improve reception quality for the SOI.

The computational complexity of an adaptive processor, MOE, GSC or MMSE, is the function of the rank of the filter and the requirements of the adaptive algorithm. The filter rank is conventionally chosen to satisfy the desired Wiener solution and the resulting steady state MMSE or output signal-to-interference-plus-noise ratio (SINR). The complexity of the

algorithm determines how quickly the filter coefficients converge to the Wiener solution. For recursive least squares (RLS) algorithms, with $\mathcal{M}$ being the number of adaptive weights, the computational complexity is $\mathcal{M}^2$ and convergence is obtained in approximately $2\mathcal{M}$ adaptation [37], yielding a complexity of $2\mathcal{M}^3$ for convergence. Due to this large computational complexity, it is very important to reduce $\mathcal{M}$ to a level which is realizable for the platform. The partially adaptive filtering uses only a portion of the available degrees of freedom offered by the adaptive weights. The advantage of partially adaptive filtering include: reduced complexity, faster convergence and the ability to improve the quiescent response with the unused degrees of freedom. Much of the previous work on partially adaptive interference suppression has been based on principal components (PC) in which the received vector is projected onto an estimate of the lower dimensional signal subspace with the largest energy [36, 38]. When used with GSC, the partially adaptive filtering can be employed to reduce the size of blocking matrix [39, 40]. There are several methods proposed for determining the low rank subspace of blocking matrix.

1.5 Outline of Thesis

In this thesis, we propose a class of pre-despread and post-despread blind 2-D RAKE receivers. In addition to conventional space-time 2-D RAKE receivers working on antenna elements directly, beamspace-time 2-D RAKE receivers which utilize a set of diversity beamformers are developed. The beamspace-time receiver is suitable for sectorized communications in which the desired signal is captured from inside a designated angular sector. In particular, a new method of beamfoming is propsed which leads to reliable signal reception and interference suppression. For real time implementation, we suggest efficient adaptive algorithms for time-varying mobile environments, and methods for enhancing their robustness. Furthermore, partially adaptive schemes are also proposed for reduced complexity processing and faster convergence. Finally, a new scheme of sectorization is developed which can effectively combat narrowband interference from inside the sector. In summary, the thesis presents an alternative approach to the conventional space-time receiver for CDMA systems by incorporating beamspace processing. The new receiver structure proves to be near-far

resistant, and requires a significantly lower complexity. It can be operated even in a nearly blind mode without the need of many training symbols that consume the system throughput. The proposed receiver is well suited to the so-called multi-beam sectored system considered to be a promising candidate for future smart antenna technologies. The thesis is organized as follows.

In Chapter 1, we introduce the multiple access techniques, space-time processing and give a historical review of various blind and nonblind linear CDMA receivers. Chapter 2 establishes the basic system models and theoretical background of the research. It shows a continuous time model of CDMA systems over multipath fading channels. This model was derived into an equivalent discrete time model for the purpose of digital signal processing. It also analyzes some key concepts in linear multiuser or single-user detection techniques, including MMSE detection, decorrelating detection, and MOE detection. In the last part of this chapter, we propose a blind CDMA receiver based on a modified GSC structure for multipath reception and interference suppression.

In Chapter 3, the system model is extended from the time-only to space-time domain by the incorporation of an antenna array. In particulr, a class of 2-D RAKE receivers will be discussed and analyzed. The temporal domain processing leads to pre-despread and post-despread processors and spatial domain processing leads to antenna space and beamspace processors, respectively. The temporal and spatial domain processing can be done either in a joint or cascade manner. In addition to various space-time detectors, the parallel interference cancellation (PIC) and successive interference cancellation (SIC) CDMA receivers are also discussed in detail. Finally, blind space-time CDMA receivers based on the GSC technique is proposed. The GSC technique is similar to the conventional linearly constrained minimum variance (LCMV) technique, and known to be sensitive to the mismatch of signature vectors. To avoid such sensitivity problems, we include some modifications in the GSC to successfully enhance its reliability.

In Chapter 4, we propose several beamspace-time 2-D RAKE receivers for sectored CDMA systems. In a sectored cellular system, the entire field-of-view is divided into several contiguous sectors, with each sector responsible for a distinctive set of users. With antenna array incorporated, sectorization can be done adaptively to meet two major requirements.

First, multiple beams are formed to collect multipath components of the desired signal with angle diversity. Second, strong MAI outside the sector is suppressed in the sidelobe region of these beams. The outputs of the beamformers are then processed by a bank of adaptive correlators, which are formed by a set of modified GSC's to collect the multipath components of the desired signal and to suppress the in-sector MAI.

In Chapter 5, for a practical implementation of the proposed CDMA receivers, adaptive algorithms are introduced to avoid matrix inversion in GSC and to adapt the receiver to time-varying mobile environments. Note that with the channel being nonstationary, matrix inversion is usually required repeatedly, resulting in tremendous amount of computational loading. The adaptive algorithms are realized in a time recursive fashion such as the popular least mean squares (LMS) and RLS algorithms. Robust techniques are also included that are shown to effectively improve the system performance. Finally, an adaptive algorithm is presented for tracking the principle eigen-component required for maximum ratio combining.

Chapter 6 discusses miscellaneous issues about practical implementation and performance enhancement. First, the technique of diagonal loading in the correlation matrix increases the robustness of adaptive GSC algorithms. Second, several partially adaptive algorithms are presented with their convergence behaviors compared. In particular, a new method is proposed for the multiuser scenario in which both the signal and MAI's signatures are available. Third, a near maximum SINR (MSINR) CDMA receiver is developed which exhibits enhanced convergence performance as compared to the original GSC based receiver. An analysis of LCMV beamformers reveals that the main cause of its poor convergence is the presence of a non-zero crosscorrelation between the signal and interference-plus-noise due to finite samples. The crosscorrelation term induces a perturbation on the weight vectors of beamformers, which in turn causes a drop in output SINR. The same statements apply to GSC. To remedy this, we propose an iterative procedure in which the signal is estimated, reconstructed at the prsent iteration, and subtracted from the input data at the next iteration. Finally, the NBI issue is considered. A strong NBI acts like a nonstationary signal within the processing window of the conventional receiver. So the temporal processing is not effective in suppressing the NBI. Fortunately, the NBI can be easily suppressed in the spatial domain by using an antenna array, because the spatial signature of the NBI is usually much

more stationary than its temporal signature. We propose to use a set of diversity beams to suppress the NBI and present a scheme of dynamic sector synthesis to adapt to the traffic of the CDMA system. The dynamic sector synthesis can be implemented for different angular regions. This allows the operator to balance the traffic loading across sectors, to manage handoff overhead, and to control the interference. As a conclusion, Chapter 7 summarizes the thesis and gives a sketch of some future work.
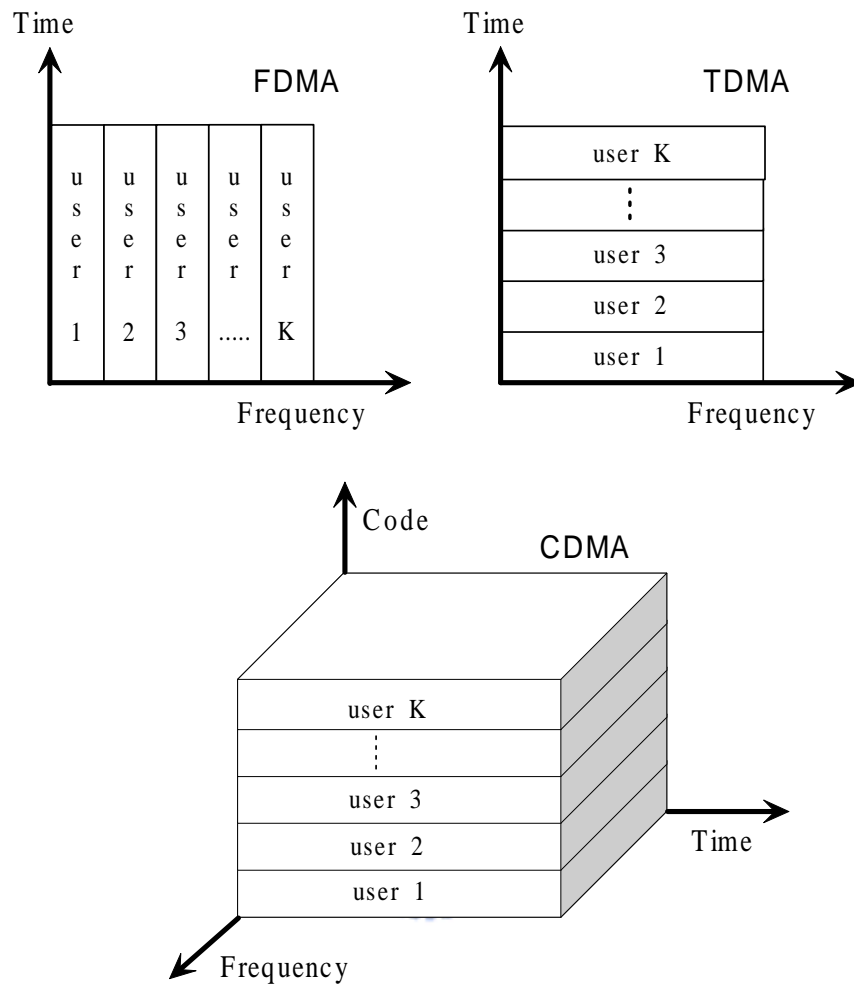
Figure 1.1: Multiple access techniques
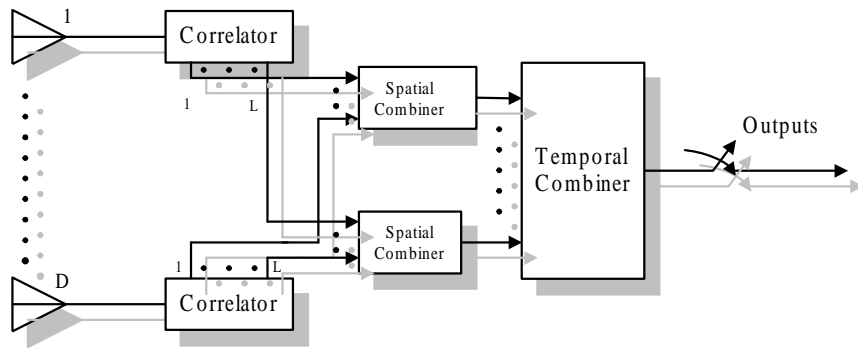
(a) time-space
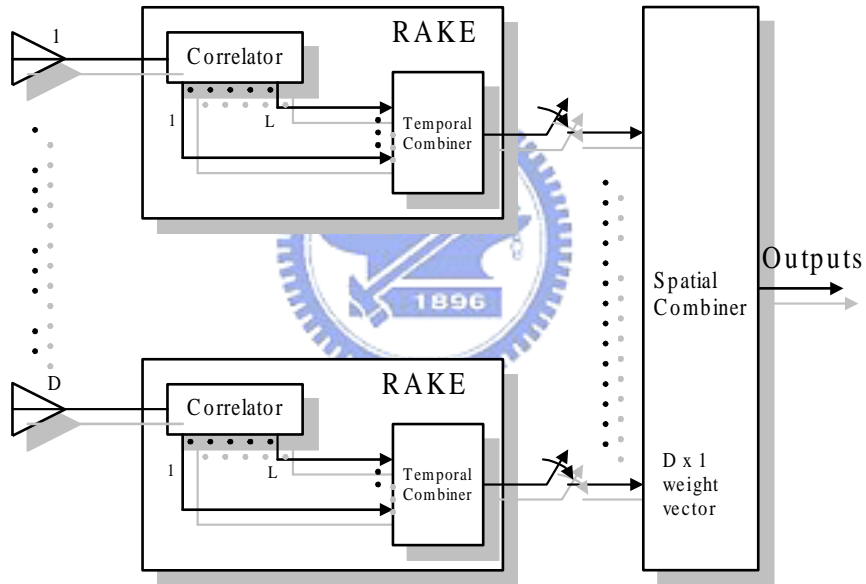
(b) space-time

Figure 1.2: Space-time and time-space cascade 2-D RAKE receivers
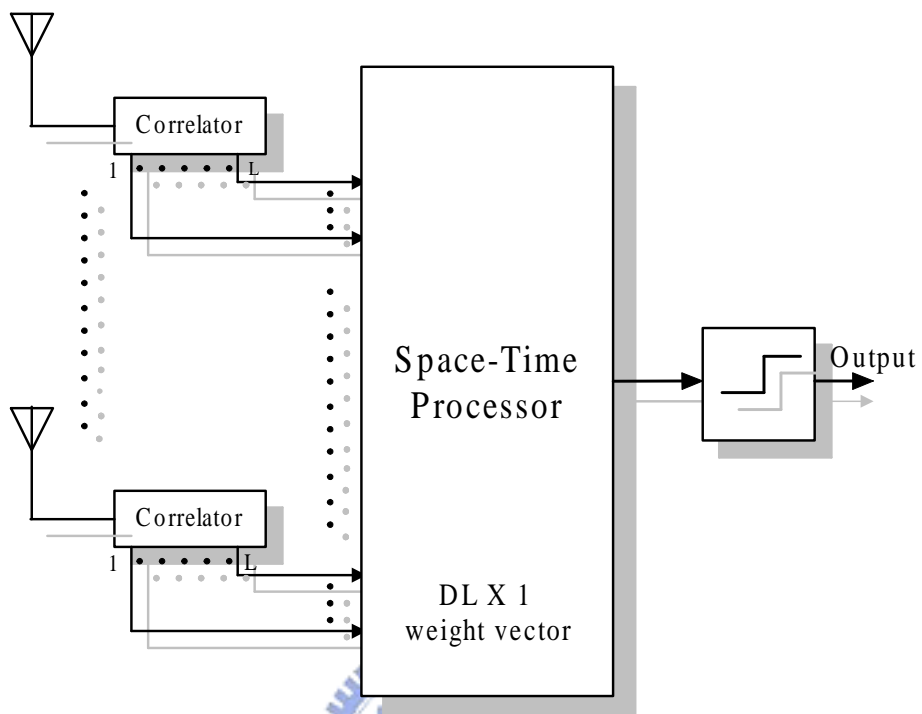
Figure 1.3: Space-time joint processing in CDMA systems

16

Chapter 2

CDMA Receivers in Multipath Fading Channels

In this chapter, we provide a mathematical framework for describing CDMA systems. Some fundamental parameters of CDMA systems and performance measures are defined. CDMA receivers may be categorized broadly into multiuser receivers and single-user receivers. This classification is based on the structures of receivers, i.e., based on whether the receivers demodulate a single-user or jointly demodulate some or all of the active users in the system. The optimal receiver is the maximum likelihood (ML) multiuser receiver which requires joint estimation of channel parameters and data symbols [41]. The optimal receiver is too complex for practical implementation and hence several suboptimal receivers have been proposed as alternatives [42]. When considering downlink receivers, only the signal of interest (SOI) should be demodulated while suppressing the interference due to other users. The single-user detectors are thus options for the downlink receivers. A popular single-user receiver is the RAKE receiver [43] which constructively combines the multipath components of the SOI. Due to the imperfect correlation properties of the spreading codes, the RAKE receiver is sensitive to multipath and near-far problems [12]. Significant improvements can be obtained with linear MMSE or decorrelating receivers. Either MMSE or decorrelating receiver needs training signals. Adding training signals consumes the available bandwidth and reduces spectral efficiency. In addition, the training method is not efficient in rapidly time-varying channels or in protocols with small short message packages. In the absence of

training signals however, the development of a linear receiver with performance equal or close to that of the MMSE solution presents a significant challenge. In this chapter, we introduce the optimal ML multiuser detector and some linear multiuser detectors. We also discuss nonblind and blind single-user receivers. Finally we develop a single-user detector based on GSC structure to collect the multipath signals and to suppress MAI simultaneously.

2.1 Data Model

A standard model for an asynchronous DS/CDMA system with K users and L propagation paths are considered. The signal of the kth user is modulated by binary phase shift keying (BPSK) and the modulated signal are spread with a unique signature waveform given by

$$c_k(t) = \sum_{n=0}^{N-1} c_k[n]p(t - nT_c) \tag{2.1}$$

where N denotes the number of the chips per symbol, i.e., processing gain or spreading factor, $c_k[n] \in \{-1, 1\}$ is the nth chip of the kth user, $p(t)$ is the chip waveform, and T_c is the chip interval. Assume that the period of signature waveform equals one symbol interval, then the contribution of user k to the received signal over an I-symbol interval can be written as

$$r_k(t) = \sigma_k \sum_{i=1}^{I} b_k(i)c_k(t - iT) \tag{2.2}$$

where I is the number of the symbols within the processing window, $b_k(i)$ denotes the ith transmitted symbol, assumed to be i.i.d. with zero-mean and unit variance, σ_k is the transmitted amplitude of the user k, and T is the symbol interval. The complex envelope of the received signal is expressed as

$$x(t) = \sum_{i=1}^{I} \sum_{k=1}^{K} r_k(t) * h_k(t) + n(t) \tag{2.3}$$

The $n(t)$ is the additive white Gaussian noise process with two-sided power spectral density σ_n^2 and the symbol $*$ denotes the convolution operation. The $h_k(t)$, which denotes the impulse response of channel for user k, is given by

$$h_k(t) = \sum_{l=1}^{L} \alpha_{k,l}\delta(t - \tau_{k,l}) \tag{2.4}$$

18

where L is number of the resolved Rayleigh fading multipaths, $\alpha_{k,l}$ is the complex fading gain, $\tau_{k,l}$ is the propagation delay of the lth path of user k and $\delta(t)$ is the Dirac's delta function. Evaluating the equation (2.3) with (2.4), the received signal is given by

$$x(t) = \sum_{i=1}^{I} \sum_{k=1}^{K} \sum_{l=1}^{L} \sigma_k b_k(i) \alpha_{k,l} c_k(t - iT - \tau_{k,l}) + n(t) \tag{2.5}$$

To fully exploit the temporal signature of the received signal, $x(t)$ is passed through chip matched filter and then is chip rate sampled at $t = (i-1)T + nT_c + T_c/2$ over the processing window of interest, i.e., I-symbol interval. The received data in discrete time form over a block of I-symbol data is given by

$$\mathbf{x}(i) = \mathbf{SFAb}(i) + \mathbf{n}(i) \tag{2.6}$$

where the chip-sampled data vector also is given by

$$\mathbf{x}(i) = \left[\bar{\mathbf{x}}^T(i+1), \bar{\mathbf{x}}^T(i+2), \cdots, \bar{\mathbf{x}}^T(i+I) \right]_{NI \times 1}^T \tag{2.7}$$

and $\bar{\mathbf{x}}^T(i)$ is the chip-sampled vector of the received data over the ith symbol interval, given by

$$\bar{\mathbf{x}}^T(i) = \left[x(t)|_{t=(i-1)T+T_c/2}, x(t)|_{t=(i-1)T+T_c+T_c/2}, \cdots, x(t)|_{t=(i-1)T+(N-1)T_c+T_c/2} \right]_{N \times 1}^T \tag{2.8}$$

where $[\cdot]^T$ denotes the transpose. The $\mathbf{S}(i)$ is the chip-sampled signature sequence matrix over an I-symbol interval given by

$$\mathbf{S}(i) = \left[\bar{\mathbf{S}}(i+1), \bar{\mathbf{S}}(i+2), \cdots, \bar{\mathbf{S}}(i+I) \right]_{NI \times KLI} \tag{2.9}$$

where $\bar{\mathbf{S}}(i)$ is the chip-sampled signature sequence associated with the ith symbol only. It means that although the column vectors spanned over an I-symbol interval, the entries of the vectors happen to be non-zero only on the chip-sampled interval during the ith symbol period. The matrix is given by

$$\bar{\mathbf{S}}(i) = \begin{bmatrix} \mathbf{0} & \cdots & \mathbf{0} & \cdots & \mathbf{0} \\ \mathbf{c}_{\tau_{1,1}} & \cdots & \mathbf{c}_{\tau_{1,L}} & \cdots & \mathbf{c}_{\tau_{k,L}} \\ \mathbf{0} & \cdots & \mathbf{0} & \cdots & \mathbf{0} \\ \vdots & \ddots & \vdots & \ddots & \vdots \\ \mathbf{0} & \cdots & \mathbf{0} & \cdots & \mathbf{0} \end{bmatrix}_{NI \times KL} \tag{2.10}$$

where each column of $\bar{\mathbf{S}}(i)$ has about $(i-1)N$ leading zero entries and a non-zero sequence, $\mathbf{c}_{\tau_{k,l}}$, which is the augmented signature sequence given by one of the column of $\mathbf{C}_k$:

$$
\mathbf{C}_k = \begin{bmatrix} c_k[0] & 0 & \cdots & 0 \\ \vdots & c_k[0] & \ddots & \vdots \\ c_k[N-1] & \vdots & \ddots & 0 \\ 0 & c_k[N-1] & \ddots & c_k[0] \\ \vdots & \vdots & \ddots & \vdots \\ 0 & 0 & \cdots & c_k[N-1] \end{bmatrix}_{(N+L-1)\times L} \tag{2.11}
$$
$$
= \begin{bmatrix} \mathbf{c}_{k,1} & \mathbf{c}_{k,2} & \cdots & \mathbf{c}_{k,L} \end{bmatrix}
$$

where $c_k[n]$ is the nth chip-sampled data of the signature waveform, $c_k(t)$. The $\mathbf{c}_{k,l}$ is the augmented signature sequence associated with the path of l chips delay of user k. The channel coefficient matrix is given by

$$
\mathbf{F} = \mathrm{diag}\begin{bmatrix} \bar{\mathbf{F}}, \bar{\mathbf{F}}, \cdots, \bar{\mathbf{F}} \end{bmatrix}_{KLI \times KI} \tag{2.12}
$$

where

$$
\bar{\mathbf{F}} = \mathrm{diag}\begin{bmatrix} \begin{bmatrix} \alpha_{1,1} \\ \vdots \\ \alpha_{1,L} \end{bmatrix}, \cdots, \begin{bmatrix} \alpha_{K,1} \\ \vdots \\ \alpha_{K,L} \end{bmatrix} \end{bmatrix}_{KL \times K} \tag{2.13}
$$

The received amplitude matrix is given by

$$
\mathbf{A} = \mathrm{diag}\begin{bmatrix} \bar{\mathbf{A}}, \bar{\mathbf{A}}, \cdots, \bar{\mathbf{A}} \end{bmatrix}_{KI \times KI} \tag{2.14}
$$

where

$$
\bar{\mathbf{A}} = \mathrm{diag}\begin{bmatrix} \sigma_1, \sigma_2, \cdots, \sigma_K \end{bmatrix}_{K \times K} \tag{2.15}
$$

The transmitted data vector of users' symbols over the I-symbol interval is given by

$$
\mathbf{b}(i) = \begin{bmatrix} \bar{\mathbf{b}}^T(i+1), \bar{\mathbf{b}}^T(i+2), \cdots, \bar{\mathbf{b}}^T(i+I) \end{bmatrix}^T_{KI \times 1} \tag{2.16}
$$

where

$$
\bar{\mathbf{b}}(i) = \begin{bmatrix} b_1(i), b_2(i), \cdots, b_K(i) \end{bmatrix}^T_{K \times 1} \tag{2.17}
$$

The transmitted data $b_k(i)$, $i = 1, \cdots, I$, $k = 1, \cdots, K$, is modulated with the symbol alphabet $\in \{-1, 1\}$ and $\mathbf{n}(i)$ is the channel noise vector.

2.2 Conventional RAKE Receivers

Conventional detection in multipath environments is done by filtering the received data vector by a bank of matched filter bank. This is conceptually equivalent to the MRC, and is usually termed RAKE reception as shown in Figure 2.1. The matched filter bank output is given in the vector form by

$$
\begin{aligned}
\mathbf{y}(i) &= (\mathbf{SF})^H \mathbf{x}(i) \\
&= \mathbf{F}^H \mathbf{RFAb}(i) + (\mathbf{SF})^H \mathbf{n}(i) \\
&= \mathbf{HAb}(i) + \bar{\mathbf{n}}(i) \tag{2.18}
\end{aligned}
$$

where $[\cdot]^H$ denotes the conjugate transpose, $\mathbf{H} = \mathbf{F}^H \mathbf{RF}$, and $\bar{\mathbf{n}}(i) = (\mathbf{SF})^H \mathbf{n}(i)$ with the covariance matrix $\sigma_n^2 (\mathbf{SF})^H \mathbf{SF}$. Under a reasonable assumption of delay spread less than one symbol interval, the crosscorrelation matrix, $\mathbf{R} = E\left\{\mathbf{S}^H(i)\mathbf{S}(i)\right\}$, is given by

$$
\mathbf{R} = \begin{bmatrix}
\mathbf{R}^{(0)} & \mathbf{R}^{(1)} & \mathbf{0}_{KL} & \cdots & & \cdots & \mathbf{0}_{KL} \\
\mathbf{R}^{(-1)} & \mathbf{R}^{(0)} & \mathbf{R}^{(1)} & \mathbf{0}_{KL} & & & \vdots \\
\mathbf{0}_{KL} & \mathbf{R}^{(0)} & \mathbf{R}^{(0)} & \mathbf{R}^{(1)} & \ddots & & \vdots \\
\vdots & \ddots & \ddots & & \ddots & \mathbf{0}_{KL} & \\
\vdots & \ddots & \ddots & \mathbf{R}^{(-1)} & \mathbf{R}^{(0)} & \mathbf{R}^{(1)} \\
\mathbf{0}_{KL} & \cdots & \cdots & \mathbf{0}_{KL} & \mathbf{R}^{(-1)} & \mathbf{R}^{(0)}
\end{bmatrix}_{KLI \times KLI} \tag{2.19}
$$

where

$$
\mathbf{R}^{(j)} = \begin{bmatrix}
\rho^{(j)}_{(1,1)(1,1)} & \cdots & \rho^{(j)}_{(1,1)(1,L)} & \cdots & \rho^{(j)}_{(1,1)(K,1)} & \cdots & \rho^{j}_{(1,1)(K,L)} \\
\rho^{(j)}_{(2,1)(1,1)} & \cdots & \rho^{(j)}_{(2,1)(1,L)} & \cdots & \rho^{(j)}_{(2,1)(K,1)} & \cdots & \rho^{j}_{(1,1)(K,L)} \\
\vdots & \vdots & \vdots & \vdots & \vdots & \vdots & \vdots \\
\rho^{(j)}_{(K,L)(1,1)} & \cdots & \rho^{(j)}_{(K,L)(1,L)} & \cdots & \rho^{(j)}_{(K,L)(K,1)} & \cdots & \rho^{j}_{(K,L)(K,L)}
\end{bmatrix}_{KL \times KL} \tag{2.20}
$$

$\rho^{(j)}_{(k,l)(k',l')} = \mathbf{c}^{(j)H}_{\tau_{k,l}} \mathbf{c}^{(0)}_{\tau_{k',l'}}$ for $j = -1, 0, 1$, and $\mathbf{c}^{(j)}_{\tau_{k,l}}$ is the chip-sampled signature vector of $c_k(t - jT - \tau_{k,l})$ at $t = T_c/2 + \tau_{1,l}, \cdots, (N-1)T_c + T_c/2 + \tau_{1,l}$, assuming that user 1 is the desired user.

Without loss of generality, we assume a synchronous CDMA system and each user has L multipaths with delays, $0, T_c, \cdots, (L-1)T_c$, respectively. Then, consider the sample signature

sequence matrix $\mathbf{S}(i)$ over a two-symbol duration, which can be written as

$$\mathbf{S}(i) = \left[\frac{\mathbf{C}^{(0)}}{\mathbf{C}^{(-1)}} \right] = \left[\begin{array}{c} \left[\begin{array}{ccc} \mathbf{c}_{1,1}[1:N] & \cdots & \mathbf{c}_{K,L}[1:N] \end{array} \right] \\ \hline \left[\begin{array}{ccc} \mathbf{c}_{1,1}[(N+1):(N+L-1)] & \cdots & \mathbf{c}_{K,L}[(N+1):(N+L-1)] \\ \mathbf{0}_{2N-(N+L-1)} & \cdots & \mathbf{0}_{2N-(N+L-1)} \end{array} \right] \end{array} \right]_{2N \times KL}$$

(2.21)

where $\mathbf{c}_{k,l}[1:N]$ denotes a vector with the entries of the vector $\mathbf{c}_{k,l}$ indexed from 1 to N. Then $\mathbf{R}^{(0)} = \mathbf{C}^{(0)H}\mathbf{C}^{(0)}$ and $\mathbf{R}^{(-1)} = \mathbf{C}^{(-1)H}\mathbf{C}^{(0)} = \mathbf{C}^{(0)H}\mathbf{C}^{(-1)} = \mathbf{R}^{(1)}$.

The decision strategy of the RAKE receiver is that the bit $\mathbf{b}[n]$, which is the nth entry of the symbol vector $\mathbf{b}(i)$, $(\mathbf{b}[n] = b_n(i)$, if $I = 1)$, is decided by the sign of the nth entry of $\mathbf{y}(\mathrm{i})$. The decision criterion is given by

$$\mathbf{b}[n] = \mathrm{sign}\left\{\mathbf{y}(i)[n]\right\} \tag{2.22}$$

If only the desired user exists in the system, this decision is optimal in the sense that the SNR is maximized corresponding to the ML detection. If multiple users exist in the system, this is, however, not entirely true. The SNR is still maximized, but the detector is not ML due to the presence of MAI.

In order to provide more insights into the structure of $\mathbf{y}$, we consider a synchronous CDMA system with two active users with a single path each. The processing window over a one-symbol interval is sufficient, i.e, $(I = 1)$ and we assume that user 1 is the desired user. Under these assumption, $\mathbf{y}$ is given by

$$\mathbf{y}(i) = \left[\begin{array}{cc} \sigma_1 & \sigma_2\rho_{1,2} \\ \sigma_1\rho_{1,2} & \sigma_2 \end{array} \right] \left[\begin{array}{c} b_1(i) \\ b_2(i) \end{array} \right] + \bar{\mathbf{n}} \tag{2.23}$$

where $\rho_{1,2}$ is the crosscorrelation of signature sequences between user 1 and user 2 and $\bar{\mathbf{n}}$ is a Gaussian random variables with zero mean and variance equal to σ_n^2. The probability of bit error of user 1 is given by [11]

$$\begin{aligned} P_1^c(\sigma_n) &= P[b_1(i) \neq \hat{b}_1(i)] \\ &= \frac{1}{2}Q\left(\frac{\sigma_1 - \sigma_2\rho_{1,2}}{\sigma_n}\right) + \frac{1}{2}Q\left(\frac{\sigma_1 + \sigma_2\rho_{1,2}}{\sigma_n}\right) \\ &\leq Q\left(\frac{\sigma_1 - \sigma_2\left|\rho_{1,2}\right|}{\sigma_n}\right) \end{aligned} \tag{2.24}$$

22

where $Q(x)$ is the unit Gaussian tail probability given by

$$Q(x) = \frac{1}{\sqrt{2\pi}} \int_x^\infty e^{-\frac{u^2}{2}} du \tag{2.25}$$

If the relative amplitude of the interference satisfies

$$\frac{\sigma_2}{\sigma_1} > \frac{1}{|\rho_{1,2}|} \tag{2.26}$$

then the conventional receivers exhibit a highly anomalous behavior, i.e., the "near-far problem". Although the conventional detector has its limitation, it still plays an important role in multiuser detection since the output of a bank of matched filters provides a minimal sufficient statistics for detection [41].

2.3 Optimal Multiuser Receivers

The optimal detector is the ML detector which exhaustively searches all the possibility of hypotheses and finds the exact one with the maximum probability. The optimal ML detection is defined as

$$\hat{\mathbf{b}}_{ML} = \arg \max_{\mathbf{b} \in \{-1,1\}^{KI}} P\left(\mathbf{y}|\mathbf{b}\right) \tag{2.27}$$

Assuming that all the spreading codes are known and the knowledge of $\mathbf{b}$ is given, the only random component in $\mathbf{y}$ is the Gaussian noise $\bar{\mathbf{n}}$. It therefore follows that $\mathbf{y}$ is Gaussian distributed with $E\{\mathbf{A}\mathbf{y}\} = \mathbf{AHA}\mathbf{b}$, where $\mathbf{A}$ is defined in (2.14), and $var\{\mathbf{A}\mathbf{y}\} = \sigma_n^2 \mathbf{AHA}$. The corresponding probability distribution function is thus [44] given by

$$P(\mathbf{y}|\mathbf{b}) = K_0 \exp\left(-\frac{(\mathbf{A}\mathbf{y} - \mathbf{AHA}\mathbf{b})^H (\mathbf{AHA})^{-1}(\mathbf{A}\mathbf{y} - \mathbf{AHA}\mathbf{b})}{2\sigma_n^2}\right) \tag{2.28}$$

where K_0 is a constant independent of $\mathbf{y}$ and $\mathbf{b}$, and therefore

$$
\begin{aligned}
\hat{\mathbf{b}}_{ML}(i) &= \arg \min_{\mathbf{b} \in \{-1,1\}^{KI}} (\mathbf{A}\mathbf{y} - \mathbf{AHA}\mathbf{b})^H (\mathbf{AHA})^{-1}(\mathbf{A}\mathbf{y} - \mathbf{AHA}\mathbf{b}) \\
&= \arg \min_{\mathbf{b} \in \{-1,1\}^{KI}} \mathbf{b}^T \mathbf{AHA}\mathbf{b} - 2\mathcal{R}\{\mathbf{b}^T \mathbf{A}\mathbf{y}\} \\
&= \arg \min_{\mathbf{b} \in \{-1,1\}^{KI}} \Omega(\mathbf{b})
\end{aligned}
\tag{2.29}
$$

where

$$\Omega(\mathbf{b}) = \mathbf{b}^T \mathbf{AHA}\mathbf{b} - 2\mathcal{R}\{\mathbf{b}^T \mathbf{A}\mathbf{y}\} \tag{2.30}$$

23

with $\Omega(\mathbf{b})$ being the likelihood function of the matched filter output vector $\mathbf{y}$ in (2.18) conditioned on all the transmitted symbols $\mathbf{b}(i)$ and $\mathcal{R}(\cdot)$ fetching the real part of the operand. The solution to the ML problem was derived in [41], which is to exhaustively search all 2^{KI} possible data vectors using the Viterbi algorithm to guarantee a global solution. It is hence clear that the problem grows exponentially in complexity with the number of users. The structure of optimal multiuser detection is shown in Figure 2.2.

Due to the prohibitive computational complexity of the optimal ML multiuser receiver, suboptimal solutions have been studied extensively. Well-known suboptimal receivers are the linear multiuser receivers. Before discussing these receivers, we first introduce three importance performance measures in the next section.

2.4 Performance Measures

There are four important performance measures to indicate whether the specified CDMA receiver is good enough or not. These measures are asymptotic efficiency, near-far resistance, probability of bit error, and output SINR.

2.4.1 Asymptotic Efficiency

Asymptotic efficiency is a measure of the influence, which the interfering users have, on the bit error rate (BER) of the user of interest. A single user in the CDMA system with amplitude σ_k in an additive white Gaussian noise (AWGN) channel with BPSK modulation with noise variance σ_n^2 has a probability of bit error [45]:

$$P_k = Q\left(\frac{\sigma_k}{\sigma_n}\right) = Q\left(\sqrt{\frac{e_k}{\sigma_n^2}}\right) \tag{2.31}$$

where e_k is the energy of user k. With interferers the probability of error may increase. Define the effective energy $e_k(\sigma_n)$ as the energy that would be required for a single user in AWGN to achieve the BER that is observed in the presence of other users. Thus the efficiency is given by the ratio of the energy required in the multiuser system to the energy required in the single user system for the same BER performance.

$$\eta_k(\sigma_n) \equiv \frac{e_k(\sigma_n)}{\sigma_k^2} \tag{2.32}$$

24

The asymptotic efficiency is defined as the limit in the high SNR region:

$$\bar{\eta}_k = \lim_{\sigma_n \to 0} \frac{e_k(\sigma_n)}{\sigma_k^2} \tag{2.33}$$

The $\bar{\eta}_k$ lies between 0 and 1, with a value of 1 indicating that the user of interest is not affected at all by the presence of other users. The asymptotic efficiency of a conventional RAKE receiver was derived in [46]:

$$\bar{\eta}_k = \max \left\{ 0, 1 - \sum_{j \neq k} \frac{\sigma_j}{\sigma_k} |\mathbf{H}[j,k]| \right\} \tag{2.34}$$

where $\mathbf{H}[j,k]$ is the (j,k)th entry of matrix $\mathbf{H}$. The asymptotic efficiency of optimal multiuser receiver for a two-user system is given in [46]:

$$\bar{\eta}_1 = \min \left\{ 1, 1 + \left(\frac{\sigma_2}{\sigma_1} \right)^2 - 2 |\mathbf{H}[1,2]| \frac{\sigma_2}{\sigma_1} \right\} \tag{2.35}$$

2.4.2 Near-far Resistance

The near-far resistance quantifies the robustness of the receiver against unequal user power. Power inequality can cause a near-far effect whereby a weak user is swamped by interference from a strong user. The near-far resistance is defined as the worst case asymptotic efficiency measured over all relative user energies.

$$\tilde{\eta}_k \equiv \inf_{E_j > 0, j \neq k} \bar{\eta}_k \tag{2.36}$$

The near-far resistance of the conventional receiver is obtained as

$$\tilde{\eta}_k = \begin{cases} 1 & \text{if } \mathbf{H}[j,k] = 0, \ j \neq k \\ 0 & \text{otherwise} \end{cases} \tag{2.37}$$

That is, the conventional receiver is not near-far resistant unless the spreading sequences are orthogonal. The near-far resistance of the optimal multiuser receiver is given by

$$\tilde{\eta}_k = \begin{cases} \frac{1}{\mathbf{H}^+[k,k]} & \text{if the } k\text{th user signal is linearly independent} \\ 0 & \text{if } k\text{th user signal is in subspace spanned by other user} \end{cases} \tag{2.38}$$

where $\mathbf{H}^+$ is the Moore-Penrose generalized inverse of the normalized crosscorrelation matrix $\mathbf{H}$ [14], which is equivalent to the inverse if $\mathbf{H}$ is nonsingular. In the two-user case, the near-far resistance of user 1 is given by [13]

$$\tilde{\eta}_1 = 1 - \mathbf{H}[1,2]^2 \tag{2.39}$$

and similar representation for user 2 too, implying that the receiver is near-far resistant unless the spreading codes are linearly dependent.

2.4.3 Probability of Bit Error

The ultimate goal in most communication systems is to achieve low probability of bit error, i.e., low bit error rate (BER). For a conventional RAKE receiver, the BER can be expressed as

$$P_k = \frac{1}{2^{KI-1}} \sum_{\mathbf{b}(i) \in \{-1,1\}^{KI}, \mathbf{b}(i)[k]=-1} Q\left(\frac{\sigma_k - \sum_{j \neq k} \sigma_j \mathbf{H}[k,j] \mathbf{b}(i)[j]}{\sigma_n} \right) \tag{2.40}$$

This is simply the sum of the Gaussian tail probabilities for each possible choices of transmitted bit vector $\mathbf{b}(i)$ from $\{-1,1\}^{KI}$ conditioned on that the associated bit on the kth entry of $\mathbf{b}(i)$, denoted as $\mathbf{b}(i)[k]$, equals to -1. Equal probability of each user transmitting a 1 or -1 is assumed. There is no closed form expression for the optimal multiuser detection. For most of the cases, we refer to the processing window of the conventional RAKE receiver as one symbol interval, i.e., $I = 1$. Then the notation of $\mathbf{b}(i)[k]$ simply means the transmitted bit symbol of the kth user $b_k(i)$.
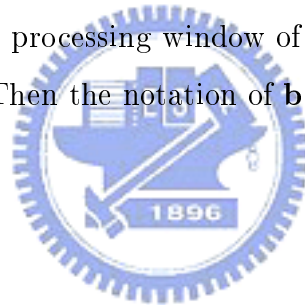
2.4.4 Output SINR

The output SINR is an important quantity that indicates the goodness of CDMA receivers. It is denoted as SINR_o (in dB) and calculated by

$$\text{SINR}_o = 10\log_{10} \frac{\text{Total Power of SOI's}}{\text{Total Power of INT's + Noise Power}}$$

For the case of two-user synchronous CDMA systems, the output SINR of user 1 is given by [13]

$$\text{SINR}_o = \frac{\sigma_1^2}{\sigma_2^2 \mathbf{H}[1,2]^2 + \sigma_n^2} \tag{2.41}$$

2.5 Linear Multiuser Receivers

As seen from the previous section, the optimal multiuser detection algorithm has a prohibitive computational complexity. In this section, we develop the alternative linear

multiuser receivers. It is assumed that the receivers have the knowledge of the spreading codes and the channel parameters of all users. This is a major distinction from linear single-user CDMA receivers, which have only the knowledge or utilization of the desired user information.

For linear multiuser detectors, a linear transformation is applied to the matched filter bank output vector $\mathbf{y}(i)$ in (2.18), known as the sufficient statistics vector in [28]. Then a local decision mechanism is applied on the transformed data vector to demodulate all the bit symbols simultaneously. The criterion of demodulation is given by

$$
\begin{aligned}
\hat{\mathbf{b}}(i) & = \text{sign}\left\{\mathcal{R}\left(\mathbf{T}^H \mathbf{y}(i)\right)\right\} \\
& = \text{sign}\left\{\mathcal{R}\left(\mathbf{T}^H \mathbf{H} \mathbf{A} \mathbf{b}(i) + \mathbf{T}^H \bar{\mathbf{n}}(i)\right)\right\}
\end{aligned} \tag{2.42}
$$

where $\mathbf{T}$ is a complex matrix with dimension $KI \times KI$. For the conventional single-user receiver, the transformation matrix is an identity matrix such that $\mathbf{T} = \mathbf{I}$. Assume that the decision is under Gaussian white noise condition, the BER of linear multiuser detector is given by

$$
\begin{aligned}
P_k & = P\left[\hat{\mathbf{b}}[k] = 1 \,\big|\, \mathbf{b}[k] = -1\right] \\
& = P\left[\left(\mathbf{T}^H \mathbf{H} \mathbf{A} \mathbf{b} + \mathbf{T}^H \bar{\mathbf{n}}\right)[k] > 0 \,\big|\, \mathbf{b}[k] = -1\right] \\
& = P\left[\left(\mathbf{T}^H \bar{\mathbf{n}}\right)[k] > \left(\mathbf{T}^H \mathbf{H} \mathbf{A}\right)[k,k] - \sum_{j \neq k}\left(\mathbf{T}^H \mathbf{H} \mathbf{A}\right)[k,j]\mathbf{b}[j]\right] \\
& = \frac{1}{2^{KI-1}} \sum_{\substack{\mathbf{b} \in \{-1,1\}^{KI} \\ \mathbf{b}[k]=-1}} P\left[\left(\mathbf{T}^H \bar{\mathbf{n}}\right)[k] > \left(\mathbf{T}^H \mathbf{H} \mathbf{A}\right)[k,k] - \sum_{j \neq k}\left(\mathbf{T}^H \mathbf{H} \mathbf{A}\right)[k,j]\mathbf{b}[j]\right] \tag{2.43}
\end{aligned}
$$

where we use the fact that the random variable $(\mathbf{T}^H \bar{\mathbf{n}})[k]$ is Gaussian with zero mean and variance equal to $(\mathbf{T}^H \mathbf{H} \mathbf{A} \mathbf{T})[k,k]\sigma_n^2$. The sum in (2.43) can be simplified as $\sigma_n \to 0$ in the following equation:

$$
P_k = \frac{1}{2^{KI-1}} Q\left(\left(\left(\mathbf{T}^H \mathbf{H} \mathbf{A}\right)[k,k] - \sum_{j \neq k}\left(\mathbf{T}^H \mathbf{H} \mathbf{A}\right)[k,j]\right)\bigg/ \sigma_n\sqrt{\left(\mathbf{T}^H \mathbf{H} \mathbf{A} \mathbf{T}\right)[k,k]}\right) \tag{2.44}
$$

Hence, according to (2.32), the asymptotic multiuser efficiency achieved by the linear transformation is

$$
\eta_k = \frac{\left(\left(\mathbf{T}^H \mathbf{H} \mathbf{A}\right)[k,k] - \sum_{j \neq k}\left|\mathbf{T}^H \mathbf{H} \mathbf{A}\right|[k,j]\right)}{\sqrt{\left(\mathbf{T}^H \mathbf{H} \mathbf{A} \mathbf{T}\right)[k,k]}} \tag{2.45}
$$

2.5.1 Decorrelating Multiuser Receivers

The decorrelating receivers are designed to recover the transmitted bits error-free in the absence of noise without requiring knowledge of the users' received amplitudes. Assume that the crosscorrelation matrix $\mathbf{H}$ in (2.18) is invertible. If we multiply the matched filter bank output vector $\mathbf{y}$ by $\mathbf{H}^{-1}$, i.e., $\mathbf{T}^H = \mathbf{H}^{-1}$, then

$$\mathbf{H}^{-1}\mathbf{y}(i) = \mathbf{H}^{-1}\mathbf{H}\mathbf{A}\mathbf{b}(i) + \mathbf{H}^{-1}\bar{\mathbf{n}}(i) = \mathbf{A}\mathbf{b}(i) + \mathbf{H}^{-1}\bar{\mathbf{n}}(i) \tag{2.46}$$

So we can simply take the sign of each of the components in (2.46) to decide the bit symbols of the transmitted data:

$$\hat{\mathbf{b}}[k] = \mathrm{sign}\left\{(\mathbf{H}^{-1}\mathbf{y})[k]\right\} = \mathrm{sign}\left\{(\mathbf{A}\mathbf{b})[k]\right\} = \mathbf{b}[k] \tag{2.47}$$

We come to a conclusion if the spreading sequences are linearly independent, then the detector in (2.47) achieves perfect demodulation for all users. For the decorrelating receiver, the signature sequences spanned over an I-symbol interval for different users are linearly independent. The interferences can be cancelled completely. This is why the detector is called "decorrelating receiver". The output of the decorrelating receiver has only two components: one due to the SOI, assumed user k, which is equal to $\sigma_k b_k$, and the other due to the background noise, which is Gaussian with zero mean and covariance matrix $\sigma_n^2 \mathbf{A}\mathbf{H}^{-1}$. Consequently, the BER of user k can be derived by replacing $\mathbf{T}^H$ as $\mathbf{H}^{-1}$ in (2.44):

$$
\begin{aligned}
P_k^d(\sigma_n) &= Q\left(\frac{\sigma_k}{\sigma_n\sqrt{\mathbf{H}^+[k,k]}}\right) \\
&= Q\left(\frac{\sigma_k}{\sigma_n}\sqrt{1 - \mathbf{v}_k^T \mathbf{H}_k^{-1}\mathbf{v}_k}\right)
\end{aligned}
\tag{2.48}
$$

The BER is shown to be independent of the interferers' amplitudes. The $\mathbf{v}_k$ is the kth column of $\mathbf{H}$ without the diagonal entries, and $\mathbf{H}_k$ is the $(K-1) \times (K-1)$ matrix that results by striking out the kth row and the kth column from $\mathbf{H}$. Substituting (2.48) into (2.33) the asymptotic efficiency can then be obtained as follows:

$$\bar{\eta}_d = \frac{1}{\mathbf{H}^+[k,k]} \tag{2.49}$$

As depicted in (2.48), the kth user's BER depends only on the SOI's amplitude as does the asymptotic efficiency in (2.49), so the decorrelating receiver is near-far resistant.

2.5.2 Linear MMSE Multiuser Receivers

The linear MMSE receivers are derived by minimizing the MSE between the transmitted data bits $\mathbf{A}\mathbf{b}(i)$ and the linear transformation of matched filter bank output vector, $\mathbf{y}(i)$, by the transformation matrix $\mathbf{T}$. The criterion of MMSE is given by

$$\min_{\mathbf{T} \in \mathcal{C}^{KI \times KI}} E\left\{ \left\| \mathbf{A}\mathbf{b}(i) - \mathbf{T}^H \mathbf{y}(i) \right\| \right\} \tag{2.50}$$

The solution to the optimization problem in (2.50) [11, 47, 48] is given by

$$\mathbf{T}^H = \left(\mathbf{H} + \sigma_n \mathbf{A}^{-2} \right)^{-1} \tag{2.51}$$

The MMSE detectors will converge to the decorrelating detectors for the background noise $\sigma_n \rightarrow 0$. Thus in this case, its asymptotic efficiency and near-far resistance are the same as those of the decorrelating detectors:

$$\bar{\eta}_m = \frac{1}{\mathbf{H}^+[k, k]} \tag{2.52}$$

If the decision statistics of the MMSE receiver is not Gaussian, but is a sum of Gaussian random variables (due to the background noise) and a binomial random variable (due to the MAI), then the analysis of BER is not as straightforward as that of the decorrelating detector.

For the synchronous case considered, the first element of the output of the linear MMSE transformation in (2.51) can be written as [11]

$$(\mathbf{T}^H \mathbf{y})[1] = \left(\left(\mathbf{H} + \sigma_n \mathbf{A}^{-2} \right)^{-1} \mathbf{y} \right)[1] = \kappa_1 \left(b_1 + \sum_{k=2}^{K} \beta_k b_k \right) + \sigma_n \tilde{n}_1 \tag{2.53}$$

where

$$\beta_k = \frac{\kappa_k}{\kappa_1}$$

$$\kappa_k = \sigma_k \left((\mathbf{H} + \sigma_n^2 \mathbf{A}^{-2})^{-1} \mathbf{H} \right)[1, k]$$

$$\tilde{n}_1 \sim \mathcal{N}\left(0, \mathbf{T}^H \mathbf{H} \mathbf{T}[1, 1] \right)$$

The "leakage coefficient" β_k quantifies the contribution of the kth interferer to the decision statistic, relative to contribution of the desired user. The BER readily follows

$$P_1^m(\sigma_n) = \frac{1}{2^{K-1}} \sum_{b_2, \cdots, b_K \in \{-1, 1\}^{K-1}} Q\left(\frac{\sigma_1 (\mathbf{T}^H \mathbf{H})[1, 1]}{\sigma_n \sqrt{(\mathbf{T}^H \mathbf{H} \mathbf{T})[1, 1]}} \left(1 + \sum_{k=2}^{K} \beta_k b_k \right) \right) \tag{2.54}$$

29

In the high SNR and low SINR environment, i.e., MAI is dominant, the MMSE receiver acts like the decorrelating detector. And for the low SNR and high SINR case, i.e., background noise is dominant, the MMSE receiver acts like the conventional RAKE receiver.

2.6   Linear Single-User Receivers

It is noted in previous sections that the optimal ML receiver has a prohibitive computational complexity for practical implementation. The suboptimal receivers of multiuser detection, with less complexity, require the knowledge of the spreading sequences of all users, accurate estimates of the phase, timing, and, in some cases, amplitudes. Accurate estimation of all of these channel parameters are almost impossible to achieve, and often, a slight loss in accuracy can result in a large degradation of the performance of these receivers [49, 50]. When the receiver is intended for a mobile unit, not only the computational complexity of multiuser detectors, but also the lack of knowledge of the spreading sequences of all of the users precludes their use. The linear single-user receivers require knowledge of only the desired user's spreading sequence. Although initial code synchronization is necessary, the timing accuracy requirement is not stringent. The chief advantage of linear single-user receivers is the case with which they can be implemented adaptively easily.

Considering the equation in (2.7), rewrite the equation with the assumption that the processing window is over the duration of the bit symbol of interest. This is a reasonable assumption for single-user detection given only the knowledge of the SOI.

$$
\begin{aligned}
\mathbf{x}(i) &= [x(0), x(1), \cdots, x(N + L - 2)]^T \\
&= \sum_{k=1}^{K} \sigma_k \sum_{l=1}^{L} \alpha_{k,l} \mathbf{c}_{k,l} b_k(i) + \mathbf{n}(i) \\
&= \mathbf{h}_1 b_1(i) + \sum_{k=2}^{K} \mathbf{h}_k b_k(i) + \mathbf{n}(i) \\
&= \mathbf{d}_s(i) + \mathbf{i}(i) + \mathbf{n}(i)
\end{aligned}
\tag{2.55}
$$

where $\mathbf{d}_s(i)$ is the signal, $\mathbf{i}(i)$ is interference, and $\mathbf{n}(i)$ is Gaussian noise vector. $\mathbf{c}_{k,l}$ is the augmented signature vector associated with the lth path of user k, given by the lth column of $\mathbf{C}_k$, defined in (2.11), and $\mathbf{h}_k$ is the effective composite signature vector (CSV) of user k

given by

$$\mathbf{h}_k = \sum_{l=1}^{L} \alpha_{k,l} \mathbf{c}_{k,l} \tag{2.56}$$

A linear single user detector weights and sums the sampled data vector to produce the output statistics from which a symbol decision is made. That is,

$$y_{SU}(i) = \mathbf{s}^H \mathbf{x}(i) \tag{2.57}$$

where $\mathbf{s}$ is the weight vector. In BPSK systems, a bit decision is made according to

$$\hat{b}_1(i) = \text{sign}\{y_{SU}(i)\} \tag{2.58}$$

There are two scalar indices often used to measure the performance of communication receivers. They are the output SINR and BER. The output SINR is defined to be the energy in the decision statistic due to the desired signal divided by the energy due to the interference-plus-noise. With the assumption of independence among all transmitted signals and noise, the output SINR is given by

$$\text{SINR}_o = \frac{\left|\mathbf{s}^H \mathbf{h}_1\right|^2}{\left|\sum_{k=2}^{K} \mathbf{s}^H \mathbf{h}_k \mathbf{h}_k \mathbf{s}^H + \sigma_n^2 \mathbf{s}^H \mathbf{s}\right|} \tag{2.59}$$

The BER is determined by the receiver output signal-to-noise ratio and the Euclidean distance between the receiver output and the decision boundary:

$$
\begin{aligned}
P_1 &= E\left\{P\left(y_{SU}(i) > 0 \,|\, b_1(i) = -1\right)\right\} \\
&= \sum_{\mathbf{b}(i) \in \{-1,1\}^K, b_1(i)=-1} P\left(y_{SU}(i) > 0 \,|\, \mathbf{b}(i)\right) P\left(\mathbf{b}(i) \,|\, b_1(i) = -1\right) \\
&= Q\left(\frac{\mathbf{s}^H \mathbf{h}_1 + \sum_{k=2}^{K} \mathbf{s}^H \mathbf{h}_k b_k(i)}{\sigma_n \left(\mathbf{s}^H \mathbf{s}\right)^{1/2}}\right)
\end{aligned}
\tag{2.60}
$$

2.6.1 Decorrelating Single-User Receivers

As the decorrelating multiuser detection, the decorrelating single-user receiver is designed such that, in the absence of noise, the detector output perfectly recovers the transmitted signal. It is clear that the $\mathbf{s}_z$ is the solution of decorrelating receiver only if it satisfies

$$\mathbf{s}_z^H \left[\begin{array}{cccc} \mathbf{h}_1 & \mathbf{h}_2 & \cdots & \mathbf{h}_K \end{array}\right] = \left[\begin{array}{cccc} 1 & 0 & \cdots & 0 \end{array}\right] \tag{2.61}$$

Let $\mathbf{H}_I$ denote the $(N + L - 1) \times (K - 1)$ matrix with columns given by $\mathbf{h}_2, \cdots, \mathbf{h}_K$ such that $\mathbf{H}_I = [\mathbf{h}_2, \mathbf{h}_3, \cdots, \mathbf{h}_k]$. The interference subspace, denoted as $\mathbf{S}_I$, is the subspace spanned by $\mathbf{h}_2, \cdots, \mathbf{h}_K$. The orthogonal projection component of $\mathbf{h}_1$ onto the interference subspace $\mathbf{S}_I$ is given by

$$\mathbf{h}_1^\perp = \mathbf{h}_1 - \mathbf{H}_I (\mathbf{H}_I^H \mathbf{H}_I)^{-1} (\mathbf{H}_I^H \mathbf{h}_1) \tag{2.62}$$

and the linear decorrelating solution was derived in [51], given by:

$$\begin{aligned} \mathbf{s}_z &= \mathbf{h}_1^\perp / \tilde{\eta}_z \\ &= \frac{1}{\tilde{\eta}_z} \left(\mathbf{I} - \mathbf{H}_I (\mathbf{H}_I^H \mathbf{H}_I)^{-1} \mathbf{H}_I^H \right) \mathbf{h}_1 \end{aligned} \tag{2.63}$$

where the scale factor $1/\tilde{\eta}_z$ is selected for $\left| \mathbf{s}_z^H \mathbf{h}_1 \right| = 1$. The quantity $\tilde{\eta}_z$ is known as the near-far resistance. It is easily shown that $(\mathbf{h}_1^\perp)^H \mathbf{h}_1 = \left\| \mathbf{h}_1^\perp \right\|^2$, so that $\tilde{\eta}_z = \left\| \mathbf{h}_1^\perp \right\|^2$. Schematically, interference suppression by a linear decorrelating detector is illustrated in Figure 2.3.

2.6.2 Linear MMSE Single-User Receivers

The linear MMSE single-user receiver minimizes the mean squared error between the decision statistic and the desired signal bit symbol only. The MMSE solution is given by

$$\mathbf{s}_{mmse} = \mathbf{R}_x^{-1} \mathbf{h}_1 \tag{2.64}$$

where

$$\mathbf{R}_x = E\{\mathbf{x}(i)\mathbf{x}(i)^H\} = \mathbf{R}_s + \mathbf{R}_{in} = \mathbf{R}_s + \mathbf{R}_i + \mathbf{R}_n \tag{2.65}$$

and $\mathbf{R}_s = E\{\mathbf{d}_s(i)\mathbf{d}_s(i)^H\} = \mathbf{h}_1 \mathbf{h}_1^H$, $\mathbf{R}_{in} = \mathbf{R}_i + \mathbf{R}_n$, $\mathbf{R}_i = E\{\mathbf{i}(i)\mathbf{i}(i)^H\}$, and $\mathbf{R}_n = E\{\mathbf{n}(i)\mathbf{n}(i)^H\}$.

If only one signal exists, $\mathbf{R}_x = \mathbf{h}_1 \mathbf{h}_1^H + \sigma_n^2$. Using the matrix inversion lemma, we have

$$\mathbf{R}_x^{-1} = \frac{1}{\sigma_n^2} \left(\mathbf{I} - \frac{\mathbf{h}_1 \mathbf{h}_1^H}{\sigma_n^2 + \|\mathbf{h}_1\|^2} \right) \tag{2.66}$$

In case of K orthogonal interference sources, successive application of the matrix inversion lemma to $\mathbf{h}_1, \mathbf{h}_2, \cdots, \mathbf{h}_K$ yields:

$$\begin{aligned} \mathbf{R}_x^{-1} &= \mathbf{R}_{in}^{-1} - \frac{\mathbf{R}_{in}^{-1} \mathbf{h}_1 \mathbf{h}_1^H \mathbf{R}_{in}^{-1}}{1 + \mathbf{h}_1^H \mathbf{R}_{in}^{-1} \mathbf{h}_1} \\ &= \frac{1}{\sigma_n^2} \left(\mathbf{I} - \mathbf{H}_I \left(\mathbf{H}_I^H \mathbf{H}_I + \sigma_n^2 \right)^{-1} \mathbf{H}_I^H \right) \mathbf{h}_1 \end{aligned} \tag{2.67}$$

Then the optimal weight vector can be written as

$$\mathbf{s}_{mmse} = \frac{1}{\sigma_n^2} \left(\mathbf{I} - \mathbf{H}_I \left(\mathbf{H}_I^H \mathbf{H}_I + \sigma_n^2 \mathbf{I} \right)^{-1} \mathbf{H}_I^H \right) \mathbf{h}_1 \tag{2.68}$$

As we compare the solution of the decorrelating detector in (2.63) to the one in (2.68), we find that the decorrelating detector is a scaled version of the MMSE detector when free of white noise, $\sigma_n^2 = 0$, or in very high SNR environment. When white noise is present, the MMSE receiver maximizes the output SINR. In particular, the MMSE solution is well-defined even when the decorrelating detection solution does not exist.

If the interferers' amplitudes are such that $\|\mathbf{h}_k\| = \sigma_k \to \infty$, it is easily seen that $\mathbf{s}_{mmse}^H \mathbf{h}_k \to 0$. Otherwise, we have the condition $\left\| \mathbf{s}_{mmse}^H \mathbf{h}_k \right\|^2 > \varepsilon \sigma_k^2 > 0$, where $\varepsilon \geq 0$ is arbitrary positive number, which is the contribution to the MSE from user k. As $\sigma_k^2 \to \infty$, the MSE $\to \infty$, which contradicts the condition MSE ≤ 1 (i.e., $\mathbf{s}_{mmse} = 0$ gives MSE=1). In fact, it can be shown that

$$\lim_{\|\mathbf{h}_k\| \to \infty} \left| \mathbf{s}_{mmse}^H \mathbf{h}_k \right| = 0 \tag{2.69}$$

which implies that as $\|\mathbf{h}_k\| = \sigma_k \to \infty$, the contribution to the MSE from user k diminishes to zero [15, 52]. To generalize (2.69), if $\|\mathbf{h}_k\| = \sigma_k \to \infty$ for all k, $k \neq 1$, then clearly $\mathbf{s}_{mmse} = \xi \mathbf{h}_1^\perp$, where ξ is a constant. Minimization of MSE by selecting ξ gives $\xi = \frac{1}{\tilde{\eta}_z + \sigma_n^2}$. We therefore conclude that as the interfering amplitudes $\|\mathbf{h}_k\| = \sigma_k \to \infty$, $k \neq 1$, we have

$$\mathbf{s}_{mmse} = \frac{\mathbf{h}_1^\perp}{\tilde{\eta}_z + \sigma_n^2} \tag{2.70}$$

and the MMSE becomes

$$\text{MMSE} = \frac{\sigma_n^2}{\tilde{\eta}_z + \sigma_n^2} \tag{2.71}$$

In addition to MMSE, the output SINR is

$$\text{SINR}_o = \frac{\mathbf{s}_{mmse}^H \mathbf{h}_1}{\sum\limits_{k=2}^{K} \mathbf{s}_{mmse}^H \mathbf{h}_k + \sigma_n^2 \|\mathbf{s}_{mmse}\|^2} \tag{2.72}$$

The bit error probability in (2.60) is also given by

$$P_1 = Q \left(\frac{\mathbf{s}_{mmse}^H \mathbf{h}_1 + \sum\limits_{k=2}^{K} \mathbf{s}_{mmse}^H \mathbf{h}_k b_k}{\sigma_n \|\mathbf{s}_{mmse}\|} \right) \tag{2.73}$$

The asymptotic efficiency of the MMSE detector, given that the interfering amplitude $\|\mathbf{h}_k\| \to \infty$ for the worst case and $\sigma_n^2 \to 0$, is therefore $\|\mathbf{h}_1\|^2$. That is, the near-far resistance of the MMSE receiver considered is the squared norm of the component of the desired signal vector that is orthogonal to the subspace spanned by the interference vectors.

2.6.3 Minimum Output Energy Receivers

An alternative approach to the above is to suppress the interference by minimizing the power of the receiver output $\|y_{SU}\|^2$ [18, 34], employing a single linear constraint constructed from the knowledge of the desired user's CSV, denotes as $\mathbf{h}_1$. The minimum output energy (MOE) optimization can be expressed as

$$\min_{\mathbf{s}} \quad \|y_{SU}(i)\|^2 = \left\|\mathbf{s}^H\mathbf{x}(i)\right\|^2 = \mathbf{s}^H\mathbf{R}_x\mathbf{s}$$
$$\text{subject to: } \mathbf{s}^H\mathbf{h}_1 = 1 \tag{2.74}$$

The optimal weight vector is given by

$$\mathbf{s}_{moe} = \left(\frac{1}{\mathbf{h}_1^H\mathbf{R}_x^{-1}\mathbf{h}_1}\right)\mathbf{R}_x^{-1}\mathbf{h}_1 \tag{2.75}$$

and the MOE at the optimal point becomes

$$\text{MOE}\left(\mathbf{h}_1\right) = \mathbf{s}_{moe}^H\mathbf{R}_x\mathbf{s}_{moe} = \frac{1}{\mathbf{h}_1^H\mathbf{R}_x^{-1}\mathbf{h}_1} \tag{2.76}$$

The MOE detector is a scaled version of the MMSE detector. Since scaling doesn't affect the output SINR, MOE has the same optimal performance as MMSE when the CSV of the desired user is accurately estimated. Unfortunately, the CSV is generally unavailable to the receiver or become inaccurate in the multipath environment, and the constrained optimization methods are known to be very sensitive to signature mismatch due to the signal cancellation effect [18]. Hence special care needs to be taken when multipaths are

present [53]. The CSV, $\mathbf{h}_1$, from (2.55) can be derived as

$$\mathbf{h}_1 = \begin{bmatrix} c_{1,1}[0] & 0 & \cdots & 0 \\ \vdots & c_{1,2}[0] & \ddots & \vdots \\ c_{1,1}[N-1] & \vdots & \ddots & 0 \\ 0 & c_{1,2}[N-1] & \ddots & c_{1,L}[0] \\ \vdots & \vdots & \ddots & \vdots \\ 0 & 0 & \cdots & c_{1,L}[N-1] \end{bmatrix} \begin{bmatrix} \alpha_{1,1} \\ \alpha_{1,2} \\ \vdots \\ \alpha_{1,L} \end{bmatrix} = \mathbf{C}_1 \mathbf{f}_a \qquad (2.77)$$

where the multipath fading parameter vector $\mathbf{f}_a = [\alpha_{1,1}, \cdots, \alpha_{1,L}]^T$, are generally unknown. It was proposed in [23] that explicit estimation be avoided by employing the constraint $|\mathbf{s}^H \mathbf{h}| = 1$, where $\mathbf{h}$ is an unknown parameter vector that approximates $\mathbf{h}_1$.

MOE with Capon's Criterion

A procedure reminiscent to the Capon's estimation method was proposed for optimizing $\mathbf{h}$. This procedure consists of selecting $\mathbf{h}$ by the conditions that $\mathrm{MOE}(\mathbf{h})$ in (2.76) is maximized and the constraint $\|\mathbf{h}\| = 1$ is satisfied. If $\mathbf{h}$ is replaced by $\mathbf{h} = \mathbf{C}_1 \mathbf{f}$, where $\mathbf{f}$ is some parameter vector approximating $\mathbf{f}_a$, we get the following optimization problem:

$$\mathbf{f}_{Capon} = \arg \max_{\mathbf{h}=\mathbf{C}_1\mathbf{f}} \frac{\mathbf{h}^H \mathbf{h}}{\mathbf{h}^H \mathbf{R}_x^{-1} \mathbf{h}} = \arg \min_{\mathbf{f}} \frac{\mathbf{f}^H \mathbf{C}_1^H \mathbf{R}_x^{-1} \mathbf{C}_1 \mathbf{f}}{\mathbf{f}^H \mathbf{C}_1^H \mathbf{C}_1 \mathbf{f}} \qquad (2.78)$$

The solution to equation (2.78) is via the generalized eigenvalue decomposition involving the matrix pencil of $(\mathbf{C}_1^H \mathbf{R}_x^{-1} \mathbf{C}_1, \mathbf{C}_1^H \mathbf{C}_1)$.

MOE with A Single Arm

An alternative approach to MOE for handling the multipath case relies on extending the number of constraints. In [20], the weight vector $\mathbf{s}$ is constrained to satisfy $\mathbf{C}_1^H \mathbf{s} = [1, 0, \cdots, 0]^T$. In this way, the response of the SOI is constrained to

$$\mathbf{s}^H \mathbf{h} = \mathbf{s}^H \mathbf{C}_1 \mathbf{f} = [1, 0, \cdots, 0]^T \mathbf{f} = \alpha_{1,1} = \text{Constant} \qquad (2.79)$$

This method avoids the signal cancellation problem by forcing the response of delayed copies of the signal of interest to zero. By doing so however, the method doesn't exploit all the energy of the received signal.

We generalize the above constraints problem by selecting the weight vector $\mathbf{s}$ and a arbitrary parameter vector to satisfy the following general constraint:

$$\mathbf{C}_1^H \mathbf{s} = \mathbf{f} \tag{2.80}$$

where $\mathbf{f}$ is a general parameter vector arbitrarily chosen. The solution subject to (2.80) yields the optimum receiver with the minimum variance:

$$\mathbf{s}_{moe} = \mathbf{R}_x^{-1} \mathbf{C}_1 \left(\mathbf{C}_1^H \mathbf{R}_x^{-1} \mathbf{C}_1 \right)^{-1} \mathbf{f} \tag{2.81}$$

Substituting (2.81) into (2.59), the output SINR is given by

$$\text{SINR}(\mathbf{f}) = \frac{\left\| \mathbf{f}^H \left(\mathbf{C}_1^H \mathbf{R}_x^{-1} \mathbf{C}_1 \right)^{-1} \mathbf{C}_1^H \mathbf{R}_x^{-1} \mathbf{h}_1 \right\|^2}{\mathbf{f}^H \left(\mathbf{C}_1^H \mathbf{R}_x^{-1} \mathbf{C}_1 \right)^{-1} \mathbf{f} - \left\| \mathbf{f}^H \left(\mathbf{C}_1^H \mathbf{R}_x^{-1} \mathbf{C}_1 \right)^{-1} \mathbf{C}_1^H \mathbf{R}_x^{-1} \mathbf{h}_1 \right\|^2} \tag{2.82}$$

which after some manipulation, and using $\mathbf{h}_1 = \mathbf{C}_1 \mathbf{f}_a$ in (2.77), reduces to

$$\text{SINR}(\mathbf{f}) = \frac{1}{\frac{\mathbf{f}^H \left(\mathbf{C}_1^H \mathbf{R}_x^{-1} \mathbf{C}_1 \right)^{-1} \mathbf{f}}{\|\mathbf{f}^H \mathbf{f}_a\|^2} - 1} \tag{2.83}$$

It is well known that the MMSE receiver maximizes the SINR [54], hence generally, we expect that

$$\text{SINR}(\mathbf{f}) \leq \text{SINR}_{MMSE} \tag{2.84}$$

It is clear from (2.81) that if $\mathbf{f} = (\mathbf{C}_1^H \mathbf{R}_x^{-1} \mathbf{C}_1) \mathbf{f}_a$, then equality is achieved in (2.84) because $\mathbf{s}_{moe}$ is now identical to the MMSE receiver weight vector $\mathbf{R}_x^{-1} \mathbf{h}_1$.

MOE with Min/Max Criterion

An improvement was proposed in [23] where the channel parameters $\mathbf{f}$ are optimized by the min/max approach. In the first step, the constraints vector $\mathbf{f}$ is set as a dummy vector. Then, the linearly constrained minimum variance (LCMV) problem is solved:

$$\min_{\mathbf{s}} \quad J = \mathbf{s}^H \mathbf{R}_x \mathbf{s}$$
$$\text{subject to:} \quad \mathbf{C}_1^H \mathbf{s} = \mathbf{f} \tag{2.85}$$

36

For a given $\mathbf{f}$, the solution to this constrained optimization problem is obtained using the Lagrange multipliers [53]:

$$\mathbf{s}_{moe} = \mathbf{R}_x^{-1}\mathbf{C}_1\left(\mathbf{C}_1\mathbf{R}_x^{-1}\mathbf{C}_1\right)^{-1}\mathbf{f} \tag{2.86}$$

This minimization suppresses the output components from interference and noise. In the second step, the received output power J_{moe} is maximized over $\mathbf{f}$, assuming that the interference and noise output energies have already been suppressed in the first step:

$$J_{moe} = \max_{\|\mathbf{f}\|=1}\quad \mathbf{s}_{moe}^H\mathbf{R}_x\mathbf{s}_{moe} \tag{2.87}$$

Ideally, this maximization optimizes the output energy of the desired signal, which is achieved when the constraint parameter $\mathbf{f}$ matches to its optimal value. The optimized linearly constrained MOE receiver is given by sequential min/max optimization in step I (2.85) and II (2.87). By substituting $\mathbf{s}_{moe}$ in (2.86) into equation (2.87), this min/max problem is equivalent to solving

$$\max_{\mathbf{f}}\quad \frac{\mathbf{f}^H(\mathbf{C}_1^H\mathbf{R}_x^{-1}\mathbf{C}_1)^{-1}\mathbf{f}}{\mathbf{f}^H\mathbf{f}} \tag{2.88}$$

This cost function in (2.88) is a Rayleigh quotient and hence the solution to this optimization problem is the eigenvector of $(\mathbf{C}_1^H\mathbf{R}_x^{-1}\mathbf{C}_1)^{-1}$ corresponding to the maximum eigenvalue, or equivalently the minimum eigenvector of $(\mathbf{C}_1^H\mathbf{R}_x^{-1}\mathbf{C}_1)$.

It has been shown [23] that the performance of this MOE detector with variable constraints is close to that of the MMSE receiver at high SNR in the presence of multipaths. However, the computational complexity is higher than using fixed constraint parameters because it requires an extra eigenvalue decomposition.

2.6.4   Proposed GSC Receivers

Here an adaptive CDMA receiver with enhanced signal reception and interference rejection is proposed for multipath channels. The design of the receiver involves a two-stage procedure. First, an adaptive correlator bank is constructed in the form of generalized side-lobe canceller (GSC) to suppress strong interference. To reduce the complexity, the partially adaptive implementation is incorporated in the design of GSC blocking matrix. Next, a

maximum ratio combining of the correlator outputs is performed to constructively collect the multipath energy. Since strong MAI has been removed, channel estimation can be done accurately, leading to improved performance compared to the conventional RAKE receiver.

In order to restore the processing gain and retain the multipath diversity, the received vector, $\mathbf{x}(i)$, is despread for each path, or finger. Specifically, the output of the correlator at the lth finger is despread by $\mathbf{s}_l$ into

$$y_{1,l} = \mathbf{s}_l^H \mathbf{x}(i) = \mathbf{s}_l^H \mathbf{h}_1 b_1(i) + \mathbf{s}_l^H \mathbf{i}(i) + \mathbf{s}_l^H \mathbf{n}(i) \tag{2.89}$$

for $l = 1, \cdots, L$, where $\mathbf{s}_l$ is the weight vector at the lth finger. For an effective suppression of MAI, the weight vector can be determined in accordance with the LCMV criterion:

$$\min_{\mathbf{s}_l} \quad \mathbf{s}_l^H \mathbf{R}_x \mathbf{s}_l$$

$$\text{subject to: } \mathbf{c}_{1,l}^H \mathbf{s}_l = 1 \tag{2.90}$$

However, the adverse phenomenon of signal cancellation usually occurs with the solution in (2.90) due to the mismatch of signature vector. With such a mismatch present, the signal can be treated as an interference. That causes a very small gain for the signal. To avoid such signal cancellation, the LCMV correlators can be implemented with multiple constraints [34]. Another better alternative solution is suggested based on the GSC technique. The GSC is essentially an indirect but simpler implementation of the LCMV receiver. It is a widely used structure that allows a constrained adaptive algorithm to be implemented in an unconstrained fashion [55]. The concept of GSC is to decompose the weights into two orthogonal parts, written in $\mathbf{s}_l = \mathbf{c}_{1,l} - \mathbf{B}_c \mathbf{g}_l$, which is shown in Figure 2.4. The matrix $\mathbf{B}_c$ is a pre-designed signal "blocking matrix" which removes user 1's signal before filtering. The goal is then to choose the adaptive part of weight vector, $\mathbf{g}_l$, to cancel the interference in $\mathbf{x}(i)$. According to the GSC scheme, $\mathbf{g}_l$ is determined by the MMSE criterion:

$$\min_{\mathbf{g}_l} \quad E\{|\mathbf{c}_{1,l}^H \mathbf{x}(i) - \mathbf{g}_l^H \mathbf{B}_c^H \mathbf{x}(i)|^2\} \equiv \|\mathbf{R}_x^{1/2} \mathbf{B}_c \mathbf{g}_l - \mathbf{R}_x^{1/2} \mathbf{c}_{1,l}\|^2 \tag{2.91}$$

Since the signal has been removed in the lower branch by the signal blocking matrix $\mathbf{B}_c$, the only way to minimize the MSE is such that $\mathbf{g}_l$ performs a mutual cancellation of the MAI

between the upper and lower branches. Solving for $\mathbf{g}_l$ and substituting it in $\mathbf{s}_l = \mathbf{c}_{1,l} - \mathbf{B}_c\mathbf{g}_l$ gives

$$\mathbf{s}_l = \left[\mathbf{I} - \mathbf{B}_c(\mathbf{B}_c^H\mathbf{R}_x\mathbf{B}_c)^{-1}\mathbf{B}_c^H\mathbf{R}_x \right] \mathbf{c}_{1,l} \tag{2.92}$$

Note that $\mathbf{B}_c$ is designed to block signals from the entire delay spread in order to avoid signal cancellation. It can be chosen to be a full rank $(N + L - 1) \times (N - 1)$ matrix whose columns are orthogonal to $\{\mathbf{c}_{1,1}, \cdots, \mathbf{c}_{1,L}\}$, i.e., $\mathbf{B}_c^H\mathbf{C}_1 = \mathbf{0}$.

With the MAI suppressed by the adaptive GSC correlators, the next step is to perform a maximum ratio combining of the correlators' outputs to collect the multipath energy of the signal. It is assumed that, with the adaptive correlator processing, the dominant interference has been eliminated and the output data $\mathbf{y}_{1,l}(i)$, $l = 1, \cdots, L$, contains the signal and colored noise only. This suggests that the maximum ratio combining (MRC) criterion can be employed to collect these components coherently to extract $b_1(i)$. Let $\mathbf{f}_{mrc}$ be the $L \times 1$ weight vector that performs the combining:

$$z_o(i) = \mathbf{f}_{mrc}^H\mathbf{y}(i) \tag{2.93}$$

where

$$\mathbf{y}(i) = [y_{1,1}, y_{1,2}, \cdots, y_{1,L}]^T \tag{2.94}$$

is the output data vector of correlators within the ith symbol, and

$$\mathbf{n}_c = \left[\mathbf{s}_1^H\mathbf{n}(i), \mathbf{s}_2^H\mathbf{n}(i), \cdots, \mathbf{s}_L^H\mathbf{n}(i) \right]^T \tag{2.95}$$

The MRC weight vector can be determined blindly as the solution to the following problem [56]:

$$\max_{\mathbf{f}_{mrc}} \quad \frac{E\left\{ \left| \mathbf{f}_{mrc}^H\mathbf{y}_c \right|^2 \right\}}{E\left\{ \left| \mathbf{f}_{mrc}^H\mathbf{n}_c \right|^2 \right\}} \equiv \frac{\mathbf{f}_{mrc}^H\mathbf{R}_{\mathbf{y}_c}\mathbf{f}_{mrc}}{\mathbf{f}_{mrc}^H\mathbf{R}_{\mathbf{n}_c}\mathbf{f}_{mrc}} \tag{2.96}$$

where $\mathbf{R}_{\mathbf{y}_c} = E\left\{ \mathbf{y}_c(i)\mathbf{y}_c^H(i) \right\}$ and $\mathbf{R}_{\mathbf{n}_c} = E\left\{ \mathbf{n}_c(i)\mathbf{n}_c^H(i) \right\}$ are the output data and noise correlation matrices, respectively. The solution to (2.96) is well known to be the principal generalized eigenvector of $\{\mathbf{R}_{\mathbf{y}_c}, \mathbf{R}_{\mathbf{n}_c}\}$.

2.7 Simulation Results

In this section, we present simulation results that illustrate the performance of some of the CDMA receivers discussed in this chapter. All results are obtained based on the assumption that the processing gain is $N = 31$, and the interferers are asynchronous with $L = 4$ independent Rayleigh fading multipaths. The multipath delays are chosen uniformly from $[0 \sim 3T_c]$. Both the desired and interference signature sequences are Gold sequences [57]. The order of RAKE receiver is 4. As an indication of the goodness of these receivers, we define the output SINR (in dB) as a criterion:

$$\text{SINR}_o = 10 \log_{10} \frac{\text{Total Power of SOI's}}{\text{Total Power of INT's} + \text{Noise Power}} \tag{2.97}$$

and the input SNR (in dB) is defined as

$$\text{SNR}_i = 10 \log_{10} \frac{\sigma_i^2}{\sigma_n^2} \tag{2.98}$$

The NFR (in dB) is defined as the ratio of the MAI power to signal power before despreading:

$$\text{NFR} = 10 \log_{10} \frac{\sigma_k^2}{\sigma_1^2} \quad \text{and} \quad \sigma_2^2 = \sigma_3^2 = \cdots = \sigma_K^2 \quad \text{for} \ \ k = 1, \cdots, K$$

N_s symbols are used to obtain sample estimates of various correlation matrices. A total of 50 Monte-Carlo runs are executed to obtain an average value of SINR_o. Unless otherwise mentioned, the following "standard" parameters will be used throughout the section: $\text{SNR}_i =$ 0 dB, $N_s =$ 500, $L = 4$ fingers and processing gain $N = 31$.

In the first set simulations, the asymptotic efficiency is evaluated in the two-user scenario. The resulting output SINR curves with respect to the NFR are plotted in Figure 2.5. Obviously the asymptotic efficiency of the decorrelating multiuser receiver (ZF-MUD) described by (2.47) is nearly a constant, which is determined only by the crosscorrelation properties of signature sequences. The MMSE multiuser receiver (MMSE-MUD), as described by (2.51), acts similar to the conventional receiver in low NFR region and similar to the ZF-MUD in high NFR region. The conventional RAKE receiver works better than the ZF-MUD in the low NFR region. This is because that the ZF-MUD has the more significant noise enhancement phenomenon in that region.

In the second set of simulations, the BER performance of the linear multiuser detections is evaluated in the two-user scenario. The resulting BER curves with respect to the NFR are

plotted in Figure 2.6. Although the power of interference increases, the ZF-MUD remains constantly reliable. The MMSE-MUD outperforms the ZF-MUD with low NFR, but degrades quickly as the NFR increase.

In the third set of simulations, the system capacity is evaluated with different user numbers K. The resulting output SINR curves are plotted in Figure 2.7 for NFR = 0 dB and NFR = 20 dB. As observed, the conventional RAKE (C-RAKE) receiver totally fails with NFR = 20 dB and a large K due to the poor crosscorrelation properties among signature sequences. The linear MMSE receiver (MMSE-SU) described by (2.64) has the best of performance among these receivers. This is due to the aid of training signal and the large degree of freedom with N. The MOE receiver with the min/max criterion (MM-MOE) described in Section 2.6.3, and the proposed GSC receiver (G-RAKE) described in Section 2.6.4 have nearly the same performance of the MMSE receiver for NFR = 0 dB. As the NFR increases to 20 dB, the output SINR of the MOE degrades quickly. This is because that the MOE receiver relies largely on the estimation of CSV. Many strong MAI users will cause the channel mismatch more severe. The proposed GSC is better than the MOE, but is slightly worse than the training based MMSE-SU receiver.

In the fourth set of simulations, the near-far resistance of the proposed GSC receiver is evaluated with different NFR values. Figure 3in shows the results obtained with $K = 5$ and $K = 25$ users. As observed, the C-RAKE receiver fails again with $K = 25$. The MM-MOE, G-RAKE and MMSE-SU receivers achieves their excellent near-far resistant by successfully cancelling the MAI using the temporal degree of freedom (N: processing gain) with $K = 5$. For the case of large number of users $K = 25$, the output SINR of the MM-MOE receiver degrades quickly as the NFR increases. The MMSE-SU gives the best performance, in which case both channel estimation and MAI suppression can be done effectively. On the other hand, the proposed G-RAKE receiver has the same degree of freedom to suppress the MAI and is not sensitive to channel error. So the proposed G-RAKE receiver has the performance somehere between the MMSE-SU and MM-MOE.

41

2.8 Summary

A CDMA receiver model is introduced and a systematic overview of the linear multiuser and single-user CDMA receivers are outlined. Also, a GSC based receiver has been proposed for multipath environments. The proposed receiver can be operated without the aid of training signals. The only information required is the signature sequence, rough timing estimation. From simulation results, it is shown that the proposed blind receiver is near-far resistant, and performs reliably in an overloaded system.
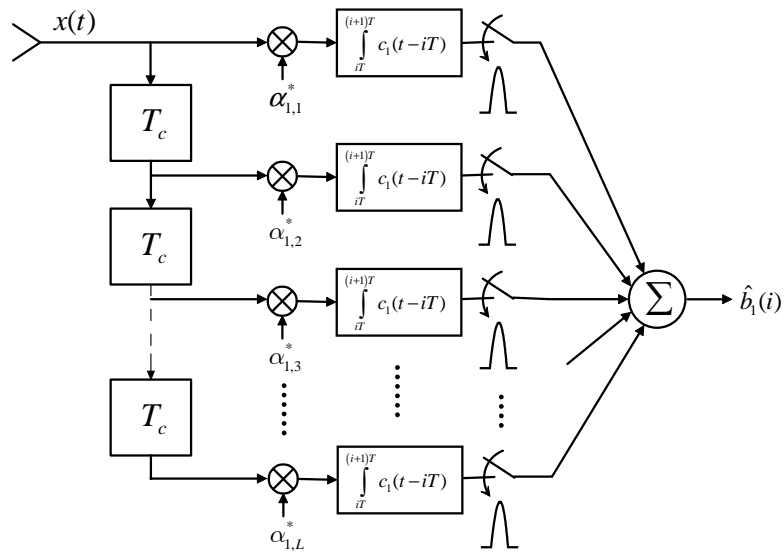
Figure 2.1: RAKE receiver for CDMA systems
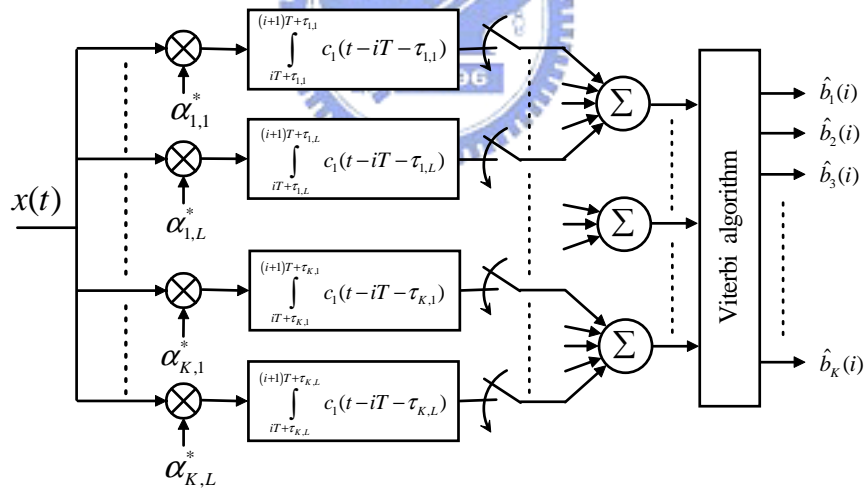
Figure 2.2: Maximum likelihood receiver for CDMA systems.
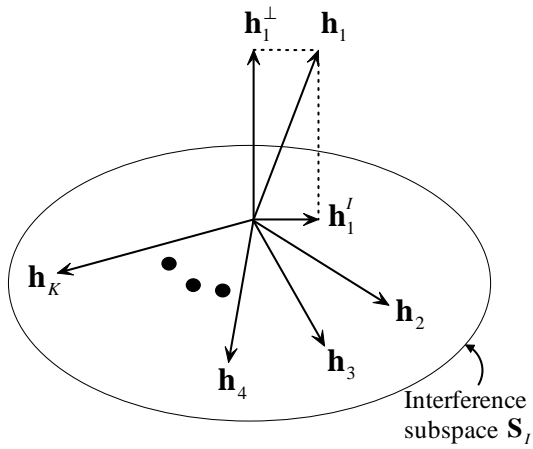
Figure 2.3: Scenario for decorrelating receivers.
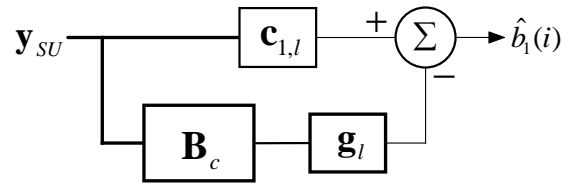
Figure 2.4: Structure of generalized sidelobe canceller.
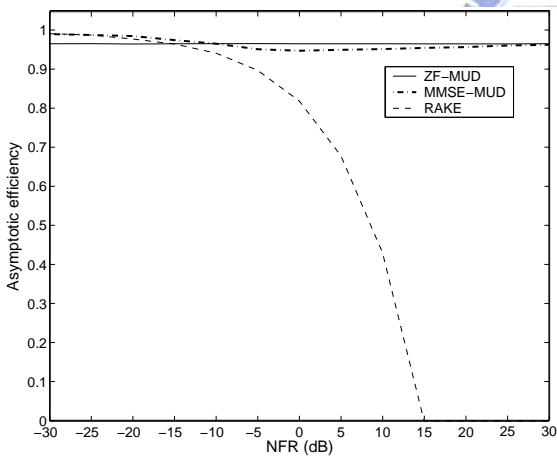
Figure 2.5: Evaluation of asymptotic efficiency with $K = 2$ and $\text{SNR}_i = 0$ dB.
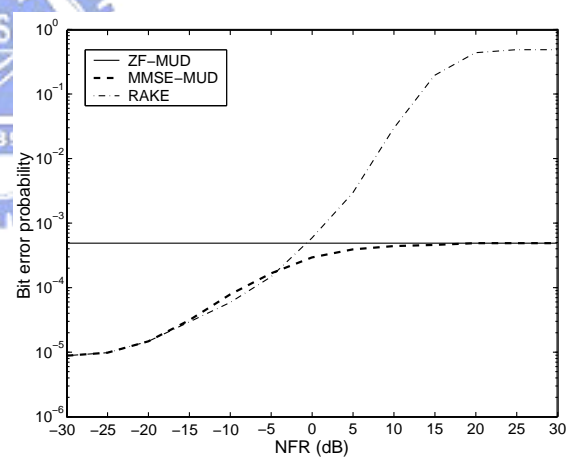
Figure 2.6: Evaluation of bit error probability with $K = 2$ and $\text{SNR}_i = 0$ dB.
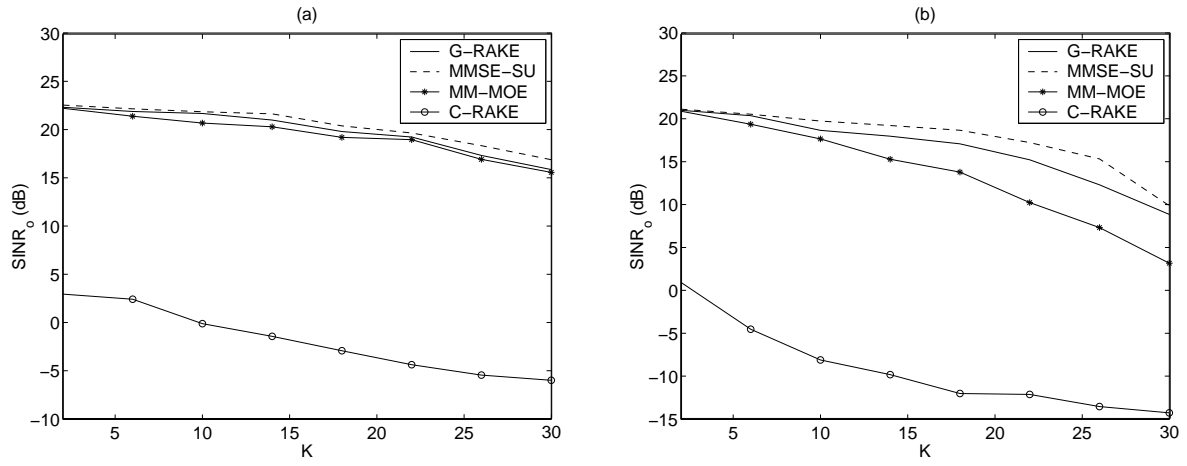
Figure 2.7: Output SINR versus number of users K, with (a) NFR = 0 dB and (b) NFR = 20 dB.
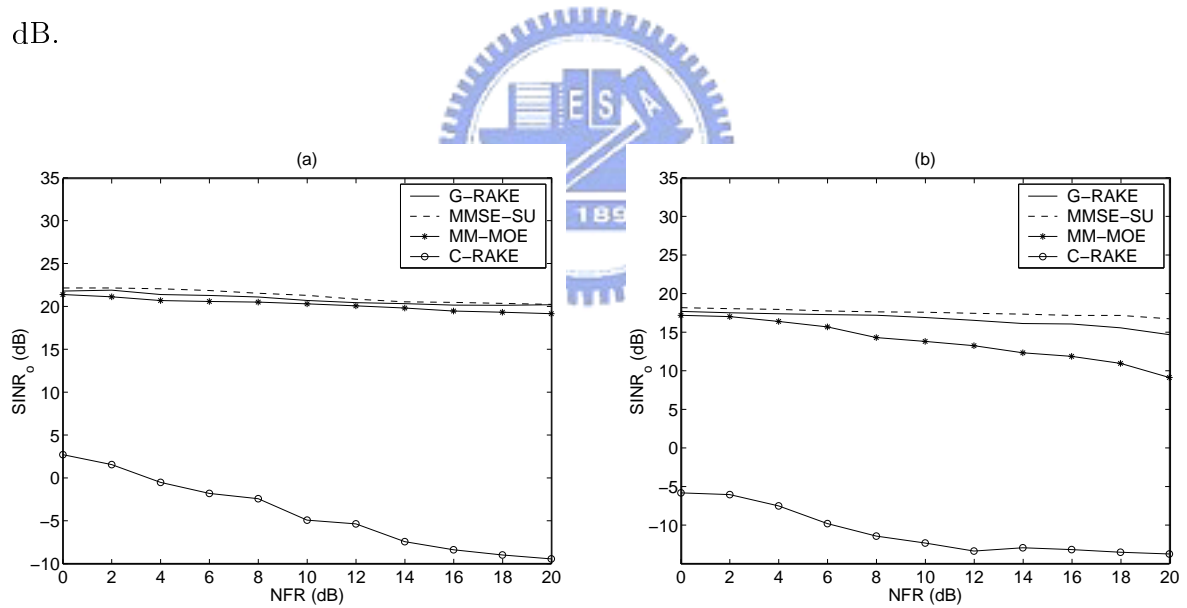
Figure 2.8: Output SINR versus near-far ratio NFR, with (a) $K = 5$ users and (b) $K = 25$ users.

Chapter 3

Space-Time Processing Techniques for CDMA Systems

As discussed in Chapter 2, signal processing in CDMA receivers include channel estimation of transmitted signal and suppression of MAI. One promising approach to improve signal processing performance is the space-time (ST) processing, which operates simultaneously on multiple antennas. A key leverage of this spatial dimension is MAI suppression. This suppression is possible since the MAI and the SOI almost always arrive at the antenna array (even in complex multipath environments) with distinct and often well-separated spatial signatures. This allows the receiver to exploit the difference to reduce the MAI. Likewise, the ST transmit processing can use spatial selectivity to deliver signals to the desired mobile while minimizing the interference to others. Filtering in the space domain can separate spectrally and temporally overlapping signals from multiple mobile units, which is referred to as space division multiple access (SDMA) [55, 58, 59, 60]. By exploiting the space domain via an adaptive antenna array, the operational benefits to the network operator were summarized as follows [61]:

- Capacity enhancement

- Coverage extension

- Increased immunity to near-far problem

- Ability to support hierarchical cell structure

In this chapter, we extend the discussion from time domain to ST domain by employing multiple antennas. Firstly, we develop the ST CDMA models in a similar way as Chapter 2 does for time domain. Then, we will derive different kinds of ST 2-D RAKE receivers for cellular DS/CDMA communication systems. The extension of conventional RAKE receiver into the 2-D RAKE receiver, a combination of the space domain (antenna array or diversity beams) and time domain (the RAKE receiver) only, is very important in the user-flooded communication environments.

3.1   Space-Time Data Model

Reconsider the DS/CDMA data model for a scenario in which the receiver of basestation is equipped with an antenna array of D elements. Assuming that each transmitter is equipped with a single antenna, the baseband multipath channel between the kth user's transmitter and the basestation receiver can be modeled as a single-input, multiple-output (SIMO) system. To develop the SIMO data model, firstly the received data at the dth antenna is written as

$$x_{(d)}(t) = \sum_{i=1}^{I} \sum_{k=1}^{K} \sum_{l=1}^{L} \sigma_k b_k(i) a_{kl,d} \alpha_{k,l} c_k(t - iT - \tau_{k,l}) + n_{(d)}(t) \tag{3.1}$$

The scheme of data model is shown in Figure 3.1. Following a chip matched filter, the discrete time complex baseband signal over a block of I symbols is given by

$$\mathbf{x}_{(d)}(i) = \mathbf{S}\tilde{\mathbf{F}}_{(d)}\mathbf{Ab}(i) + \mathbf{n}_{(d)}(i) \tag{3.2}$$

The equations (3.1) and (3.2) similar to the equations (2.5) and (2.6), which are developed in the single antenna CDMA system, except for a multiplying phase parameter $a_{kl,d}$. As developed in the previous chapter, we cascade the chip-sampled data over a block of I symbols at the dth antenna into a vector as

$$\mathbf{x}_{(d)}(i) = \left[\bar{\mathbf{x}}_{(d)}^T(i+1), \bar{\mathbf{x}}_{(d)}^T(i+2), \cdots, \bar{\mathbf{x}}_{(d)}^T(i+I) \right]_{NI \times 1}^T \tag{3.3}$$

where $\bar{\mathbf{x}}_{(d)}^T(i)$ is the chip-sampled data vector over the ith symbol duration denoted as

$$\bar{\mathbf{x}}_{(d)}^T(i) = \left[x_{(d)}(t)\big|_{t=(i-1)T+\frac{T_c}{2}}, \, x_{(d)}(t)\big|_{t=(i-1)T+T_c+\frac{T_c}{2}}, \cdots, x_{(d)}(t)\big|_{t=(i-1)T+NT_c-\frac{T_c}{2}} \right]_{N \times 1}^T \tag{3.4}$$

and $\mathbf{n}_{(d)}(i)$ is the chip-sampled white Gaussian noise vector over the I-symbol interval

$$\mathbf{n}_{(d)}(i) = \left[\bar{\mathbf{n}}_{(d)}^T(i+1), \bar{\mathbf{n}}_{(d)}^T(i+2), \cdots, \bar{\mathbf{n}}_{(d)}^T(i+I) \right]_{NI \times 1}^T \tag{3.5}$$

where $\bar{\mathbf{n}}_{(d)}^T(i)$ is the chip-sampled noise vector over the ith symbol duration denoted as

$$\bar{\mathbf{n}}_{(d)}^T(i) = \left[n_{(d)}(t)\Big|_{t=(i-1)T+\frac{T_c}{2}}, n_{(d)}(t)\Big|_{t=(i-1)T+T_c+\frac{T_c}{2}}, \cdots, n_{(d)}(t)\Big|_{t=(i-1)T+NT_c-\frac{T_c}{2}} \right]_{N \times 1}^T \tag{3.6}$$

In (3.2), $\mathbf{S}$, $\mathbf{A}$ and $\mathbf{b}$ are defined in (2.9), (2.14) and (2.16) in Chapter 2. The $\tilde{\mathbf{F}}_{(d)}$ is defined as

$$\tilde{\mathbf{F}}_{(d)} = \mathrm{diag}\left[\phi_{(d)}(i+1), \phi_{(d)}(i+2), \cdots, \phi_{(d)}(i+I) \right] \mathbf{F} \tag{3.7}$$

where

$$\phi_{(d)}(i) = \mathrm{diag}\left[a_{11,d}, \cdots, a_{1L,d}, \cdots, a_{K1,d}, \cdots, a_{KL,d} \right]_{KL \times KL} \tag{3.8}$$

for $i = 1, \cdots, I$, $\mathbf{F}$ is the channel fading matrix defined in (2.12), and $a_{kl,d}$ is the phase of the kth user associated with the lth path at the dth antenna element.

Stacking the received data at the D antennas gives

$$\mathbf{x}_{ST}(i) = \left[\mathbf{x}_{(1)}^T(i), \mathbf{x}_{(2)}^T(i), \cdots, \mathbf{x}_{(D)}^T(i) \right]_{NID \times 1}^T \tag{3.9}$$

which, in matrix form, is

$$\mathbf{x}_{ST}(i) = \tilde{\mathbf{S}}\tilde{\mathbf{F}}\mathbf{A}\mathbf{b}(i) + \mathbf{n}_{ST}(i) \tag{3.10}$$

where $\tilde{\mathbf{S}}$ is the $NID \times KLID$ block Toeplitz signature matrix with diagonal blocks $\mathbf{S}_{(d)} = \mathbf{S}$, for $d = 1, \cdots, D$, $\mathbf{S}$ is defined in (2.9), such that

$$\tilde{\mathbf{S}} = \mathrm{diag}\left[\mathbf{S}_{(1)}, \mathbf{S}_{(2)}, \cdots, \mathbf{S}_{(D)} \right]_{NID \times KLID} \tag{3.11}$$

$\tilde{\mathbf{F}}$ is the $KLID \times KI$ ST channel fading matrix:

$$\tilde{\mathbf{F}} = \left[\tilde{\mathbf{F}}_{(1)}^T, \tilde{\mathbf{F}}_{(2)}^T, \cdots, \tilde{\mathbf{F}}_{(D)}^T \right]_{KLID \times KI}^T \tag{3.12}$$

and $\mathbf{n}_{ST}(i) = \left[\mathbf{n}_{(1)}^T(i), \mathbf{n}_{(2)}^T(i), \cdots, \mathbf{n}_{(D)}^T(i) \right]_{NID \times 1}^T$ is the stacked ST received noise vector. The $\mathbf{n}_{ST}(i)$ is a vector of independent zero-mean complex white Gaussian noise processes, and σ_n^2 is the variance of the ambient noise at each antenna element.

Similar to the development of multiuser receivers in the single antenna case, which corresponds to a single-input, single-output (SISO) system, we can derive the sufficient statistics for ST multiuser detectors from the received ST stacked data vector $\mathbf{x}_{ST}(i)$ in (3.10). The ML detector finds the symbol vector estimate, $\hat{\mathbf{b}}(i)$, which maximizes the likelihood function $\exp\left[(-1/2\sigma_n^2)\left\|\mathbf{x}_{ST}(i) - \tilde{\mathbf{S}}\tilde{\mathbf{F}}\mathbf{A}\mathbf{b}(i)\right\|^2\right]$ [11]. This is equivalent to maximizing the negative of the following exponential function:

$$\Omega_{ST}(\mathbf{b}) = 2\mathcal{R}\left(\mathbf{b}\mathbf{A}\tilde{\mathbf{F}}^H\tilde{\mathbf{S}}^H\mathbf{x}_{ST}\right) - \mathbf{b}\mathbf{A}\tilde{\mathbf{F}}^H\tilde{\mathbf{S}}^H\tilde{\mathbf{S}}\tilde{\mathbf{F}}\mathbf{A}\mathbf{b} \tag{3.13}$$

Since the second term does not depend on the received signal assuming knowledge of the channel matrices, a sufficient statistic vector is given by the complex $KI \times 1$ vector:

$$\begin{aligned} \mathbf{y}_{ST}(i) &= \tilde{\mathbf{F}}^H\tilde{\mathbf{S}}^H\tilde{\mathbf{S}}\tilde{\mathbf{F}}\mathbf{A}\mathbf{b}(i) + \tilde{\mathbf{F}}^H\tilde{\mathbf{S}}^H\mathbf{n}_{ST}(i) \\ &= \bar{\mathbf{H}}\mathbf{A}\mathbf{b}(i) + \bar{\mathbf{n}}_{ST}(i) \end{aligned} \tag{3.14}$$

where $\bar{\mathbf{H}} = \tilde{\mathbf{F}}^H\tilde{\mathbf{S}}^H\tilde{\mathbf{S}}\tilde{\mathbf{F}}$ is the ST correlation matrix and $\bar{\mathbf{n}}_{ST} = \tilde{\mathbf{F}}^H\tilde{\mathbf{S}}^H\mathbf{n}_{ST}$ is the corresponding noise vector.

It is seen that the sufficient statistics are simply the ST code matched filter output. The ST code is specified by the ST channel parameter associated with the path fading gains and AOA of each user. For example, suppose the processing window I is over only one-symbol duration, the kth element of $\mathbf{y}_{ST}$ is the ST matched filter output for user k, obtained by correlating each of the D antennas received signals with its L multipath codes $[\mathbf{c}_{k,1}, \mathbf{c}_{k,2}, \cdots, \mathbf{c}_{k,L}]$, weighting them by the complex conjugate of the ST channel $[a_{k1,d}\alpha_{k,1}, a_{k2,d}\alpha_{k,2}, \cdots, a_{kL,d}\alpha_{k,L}]$, for $d = 1, \cdots, D$, and summing over all the multipath indices l and all array indices d. The procedure is illustrated in Figure 3.2. If the channel, $\tilde{\mathbf{F}}$, is not known, an alternative vector of sufficient statistics can be formed at the outputs of the code matched filter bank:

$$\begin{aligned} \tilde{\mathbf{y}}_{ST} &= \tilde{\mathbf{S}}^H\tilde{\mathbf{S}}\tilde{\mathbf{F}}\mathbf{A}\mathbf{b} + \tilde{\mathbf{S}}\mathbf{n}_{ST} \\ &= \tilde{\mathbf{H}}\mathbf{b} + \tilde{\mathbf{n}}_{ST} \end{aligned} \tag{3.15}$$

where $\tilde{\mathbf{H}} = \tilde{\mathbf{S}}^H\tilde{\mathbf{S}}\tilde{\mathbf{F}}\mathbf{A}$ is the overall channel matrix between the input vector $\mathbf{b}(i)$ and output vector $\tilde{\mathbf{y}}_{ST}(i)$. Equations (3.14) and (3.15) are two sufficient statistics models for the received

signal. Depending on the knowledge of the channel, the receivers can operate either on $\mathbf{y}_{ST}(i)$ or on $\tilde{\mathbf{y}}_{ST}(i)$.

3.2 Linear Space-Time Multiuser Receivers

Since the optimal ST multiuser detection algorithm has a prohibitive computational complexity, $\propto O(2^{KI})$, we will develop linear ST multiuser detection techniques in this section. It is assumed that the receiver has the knowledge of the spreading code and the ST channel parameters of all users.

In linear multiuser detection, a linear transformation is applied to the sufficient statistics vector, $\mathbf{y}_{ST}(i)$, then followed by local decisions for each user, that is

$$
\begin{aligned}
\hat{\mathbf{b}}(i) &= \operatorname{sign}\left\{\mathcal{R}\left\{\mathbf{T}^{H}\mathbf{y}_{ST}(i)\right\}\right\} \\
&= \operatorname{sign}\left\{\mathcal{R}\left\{\mathbf{T}^{H}\bar{\mathbf{H}}\mathbf{b}(i) + \mathbf{T}^{H}\bar{\mathbf{n}}_{ST}(i)\right\}\right\}
\end{aligned}
\tag{3.16}
$$

where $\mathbf{T}$ is a $KI \times KI$ complex matrix.

Two popular linear multiuser detectors described in Chapter 2 are the decorrelating detector and MMSE detector. The corresponding transformation matrices for these linear detectors are given, respectively, by

$$
\mathbf{T}^{H}_{ST_{DEC}} = \bar{\mathbf{H}}^{-1} \qquad [\text{ linear decorrelating multiuser detector }]
\tag{3.17}
$$

$$
\mathbf{T}^{H}_{ST_{MMSE}} = \left(\bar{\mathbf{H}} + \sigma_{n}^{2}\mathbf{A}^{-2}\right)^{-1} \quad [\text{ linear MMSE multiuser detector }]
\tag{3.18}
$$

The BER performances of linear ST multiuser detectors are similar to the previous SISO linear multiuser detectors, so what we do is to replace $\mathbf{H}$ with $\bar{\mathbf{H}}$ in (2.43), such that

$$
\begin{aligned}
P_{k} &= P\left[\hat{\mathbf{b}}[k] = 1 \,\middle|\, \mathbf{b}[k] = -1\right] = P\left[\left(\mathbf{T}^{H}\bar{\mathbf{H}}\mathbf{A}\mathbf{b} + \mathbf{T}^{H}\bar{\mathbf{n}}_{ST}\right)[k] > 0 \,\middle|\, \mathbf{b}[k] = -1\right] \\
&= P\left[\left(\mathbf{T}^{H}\bar{\mathbf{n}}_{ST}\right)[k] > \left(\mathbf{T}^{H}\bar{\mathbf{H}}\mathbf{A}\right)[k,k] - \sum_{j\neq k}\left(\mathbf{T}^{H}\bar{\mathbf{H}}\mathbf{A}\right)[k,j]\mathbf{b}[j]\right] \\
&= \frac{1}{2^{KI-1}} \sum_{\substack{\mathbf{b}\in\{-1,1\}^{KI} \\ \mathbf{b}[k]=-1}} P\left[\left(\mathbf{T}^{H}\bar{\mathbf{n}}_{ST}\right)[k] > \left(\mathbf{T}^{H}\bar{\mathbf{H}}\mathbf{A}\right)[k,k] - \sum_{j\neq k}\left(\mathbf{T}^{H}\bar{\mathbf{H}}\mathbf{A}\right)[k,j][j]\right]
\end{aligned}
\tag{3.19}
$$

and the asymptotic efficiency of ST multiuser detection can be achieved in a similar way as the equation (2.45) developed previously:

$$\bar{\eta}_k = \frac{\left(\left(\mathbf{T}^H \bar{\mathbf{H}} \mathbf{A} \right) [k, k] - \sum_{j \neq k} \left| \mathbf{T}^H \bar{\mathbf{H}} \mathbf{A} \right| [k, j] \right)}{\sqrt{\left(\mathbf{T}^H \bar{\mathbf{H}} \mathbf{A} \mathbf{T} \right) [k, k]}} \tag{3.20}$$

In order to perform a simpler analysis on the impact of a generic detector on the system capacity, one can approximate the BER as the $Q(\cdot)$ function of the square root of the received SNR where the noise is modeled as in-cell and out-of-cell Gaussian MAI:

$$Q \left(\sqrt{\frac{N}{(K - 1)\beta + K\gamma}} \right) \tag{3.21}$$

where

N processing gain;

K number of users per cell;

β percentage of MAI power remaining after any multiuser detection;

   ($\beta = 0$: no multiuser detection, $\beta = 1$: perfect removal of all MAI)

γ (the ratio of the total out-of-cell interference over K)

If the signal-to-interference ratio (SIR) increases by a factor of D, for example, due to D uncorrelated antennas, then for a fixed BER the new system can support K' users, and this K' can be solved based on the same BER assumption:

$$Q \left(\sqrt{\frac{N}{(K - 1)\beta + K\gamma}} \right) = Q \left(\sqrt{\frac{DN}{(K' - 1)\beta + K'\gamma}} \right) \tag{3.22}$$

Solving for K' and normalizing by K, we have

$$\frac{K'}{K} = D - \frac{\beta(D - 1)}{K(\beta + \gamma)} \tag{3.23}$$

which asymptotically approaches D as K approaches infinity. From (3.23), it follows that additional antennas and multiuser detection both increase the DS/CDMA system capacity.

3.3   Single-User Detection Data Model

In this section, we will derive a variety of data models applicable to 2-D RAKE single-user receivers for DS/CDMA communication systems. For single-user detection, the MAI is

51

regarded as noise and only the desired user's channel is of interest. Here, we will develop different ST CDMA data models according to whether the data modeled for detection is pre-despread or post-despread in time domain or whether the antenna-space or beamspace is considered. They will be categorized into four types of models: pre-despread antenna-space model (Pre-BT), pre-despread beamspace model (Pre-BT), post-despread antenna-space model (Post-ST) and post-despread beamspace model (Post-BT).

3.3.1 Pre-despread Antenna-space Data Model

First, we discuss the Pre-ST data model in which the data is in pre-despread form in time domain and antenna-space form in space domain. Rearranging the received data (3.1) into a stacked vector, we have the single-input multiple-output (SIMO) continuous time model as

$$
\begin{aligned}
\bar{\mathbf{x}}_{ST}(t) &= \left[x_{(1)}^T(t), x_{(2)}^T(t), \cdots, x_{(D)}^T(t) \right]^T \\
&= \sum_{i=1}^{I} \sum_{k=1}^{K} \sum_{l=1}^{L} \sigma_k b_k(i) \mathbf{a}_{k,l} \alpha_{k,l} c_k(t - iT - \tau_{k,l}) + \bar{\mathbf{n}}(t)
\end{aligned}
\tag{3.24}
$$

where $\mathbf{a}_{k,l} = [a_{kl,1}, a_{kl,2}, \cdots, a_{kl,D}]^T$ is the array response vector associated with the lth path of the kth user's.

To gain full information of the composite signatures, we chip-sample the received data $\bar{\mathbf{x}}_{ST}(t)$ at $t = iT + nT_c + \frac{1}{2}T_c$ over one symbol duration, $(n = 0, 1, \ldots, N + L - 2)$. It means that we take $(N + L - 1)$ samples to make the decision on one bit. Without loss of generality, we assume that the desired user is user 1 and the ith data bit is considered. Thus, the sampled received data can be written as a $D \times (N + L - 1)$ matrix:

$$
\begin{aligned}
\mathbf{X}(i) &= \sum_{l=1}^{L} \mathbf{a}_{k,l} \alpha_{k,l} \mathbf{c}_{1,l}^T b_1(i) + \mathbf{I}(i) + \mathbf{N}(i) \\
&= \left[\bar{\mathbf{x}}_{ST,i}(0), \bar{\mathbf{x}}_{ST,i}(1), \cdots, \bar{\mathbf{x}}_{ST,i}(N + L - 2) \right]
\end{aligned}
\tag{3.25}
$$

where $\bar{\mathbf{x}}_{ST,i}(n)$ is the received data vector sampled at $t = iT + nT_c + \frac{1}{2}T_c$, $\mathbf{c}_{1,l}$, defined in (2.11), is the augmented signature vector of the lth path of user 1, and $\mathbf{I}(i)$ consists of ISI and MAI:

$$
\mathbf{I}(i) = \sum_{l=1}^{L} \mathbf{a}_{1,l} \alpha_{1,l} \mathbf{c}_{1,l}^{(-)T} b_1(i-1) + \sum_{l=1}^{L} \mathbf{a}_{1,l} \alpha_{1,l} \mathbf{c}_{1,l}^{(+)T} b_1(i-1)
$$

$$+ \sum_{k=2}^{K} \sum_{l=1}^{L} \mathbf{a}_{k,l} \alpha_{k,l} \mathbf{c}_{k,l}^T b_k(i) + \sum_{k=2}^{K} \sum_{l=1}^{L} \mathbf{a}_{k,l} \alpha_{k,l} \mathbf{c}_{k,l}^{(-)T} b_k(i-1)$$

$$+ \sum_{k=2}^{K} \sum_{l=1}^{L} \mathbf{a}_{k,l} \alpha_{k,l} \mathbf{c}_{k,l}^{(+)T} b_k(i+1) \tag{3.26}$$

with $\mathbf{c}_{1,l}^{(-)}$ and $\mathbf{c}_{1,l}^{(+)}$ being the augmented signature vector associated with the previous and next bits, respectively. $\mathbf{c}_{k,l}$, $\mathbf{c}_{k,l}^{(-)}$ and $\mathbf{c}_{k,j}^{(+)}$ are defined in a similar fashion for the MAI. $\mathbf{N}(i)$ is complex additive spatial and temporal white Gaussian noise matrix. From (3.25), the ST signature matrix of the desired user is given by

$$\begin{aligned} \mathbf{H}_{ST} &= \sum_{l=1}^{L} \mathbf{a}_{1,l} \alpha_{1,l} \mathbf{c}_{1,l}^T \\ &= [\mathbf{h}_{ST}(0), \mathbf{h}_{ST}(1), \cdots, \mathbf{h}_{ST}(N+L-2)] \end{aligned} \tag{3.27}$$

such that

$$\mathbf{X}(i) = \mathbf{H}_{ST} b_1(i) + \mathbf{I}(i) + \mathbf{N}(i) \tag{3.28}$$

where

$$\mathbf{I}(i) = [\mathbf{i}_{ST,i}(0), \mathbf{i}_{ST,i}(1), \cdots, \mathbf{i}_{ST,i}(N+L-2)] \tag{3.29}$$

$$\mathbf{N}(i) = [\mathbf{n}_{ST,i}(0), \mathbf{n}_{ST,i}(1), \cdots, \mathbf{n}_{ST,i}(N+L-2)] \tag{3.30}$$

where $\mathbf{h}_{ST}(n)$ is the chip-sampled channel signature vector, $\mathbf{i}_{ST,i}(n)$ is the ISI and interference part of chip-sampled vector and $\mathbf{n}_{ST}(n)$ is the chip-sampled white Gaussian noise vector, all sample at $t = iT + nT_c + \frac{1}{2}T_c$.

3.3.2 Pre-despread Beamspace Data Model

The pre-despread beamspace data (Pre-BT) model is developed next. The Pre-BT receiver is constructed on a set of M diversity beams formed at the antenna array, where the number of beams is usually less than the number of antenna elements, i.e., $(M \leq D)$, and each beam is pointed at a distinctive look angle as shown in Figure 3.3. This transforms the received antenna-space data matrix $\mathbf{X}$ into a set of beamformer outputs:

$$\mathbf{y}_{BT,m}^T(i) = \mathbf{w}_m^H \mathbf{X}(i) \quad m = 1, \ldots, M \tag{3.31}$$

where $\mathbf{w}_m$, $m = 1, \ldots, M$, are the beamforming weight vectors. The look angles are chosen such that the M beams span an angular region encompassing a sector Θ_s within which the desired signal paths arrive. From (3.31), we get the $D \times M$ beamforming weight matrix $\mathbf{W}_B$ and the Pre-BT data model as

$$
\begin{aligned}
\mathbf{Y}_{BT}(i) &= \mathbf{W}_B^H \mathbf{X}(i) \\
&= \sum_{l=1}^{L} \alpha_{1,l} \mathbf{W}_B^H \mathbf{a}_{1,l} \mathbf{c}_{1,l}^T b_1(i) + \mathbf{W}_B^H \mathbf{I}(i) + \mathbf{W}_B^H \mathbf{N}(i) \\
&= [\mathbf{y}_{BT,i}(0), \mathbf{y}_{BT,i}(1), \cdots, \mathbf{y}_{BT}(N+L-2)]
\end{aligned}
\tag{3.32}
$$

where $\mathbf{y}_{BT,i}(n)$ is the chip-sampled beamspace vector at $t = iT + nT_c + \frac{1}{2}T_c$. The Pre-BT signature matrix is given accordingly by

$$
\begin{aligned}
\mathbf{H}_{BT} &= \sum_{l=1}^{L} \alpha_{1,l} \mathbf{W}_B^H \mathbf{a}_{1,l} \mathbf{c}_{1,l}^T \\
&= [\mathbf{h}_{BT}(0), \mathbf{h}_{BT}(1), \cdots, \mathbf{h}_{BT}(N+L-2)]
\end{aligned}
\tag{3.33}
$$

where $\mathbf{h}_{BT}(n)$ is the chip-sampled beamspace signature vector at $t = iT + nT_c + \frac{1}{2}T_c$. Note that the simplest choice of $\mathbf{W}_B$ is a set of fixed beams pointed at different directions in the working sector Θ_s.
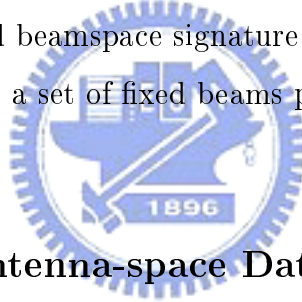
3.3.3 Post-despread Antenna-space Data Model

Post-despread antenna-space data model (Post-ST) means that the chip-sampled ST data is despread or compressed in time domain first before further processing. Assuming that the information of channel impulse responses with a delay spread of L chips is known, we may design a matched filter bank with L fingers for every antenna. The weight vector of each finger has a length of $N + L - 1$ to cover all the delay versions carrying the information bit of interest. In Post-ST data model, we despread the pre-despread data to compress the temporal dimension from $N + L - 1$ to L in an adaptive fashion to suppress MAI. From (3.25), we define the $(N + L - 1) \times L$ adaptive matched filter matrix $\mathbf{G}$:

$$
\mathbf{G} = [\mathbf{s}_1, \mathbf{s}_2, \cdots, \mathbf{s}_L]_{(N+L-1) \times L}
\tag{3.34}
$$

where $\mathbf{s}_l$, $l = 1, \ldots, L$, are the adaptive matched filter weight vectors. Note that similar to that the simplest choice of $\mathbf{W}_B$ is a set of fixed beams pointed at different direction, the

simplest choice of $\mathbf{G}$ is the $\mathbf{C}_1$ matrix as defined in (2.11). Then, the Post-ST data model is given by

$$
\begin{aligned}
\mathbf{X}_{SM}(i) &= \sum_{l=1}^{L} \alpha_{1,l} \mathbf{a}_{1,l} \mathbf{c}_{1,l}^T \mathbf{G}^* b_1(i) + \mathbf{I}(i)\mathbf{G}^* + \mathbf{N}(i)\mathbf{G}^* \\
&= [\mathbf{x}_{SM,i}(0), \mathbf{x}_{SM,i}(1), \cdots, \mathbf{x}_{SM,i}(L-1)]
\end{aligned}
\tag{3.35}
$$

where $\mathbf{x}_{SM,i}(n)$ is the post-despread data vector at the nth finger. The Post-ST signature matrix is given by

$$
\begin{aligned}
\mathbf{H}_{SM} &= \sum_{l=1}^{L} \alpha_{1,l} \mathbf{a}_{1,l} \mathbf{c}_{1,l}^T \mathbf{G}^* \\
&= [\mathbf{h}_{SM}(0), \mathbf{h}_{SM}(1), \cdots, \mathbf{h}_{SM}(L-1)]
\end{aligned}
\tag{3.36}
$$

and Post-ST interference and noise components are given by

$$
\begin{aligned}
\mathbf{I}_{SM}(i) &= \mathbf{I}(i)\mathbf{G}^* \\
&= [\mathbf{i}_{SM,i}(0), \mathbf{i}_{SM,i}(1), \cdots, \mathbf{i}_{SM,i}(L-1)]
\end{aligned}
\tag{3.37}
$$

$$
\begin{aligned}
\mathbf{N}_{SM}(i) &= \mathbf{N}(i)\mathbf{G}^* \\
&= [\mathbf{n}_{SM,i}(0), \mathbf{n}_{SM,i}(1), \cdots, \mathbf{n}_{SM,i}(L-1)]
\end{aligned}
\tag{3.38}
$$

3.3.4 Post-despread Beamspace Data Model

The last data model is obtained by compressing the temporal and spatial dimension by a set of adaptive correlators and a set of beamformers, respectively. The compressed data model is called the post-despread beamspace data model (Post-BT) which is suitable for sectored and post-despread systems. The Post-BT data model is given by

$$
\begin{aligned}
\mathbf{Y}_{BM}(i) &= \mathbf{W}_B^H \mathbf{X}(i)\mathbf{G}^* \\
&= \sum_{l=1}^{L} \alpha_{1,l} \mathbf{W}_B^H \mathbf{a}_{1,l} \mathbf{c}_{1,l}^T \mathbf{G}^* b_1(i) + \mathbf{W}_B^H \mathbf{I}(i)\mathbf{G}^* + \mathbf{W}_B^H \mathbf{N}(i)\mathbf{G}^* \\
&= [\mathbf{y}_{BM,i}(0), \mathbf{y}_{BM,i}(1), \cdots, \mathbf{y}_{BM,i}(L-1)]
\end{aligned}
\tag{3.39}
$$

and the Post-BT signature matrix is given by

$$
\begin{aligned}
\mathbf{H}_{BM} &= \sum_{l=1}^{L} \alpha_{1,l} \mathbf{W}_B^H \mathbf{a}_{1,l} \mathbf{c}_{1,l}^T \mathbf{G}^* \\
&= [\mathbf{h}_{BM}(0), \mathbf{h}_{BM}(1), \cdots, \mathbf{h}_{BM}(L-1)]
\end{aligned}
\tag{3.40}
$$

55

The corresponding Post-BT interference matrix $\mathbf{I}_{BM}(i)$ and noise matrix $\mathbf{N}_{BM}(i)$ are given by

$$
\begin{aligned}
\mathbf{I}_{BM}(i) &= \mathbf{W}_B^H \mathbf{I}(i) \mathbf{G}^* \\
&= [\mathbf{i}_{BM,i}(0), \mathbf{i}_{BM,i}(1), \cdots, \mathbf{i}_{BM,i}(L-1)]
\end{aligned}
\tag{3.41}
$$

$$
\begin{aligned}
\mathbf{N}_{BM}(i) &= \mathbf{W}_B^H \mathbf{N}(i) \mathbf{G}^* \\
&= [\mathbf{n}_{BM,i}(0), \mathbf{n}_{BM,i}(1), \cdots, \mathbf{n}_{BM,i}(L-1)]
\end{aligned}
\tag{3.42}
$$

3.4 Space-Time 2-D RAKE Receivers

In this section, we develop different types of ST 2-D RAKE receivers based on the four types of data models (Pre-ST, Pre-BT, Post-ST and Post-BT) discussed in the previous section. These 2-D RAKE receivers are distinguished by pre-despread and post-despread in time domain and by antenna-space and beamspace in space domain.

A 2-D RAKE receiver is implemented to perform two main tasks: (1) identifies and removes the signature matrix (or vector) of the desired user in order to recover the original data bit; (2) suppresses MAI, ISI, NBI and noise.

3.4.1 Pre-despread Antenna-space 2-D RAKE Receivers

Firstly, we employ the ST data model from section 3.3.1 for pre-despread antenna-space (Pre-ST) DS/CDMA systems. In order to formulate the data structure for ST joint processing, we denote the data vector of size $(N+L-1)D \times 1$ from (3.25):

$$
\begin{aligned}
\mathbf{x}_{c-ST}(i) &= \text{vec}\{\mathbf{X}(i)\} \\
&= \left[\bar{\mathbf{x}}_{ST,i}^T(0), \bar{\mathbf{x}}_{ST,i}^T(1), \cdots, \bar{\mathbf{x}}_{ST,i}^T(N+L-2)\right]_{(N+L-1)D \times 1}^T \\
&= \mathbf{h}_{c-ST} b_1(i) + \mathbf{i}_{c-ST}(i) + \mathbf{n}_{c-ST}(i)
\end{aligned}
\tag{3.43}
$$

where $vec(\cdot)$ is the operation that concatenates a matrix into a column vector, column by column. In this way, the concatenated Pre-ST signature vector from (3.27) is given by

$$
\mathbf{h}_{c-ST} = \text{vec}\{\mathbf{H}_{ST}\} = \text{vec}\left\{\sum_{l=1}^{L} \mathbf{a}_{1,l} \alpha_{1,l} \mathbf{c}_{1,l}^T\right\}
$$

$$= \left[\mathbf{h}_{ST}^T(0), \mathbf{h}_{ST}^T(1), \cdots, \mathbf{h}_{ST}^T(N+L-2), \right]_{(N+L-1)D\times 1}^T \tag{3.44}$$

The concatenated Pre-ST interference vector $\mathbf{i}_{c-ST}(i)$ and noise vector $\mathbf{n}_{c-ST}(i)$ are given by

$$\mathbf{i}_{c-ST}(i) = \left[\bar{\mathbf{i}}_{ST,i}^T(0), \bar{\mathbf{i}}_{ST,i}^T(1), \cdots, \bar{\mathbf{i}}_{ST,i}^T(N+L-2) \right]_{(N+L-1)D\times 1}^T \tag{3.45}$$

and

$$\mathbf{n}_{c-ST}(i) = \left[\bar{\mathbf{n}}_{ST,i}^T(0), \bar{\mathbf{n}}_{ST,i}^T(1), \cdots, \bar{\mathbf{n}}_{ST,i}^T(N+L-2) \right]_{(N+L-1)D\times 1}^T \tag{3.46}$$

A variety of receivers can be developed based on the concatenated Pre-ST vector in (3.43). For example, the Pre-ST RAKE receivers combine the entries of the Pre-ST data vector via a linear operation, with a specified weight vector $\mathbf{q}$, into an estimate of $b_1(i)$:

$$\hat{b}_1(i) = \text{sign}\left\{ \left(\mathbf{q}^H \mathbf{x}_{c-ST} \right) \right\} \tag{3.47}$$

The weight vector can be chosen in accordance with the coherent or MMSE criterion [31]. For the coherent Pre-ST 2-D RAKE receiver, the weight vector $\mathbf{q}$ in (3.47) is given by

$$\begin{aligned} \mathbf{r}_{st} &= \hat{\mathbf{h}}_{c-ST} = E\left\{ \mathbf{x}_{c-ST}(i)b_1^*(i) \right\} \\ \mathbf{q} &= \mathbf{r}_{st} \end{aligned} \tag{3.48}$$

Here $\mathbf{r}_{st}$ is formed to estimate the concatenated signature vector $\mathbf{h}_{c-ST}$. For the Pre-ST MMSE receiver,

$$\mathbf{q} = \mathbf{R}_{c-ST}^{-1} \mathbf{r}_{st} \tag{3.49}$$

Another receiver similar to the MMSE receiver is the Pre-ST MVDR receiver, which is given by

$$\mathbf{q} = \left(\mathbf{h}_{c-ST}^H \mathbf{R}_{c-ST}^{-1} \mathbf{h}_{c-ST} \right)^{-1} \mathbf{R}_{c-ST}^{-1} \mathbf{h}_{c-ST} \tag{3.50}$$

where $\mathbf{R}_{c-ST} = E\left\{ \mathbf{x}_{c-ST}(i)\mathbf{x}_{c-ST}^H(i) \right\}$ is the Pre-ST data correlation matrix, and $\mathbf{h}_{c-ST}$ is the Pre-ST channel vector obtained by concatenating the columns of $\mathbf{H}_{ST}$. In practice, $\mathbf{r}_{st}$ and $\mathbf{R}_{c-ST}$ are usually estimated by

$$\hat{\mathbf{r}}_{st} = \frac{1}{N_s} \sum_{i=1}^{N_s} \mathbf{x}_{c-ST}(i)b_1^*(i) \tag{3.51}$$

57

$$\hat{\mathbf{R}}_{c-ST} = \frac{1}{N_s} \sum_{i=1}^{N_s} \mathbf{x}_{c-ST}(i) \mathbf{x}_{c-ST}^H(i) \tag{3.52}$$

where N_s is the number of symbols. The output SINR of the linear receivers is given by

$$\text{SINR}_o = \frac{\left| \mathbf{q}^H \mathbf{h}_{c-ST} \right|^2}{\mathbf{q}^H \hat{\mathbf{R}}_{c-ST} \mathbf{q} - \mathbf{q}^H \mathbf{h}_{c-ST} \mathbf{h}_{c-ST}^H \mathbf{q}} \tag{3.53}$$

and the bit error probability is determined by the receiver output SNR and the Euclidean distance between the receiver output and decision boundary:

$$\begin{aligned} P_1 &= E_{\mathbf{b} \in \{-1,1\}^K} \left\{ P\left(\mathbf{q}^H \mathbf{x}_{c-ST}(i) > 0 \,|\, b_1(i) = -1 \right) \right\} \\ &= Q\left(\frac{\mathbf{q}^H \mathbf{h}_{c-ST} + \mathbf{q}^H E_{\bar{\mathbf{b}} \in \{-1,1\}^{K-1}, \bar{\mathbf{b}} = b_2, \cdots, b_k} \left\{ \mathbf{i}_{c-ST}(i) \right\}}{\sigma_n (\mathbf{q}^H \mathbf{q})^{1/2}} \right) \end{aligned} \tag{3.54}$$

Although the Pre-ST 2-D RAKE receiver has the maximum degree of freedom $(N + L - 1)D$ to suppress MAI, noise or NBI, it needs a higher computational complexity and suffers from poor convergence. A simplified approache of performing ST processing is of course to separate the spatial and the temporal processing. In this way, we can have spatial beamformers and temporal correlators (or matched filters) wotk independently. This results in the so-called cascade ST and cascade time-space 2-D RAKE receivers [29].

3.4.2 Post-despread Antenna-space 2-D RAKE Receivers

For post-despread antenna-space (Post-ST) DS/CDMA systems, we despread the received data in the time domain by a set of matched filters. Then we get the concatenated Post-ST data vector of size $LD \times 1$ from (3.35) as follows:

$$\begin{aligned} \mathbf{x}_{c-SM}(i) &= \text{vec}\left\{ \mathbf{X}_{SM}(i) \right\} \\ &= \left[\mathbf{x}_{SM,i}^T(0), \mathbf{x}_{SM,i}^T(1), \cdots, \mathbf{x}_{SM,i}^T(L-1) \right]_{LD \times 1}^T \\ &= \mathbf{h}_{c-SM} b_1(i) + \mathbf{i}_{c-SM}(i) + \mathbf{n}_{c-SM}(i) \end{aligned} \tag{3.55}$$

where the concatenated Post-ST signature vector from (3.36) is given by

$$\begin{aligned} \mathbf{h}_{c-SM} &= \text{vec}\left\{ \mathbf{H}_{SM} \right\} = \text{vec}\left\{ \sum_{l=1}^{L} \mathbf{a}_{1,l} \alpha_{1,l} \mathbf{c}_{1,l}^T \mathbf{G}^* \right\} \\ &= \left[\mathbf{h}_{SM}^T(0), \mathbf{h}_{SM}^T(1), \cdots, \mathbf{h}_{SM}^T(L-1) \right]_{LD \times 1}^T \end{aligned} \tag{3.56}$$

The concatenated Post-ST interference vector $\mathbf{i}_{c-SM}(i)$ and noise vector $\mathbf{n}_{c-SM}(i)$ are given by

$$\mathbf{i}_{c-SM}(i) = \left[\mathbf{i}_{SM,i}^T(0), \mathbf{i}_{SM,i}^T(1), \cdots, \mathbf{i}_{SM,i}^T(L-1)\right]_{LD \times 1}^T \tag{3.57}$$

$$\mathbf{n}_{c-SM}(i) = \left[\mathbf{n}_{SM,i}^T(0), \mathbf{n}_{SM,i}^T(1), \cdots, \mathbf{n}_{SM,i}^T(L-1)\right]_{LD \times 1}^T \tag{3.58}$$

The Post-ST RAKE receivers combine the entries of the Post-ST data vector via a linear operation, with a specified weight vector $\mathbf{q}$, into an estimate of $b_1(i)$:

$$\hat{b}_1(i) = \text{sign}\left\{\left(\mathbf{q}^H \mathbf{x}_{c-SM}\right)\right\} \tag{3.59}$$

For the coherent Post-ST 2-D RAKE receiver, the weight vector $\mathbf{q}$ in (3.59) is given by

$$\begin{aligned} \mathbf{r}_{sm} &= E\left\{\mathbf{x}_{c-SM}(i)b_1^*(i)\right\} \\ \mathbf{q} &= \mathbf{r}_{sm} \end{aligned} \tag{3.60}$$

Here $\mathbf{r}_{sm}$ is formed to estimate the concatenated signature vector $\mathbf{h}_{c-SM}$. For the Post-ST MMSE receiver,

$$\mathbf{q} = \mathbf{R}_{c-SM}^{-1}\mathbf{r}_{sm} \tag{3.61}$$

where $\mathbf{R}_{c-SM} = E\left\{\mathbf{x}_{c-SM}(i)\mathbf{x}_{c-SM}^H(i)\right\}$. For the Post-ST MVDR receiver,

$$\mathbf{q} = \left(\mathbf{h}_{c-SM}^H \mathbf{R}_{c-SM}^{-1} \mathbf{h}_{c-SM}\right)^{-1} \mathbf{R}_{c-SM}^{-1} \mathbf{h}_{c-SM} \tag{3.62}$$

In practice, $\mathbf{R}_{c-SM}$ and $\mathbf{r}_{sm}$ are usually estimated by

$$\hat{\mathbf{r}}_{sm} = \frac{1}{N_s}\sum_{i=1}^{N_s}\mathbf{x}_{c-SM}(i)b_1^*(i) \tag{3.63}$$

$$\hat{\mathbf{R}}_{c-SM} = \frac{1}{N_s}\sum_{i=1}^{N_s}\mathbf{x}_{c-SM}(i)\mathbf{x}_{c-SM}^H(i) \tag{3.64}$$

3.4.3   Pre-despread Beamspace 2-D RAKE Receivers

Similar to the development of the Pre-ST and Post-ST 2-D RAKE receivers, the pre-despread beamspace 2-D (Pre-BT) 2-D RAKE receiver is developed next. Instead of processing the antenna-space data, we concatenate the BT data matrix $\mathbf{Y}_{BT}(i)$ into a vector $\mathbf{y}_{c-BT}$ for Pre-BT 2-D RAKE receiver. From (3.32), we obtained

$$\mathbf{y}_{c-BT} = \text{vec}\left\{\mathbf{Y}_{BT}\right\} \tag{3.65}$$

And the concatenated CSV $\mathbf{h}_{c-BT}$ is obtained by concatenating the columns of $\mathbf{H}_{BT}$:

$$\mathbf{h}_{c-BT} = \text{vec}\left\{\mathbf{H}_{BT}\right\} \tag{3.66}$$

The Pre-BT 2-D RAKE receivers combine the entries of Pre-BT data vector via a linear operation, with a specified weight vector $\mathbf{q}$, into an estimate of $b_1(i)$:

$$\hat{b}_1(i) = \text{sign}\left\{\left(\mathbf{q}^H \mathbf{y}_{c-BT}\right)\right\} \tag{3.67}$$

The weight vector can be chosen in accordance with the coherent, MMSE or MVDR criterion. For the coherent Pre-BT 2-D RAKE receiver, the weight vector $\mathbf{q}$ in (3.67) is given by

$$
\begin{aligned}
\mathbf{r}_{bt} &= \hat{\mathbf{h}}_{c-BT} = E\left\{\mathbf{y}_{c-BT}(i)b_1^*(i)\right\} \\
\mathbf{q} &= \mathbf{r}_{bt}
\end{aligned} \tag{3.68}
$$

Here $\mathbf{r}_{bt}$ is formed to estimate the concatenated signature vector $\mathbf{h}_{c-BT}$. For the Pre-BT MMSE receiver,

$$\mathbf{q} = \mathbf{R}_{c-BT}^{-1}\mathbf{r}_{bt} \tag{3.69}$$

where $\mathbf{R}_{c-BT} = E\left\{\mathbf{y}_{c-BT}(i)\mathbf{y}_{c-BT}^H(i)\right\}$. For Pre-BT MVDR receiver,

$$\mathbf{q} = \left(\mathbf{h}_{c-BT}^H \mathbf{R}_{c-BT}^{-1}\mathbf{h}_{c-BT}\right)^{-1}\mathbf{R}_{c-BT}^{-1}\mathbf{h}_{c-BT} \tag{3.70}$$

In practice, $\mathbf{R}_{c-BT}$ and $\mathbf{r}_{bt}$ are usually estimated by

$$\hat{\mathbf{r}}_{bt} = \frac{1}{N_s}\sum_{i=1}^{N_s}\mathbf{y}_{c-BT}(i)b_1^*(i) \tag{3.71}$$

$$\hat{\mathbf{R}}_{c-BT} = \frac{1}{N_s}\sum_{i=1}^{N_s}\mathbf{y}_{c-BT}(i)\mathbf{y}_{c-BT}^H(i) \tag{3.72}$$

3.4.4   Post-despread Beamspace 2-D RAKE Receivers

The same development is done for the Post-BT 2-D RAKE receiver. We concatenate the beamspace and matched filter matrix $\mathbf{Y}_{BM}(i)$ into a vector $\mathbf{y}_{c-BM}$ for Post-BT 2-D RAKE receivers. The Post-BT concatenates composite signature vector $\mathbf{h}_{c-BM}$ is obtained by concatenating the columns of matrix $\mathbf{H}_{BM}$. From (3.39) and (3.40), we obtain

$$\mathbf{y}_{c-BM} = \mathrm{vec}\left\{\mathbf{Y}_{BM}\right\} \tag{3.73}$$

$$\mathbf{h}_{c-BM} = \mathrm{vec}\left\{\mathbf{H}_{BM}\right\} \tag{3.74}$$

The Post-BT 2-D RAKE receivers combine the entries of Post-BT data vector via a linear operation, with a specified weight vector $\mathbf{q}$, into an estimate of $b_1(i)$:

$$\hat{b}_1(i) = \mathrm{sign}\left\{\left(\mathbf{q}^H \mathbf{y}_{c-BM}\right)\right\} \tag{3.75}$$

Again, the weight vector can be chosen in accordance with the coherent, MMSE or MVDR criterion. For coherent Post-BT 2-D RAKE receiver, the weight vector $\mathbf{q}$ in (3.75) is given by

$$\begin{aligned}
\mathbf{r}_{bm} &= \hat{\mathbf{h}}_{c-BM} = E\left\{\mathbf{y}_{c-BM}(i)b_1^*(i)\right\} \\
\mathbf{q} &= \mathbf{r}_{bm}
\end{aligned} \tag{3.76}$$

Here $\mathbf{r}_{bm}$ is formed to estimate the cxoncatenated signature vector $\mathbf{h}_{c-BM}$. For Post-BT MMSE receiver,

$$\mathbf{q} = \mathbf{R}_{c-BM}^{-1}\mathbf{r}_{bm} \tag{3.77}$$

where $\mathbf{R}_{c-BM} = E\left\{\mathbf{y}_{c-BM}(i)\mathbf{y}_{c-BM}^H(i)\right\}$, and for Post-BT MVDR receiver,

$$\mathbf{q} = \left(\mathbf{h}_{c-BM}^H \mathbf{R}_{c-BM}^{-1} \mathbf{h}_{c-BM}\right)^{-1} \mathbf{R}_{c-BM}^{-1} \mathbf{h}_{c-BM} \tag{3.78}$$

In practice, $\mathbf{R}_{c-BM}$ and $\mathbf{r}_{bm}$ are usually estimated by

$$\hat{\mathbf{r}}_{bm} = \frac{1}{N_s}\sum_{i=1}^{N_s}\mathbf{y}_{c-BM}(i)b_1^*(i) \tag{3.79}$$

$$\hat{\mathbf{R}}_{c-BM} = \frac{1}{N_s}\sum_{i=1}^{N_s}\mathbf{y}_{c-BM}(i)\mathbf{y}_{c-BM}^H(i) \tag{3.80}$$

3.4.5 Principal Component Based Blind 2-D RAKE Receivers

The training signal based 2-D RAKE receiver is easy to implement and its performance is reliable. However, it consumes the spectrum and time resources. In GSM, for example, about 20% of the bits are dedicated for training. Moreover, in a rapidly varying mobile channel, we must retrain the 2-D processor frequently, resulting in poor spectral efficiency. Hence, there is an increased interest in blind methods in which one can estimate the communication channel without any explicit training signal. It is noteworthy that the performance of blind methods will be sensitive to the validity of structural properties assumed [62]. In [30, 63], the principal component (PC) method is proposed to estimate the channel response blindly by exploiting the feature of pre-despread data correlation matrix and post-despread data correlation matrix differed by a rank one contribution due to the desired user. For this reason, we need the pre-despread and post-despread data correlation matrices with the same dimension. Since the concatenated Post-ST data vector is LD-dimensional, we should find the concatenated ST data matrix $LD \times LD$. From equation (3.35), we form the modified concatenated ST data vector to fit the PC algorithm:

$$\mathbf{X}_c(i) = \begin{bmatrix} \mathbf{x}_i(0) & \mathbf{x}_i(1) & \cdots & \mathbf{x}_i(N-1) \\ \mathbf{x}_i(1) & \mathbf{x}_i(2) & \cdots & \mathbf{x}_i(N) \\ \vdots & \vdots & \vdots & \vdots \\ \mathbf{x}_i(L-1) & \mathbf{x}_i(L) & \cdots & \mathbf{x}_i(N+L-2) \end{bmatrix} \tag{3.81}$$

where $\mathbf{x}_i(n)$ is the chip-sampled data vector during the ith symbol at the antenna array. Then the pre-despread data correlation matrix is given by

$$\mathbf{R}_{\mathbf{X}_c} = E\left\{\mathbf{X}_c(i)\mathbf{X}_c^H(i)\right\} \tag{3.82}$$

It is readily seen that

$$\mathbf{R}_{\mathbf{x}_{c-SM}} - \mathbf{R}_{\mathbf{x}_c} = N(N-1)\mathbf{h}_{c-SM}\mathbf{h}_{c-SM}^H \tag{3.83}$$

From equation (3.83) in [63], the estimated concatenated Post-ST composite signature vector of the desired user, $\hat{\mathbf{h}}_{c-SM}$, can be found by the principal eigenvector of $\mathbf{R}_{\mathbf{x}_{c-SM}} - \mathbf{R}_{\mathbf{x}_c}$. From equation (3.52), the pre-despread data correlation matrix can be estimated as:

$$\hat{\mathbf{R}}_{\mathbf{x}_c} = \frac{1}{N_s}\sum_{i=1}^{N_s}\mathbf{x}_c(i)\mathbf{x}_c^H(i) \tag{3.84}$$

The PC algorithm procedure can be summarized as follows:

1. Calculate the data correlation matrices as shown in equations (3.84) and (3.52).

2. Calculate $\mathbf{r}$ as the principal eigenvector of $\hat{\mathbf{R}}_{\mathbf{x}_c} - \hat{\mathbf{R}}_{\mathbf{x}_{c-SM}}$.

3. The PC based coherent combining weight vector is $\mathbf{w} = \mathbf{r}$ and the MMSE weight vector is $\mathbf{w} = \hat{\mathbf{R}}_{x_c}^{-1}\mathbf{r}$.

3.5 Beamspace-Time 2-D RAKE Receivers for Sectored CDMA Systems

Sectorization is a widely used method for increasing the cellular wireless communication system capacity [64]. Although it can increase the system capacity, working with sectorization usually causes extra computational load in the MSC, e.g., inter-sector hand-offs. A major requirement for sectored antennas is that they should exhibit a sufficient attenuation for out-of-sector MAI so that the SINR can be enhanced for in-sector signals. In this section, we will discuss the antenna array based sectorization techniques which offer effective MAI suppression.

3.5.1 Concept of Traditional Sectored Wireless Systems

In cellular wireless communication systems, various methods have been proposed to achieve the goal of increasing system capacity. Among these methods, the commonly used is cell sectorization. The concept of sectorization is described briefly below.

As shown in Figure 3.4, for example, each cell is split into three sectors by directional antennas located at the center of the cell. Signals of different users in the same sector are received by the same sector antenna. Each base station is connected to the MSC via fiber optics or microwave links, which monitors all users in these sectors, and decisions about call initialization, power control, handoffs, frequency band or time slot assignment, etc. are made here. When some mobile unit moves from the current sector to another one, the inter-cell handoff must be executed. From [64, 65], the more sectors in one cell are used, the larger

of capacity will be. However, cell sectorization also increases the MSC computational load because of the inter-cell handoffs are decided in the MSC. In addition to the increase in the MSC loading, sectorization also decreases the trunking efficiency though the SINR for each user in the system is improved [64]. The decrease in the trunking efficiency means that the probability of being blocked or being delayed increases.

3.5.2 Beamspace Processing via Antenna Array for Sectored Wireless Systems

Conventional Fourier beamforming techniques can form a narrow beam in a prescribed look direction. In a multipath fading environment, the desired signal is spread out and we need to form a certain number of mainbeams in order to collect all the multipaths from different directions. Working with a set of beamformers has the effect of transforming the antenna space array data into the beamspace data, which can then be fed into a beamspace-time (BT) processor to compensate for the channel impairments and combine the multipaths constructively. These multiple beams cover the field-of-view with a high in-sector gain and suppress the out-of-sector MAI. This is similar to the operation of the conventional sectorization schemes. The difference between the two methods is that the MSC needs to perform additional handoffs, as mentioned previously, when conventional sectorization is applied. However, for sectorization via antenna arrays, we just adjust the look directions of these beams to form a new sector to cover the desired user. In other words, the sector formed by the antenna array is changed adaptively with the DOA of the desired user. Handoffs are unnecessary and the computational load of MSC does not increase. Due to the reduction of array data dimension, sectorization via antenna arrays can effectively reduce the computational complexity and perform MAI suppression for the system. Beamspace processing techniques can be readily applied with sectorization, with the set of beamformers acting as the beamforming matrix. In the next chapter, we will propose the technique about the development of beamforming matrix. We will address not only the conversion from Pre-ST to Pre-BT or Post-ST to Post-BT for computational complexity reduction, (from D-dimensional to M-dimensional), but also suppression of out-of-sector MAI.

3.6 Simulation Results

In this chapter, we present space-time multiuser detectors and various blind or nonblind 2-D RAKE receivers. In this section, we will illustrate the performance of these receivers by simulating results. We evaluate the performance of these CDMA detectors using an antenna array at the basestation. The array is linear and composed of D identical omni-directional elements uniformly spaced by a $1/\sqrt{3}$ wavelength. The inter-element spacing is chosen due to the assumption that the array is used to cover the field-of-view $[-60°, 60°]$. In this case, D orthogonal beams can be formed within the $120°$ angular region. This is in contrast to the conventional linear array with an inter-element spacing of $1/2$ wavelength, in which orthogonal beams are formed in the entire $180°$ region. For simplicity, the elements are assumed to be ideal omnidirectional antennas, leading to the following steering vector structure:

$$\mathbf{a}(\theta) = \left[1, e^{j\frac{2\pi}{\sqrt{3}}\sin\theta}, e^{j\frac{4\pi}{\sqrt{3}}\sin\theta}, \cdots, e^{j\frac{2(D-1)\pi}{\sqrt{3}}\sin\theta} \right]^T$$

where θ is measured with respect to the normal to the array axis. In practical systems, however, directional antennas with a suitable front-to-back ratio should be employed to avoid backward radiation [64]. The sector of interest is $\Theta_s = [-16.8°, 16.8°]$, which represents about one third of the field-of-view. As an indication of the goodness of these receivers, we define the output SINR_o (in dB) as a criterion:

$$\mathrm{SINR}_o = 10\log_{10}\frac{\text{output power of signal}}{\text{output power of interference plus noise}}$$

The input SNR (in dB) is defined as $\mathrm{SNR}_i = 10\log_{10}\frac{\sigma_1^2}{\sigma_n^2}$, and the NFR (in dB) is defined as $\mathrm{NFR} = 10\log_{10}\frac{\sigma_k^2}{\sigma_1^2}$, where $\sigma_2^2 = \sigma_3^2 = \cdots = \sigma_K^2$, for $k = 1, \cdots, K$. We assumed that the AOA's of the desired signal's multipaths are uniformly distributed in the sector of interest, and the AOA's of MAI's multipaths are uniformly distributed in the entire field-of-view. The simulation parameters are: $N = 31$ with Gold codes, $L = 4$ fingers, the number of antenna elements $D = 9$, and the input $\mathrm{SNR}_i = 0$ dB. We use $N_s = 500$ symbols for training and estimation of correlation matrices. A total of 100 Monte-Carlo runs are done for each simulation in this section. Unless otherwise mentioned, the above standard parameters will be used throughout the section.

In the first set of simulations, we compare the BER performances of linear ST 2-D RAKE CDMA receivers, MMSE-MUD described by (3.18) and ZF-MUD described by (3.17), versus input SNR with $K = 5$. The simulation results are shown in Figure 3.5 for NFR = 0 dB and NFR = 20 dB. We introduce the BER performance of single-user environment as the lower bound of those mentioned receivers for comparison. We see that the conventional ST 2-D RAKE receiver (CST-RAKE) described by (3.60) and PC method (PC-RAKE) described in subsection 3.4.5 strongly depends on the relative power of MAI. While the BER performances of the MMSE-MUD and ZF-MUD are invariant to the NFR values. The linear ST MMSE 2-D RAKE receiver (MST-RAKE) described by (3.61) has little performance degradation than those of the MMSE-MUD and ZF-MUD. This is because the multiuser detections not only use the ST signature of themselves to enhance the output SNR, but also utilize the crosscorrelation with the other users' ST signature to suppress MAI simultaneously. The MST-RAKE also has enough degree of freedom ($DL = 36$) to suppress the MAI and to estimate the channel correctively.

In the second set of simulations, the system capacity is evaluated in Figure 3.6 with NFR=0 dB and 20 dB. As expected, pre-despread 2-D RAKE receivers in MMSE criterion, PST-RAKE described by (3.49) and PBT-RAKE described by (3.69) with three fixed beams formed at look directions $\{\theta_1, \theta_2, \theta_3\} = \{-12.5°, 0°, 12.5°\}$, perform reliably on large user numbers and high NFR due to their large temporal and spatial degree of freedom. The post-despread 2-D RAKE receivers, MST-RAKE and MBT-RAKE described by (3.77) with three fixed beams formed at the same look directions as that of PBT-RAKE, perform well in the small range of number of users and in the low NFR region, in which case both channel estimation and MAI suppression can be done effectively. On the other hand, the conventional CST-RAKE totally fails with NFR=20 dB even in the small number of users due to their lack of degree of freedom to suppress the MAI.

In the third set of simulations, we consider the near-far problem in reverse link of DS/CDMA systems. Since the distances of each user to basestation are always not the same and propagation path loss of user closed to basestation is small, the closest user is able to "capture" the basestation because of small propagation loss. To avoid to this problem, we examine the ST 2-D RAKE CDMA receivers whether they are near-far resistant

or not. First we suppose that there are $K=5$ users in this cell, we show that in Figure 3.7(a) the PST-RAKE and PBT-RAKE, are "near-far" resistant due to that its large degree of freedom allow for successful MAI suppression. The MST-RAKE and MBT-RAKE receiver are near-far resistant, too. But the PC-RAKE and CST-RAKE receivers are not near-far resistant due to that the increased interference power causes a larger channel estimation error more serious. Next, we suppose that there are $K=25$ users in this cell. As shown in Figure 3.7(b), the PST-RAKE and PBT-RAKE are still near-far resistant but the MST-RAKE and MBT-RAKE receivers get worse as compared with the $K=5$ users case. When the number of users increase to 20, it is interesting to notice that the PC-RAKE and CST-RAKE receivers are all breakdown. It is conceivable since with many users and rich multipath components, the degree of freedom of the post-despread methods can not perform MAI suppression successfully.

The final set of simulations, we investigate the output SINR of MST-RAKE receiver for different number of users with respect to different antenna size with NFR=10 dB. In order to compare the performance of different antenna array size, the output SINR curves are evaluated by the number of antenna elements for $D = 1, 2, 4, 8, 12$. The results shown in Figure 3.8 demonstrate a significant performance improvement for a given number of users, by increasing the size of antenna array. For the $D = 2$ antennas case, the coherent combining improves the output SINR on average by about 3 dB than that of single antenna element. Figure 3.9 shows the output SINR of MST-RAKE for different numbers of users with respect to a variety of code length for NFR = 10 dB. The output SINR curves are evaluated by the length of spreading code with Walsh code for $N = 8, 16, 32, 64, 128$. The simulation results also show a great improvement on output SINR for a given number of users by increasing the length of spreading code.

3.7 Summary

In this chapter, we have discussed nonblind and blind 2-D RAKE receivers. The 2-D RAKE receivers appear to be a promising approach to increasing the capacity of CDMA systems. Several algorithms have been compared. The training-signal based nonblind 2-

D RAKE receivers are straightforward, and their performances are better than the blind methods. However, they waste the spectrum or the time resources and may suffer from problems in a fast fading environment. On the contrary, the blind 2-D RAKE receivers do not need to know any training signal, but more computational load is usually needed. The joint processing methods, which take the spatial and the temporal dimensions together into consideration, exhibit better performance than the separate processing methods.

We also compare the performance of linear space-time multiuser and single-user DS/CDMA receivers. As long as they have enough degrees of freedom, they can retain near-far resistance. However, in a fast fading and overloaded environment, the post-despread methods lack the degree of freedom and suffer the near-far problem. The pre-despread methods have relatively more degrees of freedom for suppressing the MAI and exhibit better performance, but they require more computational complexity and a large number of filter taps. They are hard to implemente and exhibit poor convergence in the adaptive mode. In order to reduce the computational complexity, we propose the sectorization concept in which reduced-dimensional beamspace data are processed. Beamspace processing techniques not only reduce the computational complexity but also suppress out-of-sector MAI. In the next chapter, we will propose three beamspace-time 2-D RAKE receivers for sectored CDMA systems.
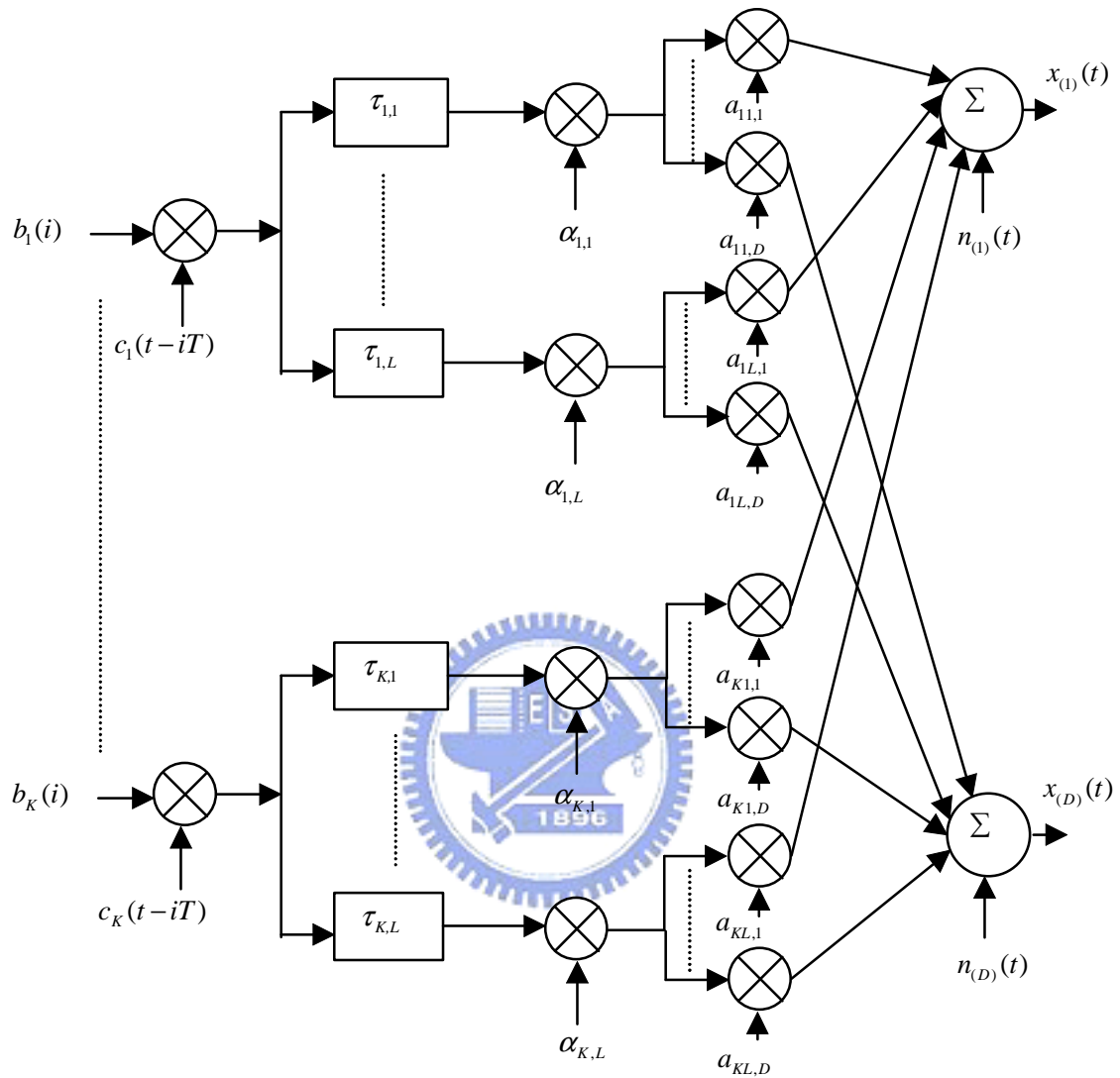
Figure 3.1: Scheme of multiple input multiple output (MIMO) model

69
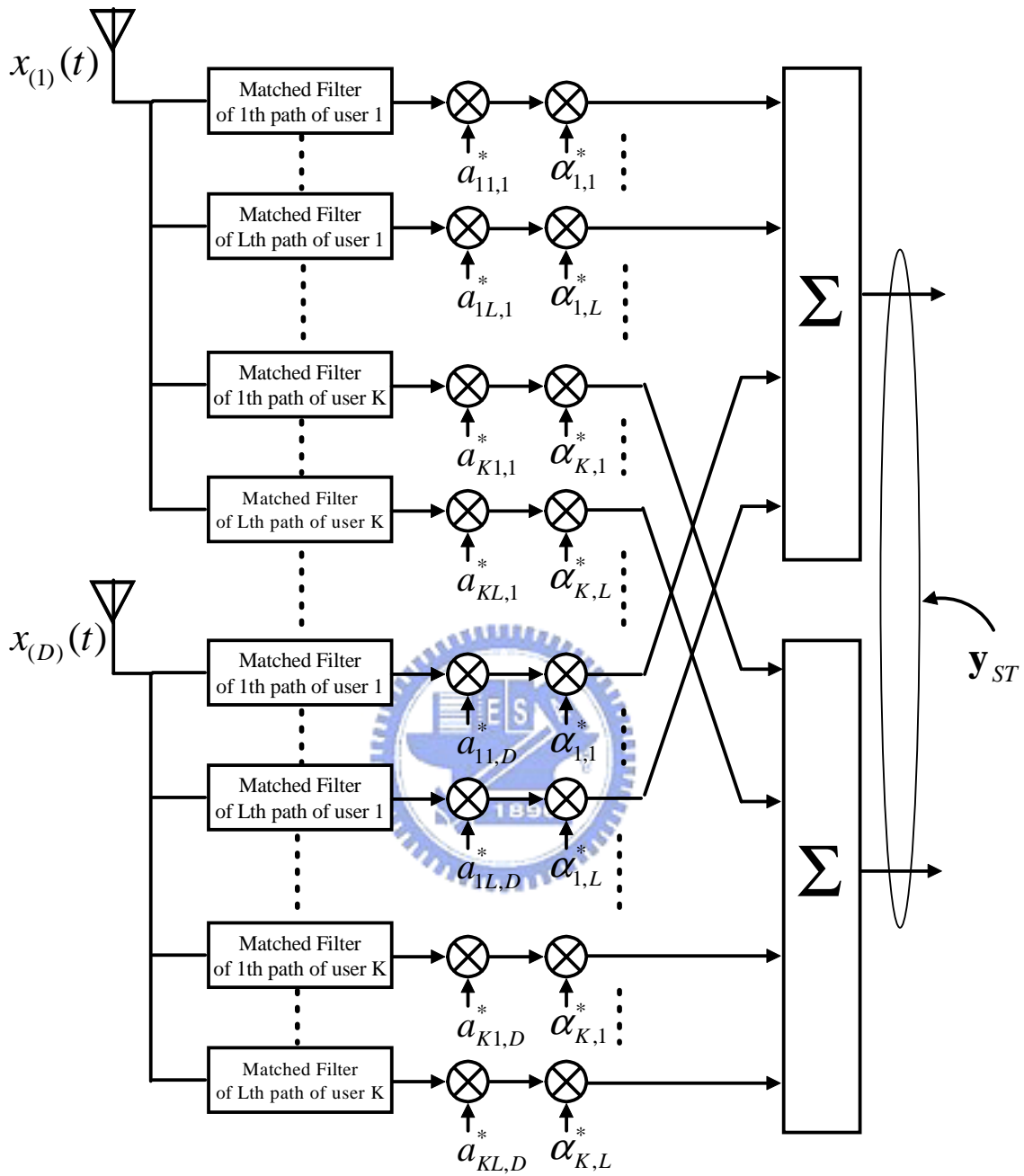
Figure 3.2: Optimal ST multiuser receiver
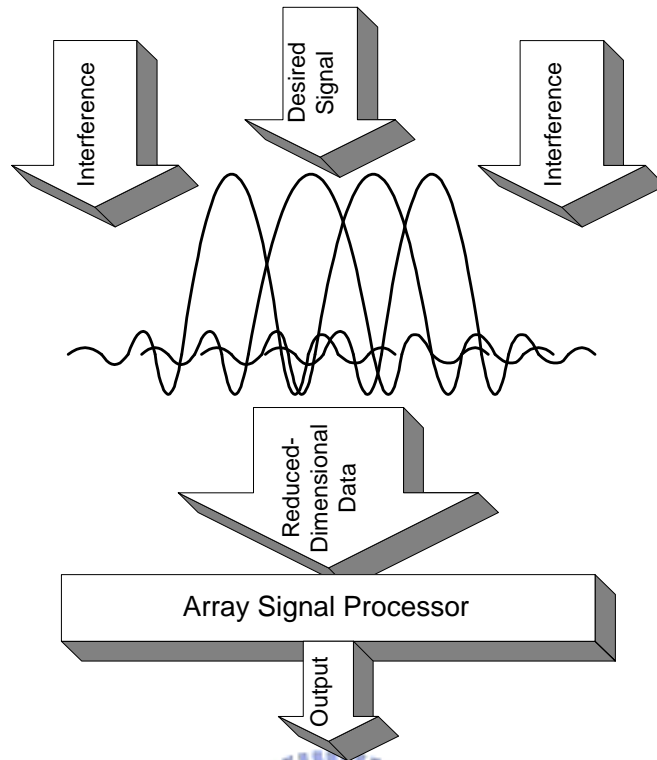
Figure 3.3: Beamspace processing for antenna array
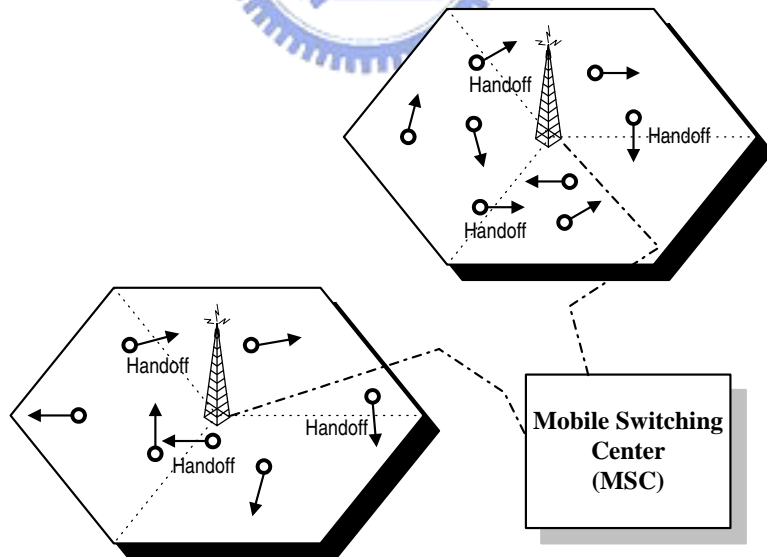
Figure 3.4: Conventional sectored wireless systems
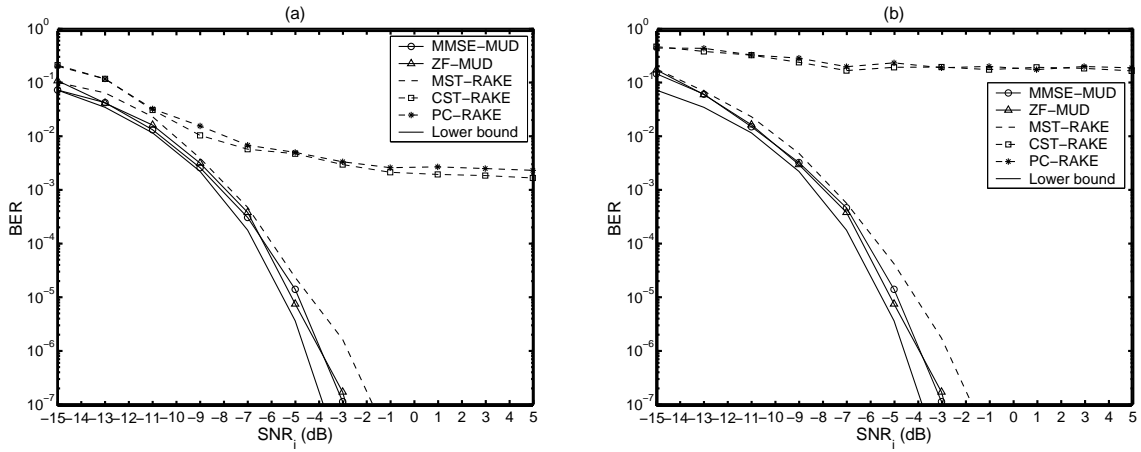
Figure 3.5: Probability of bit error versus input SNR, with $K = 5$, (a) NFR = 0 dB, and (b) NFR = 20 dB.
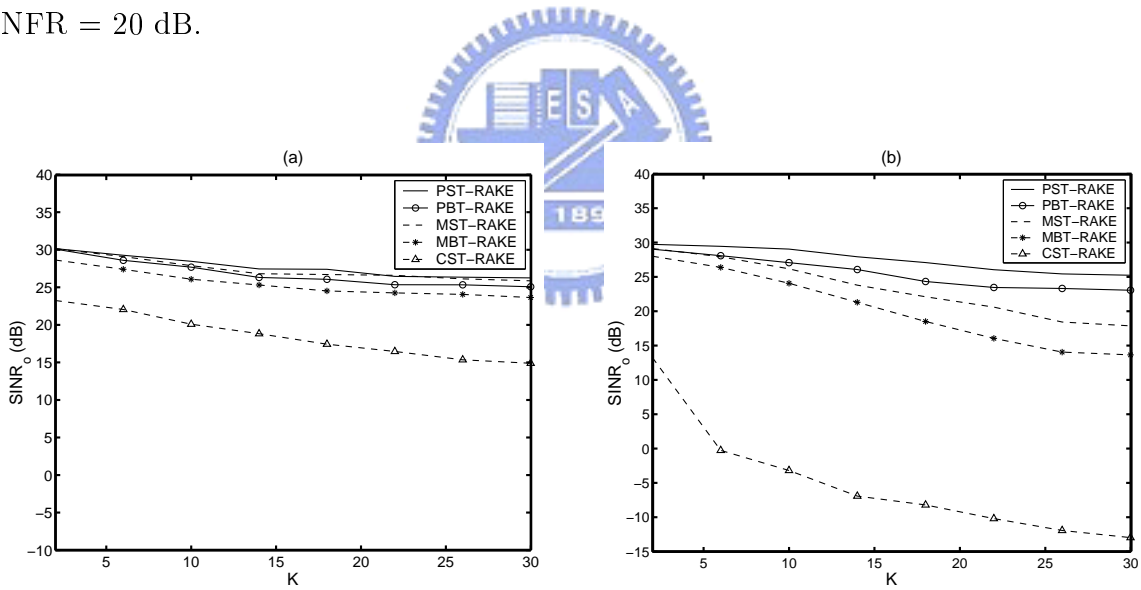
Figure 3.6: Output SINR versus number of users K, with $\mathrm{SNR}_i = 0$ dB, (a) NFR = 0 dB, and (b) NFR = 20 dB.
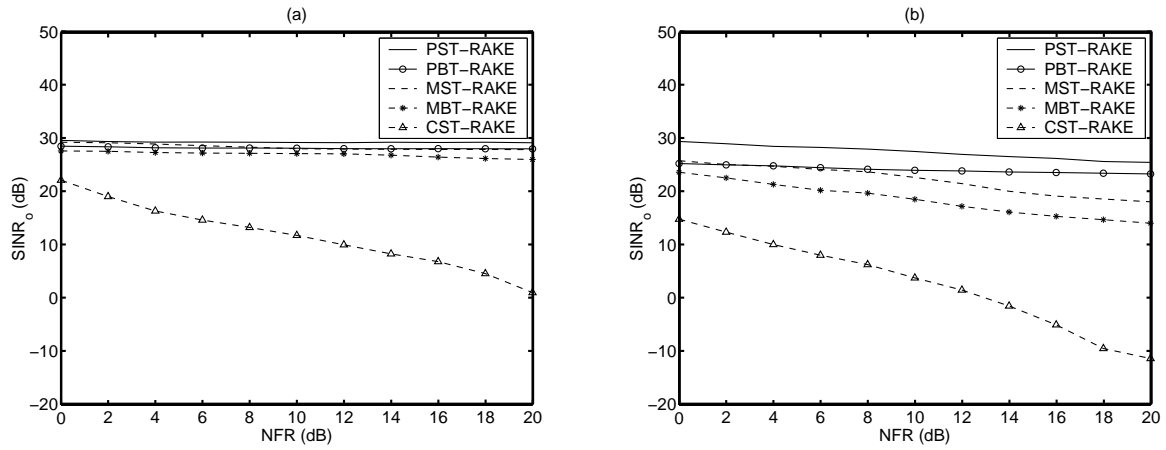
Figure 3.7: Output SINR versus near-far ratio NFR, with $\mathrm{SNR}_i = 0$ dB, (a) $K = 5$ users, and (b) $K = 25$ users.
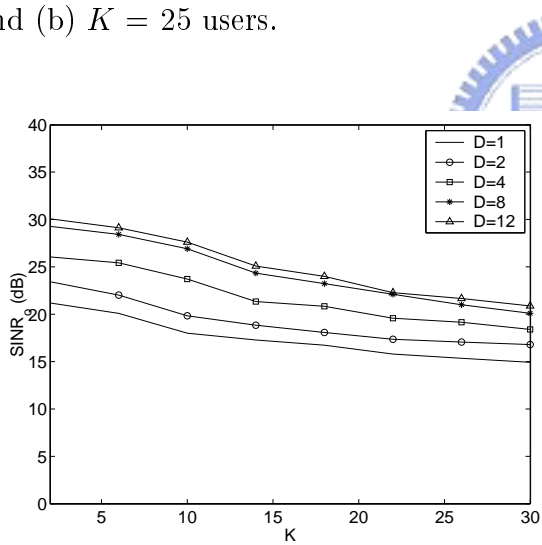
Figure 3.8: Output SINR of Post-ST MMSE receiver versus number of users K, with $\mathrm{SNR}_i = 0$ dB, $N = 31$, and NFR = 10 dB.
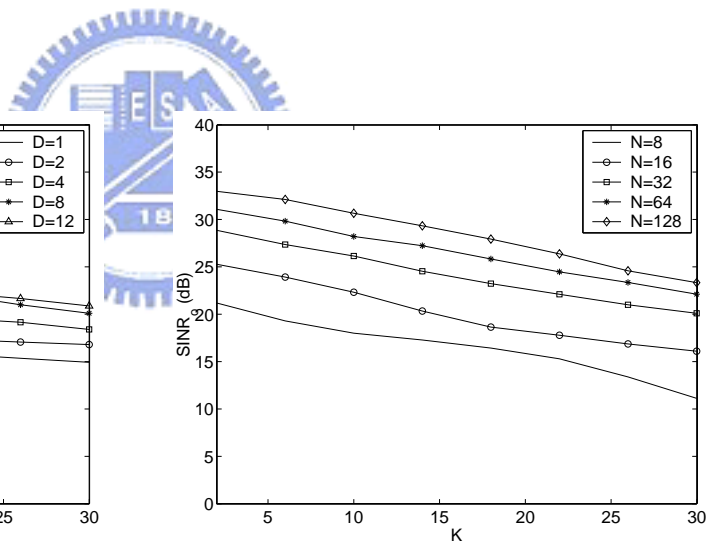
Figure 3.9: Output SINR of Post-ST MMSE receiver versus length of spreading code, with $\mathrm{SNR}_i = 0$ dB, $D = 8$, and NFR = 10 dB.

Chapter 4

Proposed Beamspace-Time 2-D RAKE Receivers for Sectored CDMA Communication Systems

Most existing cellular and PCS systems usually make use of sectoring, in which each cell is divided into several angular regions. Typically, each cell is divided into 3 sectors which are 120° wide or 6 sectors which are 60° wide [1, 64, 66]. It is useful to consider to utilize adaptive beamspace diversity techniques for sectored signal reception [82].

In this chapter, we proposed some beamspace-time receivers for interference suppression and multipath diversity reception in sectored wireless DS/CDMA communications. The scheme involves two processors, a set of adaptive beamformers and a set of adaptive correlators (or a set of matched filter bank), which are jointly or cascaded employed. The set of adaptive beamformers is constructed which provides effective suppression of unwanted interference and reception of signals from a prescribed working sector. The set of adaptive correlators is constructed to suppress the in-sector strong MAI and to receive the diversity paths from prescribed time region. Finally, the output data obtained by these processors are maximum ratio combined to capture the signal multipath components coherently. The proposed BT receivers are blind in that no training signal is needed. The only information required is the signature sequence, timing and a rough estimate of the angle of arrival of the signal for selecting the sector of interest.

4.1 A Beamspace-Time Blind 2-D RAKE Receiver for Sectored CDMA Systems

In this section, an adaptive ST 2-D RAKE receiver is proposed for sectored CDMA systems [64]. In a sectored system, the entire field-of-view of the receiver is divided into several angular sectors, with each sector responsible for a distinctive set of users. With an antenna array incorporated, sectorization can be done adaptively to meet the following two requirements. First, multiple beams are formed to collect desired signal multipath components in a designated angular sector. Second, strong MAI from outside the sector are suppressed in the sidelobe of these beams. These can be achieved by performing adaptive nulling on a set of beams steered to different look directions. To avoid signal cancellation incurred with coherent multipaths or mismatch of steering vectors in adaptive nulling, a modified GSC is employed to construct a set of linearly constrained minimum variance (LCMV) beamformers [55]. The output of these beamformers are processed by a bank of adaptive correlators, which can be regarded as a set of LCMV combiners in the time domain. A modified GSC is again employed to collect the multipath components and suppress the in-sector MAI. The beamformers and correlators together constitute a pre-despread beamspace-time (BT) processor, which performs the function of a RAKE receiver. With MAI successfully suppressed, a simple maximum ratio combining (MRC) criterion can be used to determine the weights of the BT RAKE receiver. Compared to the conventional ST receiver, beamspace sectored processing can potentially increase the system capacity by suppressing out-of-sector MAI, and also lower the computational complexity by reducing the spatial dimension. The proposed BT receiver is blind in that the construction of adaptive beamformers, correlators, and MRC is done without the aid of a training signal. The only information required is the spreading sequence, timing and a rough estimate of the AOA of the desired signal for sector selection. Compared to conventional ST CDMA receivers [30, 56, 87], in which spatial processing is done by direct beamforming, the proposed receiver performs "beamspace" beamforming in which array data are first pre-processed by a set of diversity beamformers encompassing an angular sector. This has two advantages. First, with sectorization, the capacity of the system can be potentially increased. Second, MAI and NBI from outside the

sector can be suppressed adaptively, leading to improved reception quality for the SOI. As for adaptive correlators in GSC form, the proposed receiver is similar to that of [87]. A major distinction, however, is that the proposed method works with a temporal blocking matrix designed to eliminate all multipath signals instead of just a specific path. This can avoid signal cancellation incurred with coherent multipaths. In particular, a simple and effective partially adaptive implementation is suggested to reduce the adaptive weights dimension. Furthermore, with sectorization, only a rough AOA estimator (to determine the right sector) is needed for beamforming. In contrast, the method in [87] relies on ML AOA estimation which requires a small multipath angle spread. In summary, the proposed receiver is designed to combat strong interference by adaptive spatial pre-processing (diversity beamforming), to incorporate pre-despread temporal processing to enhance suppression of in-sector MAI, and to handle multipaths by spatial/temporal post-processing (maximum ratio combining).

The proposed BT RAKE receiver is developed via the following three-stage procedure. First, a set of adaptive diversity beamformers is constructed for each finger to collect in-sector signals and suppress out-of-sector MAI. Second, a set of adaptive correlators is attached to each beamformer to perform despreading and in-sector MAI suppression. Finally, the correlator outputs are combined coherently for an optimal detection of signal symbols. For the ease of notation, the subscript 1 will be omitted in the expressions of data associated with user 1, which is the desired user.

4.1.1 Construction of Adaptive Beamformers

Suppose that the field-of-view of the receiver is divided into several sectors, and that the AOA's and delays of the multipaths of the SOI (user 1) are roughly known such that an angular sector Θ_s and a time duration T_D can be chosen to accommodate these multipaths. With an antenna array employed, the sectorization can be achieved by forming a set of M diversity beams for each of the L fingers, with the beam patterns encompassing the designated sector. Specifically, the beamformers for the lth finger act on the post-despread data vector given by

$$\tilde{\mathbf{x}}_l(i) = \mathbf{X}(i)\mathbf{c}_{1,l}^*$$

76

$$= \mathbf{H}_{ST}\mathbf{c}_{1,l}^{*}b_1(i) + \mathbf{I}(i)\mathbf{c}_{1,l}^{*} + \mathbf{N}(i)\mathbf{c}_{1,l}^{*} \tag{4.1}$$

where $\mathbf{X}(i)$ and $\mathbf{H}_{ST}$ are defined in (3.25) and (3.27), and $\mathbf{c}_{1,l}$ is the lth column of the augmented signature matrix of user 1 in (2.11). After despreading, $\tilde{\mathbf{x}}_l(i)$ contains essentially the strong MAI and multipath signals of the delay corresponding to $\mathbf{c}_{1,l}$. To ensure an effective suppression of strong out-of-sector MAI, adaptive nulling is performed for each of the diversity beamformers. A popular nulling scheme is based on the LCMV criterion [55], which says that the beamforming weight vector should be chosen in accordance with

$$\min_{\mathbf{w}_{l,m}} \quad \mathbf{w}_{l,m}^{H}\mathbf{R}_{\tilde{\mathbf{x}}_l}\mathbf{w}_{l,m}$$

$$\text{subject to: } \mathbf{w}_{l,m}^{H}\mathbf{a}(\theta_m) = 1 \tag{4.2}$$

for $l = 1, \ldots, L$ and $m = 1, \ldots, M$, where $\mathbf{w}_{l,m}$ is the weight vector of the mth beamformer at the lth finger,

$$\mathbf{R}_{\tilde{\mathbf{x}}_l} = E\left\{\tilde{\mathbf{x}}_l(i)\tilde{\mathbf{x}}_l^{H}(i)\right\} \tag{4.3}$$

is the post-despread space-only data correlation matrix at the lth finger. Finally, θ_m is the look angle of the mth beam. A major problem of the LCMV beamformer is the phenomenon of desired signal cancellation [83] due to the mismatch between the look angle steering vectors $\mathbf{a}(\theta_m)$'s and the actual steering vectors associated with the multipath signals. By signal cancellation, it is meant that with a certain mismatch, the weight vector in (4.2) will tend to treat the signal as interference, and attempt to cancel it in order to minimize the output power. The sensitivity of the LCMV beamformer to steering vector mismatch increases as the array size D or SNR increases, in which case the beamformer will put more efforts to cancel the signal. An effective remedy suggested herein is to use a modified GSC to block the signal before beamforming [55]. The GSC is essentially an indirect but simpler implementation of the LCMV beamformer. In GSC, the weight vector is decomposed as $\mathbf{w}_{l,m} = \mathbf{a}(\theta_m) - \mathbf{B}_a\mathbf{v}_{l,m}$ into two orthogonal components which lie in the range and null space of the constraint, respectively. The matrix $\mathbf{B}_a$ is a pre-designed "signal blocking" matrix which removes the signal (and MAI) in the sector. The goal is then to choose the adaptive

weight vector $\mathbf{v}_{l,m}$ to cancel the out-of-sector MAI. Following the standard procedure of GSC, the adaptive weight vectors are determined by solving the MMSE problem:

$$\min_{\mathbf{v}_{l,m}} \quad E\{|\mathbf{a}^H(\theta_m)\tilde{\mathbf{x}}_l(i) - \mathbf{v}_{l,m}^H\mathbf{B}_a^H\tilde{\mathbf{x}}_l(i)|^2\} \tag{4.4}$$

or equivalently

$$\min_{\mathbf{v}_{l,m}} \quad [\mathbf{a}(\theta_m) - \mathbf{B}_a\mathbf{v}_{l,m}]^H\mathbf{R}_{\tilde{\mathbf{x}}_l}[\mathbf{a}(\theta_m) - \mathbf{B}_a\mathbf{v}_{l,m}] \tag{4.5}$$

Taking the gradient of (4.5) with respect to $\mathbf{v}_{l,m}$ and setting to zero, we have

$$\mathbf{B}_a^H\mathbf{R}_{\tilde{\mathbf{x}}_l}[\mathbf{a}(\theta_m) - \mathbf{B}_a\mathbf{v}_{l,m}] = \mathbf{0} \tag{4.6}$$

which gives

$$\mathbf{v}_{l,m} = (\mathbf{B}_a^H\mathbf{R}_{\tilde{\mathbf{x}}_l}\mathbf{B}_a)^{-1}\mathbf{B}_a^H\mathbf{R}_{\tilde{\mathbf{x}}_l}\mathbf{a}(\theta_m) \tag{4.7}$$

Substituting this in $\mathbf{w}_{l,m} = \mathbf{a}(\theta_m) - \mathbf{B}_a\mathbf{v}_{l,m}$ and putting in matrix form, we get

$$\begin{aligned} \mathbf{W}_l &= [\mathbf{w}_{l,1}, \ldots, \mathbf{w}_{l,M}] \\ &= [\mathbf{I} - \mathbf{B}_a(\mathbf{B}_a^H\mathbf{R}_{\tilde{\mathbf{x}}_l}\mathbf{B}_a)^{-1}\mathbf{B}_a^H\mathbf{R}_{\tilde{\mathbf{x}}_l}][\mathbf{a}(\theta_1), \ldots, \mathbf{a}(\theta_M)] \end{aligned} \tag{4.8}$$

for $l = 1, \ldots, L$.

The choosing of the blocking matrix $\mathbf{B}_a$ depends on the sector size and required degree of freedom of the adaptive weight vector $\mathbf{v}_{l,m}$. Let $\mathbf{v}_{l,m}$ be a $D' \times 1$ vector. Then $\mathbf{B}_a$ can be chosen to be a full rank $D \times D'$ matrix with columns orthogonal to a set of steering vectors $\{\mathbf{a}(\theta_1^t), \mathbf{a}(\theta_2^t), \ldots, \mathbf{a}(\theta_{D-D'}^t)\}$ well representing the desired sector. As an alternative, the set of steering vectors can be replaced by the eigenvectors associated with the $D - D'$ largest eigenvalues of the matrix:

$$\mathbf{A}_{\Theta_s} = \int_{\Theta_s} \mathbf{a}(\theta)\mathbf{a}^H(\theta)d\theta \tag{4.9}$$

leading to the eigenvector constrained method [84]. The advantage of using eigenvector constraints lies in its fuzzy mode of operation, which offers robustness to the variation in multipath scenario of the signal. The choosing of D' is a trade-off between the blocking effect and adaptive nulling performance. In general, a small D' gives better "mainlobe performance" (reception of desired signal), and a large D' gives better "sidelobe performance"

(suppression of out-of-sector MAI). A practical criterion is that the ratio $(D - D')/D$ is approximately equal to the ratio of the sector size to entire field-of-view of the antenna array. That is, the degree of freedom $D - D'$ for blocking is proportional to the relative size of the sector. However, numerical results show that a smaller D' is required to warrant a "clean" blocking effect for better handling the signal cancellation problem. With the assumption that a single sector is responsible for about one third the field-of-view of the antenna array, a suitable choice for D' would be $D/2$.

4.1.2 Construction of Adaptive Correlators

The beamforming matrices $\mathbf{W}_l$'s are applied at the L fingers to convert the $D \times (N + L - 1)$ ST chip-sampled data matrix $\mathbf{X}(i)$ into a set of L BT data matrices of dimension $M \times (N + L - 1)$:

$$
\begin{aligned}
\mathbf{Y}_l(i) &= \mathbf{W}_l^H \mathbf{X}(i) \\
&= \begin{bmatrix} \mathbf{y}_{l,1}^T(i) \\ \mathbf{y}_{l,2}^T(i) \\ \vdots \\ \mathbf{y}_{l,M}^T(i) \end{bmatrix}
\end{aligned} \tag{4.10}
$$

for $l = 1, \ldots, L$, where $\mathbf{y}_{l,m}(i)$ is the chip-sampled data vector obtained at the mth beam of the lth finger, given by

$$
\begin{aligned}
\mathbf{y}_{l,m}(i) &= \mathbf{X}^T(i)\mathbf{w}_{l,m}^* \\
&= \mathbf{H}_{ST}^T \mathbf{w}_{l,m}^* b_1(i) + \mathbf{I}^T(i)\mathbf{w}_{l,m}^* + \mathbf{N}^T(i)\mathbf{w}_{l,m}^*
\end{aligned} \tag{4.11}
$$

The next step is then to perform despreading on $\mathbf{y}_{l,m}(i)$ to restore the processing gain. In order to better handle the MAI, this is done with an adaptive correlator as follows:

$$
\begin{aligned}
z_{l,m}(i) &= \mathbf{s}_{l,m}^H \mathbf{y}_{l,m}(i) \\
&= \mathbf{w}_{l,m}^H \mathbf{X}(i)\mathbf{s}_{l,m}^* \\
&= \mathbf{w}_{l,m}^H \mathbf{H}_{ST}\mathbf{s}_{l,m}^* b_1(i) + \mathbf{w}_{l,m}^H \mathbf{I}(i)\mathbf{s}_{l,m}^* + \mathbf{w}_{l,m}^H \mathbf{N}(i)\mathbf{s}_{l,m}^*
\end{aligned} \tag{4.12}
$$

where $\mathbf{s}_{l,m}$ is the despreading weight vector of the mth beam at the lth finger. As the temporal analogy of the beamforming weight vector $\mathbf{w}_{l,m}$, $\mathbf{s}_{l,m}$ can be determined using

79

the GSC scheme described above with the steering vector $\mathbf{a}(\theta)$ replaced by the augmented signature vector $\mathbf{c}_{1,l}$. Following the development in (4.2)-(4.8), we have $\mathbf{s}_{l,m} = \mathbf{c}_{1,l} - \mathbf{B}_c \mathbf{g}_{l,m}$, where $\mathbf{B}_c$ is the signal blocking matrix which removes user 1's signal. Note that instead of blocking signals with a specific delay, $\mathbf{B}_c$ must block signals within the entire delay spread in order to avoid signal cancellation due to coherent multipaths. The goal is then to choose the adaptive weight vectors $\mathbf{g}_{l,m}$ to cancel the in-sector MAI (and possibly out-of-sector MAI not canceled by the beamformers). Similar to GSC beamforming, the adaptive weight vectors are determined by

$$\min_{\mathbf{g}_{l,m}} \quad E\{|\mathbf{c}_{1,l}^H \mathbf{y}_{l,m}(i) - \mathbf{g}_{l,m}^H \mathbf{B}_c^H \mathbf{y}_{l,m}(i)|^2\} \tag{4.13}$$

or equivalently

$$\min_{\mathbf{g}_{l,m}} \quad [\mathbf{c}_{1,l} - \mathbf{B}_c \mathbf{g}_{l,m}]^H \mathbf{R}_{\mathbf{y}_{l,m}} [\mathbf{c}_{1,l} - \mathbf{B}_c \mathbf{g}_{l,m}] \tag{4.14}$$

where

$$\mathbf{R}_{\mathbf{y}_{l,m}} = E\left\{ \mathbf{y}_{l,m}(i) \mathbf{y}_{l,m}^H(i) \right\} \tag{4.15}$$

is the pre-despread time-only data correlation matrix at the mth beam of the lth finger. Solving for $\mathbf{g}_{l,m}$ in the same way as for $\mathbf{v}_{l,m}$, and substituting in $\mathbf{s}_{l,m} = \mathbf{c}_{1,l} - \mathbf{B}_c \mathbf{g}_{l,m}$, we get

$$\mathbf{s}_{l,m} = [\mathbf{I} - \mathbf{B}_c (\mathbf{B}_c^H \mathbf{R}_{\mathbf{y}_{l,m}} \mathbf{B}_c)^{-1} \mathbf{B}_c^H \mathbf{R}_{\mathbf{y}_{l,m}}] \mathbf{c}_{1,l} \tag{4.16}$$

for $l = 1, \ldots, L$ and $m = 1, \ldots, M$.

The choosing of the temporal blocking matrix $\mathbf{B}_c$ is similar to the choosing of $\mathbf{B}_a$. That is, $\mathbf{B}_c$ can be chosen to be a full rank $(N+L-1) \times (N-1)$ matrix with columns orthogonal to the set of augmented signature vectors $\{\mathbf{c}_{1,1}, \mathbf{c}_{1,2}, \ldots, \mathbf{c}_{1,L}\}$ well representing the multipath delay spread. For a more reliable operation, extra signature vectors can be included to extend the blocking interval to a larger delay spread. This will help to avoid possible signal cancellation due to undetected multipath arrivals. For example, two extra signature vectors

$$\mathbf{c}_{1,1}^{(-)} = [c_{1,1}[1], c_{1,1}[2], \ldots, c_{1,1}[N-1], 0, \ldots, 0]^T$$

$$\mathbf{c}_{1,L}^{(+)} = [0, \ldots, 0, c_{1,1}[0], c_{1,1}[1], \ldots, c_{1,1}[N-2]]^T \tag{4.17}$$

can be added to the original set to extend by one chip at both ends of the blocking interval.

Note that the above ST processors is developed based on the assumption of short spreading codes. Although the adaptive beamformers can be used with long codes, the adaptive correlators cannot. This is because that the adaptive correlators are designed to respond to fixed temporal signatures (composite spreading codes due to multipaths). Only with fixed temporal signatures can the adaptive correlators "recognize" and suppress strong MAI.

4.1.3 Maximum Ratio Combiner

Suppose that, after adaptive beamforming and despreading, the MAI are successfully suppressed, the correlator outputs $z_{l,m}(i)$'s contain essentially the desired signal and colored noise only. In this case, the MRC criterion can be applied to combine these outputs coherently to extract the signal. Let

$$
\begin{aligned}
\mathbf{z}(i) \quad = \quad & [z_{1,1}(i), \ldots, z_{1,M}(i), z_{2,1}(i), \ldots, z_{2,M}(i), \ldots, \\
& z_{L,1}(i), \ldots, z_{L,M}(i)]^T \approx \mathbf{h}_z b_1(i) + \mathbf{n}_z(i)
\end{aligned}
\tag{4.18}
$$

be the beamspace correlator output data vector, with $\mathbf{h}_z$ and $\mathbf{n}_z(i)$ being the corresponding composite signature and noise vectors, respectively, given by

$$
\begin{aligned}
\mathbf{h}_z \quad = \quad & \big[\mathbf{w}_{1,1}^H \mathbf{H}_{ST} \mathbf{s}_{1,1}^*, \ldots, \mathbf{w}_{1,M}^H \mathbf{H}_{ST} \mathbf{s}_{1,M}^*, \mathbf{w}_{2,1}^H \mathbf{H}_{ST} \mathbf{s}_{2,1}^*, \ldots, \\
& \mathbf{w}_{2,M}^H \mathbf{H}_{ST} \mathbf{s}_{2,M}^*, \ldots, \mathbf{w}_{L,1}^H \mathbf{H}_{ST} \mathbf{s}_{L,1}^*, \ldots, \mathbf{w}_{L,M}^H \mathbf{H}_{ST} \mathbf{s}_{L,M}^* \big]^T
\end{aligned}
\tag{4.19}
$$

$$
\begin{aligned}
\mathbf{n}_z(i) \quad = \quad & \big[\mathbf{w}_{1,1}^H \mathbf{N}(i) \mathbf{s}_{1,1}^*, \ldots, \mathbf{w}_{1,M}^H \mathbf{N}(i) \mathbf{s}_{1,M}^*, \mathbf{w}_{2,1}^H \mathbf{N}(i) \mathbf{s}_{2,1}^*, \ldots, \\
& \mathbf{w}_{2,M}^H \mathbf{N}(i) \mathbf{s}_{2,M}^*, \ldots, \mathbf{w}_{L,1}^H \mathbf{N}(i) \mathbf{s}_{L,1}^*, \ldots, \mathbf{w}_{L,M}^H \mathbf{N}(i) \mathbf{s}_{L,M}^* \big]^T
\end{aligned}
\tag{4.20}
$$

The final operation of the receiver is then a linear combination on $\mathbf{z}(i)$ using an $ML \times 1$ weight vector $\mathbf{f}_{mrc}$:

$$
z_o(i) = \mathbf{f}_{mrc}^H \mathbf{z}(i)
\tag{4.21}
$$

The weight vector $\mathbf{f}_{mrc}$ that leads to MRC can be determined by solving the following problem [63]:

$$
\max_{\mathbf{f}_{mrc}} \quad \frac{E\{|\mathbf{f}_{mrc}^H \mathbf{z}(i)|^2\}}{E\{|\mathbf{f}_{mrc}^H \mathbf{n}_z(i)|^2\}} = \frac{\mathbf{f}_{mrc}^H \mathbf{R}_z \mathbf{f}_{mrc}}{\mathbf{f}_{mrc}^H \mathbf{Q}_z \mathbf{f}_{mrc}}
\tag{4.22}
$$

where $\mathbf{R}_z = E\{\mathbf{z}(i)\mathbf{z}^H(i)\}$ and $\mathbf{Q}_z = E\{\mathbf{n}_z(i)\mathbf{n}_z^H(i)\}$ are the beamspace correlator output data and noise correlation matrices, respectively. Note that $\mathbf{Q}_z$ can be determined with the knowledge of $\mathbf{w}_{l,m}$'s, $\mathbf{s}_{l,m}$'s, and the whiteness of $\mathbf{N}(i)$. The solution to (4.22) is well known to be the principle generalized eigenvector of the matrix pair $\{\mathbf{R}_z, \mathbf{Q}_z\}$. As a final remark, we point out that, as opposed to the conventional ST 2-D RAKE receiver in which a single beam is responsible for a finger, the proposed BT 2-D RAKE receiver requires M beams for a finger. This is because that the BT 2-D RAKE receiver does not have the exact AOA or channel information about the signal paths. So the best strategy would be to "collect" the in-sector multipath signals using a set of diversity beams encompassing the entire sector. In fact, using multiple beams for a single finger is the price in complexity paid for not using a training sequence.

4.1.4 AOA Estimation and Sector Selection

To determine the working sector Θ_s, some kind of location techniques are required to obtain a coarse estimate of the signal AOA. For the proposed receiver, a suitable choice is the multi-beam (MB) technique described in [85]. The MB technique works with a bank of beams pointed at different directions, and determines the signal AOA by comparing the signal power levels observed at these beamformer outputs. The beamformer with the maximum output power is likely to be the one pointed at the signal, and its look direction is taken to be the estimate of the signal AOA. Finally, the working sector is chosen to be the one that contains the estimated AOA. To apply the MB technique in the proposed receiver, a set of beams is formed simultaneously whose patterns encompass the entire field-of-view of the antenna array. Power comparison is then performed on the post-despread data observed at these beamformer outputs to determine the signal AOA and sector location. In a nonstationary environment in which the signal source moves with time, it is necessary to keep track of the signal to update the working sector via some prescribed hand-off procedure. A more detailed description about AOA estimation will be given shortly in Section 4.2.3.

4.1.5 Algorithm Summary

In practice, the data correlation matrices are usually estimated by the sample average versions:

$$\mathbf{R}_{\tilde{\mathbf{x}}_{l,m}} \approx \frac{1}{N_s} \sum_{i=1}^{N_s} \tilde{\mathbf{x}}_l(i) \tilde{\mathbf{x}}_l^H(i) \tag{4.23}$$

$$\mathbf{R}_{\mathbf{y}_{l,m}} \approx \frac{1}{N_s} \sum_{i=1}^{N_s} \mathbf{y}_{l,m}(i) \mathbf{y}_{l,m}^H(i) \tag{4.24}$$

$$\mathbf{R}_z \approx \frac{1}{N_s} \sum_{i=1}^{N_s} \mathbf{z}(i) \mathbf{z}^H(i) \tag{4.25}$$

where $\tilde{\mathbf{x}}_l(i)$, $\mathbf{y}_{l,m}(i)$ and $\mathbf{z}(i)$ are given by (4.1), (4.11) and (4.18), respectively, and N_s is the number of symbols used during the processing period. With these estimates, the algorithm of the proposed BT RAKE receiver is summarized as follows:

1. Determine working sector Θ_s, look angles θ_m's and GSC blocking matrices $\mathbf{B}_a$ and $\mathbf{B}_c$.

2. Compute in parallel $\mathbf{W}_l$, $l = 1, \ldots, L$, according to (4.8), with $\mathbf{R}_{\tilde{\mathbf{x}}_{l,m}}$ estimated by (4.23).

3. Compute in parallel $\mathbf{s}_{l,m}$, $l = 1, \ldots, L$, $n = 1, \ldots, M$, according to (4.16), with $\mathbf{R}_{\mathbf{y}_{l,m}}$ estimated by (4.24).

4. Obtain $\mathbf{Q}_z$ and compute $\mathbf{f}_{mrc}$ according to (4.22), with $\mathbf{R}_z$ estimated by (4.25).

The corresponding schematic diagram is depicted in Figure 4.1.

4.1.6 Recursive Computation of Weight Vectors

For a more efficient and practical implementation, the GSC can be realized in a time-recursive fashion using stochastic gradient algorithms such as least mean square (LMS) [21]. This leads to recursive formulation of the solutions to (4.4) and (4.13), respectively:

$$\mathbf{v}_{l,m}(i+1) = \mathbf{v}_{l,m}(i) + \mu_v \left[\mathbf{a}^H(\theta_m) \tilde{\mathbf{x}}_l(i) - \mathbf{v}_{l,m}^H \mathbf{B}_a^H \tilde{\mathbf{x}}_l(i) \right]^* \mathbf{B}_a^H \tilde{\mathbf{x}}_l(i) \tag{4.26}$$

$$\mathbf{g}_{l,m}(i+1) = \mathbf{g}_{l,m}(i) + \mu_g \left[\mathbf{c}_{1,l}^H \mathbf{y}_{l,m}(i) - \mathbf{g}_{l,m}^H \mathbf{B}_c^H \mathbf{y}_{l,m}(i) \right]^* \mathbf{B}_c^H \mathbf{y}_{l,m}(i) \tag{4.27}$$

for $i = 1, 2, \ldots$, where μ_v and μ_g are the stepsizes of adaptation. It was shown that the convergence of blind adaptive algorithms is slow and noisy compared to the non-blind training signal based algorithm. This is more significant when the dimension of weight vectors and/or SNR is large. In view of this drawback, it is suggested that blind algorithms be employed in the initialization stage, and be switched to the decision-directed mode once the SINR has improved to offer a reliable decision reference [33]. In the decision-directed mode, the detected symbols are treated as correct and fed back as a training signal to "direct" the operation of the MMSE receiver. Of course, blindly detected symbols contain an arbitrary phase rotation which should be removed by incorporating differential encoding, or a short training sequence (much shorter than would be needed for regular training based methods).

On the other hand, the generalized eigenvector required for the computation of the MRC weight vector in (4.22) can be also obtained via a time-recursive algorithm without the need of a complicated eigenvalue decomposition (EVD) [63, 86]. The required computational complexity is of the order NL (BT dimension) per iteration. The adaptive algorithm of the proposed BT receiver is summarized in Table 4.1.

4.1.7   Partially Adaptive Implementation

The degree of freedom for the adaptive correlators is on the order of N, which can be quite large in wideband applications. A large degree of freedom requires a high computational complexity and is likely to incur poor convergence behaviors [55]. To alleviate this, partially adaptive (PA) methods can be applied to reduce the dimension of $\mathbf{g}_{l,m}$'s. Partial adaptivity can be achieved by either working with a reduced-size input data or with a reduced-size blocking matrix [38, 39]. A more detailed description about partially adaptive receivers will be given in Section 6.2.

4.1.8   Complexity and Performance

The trade-off between system performance and computational complexity is an issue depending on the number of antennas D and processing gain N of the system. In general, more antennas and a larger processing gain will provide better interference suppression, but lead

to high computational complexity and poor convergence behaviors. However, the spatial and temporal dimensions (D and N) do not affect the complexity of the eigenvector computation in MRC because the MRC weight vector has a size of ML, regardless of D and N. The major computations in the proposed algorithm involves the inversion of $(\mathbf{B}_c^H \mathbf{R}_{\mathbf{y}_{l,m}} \mathbf{B}_c)^{-1}$ with size $(N-1) \times (N-1)$ in (4.16), inversion of $(\mathbf{B}_a^H \mathbf{R}_{\tilde{\mathbf{x}}_{l,m}} \mathbf{B}_a)^{-1}$ with size $D' \times D'$ in (4.7), and a principal eigenvector computation with size $ML \times ML$ in (4.22). The overall complex is about $O(MLN^3 + MD'^3 + M^3L^3)$. For recursive processing as described in the previous section, the complexity for each iteration is about $O(MLN + MD' + ML)$ for the proposed receiver. With partially adaptive method and parallel computation mechanism, the computational loading will be greatly reduced.

4.1.9　Simulation Results

Computer simulations are conducted to demonstrate the performance the proposed BT GSC based RAKE (GSC1-RAKE) receiver. The antenna employed is a linear array consisting of $D = 8$ identical elements uniformly spaced by a $1/\sqrt{3}$ wavelength. The inter-element spacing is chosen for the field-of-view $[-60°, 60°]$, which represents the effective angular region of operation for a linear array [64]. Note that with the inter-element spacing chosen to be a $1/\sqrt{3}$ wavelength, $D = 8$ orthogonal beams can be formed in the $120°$ region, with two adjacent beams spaced by a half 3-dB beamwidth. The sector of interest in our simulations is $[-20°, 20°]$, and $M = 3$ diversity beams are formed at look directions $\{-12.5°, 0°, 12.5°\}$ to cover the $40°$ region. The blocking matrix $\mathbf{B}_a$ is constructed with $D' = 4$ by the eigenvector constrained method described in [55]. It is assumed that the multipaths of all users followed the discrete uniform distribution model [64] with the same angle spread of $10°$. That is, J paths are generated with their AOA's evenly distributed in a $10°$ angular interval centered at the line-of-sight (LOS) angle of the source. Moreover, the LOS angle of the signal is randomly selected in the working sector, and the LOS angles of the MAI's are randomly selected in the entire $120°$ field-of-view. The path gains $\alpha_{k,j}$'s are assumed independent, identically distributed unit variance complex Gaussian random variables, the path delays $\tau_{k,j}$'s are assumed uniform over $[0, 2T_c]$, and the number of paths is $J = 3$ for all users. All CDMA signals are generated using the Gold code of length $N = 31$. Finally, the number of

85

fingers of the receiver is $L = 3$, and the temporal blocking matrix $\mathbf{B}_c$ is chosen, according to Section 3.2, to be the matrix whose columns are orthogonal to $\{\mathbf{c}_{1,1}, \mathbf{c}_{1,2}, \mathbf{c}_{1,3}\}$.

As a performance index, we defined the output SINR to be the ratio of the signal power to the interference-plus-noise power at the receiver output $z_o(i)$:

$$\text{SINR}_o = 10 \log_{10} \frac{\text{output power of signal in } z_o(i)}{\text{output power of (interference+noise) in } z_o(i)}$$

The input SNR is defined as $\text{SNR}_i = 10 \log_{10} \frac{\sigma_1^2}{\sigma_n^2}$. For simplicity, we assumed that all out-of-sector MAI's had the same power, and defined the near-far-ratio (NFR) to be the ratio of the out-of-sector MAI power to signal power before beamforming and despreading, i.e., $\text{NFR} = 10 \log_{10} \frac{\sigma_k^2}{\sigma_1^2}$ with k belonging to the out-of-sector MAI indices. Except for one case, the in-sector MAI is assumed power controlled with the signal, i.e., $\sigma_k = \sigma_1$ for k belonging to the in-sector MAI indices (this is not strictly necessary since in-sector MAI not power controlled can be suppressed by the adaptive correlators). For each result in the simulations, N_s symbols are used to estimate the correlation matrices, and a total of 50 Monte-Carlo runs are executed to obtain an average SINR_o, with each trial using a different set of $\alpha_{k,j}$'s, $\tau_{k,j}$'s and LOS angles of the users. For comparison, we also included the results obtained with the non-blind ST coherent RAKE (CST-RAKE) and MMSE receivers (MST-RAKE) described in (3.60) and (3.61), respectively, with the channel vector and post-despread ST data correlation matrix using the same N_s symbols as the training signal. The simulation parameters are: $N = 31$ with Gold codes, $L = 3$ fingers, the number of paths $J = 3$, the number of antenna elements $D = 8$, the number of training symbols $N_s = 500$, and the input $\text{SNR}_i = 0$ dB. Unless otherwise mentioned, the above standard parameters will be used throughout the section.

First, the system capacity is evaluated in Figure 4.2 with NFR = 0 dB and 20 dB. As expected, the MST-RAKE gives the best performance with a small user number K and low NFR, in which case both channel estimation and MAI suppression can be done effectively. On the other hand, the proposed GSC receiver (GSC1-RAKE) performs reliably for a wide range of K, even in the presence of strong MAI. In fact, the GSC1-RAKE receiver outperforms the MST-RAKE receiver with a moderately large K and high NFR, indicating that the adaptive beamformers and correlators have successfully eliminated the strong MAI. The CST-RAKE

86

receiver totally fails with NFR = 20 dB due to the lack of MAI suppression.

In Figure 4.3, the patterns of the diversity beams for the first and third fingers are plotted for the case $K = 5$ users and NFR = 10 dB. The mainlobes and deep nulls confirm that the adaptive beamformers can effectively collect the in-sector signals and suppress out-of-sector MAI.

Next, the near-far resistance of the proposed receiver is evaluated with different NFR values. Figure 4.4 shows the results obtained with $K = 5$ and 25 users, with the input SNR equal to 0 dB and $N_s = 500$. It is observed that the CST-RAKE receiver fails again, and the MST-RAKE receiver loses its near-far resistance with $K = 25$ due to the exhaustion of degree of freedom ($8 \times 3 = 24$) for strong MAI suppression. On the contrary, the GSC1-RAKE receiver achieves its excellent near-far resistance by successfully canceling the MAI using the temporal degree of freedom ($31 + 3 - 1 = 33$) offered by the pre-despread chip-sampled data.

To demonstrate the efficacy of the adaptive correlators in handling in-sector MAI, we repeated the same simulation with power control of in-sector MAI "turned off". In this case, the in-sector and out-of-sector MAI had the same power determined by the NFR value. The results shown in Figure 4.5 confirm that the non-power-controlled in-sector MAI have little effect on the GSC1-RAKE receiver even with $K = 25$ since they can be effectively suppressed as long as a sufficient degree of freedom is available for adaptive processing.

Finally, the convergence behaviors of the three RAKE receivers are evaluated by varying the data sample size N_s. The resulting output SINR are plotted in Figure 4.6 with NFR = 0 dB and 20 dB. The number of users is $K = 25$. As expected, the output SINR increases as N_s increases for the three receivers. The MST-RAKE receiver converges significantly faster than the GSC1-RAKE receiver with a low NFR, but loses this advantage in the presence of strong MAI. The GSC1-RAKE receiver achieves 95% of its maximum $SINR_o$ in about 500 symbols, and takes another 500 symbols to reach its full performance. This is observed to be due to the errors in blind beamforming operation. It should be mentioned, however, that the relatively slow convergence of GSC1-RAKE receiver does not raise practical problems since the receiver can be switched to the decision directed mode as long as the MAI has been sufficiently suppressed. From simulation results, we have shown that the proposed RAKE receiver is near-far resistant, and performs reliably in a heavily loaded system.

87

4.2 Space-Time Alternating 2-D RAKE Receiver for Sectored CDMA Systems

In this section, another blind adaptive pre-despread beamspace-time (Pre-BT) receiver is proposed for sectored CDMA communications. The receiver is designed with the following procedure. First, a set of ST diversity processors, in the form of beamformer-correlator (BC) pairs is constructed to collect the multipath signals in a prescribed angular sector and time duration, and to suppress MAI and NBI. This is done by performing adaptive nulling on a set of linearly constrained minimum variance (LCMV) ST processors "steered" to different look directions and delays. To avoid signal cancellation incurred with the mismatch of spatial/temporal signatures, a modified GSC is employed. Second, the outputs of these BC pairs corresponding to different look directions and delays are coherently combined to collect the multipath energy. The beamformers and correlators together constitute a beamspace-time (BT) receiver which operates without the aid of a training signal. The only information required is a rough estimate of the AOA of the SOI for sector selection.

4.2.1 Construction of Space-Time Alternating Processors

In sectored communications, the entire field-of-view of the receiver is divided into several angular sectors, each responsible for a subset of users [64]. Assume that the AOA's and delays of the multipaths of the SOI (user 1) are roughly known such that an angular sector Θ_s and a time duration T_D can be chosen to accommodate these multipaths. In order to effectively collect the multipath energy, a set of M diversity beams is formed with their patterns encompassing Θ_s, and a set of L diversity correlators is formed with their responses matched to the L fingers in T_D. This leads to a set of ML beamformer-correlator (BC) pairs, or ST processors, operating on the Pre-ST data matrix. Let $\{\theta_m, m = 1, \ldots, M\}$, be the set of angles well representing Θ_s and denote as $\mathbf{a}_m = \mathbf{a}(\theta_m)$. Also let $\mathbf{c}_{1,l}$ be the lth column of $\mathbf{C}_1$, which is the signature matrix of user 1. The ST processor transforms the Pre-ST data matrix into a scalar output:

$$\tilde{z}_{l,m}(i) = \mathbf{a}_m^H \mathbf{X}(i)\mathbf{c}_{1,l}^* \tag{4.28}$$

with $m = 1, \ldots, M$ and $l = 1, \ldots, L$.

To ensure an effective suppression of strong interference, adaptive cancellation is performed for each of the ST diversity processors. As mentioned before, an effective solution is to employ the scheme of generalized sidelobe canceller (GSC) [55]. The GSC decomposes the weight vector $\tilde{\mathbf{w}}_{l,m}$ into: $\tilde{\mathbf{w}}_{l,m} = \mathbf{a}_m - \mathbf{B}_a \mathbf{v}_{l,m}$, where $\mathbf{a}_m$ is the fixed weight vector and $\mathbf{B}_a$ is the blocking matrix which removes the signal before beamforming. The goal is to choose the adaptive weight vector $\mathbf{v}_{l,m}$ to cancel the interference. To apply the GSC concept for ST processors, some modifications should be made. First, instead of blocking signals with a specific direction or delay, the blocking matrix must remove signals from the entire Θ_s and T_D. Second, instead of using a different blocking matrix for each ST processor, the same matrix is shared by all of the ML beam-finger pairs. Let $\mathbf{v}_{l,m}$ and $\mathbf{g}_{l,m}$ be the spatial and temporal adaptive weight vectors, respectively. The GSC formulation leads to the following ST operation:

$$
\begin{aligned}
\tilde{z}_{l,m}(i) &= (\mathbf{a}_m - \mathbf{B}_a \mathbf{v}_{l,m})^H \mathbf{X}(i)(\mathbf{c}_{1,l} - \mathbf{B}_c \mathbf{g}_{l,m})^* \\
&= h_{l,m} b_1(i) + i_{l,m}(i) + n_{l,m}(i)
\end{aligned}
\tag{4.29}
$$

where $\mathbf{B}_a$ and $\mathbf{B}_c$ are the spatial and temporal blocking matrices, respectively, and

$$
h_{l,m} = (\mathbf{a}_m - \mathbf{B}_a \mathbf{v}_{l,m})^H \mathbf{H}_{ST} (\mathbf{c}_{1,l} - \mathbf{B}_c \mathbf{g}_{l,m})^*
\tag{4.30}
$$

$$
i_{l,m}(i) = (\mathbf{a}_m - \mathbf{B}_a \mathbf{v}_{l,m})^H \mathbf{I}(i)(\mathbf{c}_{1,l} - \mathbf{B}_c \mathbf{g}_{l,m})^*
\tag{4.31}
$$

$$
n_{l,m}(i) = (\mathbf{a}_m - \mathbf{B}_a \mathbf{v}_{l,m})^H \mathbf{N}(i)(\mathbf{c}_{1,l} - \mathbf{B}_c \mathbf{g}_{l,m})^*
\tag{4.32}
$$

Following the standard procedure of GSC, the adaptive weight vectors are determined by solving the MMSE problem:

$$
\min_{\mathbf{v}_{l,m}, \mathbf{g}_{l,m}} E\left\{ |\tilde{z}_{l,m}(i)|^2 \right\} \equiv E\left\{ |(\mathbf{a}_m - \mathbf{B}_a \mathbf{v}_{l,m})^H \mathbf{X}(i)(\mathbf{c}_{1,l} - \mathbf{B}_c \mathbf{g}_{l,m})^*|^2 \right\}
\tag{4.33}
$$

The ST processors in (4.29) utilizes the spatial and temporal degrees of freedom in a separate fashion. This is in contrast to receivers operating in a ST joint fashion. ST joint receivers are superior in terms processing dimension, but require a much higher complexity. For scenarios in which there are only few dominant interferers, ST separate receivers would be a more efficient solution.

The closed-form solution to (4.33) is not available, and an suboptimum solution can be obtained by keeping the spatial weight vector fixed and solving for the temporal weight vector, and vice versa. This leads to the development of the following alternate minimization procedure. First, the beamformer weight vector

$$\tilde{\mathbf{w}}_{l,m} = \mathbf{a}_m - \mathbf{B}_a \mathbf{v}_{l,m} \tag{4.34}$$

is initialized with a pre-determined value (e.g. $\tilde{\mathbf{w}}_{l,m} = \mathbf{a}_m$), and the temporal adaptive weight vector is obtained in accordance with

$$\min_{\mathbf{g}_{l,m}} \quad E\left\{|(\mathbf{c}_{1,l} - \mathbf{B}_c \mathbf{g}_{l,m})^H \mathbf{X}^T(i)\tilde{\mathbf{w}}_{l,m}^*|^2\right\} \tag{4.35}$$

whose solution is given by

$$\mathbf{g}_{l,m} = \hat{\mathbf{R}}_{l,m}^{-1}\hat{\mathbf{r}}_{l,m} \tag{4.36}$$

where

$$\hat{\mathbf{R}}_{l,m} = E\left\{\mathbf{B}_c^H \mathbf{X}^T(i)\tilde{\mathbf{w}}_{l,m}^* \tilde{\mathbf{w}}_{l,m}^T \mathbf{X}^*(i)\mathbf{B}_c\right\}$$
$$\hat{\mathbf{r}}_{l,m} = E\left\{\mathbf{B}_c^H \mathbf{X}^T(i)\tilde{\mathbf{w}}_{l,m}^* \tilde{\mathbf{w}}_{l,m}^T \mathbf{X}^*(i)\mathbf{c}_{1,l}\right\} \tag{4.37}$$

The correlator weight vector

$$\hat{\mathbf{s}}_{l,m} = \mathbf{c}_{1,l} - \mathbf{B}_c \mathbf{g}_{l,m} \tag{4.38}$$

with $\mathbf{g}_{l,m}$ given by (4.36), can suppress MAI with a fixed temporal signature. For time-varying NBI whose temporal signatures are not well defined, adaptive nulling in the space domain is more effective. The second step is then to fix $\hat{\mathbf{s}}_{l,m}$, and obtain the spatial adaptive weight vector in accordance with

$$\min_{\mathbf{v}_{l,m}} \quad E\left\{|(\mathbf{a}_m - \mathbf{B}_a \mathbf{v}_{l,m})^H \mathbf{X}(i)\hat{\mathbf{s}}_{l,m}^*|^2\right\} \tag{4.39}$$

whose solution is given by

$$\mathbf{v}_{l,m} = \tilde{\mathbf{R}}_{l,m}^{-1}\tilde{\mathbf{r}}_{l,m} \tag{4.40}$$

where

$$\tilde{\mathbf{R}}_{l,m} = E\left\{\mathbf{B}_a^H \mathbf{X}(i)\hat{\mathbf{s}}_{l,m}^* \hat{\mathbf{s}}_{l,m}^T \mathbf{X}^H(i)\mathbf{B}_a\right\}$$

$$\tilde{\mathbf{r}}_{l,m} = E\left\{\mathbf{B}_a^H \mathbf{X}(i)\hat{\mathbf{s}}_{l,m}^* \hat{\mathbf{s}}_{l,m}^T \mathbf{X}^H(i)\mathbf{a}_m\right\} \tag{4.41}$$

The above procedure can be iterated between (4.35) and (4.39) by substituting (4.40) in (4.34), and re-executing the steps in (4.35)-(4.41). Since both the spatial adaptive weight vector and temporal adaptive weight vector are adjusted to minimize the cost function of (4.33), and both are orthogonal to the desired signal, the minimization of cost function is solely due to the suppression of interference. In particular, at each alternate iteration, either the spatial or temporal weight vector will adjust itself to decrease the cost function with the other fixed. As a result, it can be sure that the cost function will reduce as iterations proceed. Nevertheless, the resulting solution may not lead to the global minimum of the cost function. However, as long as the degree of freedom of the adaptive weights are large enough compared to the number of interferers, the alternate procedure can always yield a converged solution that provides effective interference suppression. The proposed alternate iterative scheme is similar in principle to the iterative least square (ILS) problem described in [88]. Given $\tilde{\mathbf{w}}_{l,m}$ fixed, the minimization of cost function (4.33) is a least-squares problem for $\mathbf{g}_{l,m}$ to make the cost function approach zero. A similar situation holds for $\mathbf{v}_{l,m}$ with $\hat{\mathbf{s}}_{l,m}$ fixed. The overall system diagram is depicted in Figure 4.7.

4.2.2 Maximum Ratio Combiner

It is assumed that, with adaptive ST processing, the dominant interference has been eliminated and the BC output data $\tilde{z}_{l,m}(i)$, $l = 1, \ldots, L$, $m = 1, \ldots, M$, contain the SOI and colored noise only. This suggests that the maximum ratio combining (MRC) criterion can be employed to collect these components coherently to extract $b_1(i)$. Let $\mathbf{f}_{mrc}$ be the $LM \times 1$ weight vector that performs the combining:

$$z_o(i) = \mathbf{f}_{mrc}^H \mathbf{z}_c(i) \tag{4.42}$$

where

$$
\begin{aligned}
\mathbf{z}_c(i) &= [z_{1,1}(i), \ldots, z_{1,M}(i), z_{2,1}(i), \ldots, z_{2,M}(i), \ldots, z_{L,1}(i), \ldots, z_{L,M}(i)]^T \tag{4.43}\\
&\approx \mathbf{h}_c b_1(i) + \mathbf{n}_c(i)
\end{aligned}
$$

is the BC output data vector associated with the kth symbol, with $\mathbf{h}_c$ and $\mathbf{n}_c(i)$ being the corresponding composite signature and noise vectors, respectively, given by

$$\mathbf{h}_c = [h_{1,1}, \ldots, h_{1,M}, h_{2,1}, \ldots, h_{2,M}, \ldots, h_{L,1}, \ldots, h_{L,M}]^T \tag{4.44}$$

$$\mathbf{n}_c(i) = [n_{1,1}(i), \ldots, n_{1,M}(i), n_{2,1}(i), \ldots, n_{2,M}(i), \ldots, n_{L,1}(i), \ldots, n_{L,M}(i)]^T \tag{4.45}$$

with $\tilde{z}_{l,m}(i)$, $h_{l,m}$ and $n_{l,m}(i)$ given by (4.29), (4.30) and (4.32), respectively.

As described in Section 4.1.3, the MRC weight vector can be determined blindly as the solution to the following problem [56]:

$$\max_{\mathbf{f}_{mrc}} \quad \frac{E\{|\mathbf{f}_{mrc}^H \mathbf{z}_c(i)|^2\}}{E\{|\mathbf{f}_{mrc}^H \mathbf{n}_c(i)|^2\}} \equiv \frac{\mathbf{f}_{mrc}^H \mathbf{R}_{\mathbf{z}_c} \mathbf{f}_{mrc}}{\mathbf{f}_{mrc}^H \mathbf{R}_{\mathbf{n}_c} \mathbf{f}_{mrc}} \tag{4.46}$$

where $\mathbf{R}_{\mathbf{z}_c} = E\{\mathbf{z}_c(i)\mathbf{z}_c^H(i)\}$ and $\mathbf{R}_{\mathbf{n}_c} = E\{\mathbf{n}_c(i)\mathbf{n}_c^H(i)\}$ are the BC output data and noise correlation matrices, respectively. The solution to (4.46) is well known to be the principal generalized eigenvector $\{\mathbf{R}_{\mathbf{z}_c}, \mathbf{R}_{\mathbf{n}_c}\}$. The matrix $\mathbf{R}_{\mathbf{n}_c}$ depends on the beamformer and correlator weight vectors, and can be shown to have the (i, j)th entry given by (see Appendix)

$$[\mathbf{R}_{\mathbf{n}_c}]_{(i,j)} = \sigma_n^2 \tilde{\mathbf{w}}_{l_1,m_1}^H \tilde{\mathbf{w}}_{l_2,m_2} \hat{\mathbf{s}}_{l_1,m_1}^T \hat{\mathbf{s}}_{l_2,m_2}^* \tag{4.47}$$

where $i = (m_1 - 1)L + l_1$ and $j = (m_2 - 1)L + l_2$, with $1 \leq l_1, l_2 \leq L$ and $1 \leq m_1, m_2 \leq M$.

4.2.3   AOA Estimation and Sector Selection

To determine the working sector, some kind of preliminary location method can be used to obtain a coarse estimate the AOA of the SOI. The estimate need not be accurate as required in conventional LCMV beamforming, but should lead to a right sector for the multipath arrivals. In this section, a simple technique of AOA estimation is proposed based on the same framework for adaptive beamforming.

For simplicity, we assume that the SOI is the the sector Θ_s. The AOA estimate of the lth path of the SOI is determined as the solution to the following spectral search problem:

$$\max_{\theta} \quad P_l(\theta) \equiv \mathbf{w}_l(\theta)^H \tilde{\mathbf{R}}_l \mathbf{w}_l(\theta) \tag{4.48}$$

where

$$\tilde{\mathbf{R}}_l = E\left\{\mathbf{X}(i)\mathbf{c}_{1,l}^* \mathbf{c}_{1,l}^T \mathbf{X}^H(i)\right\} \tag{4.49}$$

is the post-despread correlation matrix for the lth finger, and

$$\mathbf{w}_l(\theta) = [\mathbf{I} - \mathbf{B}_a(\mathbf{B}_a^H\tilde{\mathbf{R}}_l\mathbf{B}_a)^{-1}\mathbf{B}_a^H\tilde{\mathbf{R}}_l]\mathbf{a}(\theta) \qquad (4.50)$$

is the optimum beamforming weight vector steered to the look direction θ. It is the weight vector obtained from (4.39), with $\mathbf{a}_m$ and $\hat{\mathbf{s}}_{l,m}$ replaced by $\mathbf{a}(\theta)$ and $\mathbf{c}_{1,l}$, respectively. For any $\theta \in \Theta_s$, $\mathbf{w}_l(\theta)$ will produce a mainlobe at θ, and suppress interference outside Θ_s. Hence by varying θ over Θ_s, a spectral peak can be observed in the spatial spectrum $P_l(\theta)$ corresponding to the AOA of the lth path. This is similar in principle to the Capon's location method [89], except that a different blocking scheme is used here to avoid signal cancellation. The same procedure can be executed for different sectors to locate all spectral peaks in the entire field-of-view. If multiple peaks are present in different sectors, then further identification is necessary to distinguish the true SOI from others.

4.2.4 Algorithm Summary

In practice, the data correlation matrices are usually estimated by the sample average versions:

$$\hat{\mathbf{R}}_{l,m} \approx \frac{1}{N_s}\sum_{i=1}^{N_s}\mathbf{B}_c^H\mathbf{X}^T(i)\tilde{\mathbf{w}}_{l,m}^*\tilde{\mathbf{w}}_{l,m}^T\mathbf{X}^*(i)\mathbf{B}_c$$

$$\hat{\mathbf{r}}_{l,m} \approx \frac{1}{N_s}\sum_{i=1}^{N_s}\mathbf{B}_c^H\mathbf{X}^T(i)\tilde{\mathbf{w}}_{l,m}^*\tilde{\mathbf{w}}_{l,m}^T\mathbf{X}^*(i)\mathbf{c}_{1,l} \qquad (4.51)$$

$$\tilde{\mathbf{R}}_{l,m} \approx \frac{1}{N_s}\sum_{i=1}^{N_s}\mathbf{B}_a^H\mathbf{X}(i)\hat{\mathbf{s}}_{l,m}^*\hat{\mathbf{s}}_{l,m}^T\mathbf{X}^H(i)\mathbf{B}_a$$

$$\tilde{\mathbf{r}}_{l,m} \approx \frac{1}{N_s}\sum_{i=1}^{N_s}\mathbf{B}_a^H\mathbf{X}(i)\hat{\mathbf{s}}_{l,m}^*\hat{\mathbf{s}}_{l,m}^T\mathbf{X}^H(i)\mathbf{a}_m \qquad (4.52)$$

$$\mathbf{R}_{\mathbf{z}_c} \approx \frac{1}{N_s}\sum_{i=1}^{N_s}\mathbf{z}_c(i)\mathbf{z}_c^H(i) \qquad (4.53)$$

where N_s is the number of symbols used during the processing period. With these estimates, the algorithm of the proposed alternating ST 2-D RAKE receiver is summarized as follows:

1. Determine working sector Θ_s, look angles θ_m's and GSC blocking matrices $\mathbf{B}_a$ and $\mathbf{B}_c$.

2. Initialize the adaptive weights $\mathbf{v}_{l,m} = \mathbf{0}$, i.e., $\tilde{\mathbf{w}}_{l,m} = \mathbf{a}_m$.

3. Compute in parallel $\mathbf{g}_{l,m}$, $l = 1, \ldots, L$, $m = 1, \ldots, M$, according to (4.36), with $\hat{\mathbf{R}}_{l,m}$ and $\hat{\mathbf{r}}_{l,m}$ estimated by (4.51).

4. Compute in parallel $\mathbf{v}_{l,m}$, $l = 1, \ldots, L$, $m = 1, \ldots, M$, according to (4.40), with $\tilde{\mathbf{R}}_{l,m}$ and and $\hat{\mathbf{r}}_{l,m}$ estimated by (4.52).

5. Iterate the procedure between step 3 and step 4 until the solutions converge. By substituting the $\tilde{\mathbf{w}}_{l,m}$ into (4.51), obtain a new $\hat{\mathbf{s}}_{l,m}$ and by substituting the one into (4.52), update the $\tilde{\mathbf{w}}_{l,m}$, iteratively.

6. Obtain $\mathbf{R}_{\mathbf{n}_c}$ and compute $\mathbf{f}_{mrc}$ according to (4.46), with $\mathbf{R}_{\mathbf{z}_c}$ estimated by (4.53).

4.2.5 Recursive Computation of Weight Vectors

To avoid matrix inversion, the GSC can be implemented in a time-recursive fashion using stochastic gradient algorithms such as LMS [21]. This leads to recursive formulation of the solutions to (4.35) and (4.39), respectively:

$$\mathbf{g}_{l,m}(i+1) = \mathbf{g}_{l,m}(i) + \mu_g \left[(\mathbf{c}_{1,l} - \mathbf{B}_c \mathbf{g}_{l,m}(i))^H \mathbf{X}^T(i) \tilde{\mathbf{w}}_{l,m}^*(i) \right]^* \mathbf{B}_c^H \mathbf{X}^T(i) \tilde{\mathbf{w}}_{l,m}^*(i) \quad (4.54)$$

$$\mathbf{v}_{l,m}(i+1) = \mathbf{v}_{l,m}(i) + \mu_v \left[(\mathbf{a}_m - \mathbf{B}_a \mathbf{v}_{l,m}(i))^H \mathbf{X}(i) \hat{\mathbf{s}}_{l,m}^*(i) \right]^* \mathbf{B}_a^H \mathbf{X}(i) \hat{\mathbf{s}}_{l,m}^*(i) \quad (4.55)$$

where μ_g and μ_v are the adaptation stepsizes. Clearly, (4.54) and (4.55) are coupled and should be executed in an alternate fashion.

On the other hand, the generalized eigenvector required for the computation of the MRC weight vector in (4.46) can be also obtained via a time-recursive algorithm. One such example is the recently developed projection approximation subspace tracking (PAST) algorithm [68], which is shown to exhibit global convergence and requires a computational complexity of the order ML (BT dimension) per iteration. The PAST algorithm was originally proposed for tracking multiple eigenvectors, and can be easily modified for the tracking of a single generalized eigenvector as dictated by (4.46) in [67]. The overall adaptive algorithm for alternate optimal beamspace-time 2-D RAKE receiver is summarized in Table 4.2.

4.2.6 Partially Adaptive Implementation

The degree of freedom for the adaptive correlators is on the order of N, which can be quite large in wideband applications. A large degree of freedom requires a high computational complexity and is likely to incur poor convergence behaviors [55]. To alleviate this, the partially adaptive (PA) methods can be applied to reduce the dimension of $\mathbf{g}_{l,m}$'s. Partial adaptivity can be achieved by either working with a reduced-dimension data vector or with a reduced-size blocking matrix [38, 39]. Here a simple approach is suggested based on the principle of maximum cross correlation [90].

Let $\mathbf{B}_p$ be the $(N + L - 1) \times P'$ reduced-size blocking matrix and $\mathbf{B}_c$ be the $(N + L - 1) \times (N - 1)$ full-size blocking matrix satisfying $\mathbf{B}_c^H \mathbf{C}_1 = 0$ and $\mathbf{B}_c^H \mathbf{B}_c = \mathbf{I}$. The maximum crosscorrelation criterion dictates that $\mathbf{B}_p$ should be composed of P' vectors that maximize the magnitude of the crosscorrelation between the upper and lower branch data of the temporal GSC described by (4.35). That is, $\mathbf{B}_p$ is chosen according to:

$$\max_{\mathbf{B}_p} \quad \left\| E\left\{ \mathbf{B}_p^H \mathbf{X}^T(k)\tilde{\mathbf{w}}_{l,m}^* \tilde{\mathbf{w}}_{l,m}^T \mathbf{X}^*(k)\mathbf{c}_{1,l} \right\} \right\|$$

$$\text{subject to:} \quad \mathbf{B}_p^H \mathbf{C}_1 = 0 \text{ and } \mathbf{B}_p^H \mathbf{B}_p = \mathbf{I} \tag{4.56}$$

Optimum solution to (4.56) requires a time consuming iterative procedure if P' is large [90]. As a simplified alternative, $\mathbf{B}_p$ can be obtained with the P' orthonormal columns of $\mathbf{B}_c$ that give the largest crosscorrelation values. Note that the crosscorrelation vector in (4.56) can be readily obtained as a sub vector of $\hat{\mathbf{r}}_{l,m}$ given in (4.37) without extra computation. Finally, the PA correlator weight vector is given by (4.36)-(4.37), with $\mathbf{B}_c$ replaced by $\mathbf{B}_p$.

4.2.7 Complexity and Performance

The trade-off between system performance and computational complexity is an issue depending on the number of antennas D and processing gain N of the system. In general, more antennas and a larger processing gain will provide better interference suppression, but lead to high computational complexity and poor convergence behaviors. However, the spatial and temporal dimensions (D and N) do not affect the complexity of the eigenvector computation in MRC because the MRC weight vector has a size of ML, regardless of D

and N. For batch processing, the major computations in the proposed algorithm involves the inversion of $\hat{\mathbf{R}}_{l,m}^{-1}$ with size $(N-1) \times (N-1)$ in (4.36), inversion of $\tilde{\mathbf{R}}_{l,m}^{-1}$ with size $D' \times D'$ in (4.40), and a principal eigenvector computation with size $ML \times ML$ in (4.46). The overall complex is about $O(N^3 + D'^3 + M^3L^3)$. For comparison, the ST post-despread receiver in [56] requires about $O(D^3L^3)$, and the ST pre-despread receiver in [87] requires about $O(N^3 + D + L)$ for batch processing. The higher complexity of the proposed receiver and that in [63] is the price paid for not using a training sequence for channel estimation.

For recursive processing as described in the previous section, the complexity for each iteration is about $O(N + D' + ML)$ for the proposed receiver, $O(DL)$ for the receiver in [56], and $O(N + D^3)$ for the receiver in [87]. The proposed receiver can be further simplified by incorporating partial adaptivity in temporal processing to reduce N to a smaller P'. As long as P' is large compared to the number of strong interferers, the performance of the receiver will be virtually unaffected.

In the flat-fading case, the multipath delay spread is smaller than the chip period such that the receiver would require only a single finger to work with. As a result, only a single adaptive correlator is needed for each diversity beam. On the other hand, in time-invariant channels without the Doppler shift, it will be easier for the adaptive algorithms to converge and keep track of SOI. In addition, since the fading gain remains constant at each beam-finger pair, the maximum ratio combining weights need not be computed frequently. This should alleviate the load for eigenvector computation.

4.2.8   Simulation Results

Here the performance of the proposed BT receiver is evaluated using a linear array of $D = 12$ identical antennas uniformly spaced by a $1/\sqrt{3}$ wavelength. The inter-antenna spacing is chosen for the field-of-view $[-60°, 60°]$. The working sector is $\Theta_s = [-20°, 20°]$, and $M = 4$ diversity beams are formed at look directions $\{-12.45°, -4.15°, 4.15°, 12.45°\}$. The spatial blocking matrix $\mathbf{B}_a$ is constructed with $D' = 6$ using the eigenvector constrained method. It is assumed that the SOI is in Θ_s, and the MAI are uniformly distributed in the entire field-of-view, with each user having the same multipath angle spread of $10°$. For all users, $J = 4$ paths are generated with delays chosen from $\{0, T_c, 2T_c, 3T_c\}$, and fading gains

being i.i.d. unit variance complex Gaussian random variables. All CDMA signals are BPSK data modulated and spread with the Gold code of length $N = 31$. In addition to the MAI, there are two equal power BPSK NBI's arriving from $30°$ and $-45°$, with a bit rate being 0.8 times that of the CDMA signals. Finally, the number of fingers is $L = 4$, and the temporal blocking matrix $\mathbf{B}_c$ is chosen, according to Section 4.1.2, to be the 34×28 matrix whose columns formed an orthogonal complement to $[\mathbf{c}_{1,1}^{(-)}, \mathbf{c}_{1,1}, \mathbf{c}_{1,2}, \mathbf{c}_{1,3}, \mathbf{c}_{1,4}, \mathbf{c}_{1,4}^{(+)}]$.

As a performance index, the output SINR (in dB) is defined as

$$\text{SINR}_o = 10 \log_{10} \frac{\text{output power of signal in } z_o(i)}{\text{output power of (MAI+NBI+noise) in } z_o(i)}$$

and the input SNR (in dB) is defined as $\text{SNR}_i = 10 \log_{10} \frac{\sigma_1}{\sigma_n^2}$. The near-far-ratio (NFR) is the ratio of the MAI power to signal power before despreading, and the NBI-to-signal-ratio (NSR) is the ratio of the NBI power to signal power before despreading. For all but one result in the simulations, N_s symbols are used to obtain sample estimates of $\hat{\mathbf{R}}_{l,m}$, $\hat{\mathbf{r}}_{l,m}$, $\tilde{\mathbf{R}}_{l,m}$, $\tilde{\mathbf{r}}_{l,m}$ and $\mathbf{R}_{\mathbf{z}_c}$, and a total of 50 Monte-Carlo runs are executed to obtain an average SINR_o. For performance comparison, we included the results obtained with the blind principal component 2-D RAKE receivers (ST-PC) in [56] and the non-blind coherent Post-ST RAKE (CST-RAKE), MMSE Post-ST RAKE (MST-RAKE), coherent BT Post-BT RAKE (CBT-RAKE), and MMSE Post-BT RAKE (MBT-RAKE) receivers described in Chapter 3. For non-blind receivers, the Post-ST and Post-BT channel vectors are estimated using the same N_s symbols as the training sequence. For CBT-RAKE and MBT-RAKE receivers, the beamforming matrix is constructed using the four steering vectors $\{\mathbf{a}_1, \mathbf{a}_2, \mathbf{a}_3, \mathbf{a}_4\}$ associated with the look directions of the diversity beams. The simulation parameters are: $N = 31$ with Gold codes, $L = 4$ fingers, the number of antenna elements $D = 12$, the number of training symbols $N_s = 500$, the NSR = 20 dB and the input $\text{SNR}_i = 0$ dB. Unless otherwise mentioned, the above standard parameters will be used throughout the section.

To demonstrate the efficacy of AOA estimation described in Section 4.2.3, the spatial spectrum are computed for the three sectors $[-60°, -20°]$, $[-20°, 20°]$, and $[20°, 40°]$. Figure 4.8 shows the result for the first and third fingers ($l = 1, 3$), with $K = 10$ users and NFR = 0 dB. The peak in the working sector gives the AOA of the SOI, and those in other sectors are "false peaks" due to NBI and can be easily detected by the system.

In the first set of simulations, the system capacity is evaluated with different user numbers K. The resulting output SINR curves are plotted in Figure 4.9 for NFR = 0 dB and 20 dB. As observed, the proposed BT receiver (GSC2-RAKE) performs reliably for a wide range of K, even outperforming the MST-RAKE receiver with a moderately large K and high NFR. This indicates that the adaptive beamformers and correlators have successfully eliminated the strong NBI and MAI, respectively. The CST-RAKE, CBT-RAKE and ST-PC receivers totally fail with NFR = 20 dB and a large K due to the lack of interference suppression and poor channel estimation. In Figure 4.10, the patterns of the diversity beams for the first and third fingers ($l = 1, 3$) are plotted for the case $K = 5$ users and NFR = 0 dB. The mainlobes and deep nulls confirm that the adaptive beamformers can effectively collect the in-sector signals and suppress the strong NBI.

In the second set of simulations, the near-far resistance of the proposed BT receiver is evaluated with different NFR values. Figure 4.11 shows the results obtained with $K = 5$ and 25 users. As observed, with $K = 25$, the CST-RAKE, CBT-RAKE and ST-PC receivers fail again, and the MST-RAKE receiver loses its advantage due to ineffective interference suppression. On the contrary, the proposed BT receiver achieves excellent near-far resistance by successfully canceling the MAI and NBI simultaneously. The proposed receiver performs well with $K = 5$, in which case the temporal GSC has a sufficient degree of freedom to handle the NBI.

In the third set of simulations, the efficacy of partial adaptivity, which is described in Section 4.2.6, is demonstrated through system capacity evaluation. Figure 4.12 shows the results obtained with the fully adaptive (FA) BT receiver, partially adaptive BT receiver with $P' = 10$ (PA-10), and partially adaptive BT receiver with $P' = 20$ (PA-20), for NFR = 0 dB and 20 dB. As expected, the PA receivers perform reliably as compared to the FA receiver with a small K, and degrade as K increases due to the exhaustion of the temporal degree of freedom for interference suppression.

In the fourth set of simulations, the convergence behaviors of the proposed FA BT receiver, PA-10 receiver, ST-PC receiver and MST-RAKE receiver are evaluated by varying the data sample size N_s. The resulting output SINR are plotted in Figure 4.12 with $K = 5$, and NFR = 0 dB and 20 dB. As observed, the output SINR increases as N_s increases for all

receivers. The MST-RAKE receiver converges fastest due to the use of a training sequence. The PA-10 receiver converges faster than the FA receiver, confirming the well known fact that adaptive filters of smaller size converge faster.

Finally, to demonstrate the effectiveness of the recursive algorithms for weight adaptation and eigenvector computation, we replaced direct matrix inversions by the formulae given in (4.54) and (4.55), and direct eigenvector computation by the PAST algorithm. The adaptation stepsizes are chosen as $\mu_g = \mu_v = 10^{-6}$. Figure 4.14(a) shows the resulting learning curve of the FA BT receiver, with NFR = 0 dB and $K = 5$. To show the tracking capability of the algorithm, we repeated the same simulation, but deliberately changed the AOA's of the two NBI's to $40°$ and $-50°$, respectively, at the 500th iteration. The learning curves given in Figure 4.14(b) confirm that the recursive receiver successfully adjusted its weights to suppress the NBI.

For an efficient implementation, recursive algorithms are employed for weight vector adaptation and eigenvector computation, and a simple partially adaptive solution is given based on the maximum crosscorrelation principle. The proposed receiver can be operated without the aid of a training signal. The only information required is the signature sequence, timing and a rough estimate of the angle of arrival of the signal for selecting the sector of interest. Compared to the conventional ST receivers, the proposed beamspace receiver enhances the the SINR by suppressing interference via adaptive nulling, and increases system capacity by sectorization. From simulation results, it is shown that the proposed blind receiver is near-far resistant, and performs reliably in an overloaded system.

4.3 Post-despread Beamspace-Time 2-D RAKE Receiver for Sectored CDMA systems

In this section, a blind post-despread RAKE receiver suitable for sectored systems is developed by a two stage procedure. First, a set of adaptive ST beamformers is designed which provide effective reception of the SOI in a prescribed sector, and suppression of out-of-sector MAI on the post-despread data. Second, the outputs of these ST beamformers are

constructively combined to extract the SOI's symbols.

4.3.1 Construction of Space-Time Beamformers

In sectored communications, the entire field-of-view of the receiver is divided into several angular sectors, each responsible for a subset of users [64]. Assumed that the AOA's and delays of the multipaths of the SOI (user 1) are roughly known such that an angular sector Θ_s and delay spread T_D can be chosen to accommodate these multipaths. In order to effectively collect the multipath energy, a set of diversity beams is formed with their patterns encompassing Θ_s. As opposed to the previously developed beamforming scheme, here we propose another approach that yields a set of ST beamformers operating on the Post-ST data vector $\mathbf{x}_{c-SM}(i)$ as defined in (3.55). Let θ_m, $m = 1, \ldots, M$, be the set of angles well representing Θ_s and denote as $\mathbf{a}_m = \mathbf{a}(\theta_m)$, where $\mathbf{a}_m$ is associated with the space-only array data. We can define the signature vectors associated with the Post-ST data vector as

$$\bar{\mathbf{A}}_m = [\bar{\mathbf{a}}_{l,m}, \bar{\mathbf{a}}_{2,m}, \ldots, \bar{\mathbf{a}}_{L,m}] = \begin{bmatrix} \mathbf{a}_m & \mathbf{0} & \cdots & \mathbf{0} \\ \mathbf{0} & \mathbf{a}_m & \cdots & \vdots \\ \vdots & \vdots & \ddots & \mathbf{0} \\ \mathbf{0} & \mathbf{0} & \cdots & \mathbf{a}_m \end{bmatrix} \tag{4.57}$$

where the lth column $\bar{\mathbf{a}}_{l,m}$ is the concatenation of L segments, with the lth segment being $\mathbf{a}_m$, and zero elsewhere. Specifically, the ST signatures for the AOA θ_m can be represented by a set of L linearly independent vectors $\bar{\mathbf{a}}_{l,m}$, $l = 1, \ldots, L$, corresponding to the L fingers. If M diversity beams are to be formed at θ_m, $m = 1, \ldots, M$, then we need a total of ML ST signature vectors (STSV).

To ensure an effective suppression of strong out-of-sector MAI and NBI, adaptive nulling is performed for each of the diversity beamformers. This is done by choosing the beamforming weight vectors in accordance with the LCMV criterion [55]:

$$\min_{\bar{\mathbf{w}}_{l,m}} \quad \bar{\mathbf{w}}_{l,m}^H \mathbf{R}_{\mathbf{x}_{c-SM}} \bar{\mathbf{w}}_{l,m}$$

$$\text{subject to: } \bar{\mathbf{w}}_{l,m}^H \bar{\mathbf{a}}_{l,m} = 1 \tag{4.58}$$

for $l = 1, \ldots, L$ and $m = 1, \ldots, M$, where $\mathbf{w}_{l,m}$ is the lth weight vector of the mth beamformer,

$$\mathbf{R}_{\mathbf{x}_{c-SM}} = E\{\mathbf{x}_{c-SM}(i)\mathbf{x}_{c-SM}^H(i)\} \tag{4.59}$$

where $\mathbf{R}_{\mathbf{x}_{c-SM}}$ is the Post-ST data correlation matrix. The solution to (4.58) is a ST beamformer that matches itself to $\bar{\mathbf{a}}_{l,m}$ to receive signal at the lth finger, while minimizing the total output power to suppress interference. A major problem of the LCMV beamformer is the phenomenon of signal cancellation [83] due to the mismatch of signature vectors. By signal cancellation, it is meant that each of the weight vectors in (4.58) will combine the multipath components in a destructive manner in order to minimize the output power. An effective remedy proposed herein is again to use a modified GSC to block the signal before beamforming [55]. In GSC, the weight vector is decomposed as $\bar{\mathbf{w}}_{l,m} = \bar{\mathbf{a}}_{l,m} - \bar{\mathbf{B}}_a \mathbf{v}_{l,m}$ into two orthogonal components which lie in the range and null space of the constraint, respectively. The matrix $\bar{\mathbf{B}}_a$ is a pre-designed "signal blocking" matrix which removes the signal in the sector. The goal is then to choose the adaptive weight vector $\bar{\mathbf{v}}_{l,m}$ to cancel the out-of-sector interference. To apply the GSC in constructing the ST beamformer bank, some modifications should be made. First, instead of blocking signals from a specific direction, $\bar{\mathbf{B}}_a$ must block signals from the entire sector. Second, instead of using a different blocking matrix for each beamformer, the same $\bar{\mathbf{B}}_a$ is shared by all of the M beamformers at the L fingers. Following the standard procedure of GSC, the adaptive weight vectors are determined by the following MMSE problem:

$$\min_{\bar{\mathbf{v}}_{l,m}} \quad E\{|\bar{\mathbf{a}}_{l,m}^H \mathbf{x}_{c-SM}(k) - \bar{\mathbf{v}}_{l,m}^H \bar{\mathbf{B}}_a^H \mathbf{x}_{c-SM}(k)|^2\} \tag{4.60}$$

or equivalently

$$\min_{\bar{\mathbf{v}}_{l,m}} \quad [\bar{\mathbf{a}}_{l,m} - \bar{\mathbf{B}}_a \bar{\mathbf{v}}_{l,m}]^H \mathbf{R}_{\mathbf{x}_{c-SM}} [\bar{\mathbf{a}}_{l,m} - \bar{\mathbf{B}}_a \bar{\mathbf{v}}_{l,m}] \tag{4.61}$$

Solving for $\bar{\mathbf{v}}_{l,m}$ and substituting in $\bar{\mathbf{w}}_{l,m} = \bar{\mathbf{a}}_{l,m} - \bar{\mathbf{B}}_a \bar{\mathbf{v}}_{l,m}$, we get

$$\bar{\mathbf{w}}_{l,m} = [\mathbf{I} - \bar{\mathbf{B}}_a(\bar{\mathbf{B}}_a^H \mathbf{R}_{x_{c-SM}} \bar{\mathbf{B}}_a)^{-1} \bar{\mathbf{B}}_a^H \mathbf{R}_{x_{c-SM}}]\bar{\mathbf{a}}_{l,m} \tag{4.62}$$

for $l = 1, \ldots, L$, $m = 1, \ldots, M$.

4.3.2 Structure of Blocking Matrices

The blocking matrix $\bar{\mathbf{B}}_a$ is designed to remove signal components at each of the L fingers. Since the Post-ST channel is not known, the blocking should be done in a finger-by-finger basis. This suggests that $\bar{\mathbf{B}}_a$ should have the following form:

$$
\bar{\mathbf{B}}_a = \begin{bmatrix} \mathbf{B}_a & \mathbf{O} & \cdots & \mathbf{O} \\ \mathbf{O} & \mathbf{B}_a & \cdots & \vdots \\ \vdots & \vdots & \ddots & \mathbf{O} \\ \mathbf{O} & \mathbf{O} & \cdots & \mathbf{B}_a \end{bmatrix}
\tag{4.63}
$$

where $\mathbf{B}_a$ is the "space-only" blocking matrix satisfying $\mathbf{B}_a^H \mathbf{a}(\theta) \approx \mathbf{0}$ for $\theta \in \Theta_s$. The detail of the construction of $\mathbf{B}_a$ is described in Section 4.1.1.

4.3.3 Maximum Ratio Combiner

The weight vectors $\bar{\mathbf{w}}_{l,m}$'s produce ML ST beams with diversity reception for the desired signal from Θ_s and adaptive cancellation for the interference from outside Θ_s. These beams are then linearly combined into a single beam:

$$
\begin{aligned}
\tilde{\mathbf{w}} &= \sum_{m=1}^{M} \sum_{l=1}^{L} \bar{f}_{l,m} \bar{\mathbf{w}}_{l,m} \\
&= \bar{\mathbf{W}} \bar{\mathbf{f}}
\end{aligned}
\tag{4.64}
$$

where

$$
\bar{\mathbf{W}} = \left[\bar{\mathbf{w}}_{1,1}, \ldots, \bar{\mathbf{w}}_{L,1}, \bar{\mathbf{w}}_{1,2}, \ldots, \bar{\mathbf{w}}_{L,2}, \ldots, \bar{\mathbf{w}}_{L,1}, \ldots, \bar{\mathbf{w}}_{L,M} \right]
\tag{4.65}
$$

and

$$
\bar{\mathbf{f}} = \left[\bar{f}_{1,1}, \ldots, \bar{f}_{L,1}, \bar{f}_{1,2}, \ldots, f_{L,2}, \ldots, f_{1,M}, \ldots, f_{L,M} \right]^T
\tag{4.66}
$$

is the combining coefficient vector. To achieve the optimum performance, the vector $\bar{\mathbf{f}}$ is determined in accordance with the maximum ratio combining (MRC) criterion. With adaptive ST processing, the dominant interference has been eliminated and the beamformer output data $\bar{\mathbf{w}}_{l,m}^H \mathbf{x}_{c-SM}(i)$, $m = 1, \ldots, M$, $l = 1, \ldots, L$, contain the SOI and colored noise

only. In this case, the MRC weight vector can be determined blindly as the solution to the following problem [63]:

$$\max_{\bar{\mathbf{f}}} \quad \frac{E\left\{\left|\bar{\mathbf{f}}^H \bar{\mathbf{W}}^H \mathbf{x}_{c-SM}(i)\right|^2\right\}}{E\left\{\left|\bar{\mathbf{f}}^H \bar{\mathbf{W}}^H \mathbf{n}_{c-SM}(i)\right|^2\right\}} \equiv \frac{\bar{\mathbf{f}}^H \bar{\mathbf{W}}^H \mathbf{R}_{\mathbf{x}_{c-SM}} \bar{\mathbf{W}} \bar{\mathbf{f}}}{\bar{\mathbf{f}}^H \bar{\mathbf{W}}^H \mathbf{R}_{\mathbf{n}_{c-SM}} \bar{\mathbf{W}} \bar{\mathbf{f}}} \tag{4.67}$$

where

$$\mathbf{R}_{\mathbf{n}_{c-SM}} = E\left\{\mathbf{n}_{c-SM}(i)\mathbf{n}_{c-SM}^H(i)\right\} \tag{4.68}$$

The solution to (4.67) is well known to be the principle generalized eigenvector of the matrix pair $\{\mathbf{R}_{\mathbf{x}_{c-SM}}, \mathbf{R}_{\mathbf{n}_{c-SM}}\}$. Finally, the combiner output is given by

$$z_o(i) = \tilde{\mathbf{w}}^H \mathbf{x}_{c-SM}(i) \tag{4.69}$$

Note that the blind MRC combiner exhibits an arbitrary phase ambiguity in symbol detection due to the second order cost function used in (4.67). To remove this ambiguity, differential encoding, or a short training sequence can be incorporated.

4.3.4 Algorithm Summary

In practice, the data correlation matrix is usually estimated by the sample average version:

$$\mathbf{R}_{\mathbf{x}_{c-SM}} \approx \frac{1}{N_s} \sum_{i=1}^{N_s} \mathbf{x}_{c-SM}(i)\mathbf{x}_{c-SM}^H(i) \tag{4.70}$$

assuming that $\mathbf{x}_{c-SM}(i)$ is stationary over the processing period N_s. The noise correlation matrix $\mathbf{R}n$ depends on the beamformer weight vectors, and can be shown to be given by

$$\tilde{\mathbf{R}}_n = \sigma_n^2 \bar{\mathbf{W}}^H \begin{bmatrix} \mathbf{c}_{1,1}^H \mathbf{c}_{1,1}\mathbf{I} & \mathbf{c}_{1,2}^H \mathbf{c}_{1,1}\mathbf{I} & \dots & \mathbf{c}_{1,L}^H \mathbf{c}_{1,1}\mathbf{I} \\ \mathbf{c}_{1,1}^H \mathbf{c}_{1,2}\mathbf{I} & \mathbf{c}_{1,2}^H \mathbf{c}_{1,2}\mathbf{I} & \dots & \mathbf{c}_{1,L}^H \mathbf{c}_{1,2}\mathbf{I} \\ \vdots & \vdots & \dots & \vdots \\ \mathbf{c}_{1,1}^H \mathbf{c}_{1,L}\mathbf{I} & \mathbf{c}_{1,2}^H \mathbf{c}_{1,L}\mathbf{I} & \dots & \mathbf{c}_{1,L}^H \mathbf{c}_{1,L}\mathbf{I} \end{bmatrix} \bar{\mathbf{W}} \tag{4.71}$$

where $\mathbf{I}$ is the $D \times D$ identity matrix. Using the estimate, the proposed diversity combiner is summarized as follows:

1. Determine working sector Θ_s, look angles θ_n^t's, and blocking matrix $\bar{\mathbf{B}}_a$.

103

2. Obtain $\mathbf{R}_{\mathbf{x}_{c-SM}}$ according to (4.70).

3. Obtain $\bar{\mathbf{W}}$ according to (4.62) and (4.65).

4. Obtain $\mathbf{R}_{\mathbf{n}_{c-SM}}$ according to (4.71).

5. Obtain $\bar{\mathbf{f}}$ as principle generalized eigenvector of $\{\mathbf{R}_{\mathbf{x}_{c-SM}}, \mathbf{R}_{\mathbf{n}_{c-SM}}\}$.

6. Obtain combining weight vector as $\tilde{\mathbf{w}} = \bar{\mathbf{W}}\bar{\mathbf{f}}$ and $z_o(i) = \tilde{\mathbf{w}}^H \mathbf{x}_{c-SM}$

The overall schematic diagram of the post-despread receiver is depicted in Figure 4.14.

4.3.5 Recursive Computation of Weight Vectors

To avoid matrix inversion and the incurred numerical instability, the GSC can be implemented in a time-recursive fashion using stochastic gradient algorithms such as LMS [21, 53]. This leads to recursive formulation of the solution to the MMSE problem (4.60)

$$\mathbf{v}_{l,m}(i+1) = \mathbf{v}_{l,m}(i) - \mu_v \left[\bar{\mathbf{a}}_{l,m}^H \mathbf{x}_{c-SM}(i) - \mathbf{v}_{l,m}^H(i)\bar{\mathbf{B}}_a^H \mathbf{x}_{c-SM}(i) \right]^* \bar{\mathbf{B}}_a^H \mathbf{x}_{c-SM}(i) \qquad (4.72)$$

where μ_v is the adaptation stepsizes. It was shown that the convergence of blind adaptive algorithms is slow and noisy compared to the non-blind training signal based algorithm. This is more significant when the size of weight vectors and/or SNR is large. In view of this drawback, it is suggested that blind algorithms be employed in the initialization stage, and be switched to the decision-directed mode once the SINR has improved to offer a reliable decision reference [33].

On the other hand, the generalized eigenvector required for the computation of the MRC weight vector in (4.67) can be also obtained via a time-recursive stochastic gradient (LMS-like) algorithm without the need of a complicated generalized EVD. One such example is the recently developed projection approximation subspace tracking (PAST) algorithm [68], which is shown to exhibit global convergence and requires a computational complexity of the order ML (BT dimension) per iteration. The PAST algorithm was originally proposed for tracking multiple eigenvectors, and can be easily modified for the tracking of a single generalized eigenvector as dictated by (4.67) [36]. The overall algorithm summary is tabulated in Table 4.3.

4.3.6 Complexity and Performance

The computational complexity of the proposed post-despread RAKE receiver depends on the designated blocking matrix $\bar{\mathbf{B}}_a$, which has nothing to do with the processing gain, but is related to the number of antenna D and the number of fingers L. For batch processing, the major computations in the proposed algorithm involves the inversion of $(\bar{\mathbf{B}}_a^H \mathbf{R}_{x_c-SM} \bar{\mathbf{B}}_a)^{-1}$ with size $LD' \times LD'$ in (4.62) and a principal eigenvector computation with size $ML \times ML$ in (4.67). The overall complexity is about $O(ML^4 D'^3 + M^3 L^3)$. Since the number of beams M, the number of finger L, and the degree of D', $D' < D$ are all small numbers, the proposed post-despread receiver is less computational demanding than the previously proposed pre-despread receivers.

4.3.7 Simulation Results

Here the performance of the proposed post-despread receiver is evaluated using a linear array of $D = 12$ identical antennas uniformly spaced by a $1/\sqrt{3}$ wavelength. The inter-antenna spacing is chosen for the field-of-view $[-60°, 60°]$. The working sector is $[-20°, 20°]$, and $M = 4$ diversity beams are formed at look directions $\{\theta_1, \theta_2, \theta_3, \theta_4\} = \{-12.45°, -4.15°, 4.15°, 12.45°\}$. The spatial blocking matrix $\bar{\mathbf{B}}_a$ is constructed with $D' = 6$ using the eigenvector constrained method. It is assumed that the desired signal is in the sector, and the MAI are uniformly distributed in the entire field-of-view, with each user having same multipath angle spread of $10°$. For all users, $J = 4$ paths are generated with the delays $\tau_{i,j}$'s chosen from $\{0, T_c, 2T_c, 3T_c\}$, and the corresponding path gains $\alpha_{i,j}$'s are independent, identically distributed unit variance complex Gaussian random variables. All CDMA signals are generated with BPSK data modulation and spread with the Gold code of length $N = 31$. In addition to the MAI, there are two equal power BPSK NBI's arriving from $30°$ and $-45°$, whose bit rate is 0.8 times that of the CDMA signals. Finally, the number of fingers of the receiver is $L = 4$.

As a performance index, we define the output SINR to be the ratio of the signal power to the interference-plus-noise power at the receiver output $z_o(i)$:

$$\text{SINR}_o = 10 \log_{10} \frac{\text{output power of signal in } z_o(i)}{\text{output power of (MAI+NBI+noise) in } z_o(i)}$$

The input SNR is defined as $\mathrm{SNR}_i = 10 \log_{10} \frac{\sigma_1^2}{\sigma_n^2}$. The near-far-ratio (NFR) is the ratio of the MAI power to signal power before despreading, and the NBI-to-signal-ratio (NSR) is the ratio of the NBI power to signal power before despreading. For all but one result in the simulations, N_s symbols are used to estimate the correlation matrices, and a total of 50 Monte-Carlo runs are executed to obtain an average SINR_o. For performance comparison, we also included the results obtained with the non-blind CST-RAKE, MST-RAKE and MBT-RAKE receivers described by (3.60), (3.61) and (3.77), respectively. The corresponding Post-ST channel vectors are estimated using the same N_s symbols as the training sequence. The simulation parameters are: $N = 31$ with Gold codes, $L = 4$ fingers, the number of antenna elements $D = 12$, the number of training symbols $N_s = 500$, the NSR = 20 dB and the input $\mathrm{SNR}_i = 0$ dB. Unless otherwise mentioned, the above standard parameters will be used throughout the section.

In the first set of simulations, the system capacity and interference rejection capability are evaluated with different user numbers K. The resulting output SINR curves are plotted in Figure 4.16 for NFR = 0 dB and 10 dB. As expected, the MST-RAKE receiver gives the best performance for most cases due to its large degree of freedom ($DL = 48$) for interference suppression. The MBT-RAKE receiver performs well with a small K and low NFR, in which case interference suppression can be done successfully using its smaller degree of freedom ($ML = 16$). On the other hand, the proposed beamspace-time receiver (GSC3-RAKE) performs reliably for a wide range of K, even in the presence of strong MAI. In fact, the performance of the proposed receiver is nearly the same performance as that of MST-RAKE receiver with a moderately large K and high NFR, indicating that the adaptive beamformers and correlators have successfully eliminated the strong NBI and MAI, respectively. Note that the MST-RAKE receiver cannot handle the time-varying NBI well when K is large. This is because that the time-varying NBI appears to the MST-RAKE receiver as a set of multiple time-invariant MAI [100], and requires a large degree of freedom for effective cancellation. But the NBI seems to be stationary in spatial domain and can be nulling by the adaptive beamformer of proposed receiver. The CST-RAKE receiver totally fails with NFR = 10 dB due to the lack of interference suppression and cause large channel estimation error.

In the second set of simulations, the near-far resistance of the proposed receiver is eval-

uated with different NFR values. Figure 4.17 shows the results obtained with $K = 5$ and 20 users. It is observed that the CST-RAKE fails again, and the MBT-RAKE receiver loses its near-far resistance with $K = 20$ due to the exhaustion of degree of freedom for interference suppression. On the contrary, the proposed receiver achieves its near-far resistance by successfully cancelling the MAI the strong NBI using the jointly ST degree of freedom.

Finally, to demonstrate the effectiveness of the recursive algorithms for weight adaptation and eigenvector computation, we replaced the direct matrix inversions and eigenvector computation by the formulae given in (4.72). The adaptation stepsizes are chosen as $\mu_v = 10^{-6}$. Figure 4.19(a) shows the resulting learning curve of the receiver, with NFR = 0 dB, and $K = 5$. To show the tracking capability of the algorithm, we repeated the same simulation, but deliberately changed the AOA's of the two NBI's to 40° and −50°, respectively, at the 500th iteration. The learning curves given in Figure 4.19(b) confirm that the recursive receiver successfully adjusted its weights to suppress the NBI.

4.4   Summary

Three blind adaptive beamspace-time receivers have been proposed for sectored CDMA wireless communications. The first proposed receiver was designed with a two-stage procedure. First, a set of adaptive ST diversity beamformers was constructed which provides effective suppression of unwanted interference and reception of signals from a prescribed ST region. Second, the output data obtained from these processors were maximum ratio combined to capture the signal multipath components coherently. The second proposed receiver used the beamformer-correlator pairs to alternately optimize the beamformer and correlator outputs. Finally, a post-despread receiver was proposed. The receiver constructed multiple beams for each finger, as opposed to the conventional ST receivers, which use one beam for each finger. All these proposed receivers work blindly without the aid of a training signal. The only information required is the signature sequence, timing and a rough estimate of the angle of arrival of the signal for selecting the sector of interest. For an efficient implementation, recursive algorithms are derived for weight vector adaptation and eigenvector computation. Compared to the conventional antenna level ST receivers, beamspace receivers

enhance the the SINR by suppressing interference via adaptive nulling, and lower the computational complexity by reducing data dimension. From simulation results, it is shown that the proposed blind receivers are near-far resistant, and performs reliably in an overloaded system, even in the presence of strong NBI.

Table 4.1: Algorithm summary of adaptive beamspace-time 2-D RAKE receiver

1. Determine working sector Θ_s, look angles θ_m's and GSC blocking matrices $\mathbf{B}_c$ and $\mathbf{B}_a$.

2. Initialize the coefficients μ_v , μ_g, λ_e and forgetting factor α_p of PAST

3. Initialize the adaptive weights $\mathbf{s_{l,m}} = \mathbf{c_{l,l}}$ and $\mathbf{w}_{l,m} = \mathbf{a}(\theta_m)$.

4. For $i = 1, 2, \cdots$ (Do recursive update for step $4 \sim 6$)

5. For $l = 1, \cdots, L$ and $m = 1, \cdots, M$ (ML processors in parallel).

$$\tilde{\mathbf{x}}_l(i) = \mathbf{X}(i)\mathbf{c}_{1,l}^*$$

$$\mathbf{w}_{l,m}(i) = \mathbf{a}(\theta_m) - \mathbf{B}_a\mathbf{v}_{l,m}(i)$$

$$\mathbf{y}_{l,m}(i) = \mathbf{w}_{l,m}(i)^H\mathbf{X}(i)$$

$$\mathbf{v}_{l,m}(i+1) = \mathbf{v}_{l,m}(i) + \mu_v \left[\mathbf{a}^H(\theta_m)\tilde{\mathbf{x}}_l(i) - \mathbf{v}_{l,m}^H(i)\mathbf{B}_a^H\tilde{\mathbf{x}}_l(i)\right]^* \mathbf{B}_a^H\tilde{\mathbf{x}}_l(i)$$

$$\mathbf{g}_{l,m}(i+1) = \mathbf{g}_{l,m}(i) + \mu_g \left[\mathbf{c}_{1,l}^H\mathbf{y}_{l,m}(i) - \mathbf{g}_{l,m}^H(i)\mathbf{B}_c^H\mathbf{y}_{l,m}(i)\right]^* \mathbf{B}_c^H\mathbf{y}_{l,m}(i)$$

$$\mathbf{w}_{l,m}(i+1) = \mathbf{a}(\theta_m) - \mathbf{B}_a\mathbf{v}_{l,m}(i+1)$$

$$\mathbf{s}_{l,m}(i+1) = \mathbf{c}_{1,l} - \mathbf{B}_c\mathbf{g}_{l,m}(i+1)$$

$$z_{l,m}(i+1) = \mathbf{w}_{l,m}^H(i+1)\mathbf{X}(i+1)\mathbf{s}_{l,m}^*(i+1)$$

$$\mathbf{z}(i+1) = [z_{1,1}(i+1), \cdots, z_{1,M}(i+1), z_{2,1}(i+1), \cdots, z_{2,M}(i+1), \cdots,$$
$$z_{L,1}(i+1), \cdots, z_{L,M}(i+1)]^T$$

6. Use PAST to track the principal eigenvector and do maximum ratio combiner

$$z_o(i+1) = \mathbf{f}_{mrc}^H(i)\mathbf{z}(i+1)$$

$$\hat{b}_1(i+1) = z_o(i+1)$$

$$\lambda_e(i+1) = \alpha_p\lambda_e(i) + |z_o(i+1)|^2$$

$$\mathbf{f}_{mrc}(i+1) = \mathbf{f}_{mrc}(i) + [\tilde{\mathbf{z}}(i+1) - \mathbf{f}_{mrc}(i)z_o(i)] z_o(i+1)^*/\lambda_e(i+1)$$

Table 4.2: Algorithm summary of adaptive space-time alternating 2-D RAKE receiver

1. Determine working sector Θ_s, look angles θ_m's and GSC blocking matrices $\mathbf{B}_c$ and $\mathbf{B}_a$.

2. Initialize the coefficients μ_v , μ_g, λ_e, $\mathbf{f}_{mrc}(0)$ and forgetting factor α_p of PAST

3. Initialize the adaptive weights $\hat{\mathbf{s}}_{l,m}(0) = \mathbf{c}_{l,l}$ and $\tilde{\mathbf{w}}_{l,m}(0) = \mathbf{a}_m$.

4. For $l = 1, \cdots, L$ and $m = 1, \cdots, M$ (ML processors in parallel).

5. For $i = 1, 2, \cdots$, recursive calculate step 6 and step 7.

6. Update $\hat{\mathbf{s}}_{l,m}(i)$, goto step 7

$$\mathbf{g}_{l,m}(i+1) = \mathbf{g}_{l,m}(i) + \mu_g \left[(\mathbf{c}_{1,l} - \mathbf{B}_c \mathbf{g}_{l,m}(i))^H \mathbf{X}^T(i) \tilde{\mathbf{w}}_{l,m}^*(i) \right]^* \mathbf{B}_c^H \mathbf{X}^T(i) \tilde{\mathbf{w}}_{l,m}^*(i)$$

$$\mathbf{s}_{l,m}(i+1) = \mathbf{c}_{1,l} - \mathbf{B}_c \mathbf{g}_{l,m}(i+1)$$

7. Update $\tilde{\mathbf{w}}_{l,m}(i+1)$, goto step 6

$$\mathbf{v}_{l,m}(i+1) = \mathbf{v}_{l,m}(i) + \mu_v \left[(\mathbf{a}_m - \mathbf{B}_a \mathbf{v}_{l,m}(i))^H \mathbf{X}(i) \hat{\mathbf{s}}_{l,m}^*(i) \right]^* \mathbf{B}_a^H \mathbf{X}(i) \hat{\mathbf{s}}_{l,m}^*(i)$$

$$\tilde{\mathbf{w}}_{l,m}(i+1) = \mathbf{a}(\theta_m) - \mathbf{B}_a \mathbf{v}_{l,m}(i+1)$$

8. Use PAST to track the principal eigenvector and do maximum ratio combiner

$$\tilde{z}_{l,m}(i+1) = \tilde{\mathbf{w}}_{l,m}^H(i+1) \mathbf{X}(i+1) \hat{\mathbf{s}}_{l,m}^*(i+1)$$

$$\mathbf{z}_c(i+1) = [\tilde{z}_{1,1}(i+1), \cdots, \tilde{z}_{1,M}(i+1), \tilde{z}_{2,1}(i+1), \cdots, \tilde{z}_{2,M}(i+1), \cdots,$$

$$\tilde{z}_{L,1}(i+1), \cdots, \tilde{z}_{L,M}(i+1)]^T$$

$$z_o(i+1) = \mathbf{f}_{mrc}^H(i) \mathbf{z}_c(i+1)$$

$$\hat{b}_1(i+1) = z_o(i+1)$$

$$\lambda_e(i+1) = \alpha_p \lambda_e(i) + |z_o(i+1)|^2$$

$$\mathbf{f}_{mrc}(i+1) = \mathbf{f}_{mrc}(i) + [\mathbf{z}_c(i+1) - \mathbf{f}_{mrc}(i) z_o(i)] z_o(i+1)^* / \lambda_e(i+1)$$

Table 4.3: Algorithm summary of post-despread beamspace-time 2-D RAKE receiver

1. Determine working sector Θ_s, look angles θ_m's and blocking matrices $\mathbf{B}_a$ and $\bar{\mathbf{B}}_a$.
2. Initialize the coefficients μ_v, λ_e, $\bar{\mathbf{f}}(0)$ and forgetting factor α_p of PAST
3. Initialize the adaptive weights $\bar{\mathbf{w}}_{l,m}(0) = \bar{\mathbf{a}}_{l,m}$, i.e, $\bar{\mathbf{v}}_{l,m} = \mathbf{0}$.
4. For $l = 1, \cdots, L$ and $m = 1, \cdots, M$ $(ML$ processors in parallel).
5. For $i = 1, 2, \cdots$, recursively update $\bar{\mathbf{w}}_{l,m}(i+1)$.

$$\bar{\mathbf{v}}_{l,m}(i+1) = \bar{\mathbf{v}}_{l,m}(i) - \mu_v \left[\bar{\mathbf{a}}_{l,m}^H \mathbf{x}_{c-SM}(i) - \bar{\mathbf{v}}_{l,m}^H(i) \bar{\mathbf{B}}_a^H \mathbf{x}_{c-SM}(i) \right]^* \bar{\mathbf{B}}_a^H \mathbf{x}_{c-SM}(i)$$

$$\bar{\mathbf{w}}_{l,m}(i+1) = \mathbf{a}(\theta_m) - \mathbf{B}_a \bar{\mathbf{v}}_{l,m}(i+1)$$

$$\bar{\mathbf{W}}(i+1) = [\bar{\mathbf{w}}_{1,1}(i+1), \ldots, \bar{\mathbf{w}}_{L,1}(i+1), \bar{\mathbf{w}}_{1,2}(i+1), \ldots, \bar{\mathbf{w}}_{L,2}(i+1), \ldots,$$

$$\bar{\mathbf{w}}_{L,1}(i+1), \ldots, \bar{\mathbf{w}}_{L,M}(i+1)]$$

$$\bar{\mathbf{z}}(i+1) = \bar{\mathbf{W}}(i+1)^H \mathbf{x}_{c-SM}$$

6. Use PAST to track the principal eigenvector and do maximum ratio combiner

$$z_o(i+1) = \bar{\mathbf{f}}(i)^H \bar{\mathbf{z}}(i+1)$$

$$\hat{b}_1(i+1) = z_o(i+1)$$

$$\lambda_e(i+1) = \alpha_p \lambda_e(i) + |z_o(i+1)|^2$$

$$\bar{\mathbf{f}}(i+1) = \bar{\mathbf{f}}(i) + \left[\mathbf{z}(i+1) - \bar{\mathbf{f}}(i) z_o(i) \right] z_o(i+1)^* / \lambda_e(i+1)$$
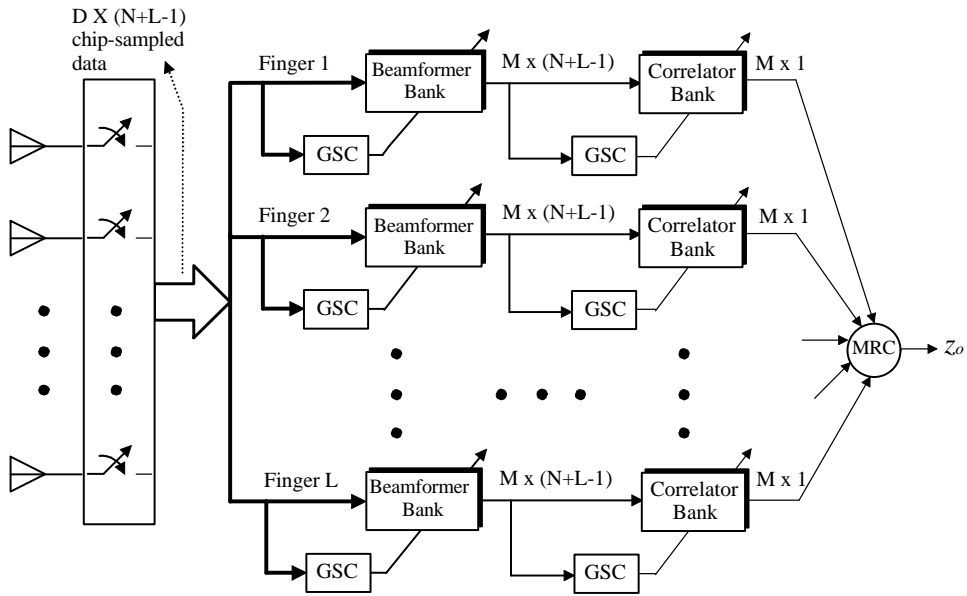
Figure 4.1: Scheme of fisrt proposed beamspace-time 2-D RAKE receiver

Figure 4.2: Output SINR versus number of users for GSC1-RAKE, MST-RAKE and CST-RAKE receivers with (a) NFR = 0 dB and (b) NFR = 20 dB.

112

Figure 4.3: Patterns of diversity beams of GSC1-RAKE receiver obtained with $K = 5$ and NFR = 10 dB for (a) Finger 1 and (b) Finger 3.
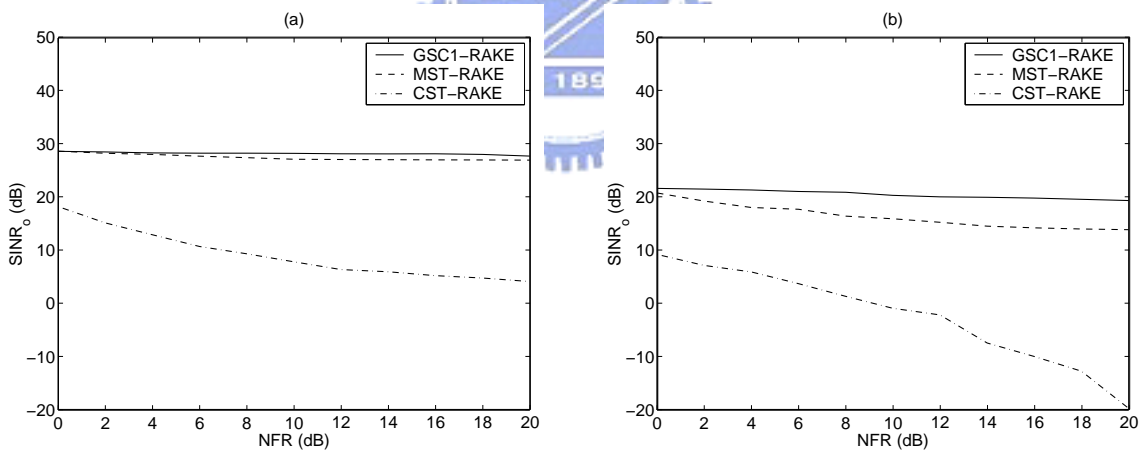
Figure 4.4: Evaluation of near-far resistance of GSC1-RAKE, MST-RAKE and CST-RAKE receivers with in-sector MAI power controlled, (a) $K = 5$ and (b) $K = 25$.
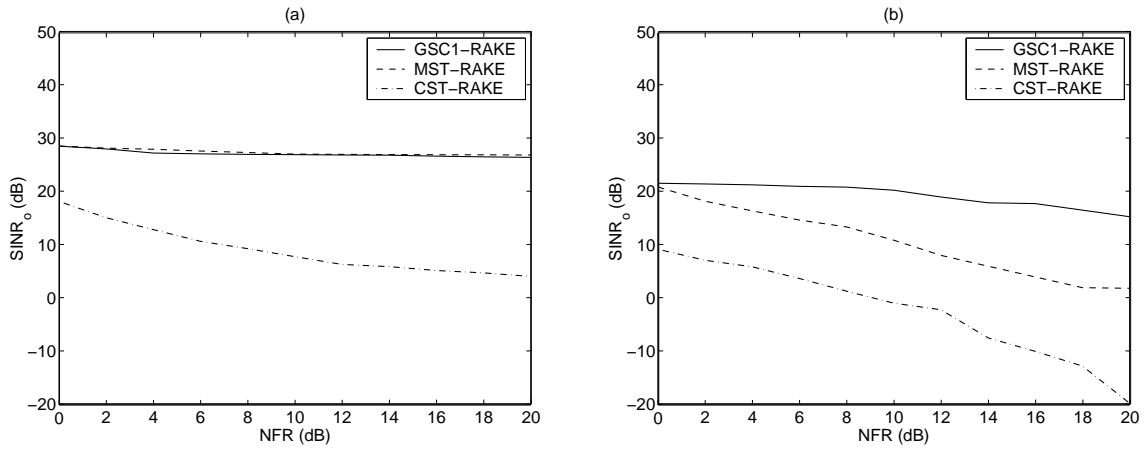
Figure 4.5: Evaluation of near-far resistance of GSC1-RAKE, MST-RAKE and CST-RAKE receivers with in-sector MAI not power controlled for (a) $K = 5$ and (b) $K = 25$.
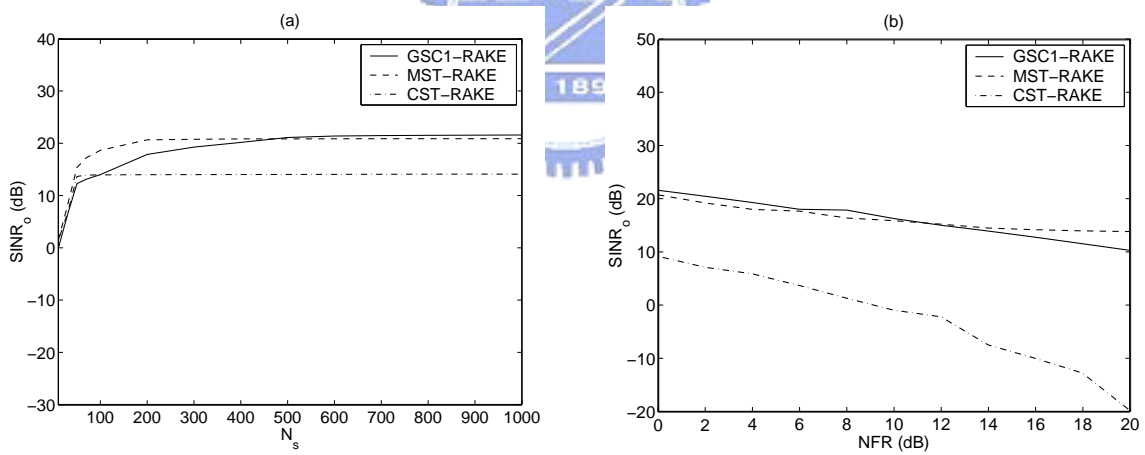
Figure 4.6: Convergence behavior of GSC1-RAKE, MST-RAKE and CST-RAKE receivers with $K = 25$, (a) NFR = 0 dB and (b) NFR = 20 dB.
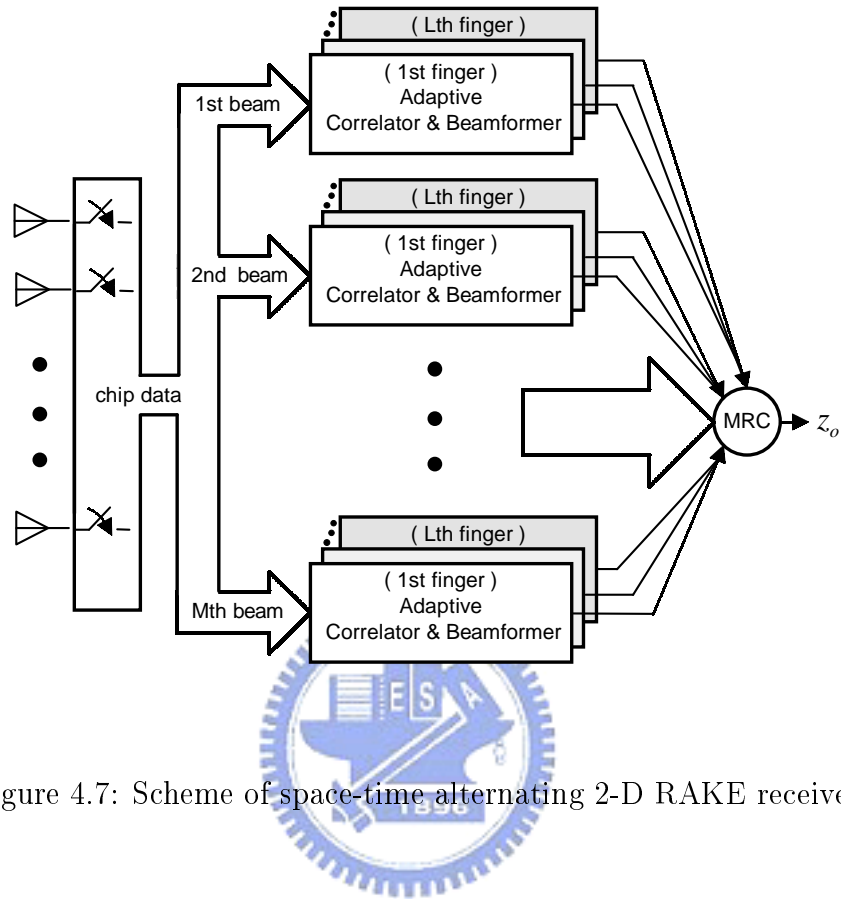
Figure 4.7: Scheme of space-time alternating 2-D RAKE receiver
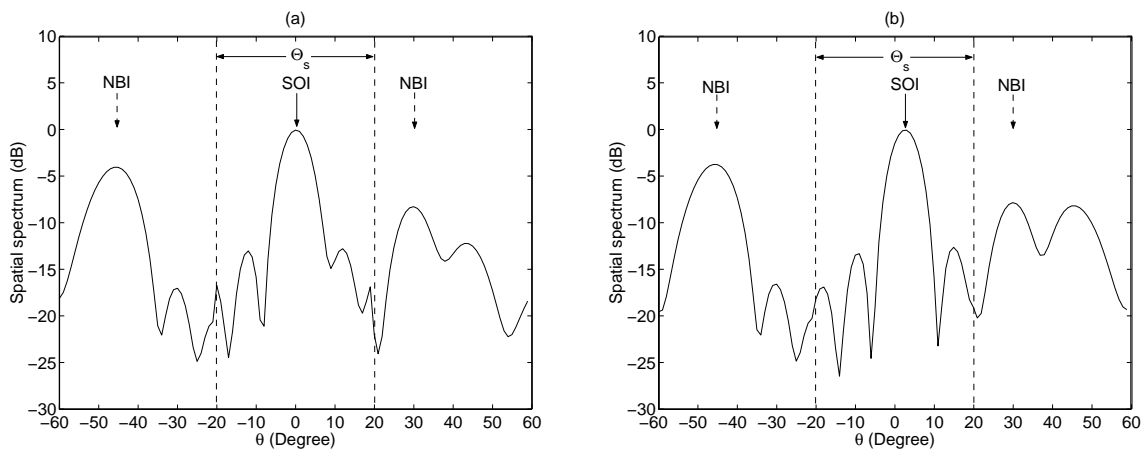
Figure 4.8: Spatial spectrum of AOA estimation of GSC2-RAKE receiver obtained with $K = 10$ users and NFR $= 0$ dB for (a) Finger 1 and (b) Finger 3.
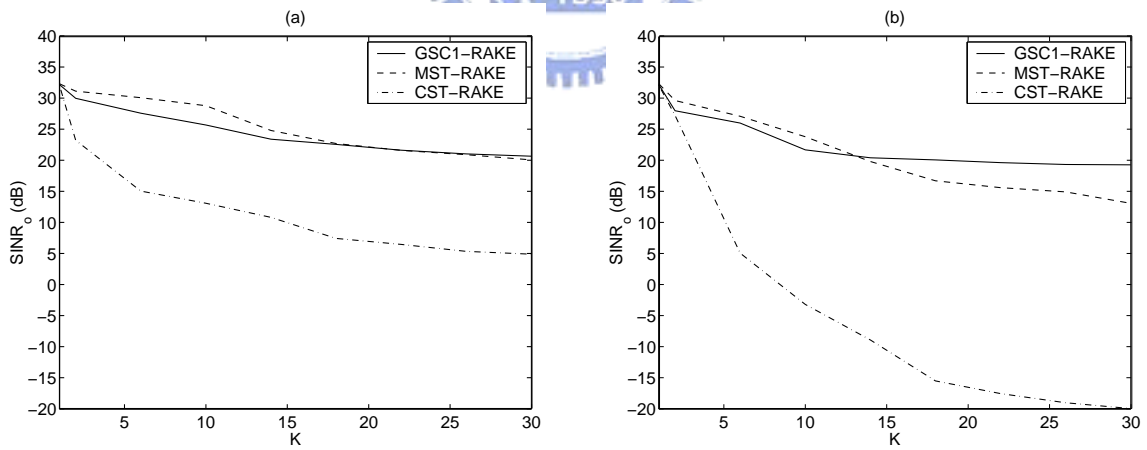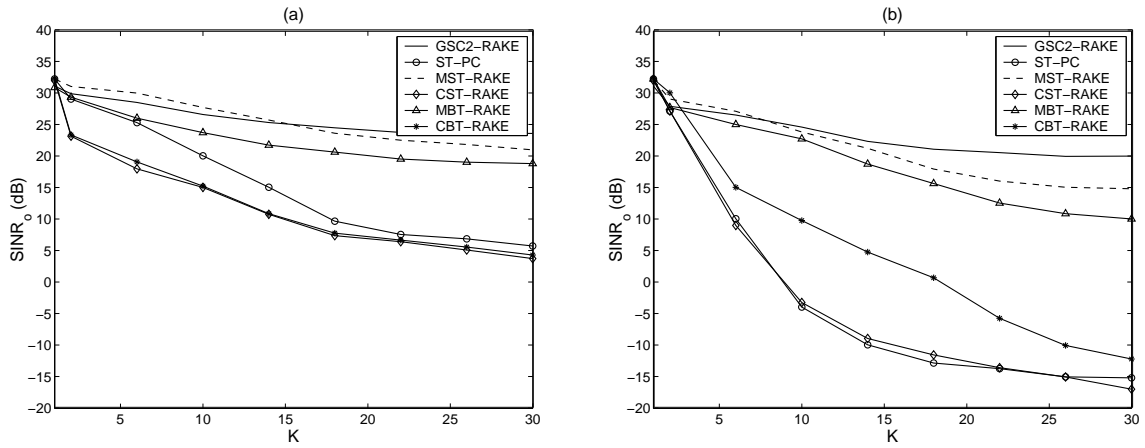
Figure 4.9: Output SINR versus number of users for GSC2-RAKE, MST-RAKE and CST-RAKE receivers with (a) NFR = 0 dB and (b) NFR = 20 dB.
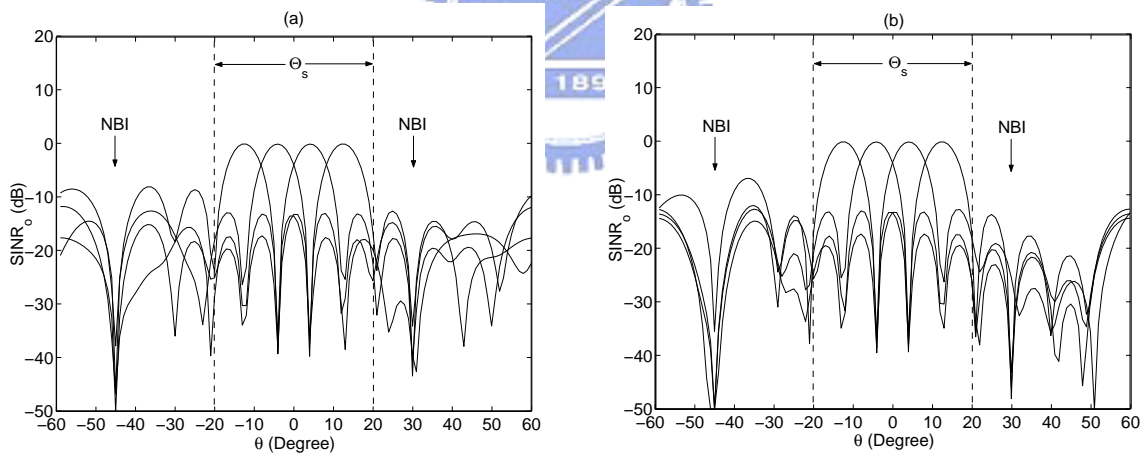
Figure 4.10: Patterns of diversity beams of GSC2-RAKE receiver obtained with $K = 5$ users and NFR = 0 dB for (a) Finger 1 and (b) Finger 3.
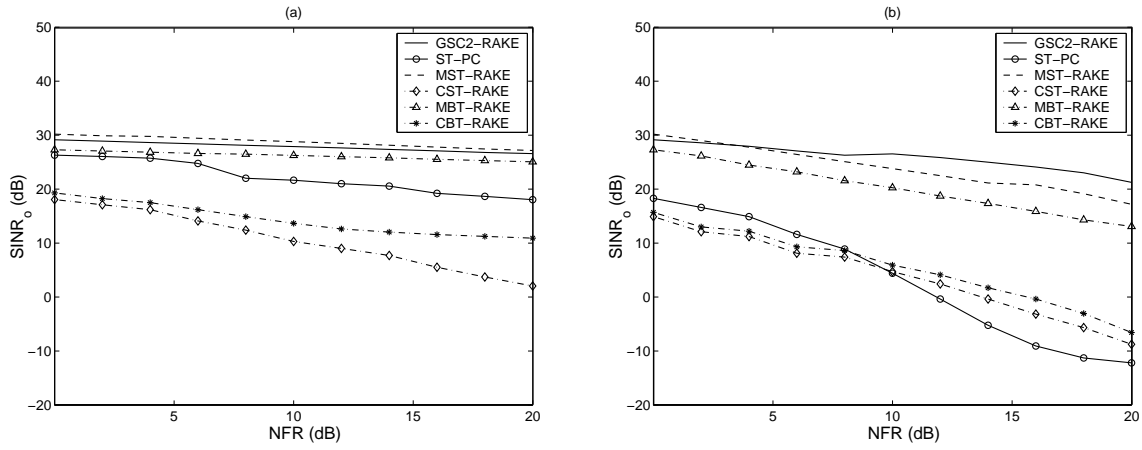
Figure 4.11: Evaluation of near-far resistance of GSC2-RAKE, MST-RAKE and CST-RAKE receivers with (a) $K = 5$ and (b) $K = 25$.
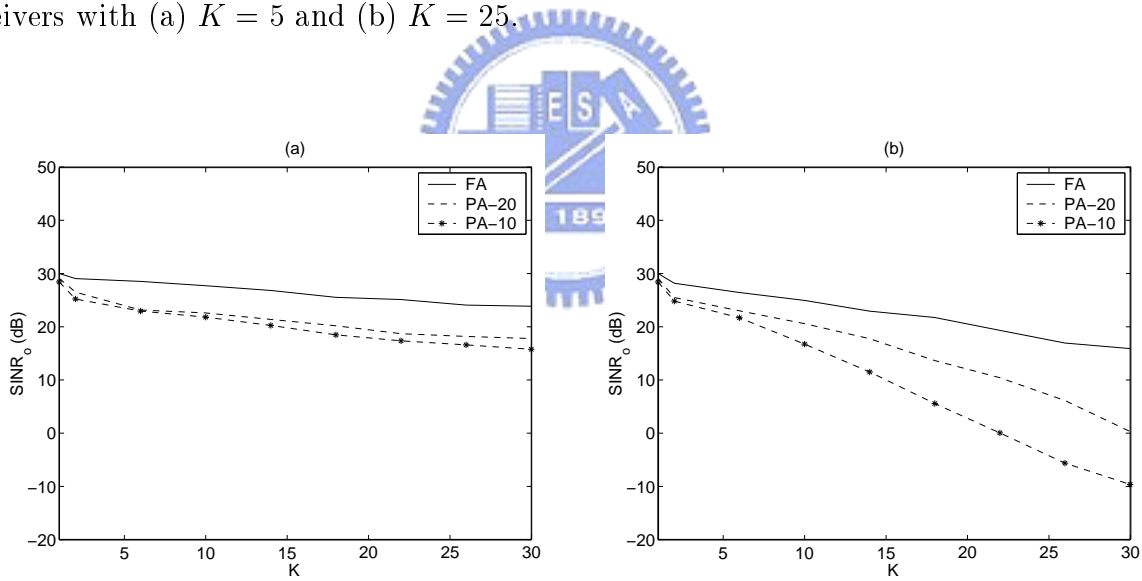
Figure 4.12: Output SINR versus number of users for FA, PA with $P' = 20$ (PA-20), and PA with $P' = 10$ (PA-10) of GSC2-RAKE receivers with (a) NFR = 0 dB and (b) NFR = 20 dB.
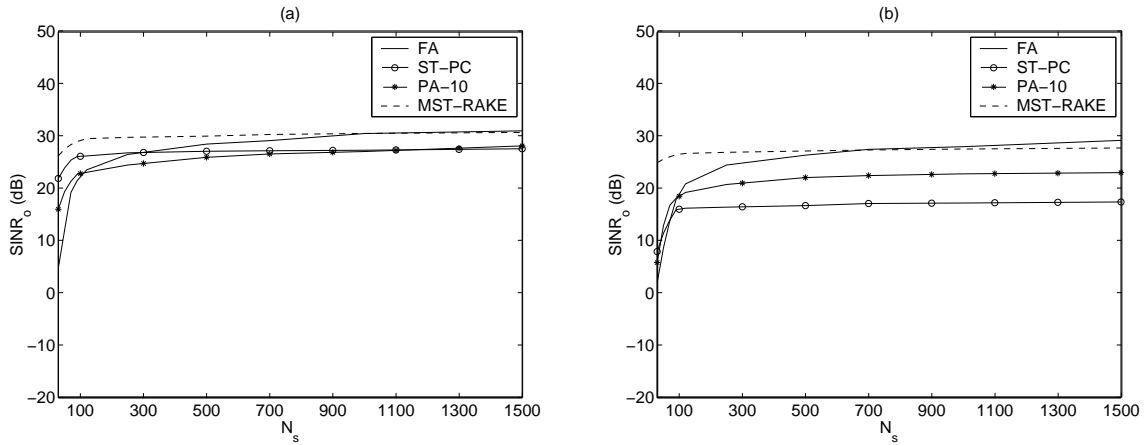
Figure 4.13: Evaluation of convergence behaviors of FA, PA-10, MST-RAKE and ST-PC receivers obtained with $K = 5$, (a) NFR = 0 dB and (b) NFR = 20 dB.
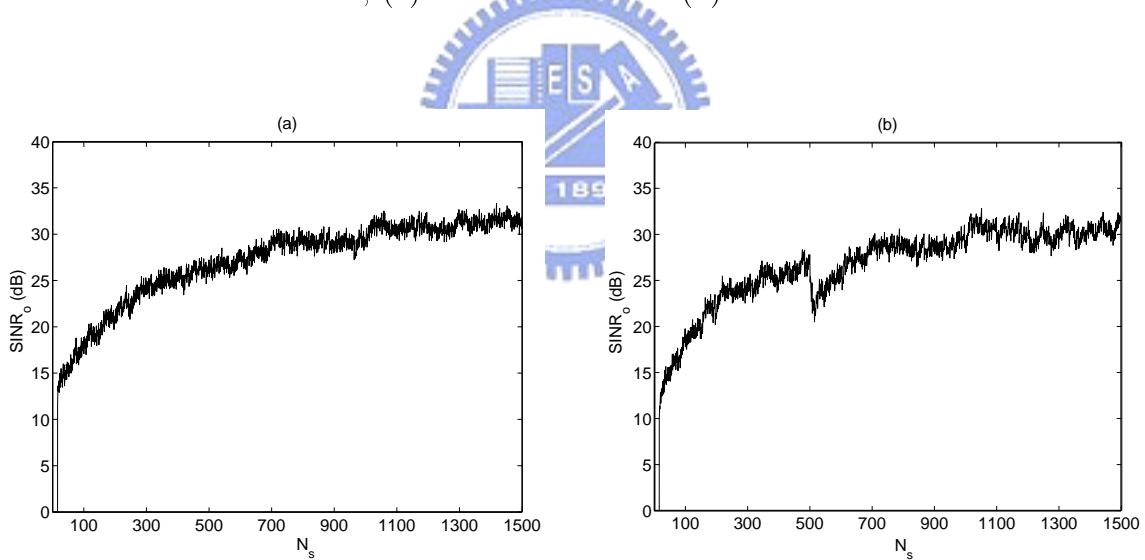
Figure 4.14: Evaluation of recursive algorithms of GSC2-RAKE receiver with $K=5$ users, NFR = 0 dB for (a) NBI's AOA fixed and (b) NBI's AOA changed at 500th iteration.
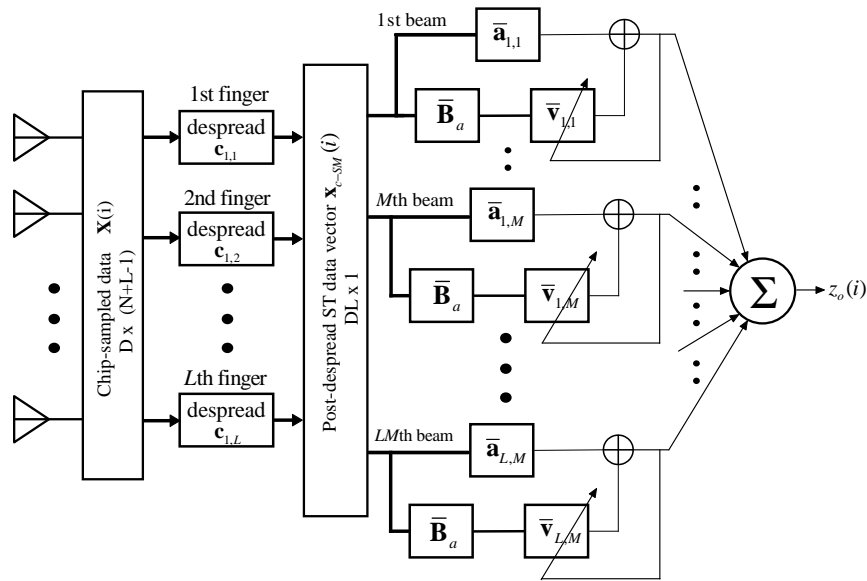
Figure 4.15: Scheme of post-despread BT 2-D RAKE receiver
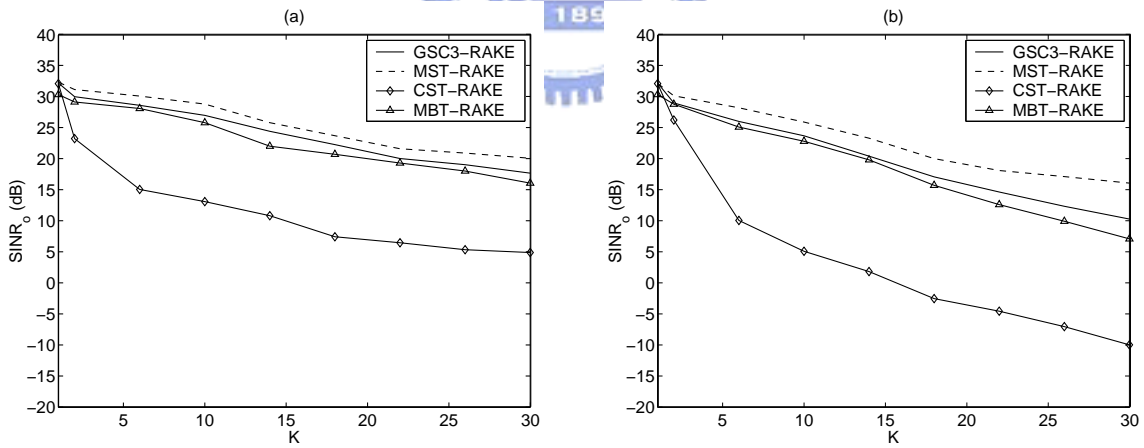
Figure 4.16: Output SINR versus number of users for GSC3-RAKE, MST-RAKE, MBT-RAKE and CST-RAKE receivers with (a) NFR = 0 dB and (b) NFR = 10 dB.
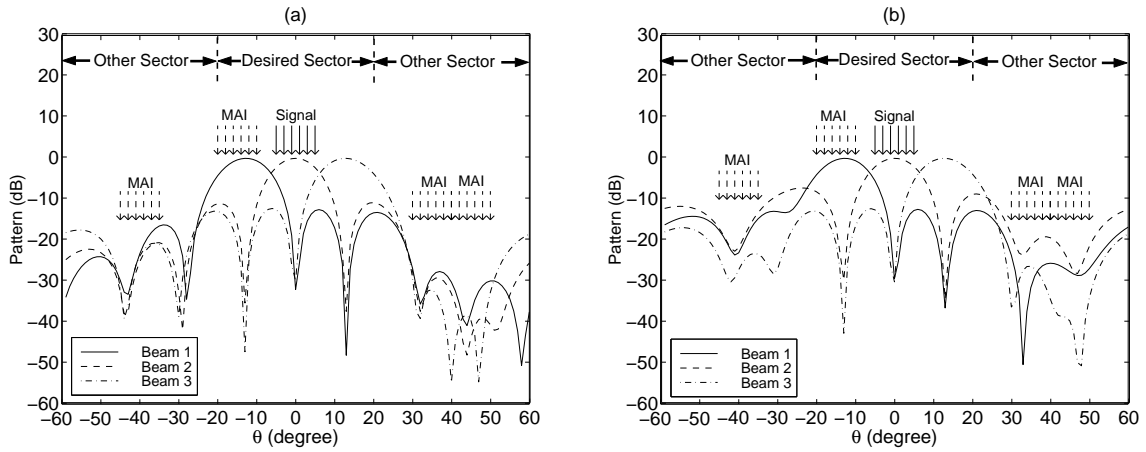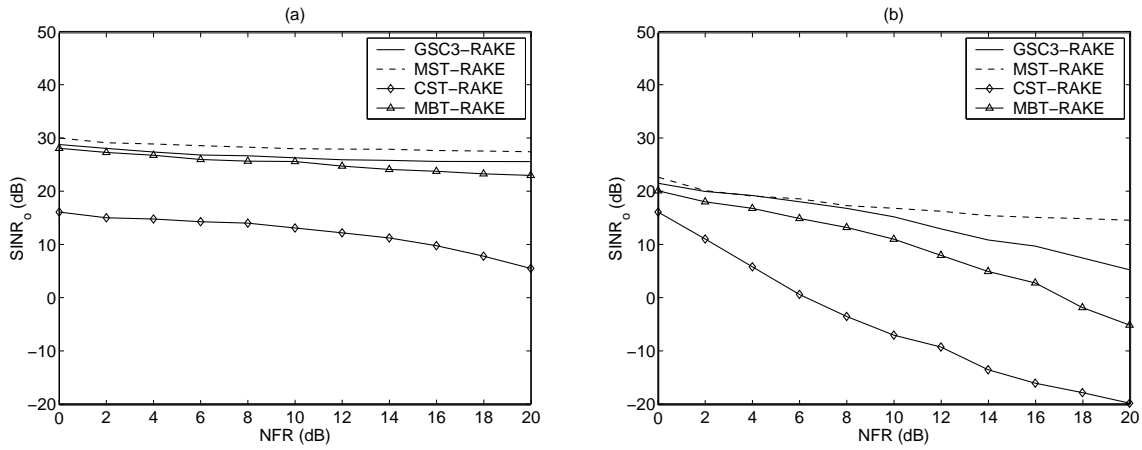
Figure 4.17: Evaluation of near-far resistance of GSC3-RAKE, MST-RAKE, MBT-RAKE and CST-RAKE receivers with (a) $K = 5$ and (b) $K = 20$.
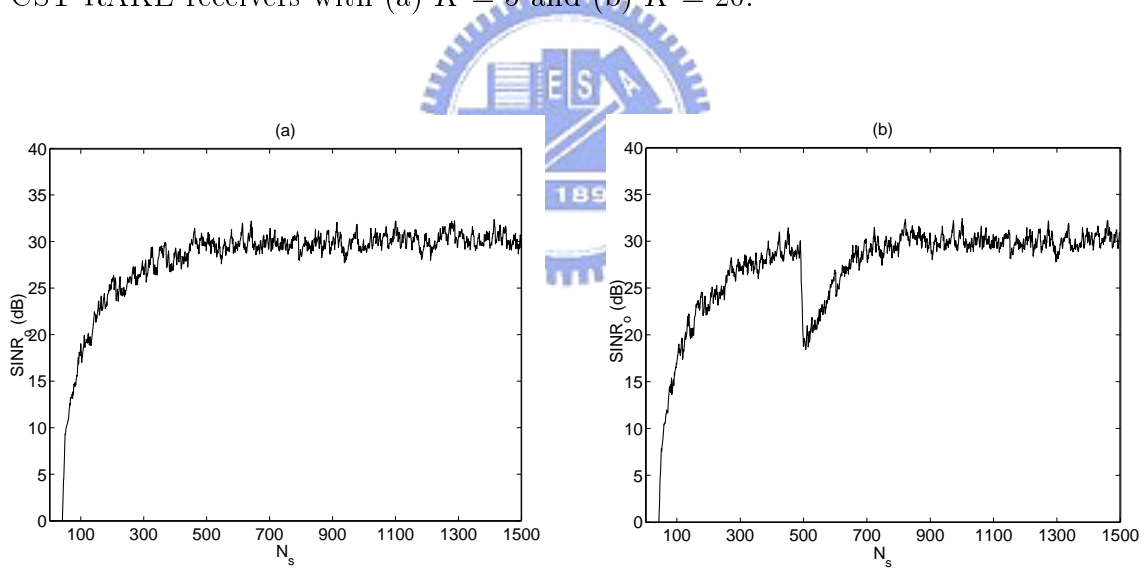
Figure 4.18: Evaluation of recursive algorithms of GSC3-RAKE receiver obtained with $K = 5$, NFR $= 0$ dB for (a) NBI's AOA fixed and (b) NBI's AOA changed at 500th iteration.

Appendix: Derivation of Entries of $\mathbf{R}_{\mathbf{n}_c}$

Let $i = (m_1 - 1)L + l_1$ and $j = (m_2 - 1)L + l_2$. From (4.45), the (i,j)th entry of $\mathbf{R}_{\mathbf{n}_c}$ is the crosscorrelation between $n_{l_1,m_1}(k)$ and $n_{l_2,m_2}(k)$:

$$
\begin{aligned}
[\mathbf{R}_{\mathbf{n}_c}]_{(i,j)} &= E\{\tilde{\mathbf{w}}^H_{l_1,m_1} \mathbf{N}(k)\hat{\mathbf{s}}^*_{l_1,m_1}\hat{\mathbf{s}}^T_{l_2,m_2}\mathbf{N}^H(k)\tilde{\mathbf{w}}_{l_2,m_2}\} \\
&= \tilde{\mathbf{w}}^H_{l_1,m_1} E\{\mathbf{N}(k)\hat{\mathbf{s}}^*_{l_1,m_1}\hat{\mathbf{s}}^T_{l_2,m_2}\mathbf{N}^H(k)\}\tilde{\mathbf{w}}_{l_2,m_2} \\
&= \tilde{\mathbf{w}}^H_{l_1,m_1} \left(\sum_{l=1}^{N+L-1} \sum_{n=1}^{N+L-1} [\hat{\mathbf{s}}^*_{l_1,m_1}]_l[\hat{\mathbf{s}}_{l_1,m_1}]_n E\{\mathbf{n}_l(k)\mathbf{n}^*_n(k)\} \right) \tilde{\mathbf{w}}_{l_2,m_2}
\end{aligned}
$$

where $[\hat{\mathbf{s}}_{l_1,m_1}]_n$ is the nth entry of $\hat{\mathbf{s}}_{l_1,m_1}$, and $\mathbf{n}_l(k)$ is the lth column of $\mathbf{N}(k)$. Using the fact that $\mathbf{n}_l(k)$ are i.i.d. random vectors with the same variance σ^2_n, we have

$$
E\{\mathbf{n}_l(k)\mathbf{n}^*_n(k)\} = \sigma^2_n\mathbf{I}\delta[l-n]
$$

where $\delta[n]$ is the Kronecker delta function. This gives

$$
\begin{aligned}
[\mathbf{R}_{\mathbf{n}_c}]_{(i,j)} &= \sigma^2_n\tilde{\mathbf{w}}^H_{l_1,m_1} \left(\sum_{n=1}^{N+L-1} [\hat{\mathbf{s}}^*_{l_1,m_1}]_l[\hat{\mathbf{s}}_{l_1,m_1}]_n \right) \tilde{\mathbf{w}}_{l_2,m_2} \qquad (4.73) \\
&= \sigma^2_n\tilde{\mathbf{w}}^H_{l_1,m_1} \tilde{\mathbf{w}}_{l_2,m_2}\hat{\mathbf{s}}^T_{l_1,m_1}\hat{\mathbf{s}}^*_{l_2,m_2} \qquad (4.74)
\end{aligned}
$$
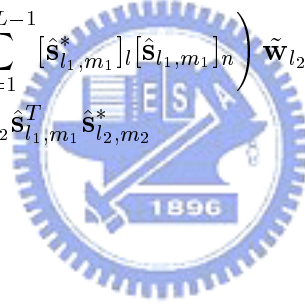
Chapter 5

Adaptive CDMA Receivers

In wireless communications, the radio propagation channel is dynamic, and the adaptation process must be continuous to allow the receiver to constantly optimize its filter weights. The algorithm must adapt the weights quickly to keep up with the changing environment. Since the adaptation algorithm is used continuously, its computational complexity is often an important issue to be considered, especially when used in single-user receivers, where power and physical space may be at a premium. The trade-off between convergence speed and complexity should be taken into careful consideration.

A variety of adaptive algorithms have been used in adaptive CDMA receivers. While some of them are classic algorithms used in adaptive equalization and interference rejection, others are new and have been specially developed for CDMA receivers. Adaptive receivers can be divided into two categories based on whether training sequences are used or not. In the first category, nonblind MMSE receivers can be adaptively implemented if the desired signal is known at the receiver [15], while in the second category, a blind approach is employed. The nonblind methods need a significant overhead for training and may not be feasible in practice. It is thus desirable to have blind algorithms that does not need any training signals.

The GSC algorithms proposed in previous chapters for wireless DS/CDMA receivers can be used in a blind or nonblind way. Since the antenna array suppresses the strong out-of-sector NBI and/or out-of-sector MAI and the set of adaptive correlators also suppress the in-sector MAI, the proposed GSC receivers can use a shorter training sequence than the MMSE receiver for the start-up procedure. The goal of this chapter is to derive adaptive algorithms

for the GSC structure based CDMA receivers. Popular conventional adaptive methods are the LMS and RLS algorithms. The LMS algorithm suffers from slow convergence, but has a low computational complexity. The RLS algorithm has a faster convergence, but tends to be sensitive to the input data. In this chapter, we will develop adaptive 2-D RAKE receivers based either on the LMS or RLS algorithm.

5.1 Adaptive Multiuser Receivers

The linear multiuser receivers such as the decorrelating and the MMSE multiuser receivers depend on signal crosscorrelations (and on the received SNR in case of MMSE detector), and the computation of their filter weights involves matrix inversions. It is particularly important to eliminate this need in multipath fading channels where crosscorrelations are time varying and in channels with time varying received power levels. It is desirable to obtain a linear multiuser detector that not only eliminates the need for on-line computation of its weights, but also adapts to the time varying environment. Here, we present some categories of adaptive algorithms for DS/CDMA multiuser detectors. The first category consists of the LMS and RLS algorithms which are well-known in the adaptive filtering theory [53, 69]. The second category is an iterative method for successive interference suppression (SIC) or parallel interference suppression (PIC).

5.1.1 LMS and RLS Adaptive Algorithms for Multiuser Receivers

In the training mode, the weight matrix of space-time MMSE multiuser receiver, $\mathbf{T}_{ST_{MMSE}}$ working on the sufficient statistics, can be obtained based on the MMSE criterion:

$$\mathbf{T}_{ST_{MMSE}} = \arg \min_{\mathbf{T} \in \mathbf{C}^{KI \times KI}} \left\{ E \left\{ \left\| \mathbf{T}^H \mathbf{y}_{ST}(i) - \mathbf{b}(i) \right\|^2 \right\} \right\} \tag{5.1}$$

The cost function of MMSE receiver is

$$\min_{\mathbf{T} \in \mathbf{C}^{KI \times KI}} J(\mathbf{T}) = E \left\{ \left\| \mathbf{T}^H \mathbf{y}_{ST}(i) - \mathbf{b}(i) \right\|^2 \right\} \tag{5.2}$$

The LMS adaptive algorithm is employed to update the weight matrix $\mathbf{T}$ at the ith input data with the recursion:

$$\mathbf{T}(i+1) = \mathbf{T}(i) + \mu \mathbf{y}_{ST}(i) \left[\mathbf{b}(i) - \mathbf{z}_{ST}(i) \right]^H \tag{5.3}$$

where $\mathbf{z}_{ST}(i) = \mathbf{T}^H(i)\mathbf{y}_{ST}(i)$ is the $KI \times 1$ filter output (one update per symbol), and $\mathbf{T}(i)$ and $\mathbf{y}_{ST}(i)$ denote the weight matrix and sufficient statistics vector at the ith iteration, respectively. The μ is the algorithm's stepsize. Each column of $\mathbf{T}$ is updated through the standard form of the single-user LMS algorithm.

A modification of the ordinary LMS algorithm to avoid noise amplification, when $\mathbf{y}_{ST}(i)$ is large, is the normalized LMS (NLMS) algorithm [53, 70]. The NLMS may be viewed as the solution to the constrained optimization problem $\mathbf{T}^H(i+1)\mathbf{y}_{ST}(i) = \mathbf{b}(i)$. This result has the following form:

$$\mathbf{T}(i+1) = \mathbf{T}(i) + \bar{\mu}\frac{\mathbf{y}_{ST}(i)}{\|\mathbf{y}_{ST}(i)\|^2}\left[\mathbf{b}(i) - \mathbf{z}_{ST}(i)\right]^H \tag{5.4}$$

where $\bar{\mu}$ is the stepsize. It can be shown that the NLMS algorithm converges in the mean square if $0 < \bar{\mu} < 1$ [53], which makes the selection of the stepsize $\bar{\mu}$ much easier than the selection of μ in the LMS algorithm. Normally, when the system employ a training signal to achieve a level of performance, the algorithm (5.4) will be switched to decision-directed mode in the form:

$$\mathbf{T}(i+1) = \mathbf{T}(i) + \bar{\mu}\frac{\mathbf{y}_{ST}(i)}{\|\mathbf{y}_{ST}(i)\|^2}\left[\mathbf{b}(i) - \hat{\mathbf{b}}(i)\right]^H \tag{5.5}$$

where $\hat{\mathbf{b}}(i) = sign\left[\mathbf{z}_{ST}(i)\right]$.

Another alternative to the LMS algorithm is the RLS algorithm which chooses the weight matrix $\mathbf{T}$ to minimize the least squares cost function:

$$\min_{\mathbf{T}\in\mathbf{C}^{KI \times KI}} J_{ls}(\mathbf{T}) = \sum_{\mathbf{j}=1}^{\mathbf{i}} \lambda_{\mathbf{ls}}^{\mathbf{i}-\mathbf{j}} \|\mathbf{z_{ST}(i)} - \mathbf{b(i)}\|^2 \tag{5.6}$$

where $\mathbf{z}_{ST}(i) = \mathbf{T}^H(i)\mathbf{y}_{ST}(i)$ is the filtered output, and λ_{ls}, $0 < \lambda_{ls} < 1$, is an exponential weighting factor that discounts past data. The correlation matrix $\mathbf{R}_{\mathbf{y}_{ST}}(i) = E\left\{\mathbf{y}_{ST}(i)\mathbf{y}_{ST}^H(i)\right\}$ is updated with a weighted sample average such as $\hat{\mathbf{R}}_{\mathbf{y}_{ST}}(i) = \sum_{j=1}^{i} \lambda_{ls}^{i-j}\mathbf{y}_{ST}(i)\mathbf{y}_{ST}^H(i)$, as well as the inverse of the covariance matrix, $\mathbf{P}_{\mathbf{y}_{ST}}(i) \doteq \hat{\mathbf{R}}_{\mathbf{y}_{ST}}^{-1}(i)$, and an adaptation gain vector $\mathbf{k}(i) \doteq \mathbf{P}_{\mathbf{y}_{ST}}(i)\mathbf{y}_{ST}(i)$.

The RLS implementation [53] iterates in the form:

- Initialization:

$$\mathbf{P}_y(0) = \delta^{-1}\mathbf{I} \qquad \delta = \text{ small positive constant} \tag{5.7}$$

$$\mathbf{T}(0) = \mathbf{0} \tag{5.8}$$

- RLS updating: $i = 1, 2, \cdot$, compute

$$\mathbf{k}(i) = \frac{\lambda_{ls}^{-1} \mathbf{P}_y(i-1) \mathbf{y}_{ST}(i)}{1 + \lambda_{ls}^{-1} \mathbf{y}_{ST}^H(i) \mathbf{P}_y(i-1) \mathbf{y}_{ST}(i)} \tag{5.9}$$

$$\xi(i) = \mathbf{b}(i) - \mathbf{T}^H(i-1) \mathbf{y}_{ST}(i) \tag{5.10}$$

$$\mathbf{T}(i) = \mathbf{T}(i-1) + \mathbf{k}(i) \xi^H(i) \tag{5.11}$$

$$\mathbf{P}_y(i) = \lambda_{ls}^{-1} \mathbf{P}_y(i-1) - \lambda_{ls}^{-1} \mathbf{k}(i) \mathbf{y}_{ST}^H(i) \mathbf{P}_y(i-1) \tag{5.12}$$

Basically, the update (5.12) is sensitive to numerical roundoff errors [51] and must therefore be closely monitored or stabilized in some manner. Also the complexity per update is $O(K^2 I^2)$ for RLS, as compared with $O(KI)$ for LMS. As with the LMS case, the desired signal for RLS can be initially accomplished through a training sequence, and subsequently by switching to decision-directed mode.

5.1.2 Adaptive Algorithms for Successive Interference Canceller

For the two linear multiuser detectors, MMSE and decorrelating receivers, the corresponding weight vector matrix are given by (3.17) and (3.18) respectively. Most of the multiuser detectors enlarge the sliding processing window to cover more symbols. This results in a large dimension of matrices in (3.17) and in (3.18). With direct inversion of the matrices, it is too costly for practical implementation. In [67], the authors considered the application of the Gauss-Seidel iteration in obtaining the detector output. This method effectively performs serial interference cancellation (SIC) on the sufficient statistic vector $\mathbf{y}_{ST}(i)$ and recursively refines the estimate of the users' transmitted symbols, denoted as $\left\{ \bar{\mathbf{d}}(i)[Ki+k] \equiv \sigma_k b_k(i) : 1 \le k \le K, 0 \le i \le I-1 \right\}$. Denote such an estimate at the jth iteration as $\bar{\mathbf{d}}^{(j)}(i)[Ki+k]$. Here we denote $\mathbf{Matrix}[m,n]$ as the (m,n)th entry of $\mathbf{Matrix}$ and denote $\mathbf{vector}[n]$ as the nth entry of $\mathbf{vector}$.

Consider and rewrite the linear system equation in (3.14) which consists of the sufficient statistics $\mathbf{y}_{ST}$, the users' transmitted symbols $\bar{\mathbf{d}}$, and the space-time correlation matrix $\bar{\mathbf{H}}$. Ignoring the Gaussian white noise, (3.14) is given by

$$\bar{\mathbf{H}} \bar{\mathbf{d}}(i) = \mathbf{y}_{ST}(i) \tag{5.13}$$

The purpose of the receiver is to update the estimates of the users' transmitted symbols, $\bar{\mathbf{d}}$, at each new data input. By using the Gauss-Seidel procedure [71] to solve the equation in 5.13), we get

$$
\bar{\mathbf{d}}^{(j)}[Ki + k] = \frac{1}{\bar{\mathbf{H}}[Ki + k, Ki + k]} \left(\mathbf{y}_{ST}[Ki + k] - \sum_{n' < (Ki+k)} \bar{\mathbf{H}}[Ki + k, n']\bar{\mathbf{d}}^{(j)}[n'] \right.
$$
$$
\left. - \sum_{n' > Ki+k} \bar{\mathbf{H}}[Ki + k, n']\bar{\mathbf{d}}^{(j-1)}[n'] \right) \tag{5.14}
$$

for $k = 1, \ldots K$, $i = 0, \ldots, I - 1$, $j = 1, 2, \ldots$ and $n' = 1, \cdots, KI$. For simplicity, we replace $Ki + k$ by n which is the entry of a vector or matrix. Then, by examining the equation in (5.14), we can find the Gauss-Seidel iteration for the SIC that obtains estimates of $\bar{\mathbf{d}}^{(j)}(i)[n]$ by subtracting the most current estimates of the interference created by all the users from the received signal $\mathbf{y}_{ST}(i)$. By the theory of Gauss-Seidel iterations, if $\bar{\mathbf{H}}$ is positive definite, the $\bar{\mathbf{d}}^{(j)}(i)$ will be guaranteed to converge to the solution of (5.13) [28, 72], i.e., the output of the decorrelating detector in (3.17):

$$
\bar{\mathbf{d}}^{(j)}(i) \to \bar{\mathbf{H}}^{-1}\mathbf{y}_{ST}(i) = \mathbf{T}^H_{ST_{DEC}}\mathbf{y}_{ST}(i) \tag{5.15}
$$

A similar way for developing the adaptive SIC toward to the MMSE solution can be obtained by the linear system of equations:

$$
\left(\bar{\mathbf{H}} + \sigma_n^2 \mathbf{A}^{-2} \right) \bar{\mathbf{d}}(i) = \mathbf{y}_{ST}(i) \tag{5.16}
$$

The corresponding Gauss-Seidel iteration is given by

$$
\bar{\mathbf{d}}^{(j)}[n] = \frac{1}{\bar{\mathbf{H}}[n, n] + \sigma_n^2 \mathbf{A}[n, n]^2} \left(\mathbf{y}_{ST}[n] - \sum_{n' < n} \bar{\mathbf{H}}[n, n']\bar{\mathbf{d}}^{(j)}[n'] - \sum_{n' > n} \bar{\mathbf{H}}[n, n']\bar{\mathbf{d}}^{(j-1)}[n'] \right) \tag{5.17}
$$

where n represents $Ki + k$ and $n, n' = 1, \ldots, KI$, $j = 1, 2, \ldots$. $\bar{\mathbf{d}}^{(j)}$ will converge to the solution of (5.16), i.e., the output of the MMSE detector in (3.18):

$$
\bar{\mathbf{d}}^{(j)}(i) \to \left(\bar{\mathbf{H}} + \sigma_n^2 \mathbf{A}^{-2} \right)^{-1} \mathbf{y}_{ST}(i) = \mathbf{T}^H_{ST_{MMSE}}\mathbf{y}_{ST}(i) \tag{5.18}
$$

The computational complexity per user per bit of the direct inversion of the matrices $\bar{\mathbf{H}}$ or $(\bar{\mathbf{H}} + \sigma_n^2 \mathbf{A}^{-2})$ is $O(K^3 I^3/KI) = O(K^2 I^2)$. The computational complexity of the adaptive SIC algorithm per user per bit is $O(\bar{j}K^2 I/KI) = O(MK)$, where $\bar{j}$ is the total number of iterations. Since the number of iteration is a small, the above adaptive SIC algorithm achieves a significant complexity reduction over the direct matrix inversion approach.

5.1.3 Adaptive Algorithms for Parallel Interference Cancellers

A natural alternative to the serial interference cancellation (SIC) method is the parallel interference cancellation (PIC) method [67, 73]. In the SIC, the new estimate of $\bar{\mathbf{d}}^j[n]$ is used to update the subsequent estimates as soon as it is available. In the PIC at the jth iteration, the $\bar{\mathbf{d}}^{(j)}[n]$ is updated using the estimates only from the previous iteration $\bar{\mathbf{d}}^{(j-1)}[n]$.

The simplest iterative method for solving the linear system in (5.13) or (5.16) in PIC is the Jacobi iteration [67, 71, 74]. The adaptive PIC decorrelating receiver with the Jacobi iteration solves the linear system of equations in (5.13):

$$\bar{\mathbf{d}}^{(j)}[n] = \frac{1}{\bar{\mathbf{H}}[n,n]} \left(\mathbf{y}_{ST}[n] - \sum_{n' \neq n} \bar{\mathbf{H}}[n,n]\bar{\mathbf{d}}^{(j-1)}[n'] \right) \tag{5.19}$$

And the adaptive PIC MMSE receiver corresponds to the Jacobi method for solving the linear system of equations in (5.16):

$$\bar{\mathbf{d}}^{(j)}[n] = \frac{1}{\bar{\mathbf{H}}[n,n] + \sigma_n^2 \mathbf{A}[n,n]} \left(\mathbf{y}_{ST}[n] - \sum_{n' \neq n} \bar{\mathbf{H}}[n,n]\bar{\mathbf{d}}^{(j-1)}[n'] \right) \tag{5.20}$$

where $n, n' = 1, 2, \ldots, KI$, and $j = 1, 2, \ldots$.

It should be noted the Jacobi iteration is not guaranteed to converge unless a specified condition is satisfied. Let the matrix $\bar{\mathbf{H}}$ be decomposed into three parts, a diagonal matrix $\mathbf{D}_{\bar{\mathbf{H}}}$, a lower left triangular matrix $\mathbf{L}_{\bar{\mathbf{H}}}$, a upper right triangular matrix $\mathbf{U}_{\bar{\mathbf{H}}}$ such that $\bar{\mathbf{H}} = \mathbf{D}_{\bar{\mathbf{H}}} + \mathbf{L}_{\bar{\mathbf{H}}} + \mathbf{U}_{\bar{\mathbf{H}}}$. The condition that guarantees the Jacobi iteration's convergence is that the spectral radius of the matrix, $\mathbf{D}_{\bar{\mathbf{H}}}^{-1}(\mathbf{L}_{\bar{\mathbf{H}}} + \mathbf{U}_{\bar{\mathbf{H}}})$, is less than 1 [72]. However, convergence can also be assured if the technique of over-relaxation is applied [75]. The modification for the Jacobi over-relaxation iteration (JOR) is given by

$$\bar{\mathbf{d}}^{(j)}[n] = \frac{\mu_p}{\bar{\mathbf{H}}[n,n]} \left(\mathbf{y}_{ST}[n] - \sum_{n' \neq n} \bar{\mathbf{H}}[n,n']\bar{\mathbf{d}}^{(j-1)}[n'] \right) + (1 - \mu_p)\bar{\mathbf{d}}^{(j-1)}[n] \tag{5.21}$$

or

$$\bar{\mathbf{d}}^{(j)}[n] = \frac{\mu_p}{\bar{\mathbf{H}}[n,n] + \sigma^2 \mathbf{A}[n,n]^2} \left(\mathbf{y}_{ST}[n] - \sum_{n' \neq n} \bar{\mathbf{H}}[n,n']\bar{\mathbf{d}}^{(j-1)}[n'] \right) + (1 - \mu_p)\bar{\mathbf{d}}^{(j-1)}[n] \tag{5.22}$$

where μ_p is a fractional parameter with $0 < \mu_p < 1$. It can easily be seen that the JOR is in fact a weighted linear PIC scheme where the interference estimate is scaled before subtraction.

127

5.2 Adaptive GSC Multiuser Receivers

The blind adaptive ST multiuser receiver was implemented based on the GSC algorithm. With the chip-sampled received data vector at each antenna element, a set of linear adaptive correlators is applied to extract the multipath path signal of the desired user and to suppress the interference caused by other users, as well as the interferers. The chip-sampled data vector at the dth antenna element, $\mathbf{x}_{(d)}(i)$, $d = 1, \cdots, D$, in (3.2), is the dth row vector of the ST data matrix $\mathbf{X}(i)$ in (3.25). The set of adaptive correlators at the dth antenna element is chosen according to the LCMV criterion [67, 76]. This leads to the criterion for determining the weight matrix, $\tilde{\mathbf{S}}_d = [\tilde{\mathbf{s}}_{d1}, \ldots, \tilde{\mathbf{s}}_{dL}]$, of the bank of correlators:

$$\min_{\tilde{\mathbf{S}}_d} \quad E\left\{\left\|\tilde{\mathbf{S}}_d \mathbf{x}_{(d)}(i)\right\|^2\right\} = \min_{\tilde{\mathbf{S}}_d} \quad \mathrm{tr}\left(\tilde{\mathbf{S}}_d^H \mathbf{R}_{\mathbf{x}_{(d)}} \tilde{\mathbf{S}}_d\right)$$

$$\text{subject to: } \tilde{\mathbf{S}}_d^H \mathbf{C}_1 = \mathbf{I}_L \tag{5.23}$$

where $trace(\cdot)$ denotes the trace operator, $\mathbf{R}_{\mathbf{x}_{(d)}} = E\left\{\mathbf{x}_{(d)}(i)\mathbf{x}_{(d)}^H(i)\right\}$ and $\mathbf{C}_1$ is the multipath signature matrix of user 1 as defined in (2.11). The solution to this LCMV optimization is given by

$$\tilde{\mathbf{S}}_{d,o} = \mathbf{R}_{\mathbf{x}_{(d)}}^{-1} \mathbf{C}_1 (\mathbf{C}_1^H \mathbf{R}_{\mathbf{x}_{(d)}} \mathbf{C}_1)^{-1} \tag{5.24}$$

The outputs of the correlator bank are concatenated to form th following vector:

$$\begin{aligned}
\bar{\mathbf{z}}(i) &= \left[(\tilde{\mathbf{S}}_{1,o}^H \mathbf{x}_{(2)}(i))^T, (\tilde{\mathbf{S}}_{2,o}^H \mathbf{x}_{(2)}(i))^T, \cdots, (\tilde{\mathbf{S}}_{D,o}^H \mathbf{x}_{(2)}(i))^T\right]_{LD \times 1}^T \\
&= \left[\mathbf{z}_1^T, \mathbf{z}_2^T, \cdots, \mathbf{z}_D^T\right]_{LD \times 1}^T
\end{aligned} \tag{5.25}$$

Finally, a linear combining vector $\mathbf{f}$ is applied to $\bar{\mathbf{z}}(i)$ to yield the decision statistic for the ith symbol of the desired user:

$$z_o(i) = \mathbf{f}^H \bar{\mathbf{z}}(i) \tag{5.26}$$

One of the most well-known adaptive algorithms for LCMV is via the GSC [76], which decomposes the weight vector at the lth finger of the dth antenna into two orthogonal components such as follows:

$$\tilde{\mathbf{s}}_{dl} = \tilde{\mathbf{s}}_{dl,c} - \mathbf{B}_c \tilde{\mathbf{s}}_{dl,a} \tag{5.27}$$

128

where $\tilde{\mathbf{s}}_{dl,c}$ is the quiescent weight vector, $\tilde{\mathbf{s}}_{dl,a}$ is the adaptive weight vector, and $\mathbf{B}_c$ is the blocking matrix such that $\mathbf{B}_c^H \mathbf{C}_1 = \mathbf{0}_{(N-1) \times L}$. Combining the equations of (5.27), for $l = 1, \cdots, L$, at the dth element of the antenna array, gives the new equation in matrix form:

$$\tilde{\mathbf{S}}_d = \tilde{\mathbf{S}}_{d,c} - \mathbf{B}_c \tilde{\mathbf{S}}_{d,a} \tag{5.28}$$

where $\tilde{\mathbf{S}}_d = [\tilde{\mathbf{s}}_{d1}, \cdots, \tilde{\mathbf{s}}_{dL}]$, $\tilde{\mathbf{S}}_{d,c} = [\tilde{\mathbf{s}}_{d1,c}, \cdots, \tilde{\mathbf{s}}_{dL,c}]$ and $\tilde{\mathbf{S}}_{d,a} = [\tilde{\mathbf{s}}_{d1,a}, \cdots, \tilde{\mathbf{s}}_{dL,a}]$. $\tilde{\mathbf{S}}_{d,c}$ is the projection obtained by projecting $\tilde{\mathbf{S}}_d$ onto the subspace spanned by the column vectors of $\mathbf{C}_1$, and $\tilde{\mathbf{S}}_{d,a}$ is the $(N-1) \times L$ adaptive weight matrix. The projection matrix is denoted as $\mathbf{P}_c = \mathbf{C}_1 (\mathbf{C}_1^H \mathbf{C})_1^{-1} \mathbf{C}_1^H$. The LCMV problem is then converted into the following unconstrained optimization problem:

$$\min_{\tilde{\mathbf{S}}_{d,a}} \quad E\left\{ \left(\tilde{\mathbf{S}}_{d,c} - \mathbf{B}_c \tilde{\mathbf{S}}_{d,a} \right)^H \mathbf{x}_{(d)}(i) \right\} \tag{5.29}$$

The LMS algorithm for updating the weights of the bank of correlators at the dth antenna is given by

$$\mathbf{z}_d(i) = \left(\tilde{\mathbf{S}}_{d,c} - \mathbf{B}_c \tilde{\mathbf{S}}_{d,a}(i) \right)^H \mathbf{x}_{(d)}(i) \tag{5.30}$$

$$\tilde{\mathbf{S}}_{d,a}(i+1) = \tilde{\mathbf{S}}_{d,a}(i) + \mu \mathbf{B}_c^H \mathbf{x}_{(d)}(i) \mathbf{z}_d^H(i) \tag{5.31}$$

Note that $\mathbf{z}_d(i)$ is the output of the L-finger correlator bank at the dth antenna element. The output of the filters at all antenna elements are concatenated to obtain $\bar{\mathbf{z}}(i)$ in (5.25).

On the other hand, we can blindly combine the filter outputs of the correlator banck at all antenna elements based on the maximum ratio criterion. The principal eigenvector of the autocorrelation matrix of $\bar{\mathbf{z}}(i)$ should be obtained in an adaptive fashion. The simple algorithm named PAST (Projection Approximation Subspace Tracking) [68, 77] can be used to track the largest eigenvalue, λ_m, and the corresponding eigenvector, $\mathbf{f}$, of the correlation matrix of $\bar{\mathbf{z}}(i)$:

$$\lambda_m(i) = \alpha \lambda_m(i-1) + |z_o(i)|^2 \tag{5.32}$$

$$\mathbf{f}(i) = \mathbf{f}(i-1) + [\bar{\mathbf{z}}(i) - \mathbf{f}(i-1)z_o(i)] z_o(i)^* / \lambda_m(i) \tag{5.33}$$

where α, $0 < \alpha < 1$, is the forgetting factor. Finally, the filter output, which is the MRC output, is given by

$$z_o(i) = \mathbf{f}^H(i-1)\bar{\mathbf{z}}(i) \tag{5.34}$$

The algorithm for adaptive GSC multiuser detection is summarized in Table 5.1. The convergence of the PAST algorithm are studied in [78]. It is shown that with the forgetting factor $\alpha = 1$ under mild conditions, this algorithm globally converges almost surely to the signal eigenvectors and eigenvalues.

5.3   Adaptive 2-D RAKE Single-User Receivers

For the four ST 2-D RAKE receivers such as Pre-ST, Post-ST, Pre-BT and Post-BT, described in Section 3.3, a generic linear filtering model is given by

$$\hat{b}_1(i) = sign(\mathbf{s}^H \mathbf{x}(i)) \tag{5.35}$$

where $\mathbf{x}(i)$ is the observation vector (for Pre-ST being $\mathbf{x}_{c-ST}$, Post-ST being $\mathbf{x}_{c-SM}$, Pre-BT being $\mathbf{y}_{c-BT}$, and Post-BT being $\mathbf{y}_{c-BM}$), and $\mathbf{s}$ is the generic weight vector.

As described before, popular adaptive filtering algorithms consist of the conventional stochastic gradient and least squares algorithms [53]. These have been applied to obtain the MMSE symbol estimates for CDMA systems [27, 79]. An important feature of the MMSE receivers is that the mean-square-error (MSE) can be minimized via the Wiener-Hopf filtering theory [53]. The MSE from a linear FIR filter $\mathbf{s}$ operating on $\mathbf{x}$ in the estimation of bit $b_1(i)$ is given by

$$J = E\left\{\left|\mathbf{s}^H \mathbf{x}(i) - b_1(i)\right|^2\right\} \tag{5.36}$$

The stochastic gradient or LMS algorithm has been successfully applied to many signal processing applications such as equalization, echo cancellation, and adaptive beamforming. The weight vector updates of the LMS algorithm is summarized as

- Initialization $\mathbf{s}(0)=\mathbf{0}$

- LMS updating: $i = 1, 2, \cdots$, compute

$$\hat{b}_1(i) = \mathbf{s}^H(i-1)\mathbf{x}(i) \tag{5.37}$$

$$e(i) = b_1(i) - \hat{b}_1(i) \tag{5.38}$$

$$\mathbf{s}(i) = \mathbf{s}(i-1) + \mu\mathbf{x}(i)e^*(i) \tag{5.39}$$

The scalar μ is the LMS stepsize, whose choosing is according to the trade-off of stability and convergence speed. With $\mathbf{s}$ set to the optimal value of Wiener solution $\mathbf{R}^{-1}\hat{\mathbf{r}}$, where $\hat{\mathbf{r}} = E\{\mathbf{x}b_1^*\}$ and $\mathbf{R} = E\{\mathbf{x}\mathbf{x}^H\}$, and for binary valued data, the MMSE is givrn by

$$J_{\min} = 1 - \hat{\mathbf{r}}^H \mathbf{R} \hat{\mathbf{r}} \tag{5.40}$$

The use of a finite, non-zero stepsize in the adaptive algorithm implies that the coefficients will wander, so there will be some filter misadjustment. The mean square error above the MMSE is termed excess mean square error $J_{ex}(i)$ at the ith iteration. The misadjustment, defined as the ratio of the steady state value $J_{ex}(\infty)$ of excess mean square error to the MMSE $J_{\min}$:

$$\begin{aligned} \kappa &= \frac{J_{ex}(\infty)}{J_{\min}} \\ &= \sum_{i=1}^{\mathcal{M}} \frac{\mu\lambda_i}{(2 - \mu\lambda_i)} \end{aligned} \tag{5.41}$$

where λ_i's are the eigenvalues of the correlation matrix $\mathbf{R}$ of dimension $\mathcal{M} \times \mathcal{M}$.

For the normalized LMS (NLMS) algorithm, the stepsize is chosen to be equal to the inverse of the instantaneous observation power [53, 70]:

$$\mu = \frac{\bar{\mu}}{\epsilon + \|\mathbf{x}(i)\|^2} \tag{5.42}$$

where $\bar{\mu}$ is the NLMS stepsize, which can be used to adjust the convergence speed, and ϵ is a small constant that ensures stability when the signal energy is small. Nominally $\bar{\mu}$ is chosen to be equal to unity. The main benefits of the LMS algorithm are its simplicity and robustness to noise. The algorithm complexity is $O(\mathcal{M})$, where $\mathcal{M}$ is the length of the weight vector.

For the RLS adaptive algorithm, the weight vector is computed in accordance with the algorithm:

- Initialization

$$\mathbf{P}(0) = \delta^{-1}\mathbf{I} \qquad \delta = \text{small positive constant} \tag{5.43}$$

$$\mathbf{s}(0) = \mathbf{0} \tag{5.44}$$

131

- RLS updating: For each $n = 1, 2, \cdots$, compute:

$$\mathbf{k}(i) = \frac{\lambda_{ls}^{-1}\mathbf{P}(i-1)\mathbf{x}(i)}{1 + \lambda_{ls}^{-1}\mathbf{x}^{H}(i)\mathbf{P}(i-1)\mathbf{x}(i)} \tag{5.45}$$

$$\xi(i) = b(i) - \mathbf{s}^{H}(i-1)\mathbf{x}(i) \tag{5.46}$$

$$\mathbf{s}(i) = \mathbf{s}(i-1) + \mathbf{k}(i)\xi^{*}(i) \tag{5.47}$$

$$\mathbf{P}(i) = \lambda_{ls}^{-1}\mathbf{P}(i-1) - \lambda_{ls}^{-1}\mathbf{k}(i)\mathbf{x}^{H}(i)\mathbf{P}(i-1) \tag{5.48}$$

where λ_{ls} is a positive constant close to, but less than, 1. When λ_{ls} equals 1, we have the ordinary method of least squares corresponding to infinite memory.

The fundamental difference between the RLS algorithm and LMS algorithm is stated as follows [53]: The stepsize parameter μ in the LMS algorithm is replaced by the inverse of the correlation matrix of the input vector $\mathbf{x}(i)$ in RLS algorithm. This modification has a profound impact on the convergence behavior of the RLS algorithm for a stationary environment, which is summarized as follows:

1. The rate of convergence of the RLS algorithm is typically an order of magnitude faster than that of the LMS algorithm.

2. The rate of convergence of the RLS algorithm is invariant to the eigenvalue spread of the ensemble-averaged correlation matrix of the input vector $\mathbf{x}(i)$

3. The excess mean-squared error $J_{ex}(i)$ of the RLS converges to zero as the number of iteration, i, approaches infinity, with the exponential weighting factor $\lambda_{ls} = 1$.

5.4 Adaptive GSC Single-User Receivers

This section provides a comprehensive treatment of blind ST adaptive GSC single-user detection. The GSC adaptive detector requires accurate knowledge of the channel characteristics of the desired user. However, when multiple antennas are deployed in the receiver, it is not straightforward to identify the propagation channel. This is due to the difficulty in performing direction finding in a rich multipath environment. For this reason, different implementations of adaptive GSC algorithms have been taken into consideration. They are classified into the ST joint or ST separate adaptive receiver structures.

5.4.1 ST Joint Adaptive GSC Single-User Receivers

An MOE receiver is proposed in [18], where the weight vector is optimized by minimizing the output energy subject to the constraint that the response to the user of interest is a constant:

$$\min_{\mathbf{s}} \quad \mathbf{s}^H \mathbf{R} \mathbf{s}$$

$$\text{subject to: } \mathbf{s}^H \tilde{\mathbf{h}}_1 = 1 \tag{5.49}$$

where $\tilde{\mathbf{h}}_1$ is the generic effective ST CSV, (for Pre-ST being $\mathbf{h}_{ST}$, for Post-ST being $\mathbf{h}_{SM}$, for Pre-BT being $\mathbf{h}_{BT}$ and for Post-BT being $\mathbf{h}_{BM}$).

By merging the ideas of the GSC and LMS algorithm, the generic weight vector $\mathbf{s}$ is decomposed into two branches, where $\mathbf{s} = \mathbf{s}_c - \mathbf{B}\mathbf{s}_a$. The upper branch weight vector $\mathbf{s}_c = \tilde{\mathbf{h}}_1$ is the fixed part that satisfies the constraint at each update. The lower branch blocks the signal with the assumed signature sequence by a designated blocking matrix $\mathbf{B}$. By dynamically updating the adaptive weight vector $\mathbf{s}_a$ of the lower branch, any signals common to the two branches' outputs will be cancelled. The blind adaptive GSC algorithm for the single-user receiver is described in Table 5.2.

5.4.2 Robust Adaptive GSC Algorithms

Unfortunately, the MOE method is known to be very sensitive to the signature mismatch due to the so-called signal cancellation effect [18]. To see the impact of signature mismatch, we consider the case of a 2-D RAKE single-user receiver with multipaths, but no interference. Instead of $\tilde{\mathbf{h}}_1$, the perturbed CSV $\boldsymbol{\Delta}\tilde{\mathbf{h}}_1$ is assumed due to mismatch, where $\boldsymbol{\Delta} = \mathbf{I} + diag[\delta_0, \delta_1, \ldots, \delta_{\mathcal{M}}]$, where the length of the CSV is $\mathcal{M}$. The output power of the MOE receiver is given by

$$
\begin{aligned}
\left(\tilde{\mathbf{h}}_1^H \mathbf{R}^{-1} \tilde{\mathbf{h}}_1\right)^{-1} &= \sigma_n^2 \left\{ \tilde{\mathbf{h}}_1 \left[\mathbf{I} - \frac{\sigma_1^2 \boldsymbol{\Delta}\tilde{\mathbf{h}}_1 (\boldsymbol{\Delta}\tilde{\mathbf{h}}_1)^H}{\mathcal{M}\sigma_1^2 + \sigma_n^2} \right] \tilde{\mathbf{h}}_1 \right\}^{-1} \\
&= \frac{\mathcal{M}\sigma_1^2 + \sigma_n^2}{\mathcal{M} + \frac{\sigma_1^2}{\sigma_n^2} \left[\mathcal{M}^2 - \left| (\boldsymbol{\Delta}\tilde{\mathbf{h}}_1)^H \tilde{\mathbf{h}}_1 \right|^2 \right]}
\end{aligned}
$$

$$= \left(\sigma_1^2 + \frac{\sigma_n^2}{\mathcal{M}} \right) \left(\frac{1 + \frac{\frac{\sigma_1^2}{\sigma_n^2}}{1 + \mathcal{M}\sigma_1^2/\sigma_n^2} \sum_m |\delta_m|^2}{1 + \frac{\sigma_1^2}{\sigma_n^2} \sum_m |\delta_m|^2} \right) \quad (5.50)$$

For a small or moderate SNR σ_1^2/σ_n^2, the factor on the right hand side nearly equals 1. As the SNR increases, however, this factor becomes proportional to $1/\sigma_1^2$, and the signal is actually suppressed:

$$\lim_{\sigma_1^2/\sigma_n^2 \to \infty} (\tilde{\mathbf{h}}_1 \mathbf{R}^{-1} \tilde{\mathbf{h}}_1)^{-1} = \frac{\sigma_n^2}{\mathcal{M}} \left(1 + \frac{1}{\sum_m |\delta_m|^2 \big/ \mathcal{M}} \right) \quad (5.51)$$

To avoid signal cancellation, a robust solution is obtained by placing a limit on the weight vector's norm [80]:

$$\min_{\mathbf{s}} \quad \mathbf{s}^H \mathbf{R} \mathbf{s}$$

$$\text{subject to: } \mathbf{s}^H \tilde{\mathbf{h}}_1 = 1 \quad \text{and} \quad \mathbf{s}^H \mathbf{s} \leq \beta_s^2 \quad (5.52)$$

where β_s is the bound on the norm. Setting the Lagrangian and taking the gradient with respect to the conjugate of the weight vector yields

$$\mathbf{R} \mathbf{s}_o + \eta_1 \tilde{\mathbf{h}}_1 + \eta_2 \mathbf{s}_o = 0 \quad (5.53)$$

where η_1 and η_2 are the Lagrange multipliers corresponding to the equality and inequality constraints, respectively. If $\eta_2 = 0$, the usual minimum variance solution results. If $\eta_2 \neq 0$, the solution is obtained by

$$\mathbf{s}_o = -\eta_1 \left(\mathbf{R} + \eta_2 \mathbf{I} \right)^{-1} \tilde{\mathbf{h}}_1 \quad (5.54)$$

Note that the multipliers do not have the same values in this solution. However, we can develop a suboptimal solution by adding a fixed identity matrix to the correlation matrix. Adding an identity matrix so as to desensitize an algorithm to errors is known as *diagonal loading* in array processing [81]. The GSC with diagonal loading can be recast for the robust adaptive algorithm:

$$\min_{\mathbf{s}_a} \quad (\mathbf{s}_c - \mathbf{B}\mathbf{s}_a)^H (\mathbf{R} + \eta_2 \mathbf{I})(\mathbf{s}_c - \mathbf{B}\mathbf{s}_a) \quad (5.55)$$

The robust formulation for GSC requires modification of the dynamic equation for the adaptive weight vector:

$$\mathbf{s}_a(i+1) = (\mathbf{I} - \eta_2 \mathbf{B}^H \mathbf{B})\mathbf{s}_a(i) + \mu z^*(i)\mathbf{x}_B(i) \tag{5.56}$$

where $z(i) =$ is the estimation error between the output of upper GSC branch and that of the lower branch, and $\mathbf{x}_B(i)$ is the input data vector after the SOI is blocked by the designated blocking matrix $\mathbf{B}$.

An alternative robust algorithm for GSC is suggested that does not require specifying the η_2 value explicitly. Usually η_2 is not known beforehand, and the norm constraint applies only to the adaptive weight vector. Because the component terms are orthogonal, the norm constraint $\|\mathbf{s}\|^2 \leq \beta_s^2$ becomes

$$\|\mathbf{B}\mathbf{s}_a\|^2 \leq \beta_s^2 - \|\mathbf{s}_c\|^2 \tag{5.57}$$

To obtain a robust algorithm, we force this weight vector to satisfy its norm constraint at each update.

The robust formulation of the GSC receiver is depicted in Table 5.3, which is based on a norm constraint placed on the weight vector. Robustness constraints limit the maximum value of the overall weight vector norm. Since the fixed weight at the upper branch does not change, only the norm of the adaptive weight vector need be limited.

5.4.3   ST Separate Adaptive GSC Single-User Receivers

A potential problem with the single constraint approach to ST joint adaptive methods is the error in estimating the ST CSV $\tilde{\mathbf{h}}_1$ in the adaptive algorithm. This problem may be due to the difficulty in finding the multipath AOA's in a multipath environment or other types of distortion [51]. To alleviate this problem, spatial and temporal filtering could be processed separately. In the time domain, an extended set of constraints, $\mathbf{C}_1^H \tilde{\mathbf{s}}_d = \mathbf{f}_d$, can be used for multipath environments at the dth antenna element [23], where $\tilde{\mathbf{s}}_d$ is the weight vector, and $\mathbf{f}_d$ is the channel parameter vector. Then, an adaptive method can be used to track the principal components for maximum ratio combining in both the space and time domain.

Firstly, we solve the multiply constrained optimization problem at the dth antenna, for a specified $\mathbf{f}_d$ as the channel parameter vector of the SOI. The solution can be obtained using Lagrange multipliers as:

$$\tilde{\mathbf{s}}_{d,o} = \mathbf{R}_{\mathbf{x}_{(d)}}^{-1} \mathbf{C}_1 (\mathbf{C}_1^H \mathbf{R}_{\mathbf{x}_{(d)}}^{-1} \mathbf{C})_1^{-1} \mathbf{f}_d \tag{5.58}$$

where $\mathbf{R}_{\mathbf{x}_{(d)}} = E\left\{\mathbf{x}_{(d)}(i)\mathbf{x}_{(d)}^H(i)\right\}$, $\mathbf{C}_1$ is the multipath signature matrix of user 1 defined in (2.11). The minimum output variance is

$$J_{\min} = \tilde{\mathbf{s}}_{d,o}^H \mathbf{R}_{\mathbf{x}_{(d)}} \tilde{\mathbf{s}}_{d,o} = \mathbf{f}_d^H (\mathbf{C}_1^H \mathbf{R}_{\mathbf{x}_{(d)}}^{-1} \mathbf{C})_1^{-1} \mathbf{f}_d \tag{5.59}$$

In [23], a scheme is proposed to optimize the unknown vector $\mathbf{f}_d$ by maximizing $J_{\min}$, that is, by maximizing the energy of the signal component after the interference has been suppressed. The Lagrangian associated with this problem equals

$$J = \tilde{\mathbf{s}}_d^H \mathbf{R}_{\mathbf{x}_{(d)}} \tilde{\mathbf{s}}_d + \lambda_d^H (\mathbf{C}_1^H \tilde{\mathbf{s}}_d - \mathbf{f}_d) + (\tilde{\mathbf{s}}_d^H \mathbf{C}_1 - \mathbf{f}_d^H)\lambda_d \tag{5.60}$$

where λ_d is the Lagrange multiplier corresponding to constraints for a specified GSC weights, $\tilde{\mathbf{s}}_d$, at the dth antenna element. Then, two update equations for $\tilde{\mathbf{s}}_d$ and $\mathbf{f}_d$ can be formed as

$$\tilde{\mathbf{s}}_d(i+1) = \tilde{\mathbf{s}}_d(i) - \mu_s \nabla_{\tilde{\mathbf{s}}_d^*} J \tag{5.61}$$

$$\mathbf{f}_d(i+1) = \mathbf{f}_d(i) + \mu_f \nabla_{\mathbf{f}_d^*} J \tag{5.62}$$

where μ_s and μ_f are stepsize of the LMS algorithm. The algorithm will adaptively minimize J with respect to $\tilde{\mathbf{s}}_d$ and maximize J with respect to $\mathbf{f}_d$. Since a change in the norm of $\mathbf{f}_d(i)$ does not affects the performance of the receiver $\tilde{\mathbf{s}}_d(i)$, we may project $\nabla_{\mathbf{f}^*} J$ onto the subspace orthogonal to $\mathbf{f}_d(i)$, to obtain the following equation for updating $\mathbf{f}_d$:

$$\mathbf{f}_d(i+1) = \mathbf{f}_d(i) + \mu_f \left(\mathbf{I} - \frac{\mathbf{f}_d(i)\mathbf{f}_d^H(i)}{\mathbf{f}_d^H(i)\mathbf{f}_d(i)} \right) \nabla_{\mathbf{f}_d^*} J \tag{5.63}$$

In order to guarantee the constraint $\|\mathbf{f}_d(i+1)\| = 1$ at each iteration, we need to normalize $\mathbf{f}_d(i+1)$. Then, by using Equations (5.60), (5.61) and (5.63), the two update eauations become

$$\tilde{\mathbf{s}}_d(i+1) = \tilde{\mathbf{s}}_d(i) - \mu_s \left(\mathbf{R}_{\mathbf{x}_{(d)}} \tilde{\mathbf{s}}_d(i) + \mathbf{C}_1 \lambda_d(i) \right) \tag{5.64}$$

$$\mathbf{f}_d(i+1) = \mathbf{f}_d(i) - \mu_f \left(\mathbf{I} - \frac{\mathbf{f}_d(i)\mathbf{f}_d^H(i)}{\mathbf{f}_d^H(i)\mathbf{f}_d(i)} \right) \lambda_d(i) \tag{5.65}$$

The Lagrange multiplier $\lambda_d(i)$ is again obtained by enforcing the constraint $\mathbf{C}_1^H \tilde{\mathbf{s}}_d(i+1) = \mathbf{f}_d(i)$, and the result is

$$\lambda_d(i) = \frac{1}{\mu_s} \left(\mathbf{C}_1^H \mathbf{C}_1 \right)^{-1} \left(\mathbf{C}^H \tilde{\mathbf{s}}_d(i) - \mu_s \mathbf{C}_1^H \mathbf{R}_{\mathbf{x}_{(d)}} \tilde{\mathbf{s}}_d(i) - \mathbf{f}_d(i) \right) \tag{5.66}$$

By substituting (5.66) into (5.64) and (5.65), we obtain the recursions:

$$\tilde{\mathbf{s}}_d(i+1) = \mathbf{P}_{\mathbf{C}_1}^{\perp} \left(\tilde{\mathbf{s}}_d(i) - \mu_s \mathbf{R}_{\mathbf{x}_{(d)}} \tilde{\mathbf{s}}_d(i) \right) + \mathbf{C}_1 \left(\mathbf{C}_1^H \mathbf{C}_1 \right)^{-1} \mathbf{f}_d(i) \tag{5.67}$$

$$\mathbf{f}_d(i+1) = \mathbf{f}_d(i) + \frac{\mu_f}{\mu_s} \left(I - \frac{\mathbf{f}_d(i)\mathbf{f}_d^H(i)}{\mathbf{f}_d^H(i)\mathbf{f}_d(i)} \right) + \left(\mathbf{C}_1^H \mathbf{C}_1 \right)^{-1} \left(\mu_s \mathbf{C}_1^H \mathbf{R}_{\mathbf{x}_{(d)}} \tilde{\mathbf{s}}_d(i) - \mathbf{C}_1^H \tilde{\mathbf{s}}_d(i) \right) \tag{5.68}$$

where

$$\mathbf{P}_{\mathbf{C}_1}^{\perp} = \mathbf{I} - \mathbf{C}_1 \left(\mathbf{C}_1^H \mathbf{C}_1 \right)^{-1} \mathbf{C}_1^H \tag{5.69}$$

And the instantaneous approximation is given by

$$\mathbf{R}_{\mathbf{x}_{(d)}}(i) = \alpha_d \mathbf{R}_{\mathbf{x}_{(d)}}(i-1) + (1 - \alpha_d)\mathbf{x}_{(d)}(i)\mathbf{x}_{(d)}^H(i) \tag{5.70}$$

where α_d, $0 \leq \alpha_d < 1$, is the smoothing factor.

The filtered output $z_d(i)$ of the adaptive multiply constrained filter at the dth antenna element is given by

$$z_d(i) = \tilde{\mathbf{s}}_d^H(i)\mathbf{x}_{(d)}(i) \tag{5.71}$$

The outputs of the GSC filter at all antenna elements are concatenated together to obtain $\tilde{\mathbf{z}}(i) = [z_1(i), \ldots, z_D(i)]^T$, which is similar to (5.25). Finally, the principal eigenvector of the autocorrelation matrix of $\tilde{\mathbf{z}}(i)$ is estimated to obtain the weight vector of the maximal ratio combiner. The PAST subspace tracking can again be used to track the eigenvector $\mathbf{e}_z$ associated with the corresponding maximum eigenvalue λ_{max} of the autocorrelation matrix of $\tilde{\mathbf{z}}(i)$. The overall adaptive algorithm is summarized in Table 5.2.

5.4.4   Blind Adaptive Beamspace-Time GSC Receivers

In addition to using adaptive GSC algorithms in the time domain, we can also use them in the space domain for beamforming. For BT sectored CDMA systems, the entire field-of-view is divided into several working sectors, the AOA of the SOI is roughly estimated, and adaptive beamforming is performed accordingly with the LCMV criterion [55]. In this case, the LCMV beamformers can be operated in an adaptive fashion using the algorithms described previously. The details of proposed adaptive algorithms for BT receivers was presented already in Chapter 4.

5.5   Simulation Results

In this Chapter, we have presented various types of adaptive ST 2-D RAKE receivers. In this section, we will illustrate the performance of these receivers by simulation results. Again, a uniform linear array (ULA) with omni-directional elements is employed. The array consists of D identical elements uniformly spaced by a $1/\sqrt{3}$ wavelength, and is used for the field-of-view $[-60°, 60°]$, which represents the effective angular region of operation for a linear array. We define the output SINR SINR_o (in dB) as a performance index:

$$\text{SINR}_o = 10 \log_{10} \frac{\text{total power of SOI's}}{\text{total power of interference plus noise}}$$

The input SNR (in dB) is defined as $\text{SNR}_i = 10 \log_{10} \frac{\sigma_1^2}{\sigma_n^2}$. The NFR (in dB) is defined as the ratio of the MAI power to signal power before despreading and beamforming as $\text{NFR} = 10 \log_{10} \frac{\sigma_k^2}{\sigma_1^2}$, where $\sigma_2^2 = \sigma_3^2 = \cdots = \sigma_K^2$ for $k = 1, \cdots, K$. Major simulation parameters include: $N = 31$ Gold code, $L = 4$ fingers, $D = 8$ antenna elements, $\text{SNR}_i = 0$ dB and NFR = 10 dB. We use $N_s = 500$ symbols for training and estimation of correlation matrices. A total of 100 Monte-Carlo runs are done for each simulation. Unless otherwise mentioned, the above standard parameters will be used throughout the section.

In the first case, we evaluate the adaptive SIC and PIC receivers for different user numbers $K = 5$ and $K = 20$ with 3 stages iteration. The simulation results are based on three stages of cancellation for each user. For comparison, the BER performances of the CST-RAKE receiver and single user bound are included. The BER performacnes versus input SINR are

shown in Figure 5.1. As we can see in the figure, a significant performance improvement is provided by SIC or PIC receivers as compared to the conventional CST-RAKE receiver. Comparing the performance of SIC and PIC, it is found that for low input SNR, PIC offers slightly better performance while SIC has a steeper descent in BER at moderate to high input SNR.

In the second case, we demonstrate the effectiveness of recursive algorithms for weight vector adaptation. We replaced the direct matrix inversion computation by the corresponding adaptive algorithms. Figure 5.2(a) shows the output SINR of the adaptive implementation of adaptive implementation of MST-RAKE and GSC single-user receivers, with $K = 5$ and $D = 1$ as a function of the number of symbols N_s for each of the following algorithms: RLS, LMS with training signals, and blind GSC. The simulation results show that the RLS algorithm converges much faster than the LMS algorithm. Specifically, the RLS converges in approximately 150 symbols, while the LMS requires about 500 symbols to converge within 95% of the steady-state output SINR. Since the GSC is blind, it need more symbols (about 600) to converge to within 95% of the steady-state of output SINR. In order to demonstrate the tracking capability of these algorithms, the multipath fading gains are deliberately changed at the 500th symbol. The resulting learning curves shown in Figure 5.2(b) show that the blind GSC algorithm converges in about 350 symbols, successfully adjusting the weights to adapt to the environment changes as well as the training based RLS and LMS algorithms.

5.6   Summary

In this Chapter, various adaptive receivers were introduced for practical implementation of CDMA receivers. The adaptive algorithms were implemented in a recursive form, using popular methods such as LMS and RLS. In particular, adaptive realization was presented for the proposed GSC algorithms. Moreover, robust methods were suggested for the adaptive GSC receivers that is shown to significantly improve system performance in the presence of signature errors. Finally, the maximal ratio combiner was also realized with an adaptive algorithm for tracking the principal component of the corresponding correlation matrix. The presented adaptive algorithms represent a collection of feasible ways of realizing advanced

CDMA receivers, and deserve further investigations in future research.

Table 5.1: Blind adaptive GSC algorithm for multiuser detection

1. Initialize the principal eigenvector $\mathbf{f}(0)$, eigenvalues $\lambda_e(0)$ and adaptive weights $\tilde{\mathbf{S}}_{d,a}(0)$.

2. Initialize coefficient μ of LMS and forgetting factor α of PAST.

3. For $i = 1, 2, \ldots$ (Do iterative step 4, 5).

4. For $d = 1$ to D (Do LMS algorithm in parallel at all antenna elements).

   (a) Calculate the correlator outputs at the dth antenna element.

   $$\mathbf{z}_d(i) = \left(\tilde{\mathbf{S}}_{d,c} - \mathbf{B}_c \tilde{\mathbf{S}}_{d,a}(i) \right)^H \mathbf{x}_{(d)}(i)$$

   (b) updating $\tilde{\mathbf{S}}_{d,a}(i)$

   $$\tilde{\mathbf{S}}_{d,a}(i+1) = \tilde{\mathbf{S}}_{d,a}(i) + \mu \mathbf{B}_c^H \mathbf{x}_{(d)}(i) \mathbf{z}_d^H$$

5. Use PAST to track principal eigenvector and eigenvalue and do maximum ratio combining.

   (a) Calculate the maximal ratio combiner output.

   $$z_o(i) = \mathbf{f}^H(i-1) \bar{\mathbf{z}}(i)$$

   (b) Get the estimate of $b_1(i)$ $\hat{b}_1(i) = z_o(i)$

   (c) Updates principal eigenvalue.

   $$\lambda_e(i) = \alpha \lambda_e(i-1) + |z_o(i)|^2$$

   (d) Updates principle eigenvector.

   $$\mathbf{f}(i) = \mathbf{f}(i-1) + [\bar{\mathbf{z}}(i) - \mathbf{f}(i-1) z_o(i)] z_o(i)^* / \lambda_e(i)$$

Table 5.2: Adaptive GSC algorithm for single-user detection

1. Initialize coefficient μ and weight vector $\mathbf{s}_a$

2. For $i = 1, 2, \ldots$, compute

$$\mathbf{x}_B(i) = \mathbf{B}^H \mathbf{x}(i)$$

$$z_c(i) = \mathbf{h}_1^H \mathbf{x}(i)$$

$$z_a(i) = \mathbf{s}_a^H(i) \mathbf{x}_B(i)$$

$$z(i) = z_c(i) - z_a(i)$$

$$\hat{b}_1(i) = sign\,(z(i))$$

$$\mathbf{s}_a(i+1) = \mathbf{s}_a(i) + \mu z^*(i) \mathbf{x}_B(i)$$

Table 5.3: Robust adaptive blind adaptive GSC algorithm

1. Initialize coefficients μ, β_s and weights $\mathbf{s}_a(0)$

2. Defined $\tilde{\mathbf{s}}_a(i) = \mathbf{B}\mathbf{s}_a(i)$

3. For $i = 1, 2, \ldots$

$$z_c(i) = \mathbf{s}_c^H \mathbf{x}(i)$$

$$z_a(i) = \tilde{\mathbf{s}}_a^H(i) \mathbf{x}(i)$$

$$z(i) = z_c(i) - z_a(i)$$

$$\hat{b}_1(i) = sign\,(z(i))$$

$$\mathbf{v}_a(i) = \tilde{\mathbf{s}}_a(i) + \mu z^*(i) \mathbf{B}\mathbf{x}_B(i)$$

$$\mathbf{s}_a(i+1) = \begin{cases} \mathbf{v}_a(i) & \|\mathbf{v}_a(i)\|^2 \leq \beta_s^2 - \|\mathbf{s}_c\|^2 \\ \sqrt{\beta_s^2 - \|\mathbf{s}_c\|^2}\,\dfrac{\mathbf{v}_a(i)}{\|\mathbf{v}_a(i)\|} & \|\mathbf{v}_a(i)\|^2 > \beta_s^2 - \|\mathbf{s}_c\|^2 \end{cases}$$

Table 5.4: Blind adaptive GSC algorithm with min/max algorithm

---

1. Initialize weights $\tilde{\mathbf{s}}_d(0)$, $\mathbf{f}_d(0)$, stepsize μ_s, μ_f, and smoothing factor α_d

2. Calculate $\mathbf{P}_{\mathbf{C}_1}^{\perp} = \mathbf{I} - \mathbf{C}_1 \left(\mathbf{C}_1^H \mathbf{C}_1\right)^{-1} \mathbf{C}_1^H$

3. Initialize forgetting factor α_p of PAST.

4. For $i = 1, 2, \ldots$ (Do iterative step 4, 5).

5. For $d = 1$ to D (Do min/max algorithm in parallel at all antennas).

$$\mathbf{R}_{\mathbf{x}_{(d)}}(i) = \alpha_p \mathbf{R}_{\mathbf{x}_{(d)}}(i-1) + (1 - \alpha_p)\mathbf{x}_{(d)}(i)\mathbf{x}_{(d)}^H(i)$$

$$\tilde{\mathbf{s}}_d(i+1) = \mathbf{P}_{\mathbf{C}_1}^{\perp} \left(\tilde{\mathbf{s}}_d(i) - \mu_s \mathbf{R}_{\mathbf{x}_{(d)}} \tilde{\mathbf{s}}_d(i)\right) + \mathbf{C}_1 \left(\mathbf{C}_1^H \mathbf{C}_1\right)^{-1} \mathbf{f}_d(i)$$

$$\tilde{\mathbf{f}}_d(i+1) = \mathbf{f}_d(i) + \frac{\mu_f}{\mu_s} \left(I - \frac{\mathbf{f}_d(i)\mathbf{f}_d^H(i)}{\mathbf{f}_d^H(i)\mathbf{f}_d(i)}\right) + \left(\mathbf{C}_1^H \mathbf{C}_1\right)^{-1} \left(\mu_s \mathbf{C}_1^H \mathbf{R}_{\mathbf{x}_{(d)}} \tilde{\mathbf{s}}_d(i) - \mathbf{C}_1^H \tilde{\mathbf{s}}_d(i)\right)$$

$$\mathbf{f}_d(i+1) = \frac{\tilde{\mathbf{f}}_d(i+1)}{\left\|\tilde{\mathbf{f}}_d(i+1)\right\|}$$

$$z_d(i+1) = \tilde{\mathbf{s}}_d(i)^H \mathbf{x}_{(d)}(i)$$

$$\tilde{\mathbf{z}}(i) = [z_1(i), z_2(i), \ldots, z_D(i)]$$

6. Use PAST to track principal eigenvector and do maximum ratio combining.

$$z_o(i) = \mathbf{f}^H(i-1)\tilde{\mathbf{z}}(i)$$

$$\hat{b}_1(i) = z_o(i)$$

$$\lambda_e(i) = \alpha_p \lambda_e(i-1) + |z_o(i)|^2$$

$$\mathbf{f}(i) = \mathbf{f}(i-1) + [\tilde{\mathbf{z}}(i) - \mathbf{f}(i-1)z_o(i)] z_o(i)^* / \lambda_e(i)$$
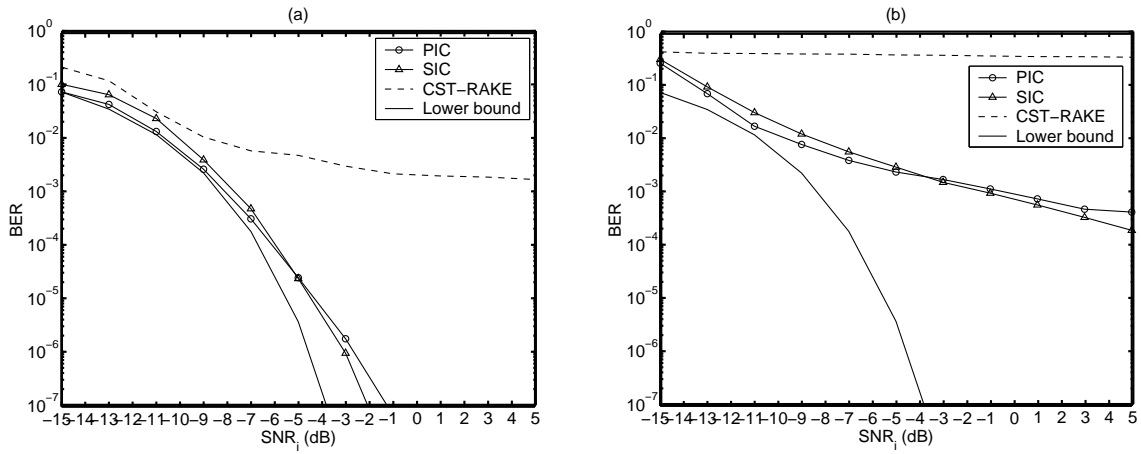

Figure 5.1: Probability of bit error versus input SNR for SIC, PIC and CST-RAKE receiver with NFR = 0 dB, (a) $K = 5$ and (b) $K = 20$.
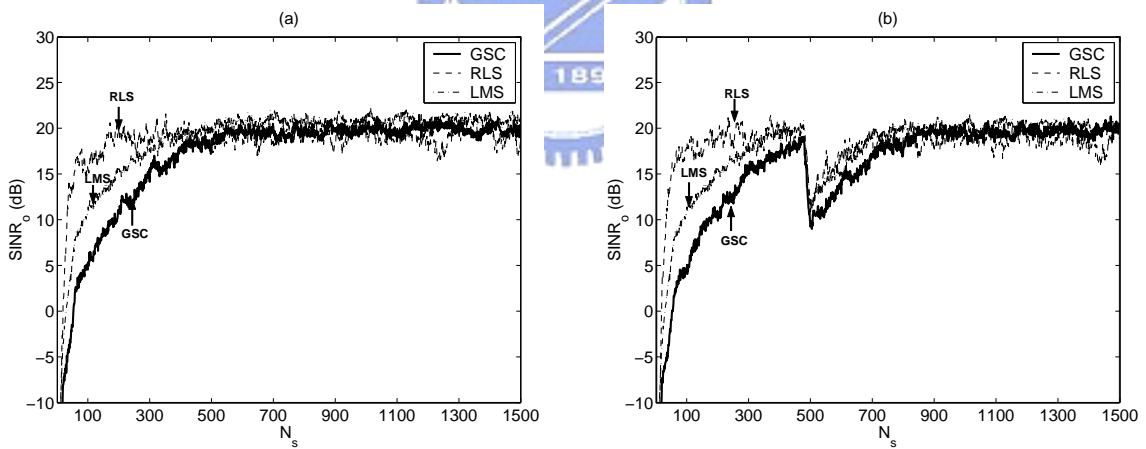
Figure 5.2: Output SINR of MST-RAKE and GSC receivers versus number of symbols for RLS, LMS and GSC algorithms with $K = 5$, $D = 1$, (a) CSV fixed and (b) CSV changed at 500th iterations.

Chapter 6

Implementation Issues and Performance Enhancement

In previous chapters, we have proposed space-time multiuser and single-user receivers. It has been demonstrated that these receivers provide substantial performance gains over detection techniques conventionally used in multiple access channels. However, the platform imposes computational and power constraints which led to hard implementation. To facilitate real-time implementation, it is necessary to alleviate the computational load, to adapt to mobile environments, to avoid system instability, and to reduce the performance degradation due to finite data samples. In this chapter, we will focus on some implementation issues and learn how to enhance the system performance.

6.1   Numerical Stability

For the direct matrix inversion implementation, the computation of temporal and spatial weight vectors for GSC or MOE algorithms all involve the inversion of correlation matrices of temporal or spatial data inputs. Numerically instability may arise when there are few strong interferers, led to ill-conditioned correlation matrices. On the other hand, the convergence of weight vectors may be slow due to the residual signal not completely removed by the blocking matrices. To remedy these, a pseudo noise term $\eta_g \mathbf{I}$ or $\eta_v \mathbf{I}$, where η_g and η_v are constants, can be added to temporal or spatial correlation matrices, respectively, to alleviate

the sensitivity problems [21, 34, 91]. The pseudo noise has the effect of deemphasizing the strong interference and masking the residual signal, and helps improve signal reception [82]. To make it clearer, we evaluate the output power of the MVDR receiver as a study case. From (3.50), the MVDR output power has the form:

$$P = \frac{1}{\mathbf{s}\mathbf{R}^{-1}\mathbf{s}} \tag{6.1}$$

where $\mathbf{s}$ is the weight vector, and $\mathbf{R}$ is the correlation matrix of the input data vector. The correlation matrix can be rewritten as

$$\mathbf{R} = \mathbf{E}\mathbf{\Lambda}\mathbf{E}^H \tag{6.2}$$

where $\mathbf{\Lambda} = diag[\lambda_1, \ldots, \lambda_\mathcal{M}]$, $\mathbf{E} = [\mathbf{e}_1, \ldots, \mathbf{e}_\mathcal{M}]$, and $\lambda_1, \ldots, \lambda_\mathcal{M}$ are the eigenvalues of $\mathbf{R}$, $\mathbf{e}_1, \ldots, \mathbf{e}_\mathcal{M}$ are the corresponding eigenvectors. It is assumed the rank of $\mathbf{R}$ is $\mathcal{M}$.

Using the matrix inversion lemma with a scaling factor $1/\lambda_{min}$, it can be shown that

$$\mathbf{R}^{-1} = \mathbf{I} - \sum_{i=1}^{\mathcal{M}} \mathbf{e}_i \frac{\lambda_i - \lambda_{min}}{\lambda_i} \mathbf{e}_i^H \tag{6.3}$$

where $1/\lambda_{min}$ is the smallest eigenvector of the inverse correlation matrix. Then the output power can now be evaluated as follows:

$$P = \frac{1}{\mathbf{s}\mathbf{R}^{-1}\mathbf{s}} = \frac{1}{\mathbf{s}^H\mathbf{s} - \sum_{i=1}^{\mathcal{M}} \frac{\lambda_i - \lambda_{min}}{\lambda_i} \left|\mathbf{s}^H\mathbf{e}_i\right|^2} \tag{6.4}$$

Inspection of the right-hand side of (6.4) shows that each eigenvalue contributes to the output with the proportional factor $(\lambda_i - \lambda_{min})$. In the case of infinite samples, every eigenvalue in the noise subspace is equal to λ_{min}, thus the noise subspace makes no contribution to the output power. In the finite samples case, the noise subspace eigenvalues are spread out, i.e., $\lambda_{q+1} > \lambda_{q+1} > \ldots > \lambda_{min}$, assuming q is the dimension of the signal subspace. In this case, $(\lambda_i - \lambda_{min})/\lambda_{min} \neq 0$, hence the noise subspace corrupts the output.

The consequence of adding the pseudo noise term $\eta_g\mathbf{I}$ or $\eta_v\mathbf{I}$ to the temporal or spatial correlation matrix has the effect of reducing the $(\lambda_i - \lambda_{min})/\lambda_{min}$ term, thus reducing the effect of the noise subspace on the output. If the eigenvalues of signal subspace are much larger than the loading level, the signal subspace's contribution to the output is minimal. The pseudo noise term should be chosen large enough to handle the ill-conditioned problem,

146

but not too large to distort the original signal scenario. A suitable choice which is proved effective is that $\eta_t\mathbf{I}$ or $\eta_s\mathbf{I}$ equals a small fraction (e.g. $0.1 \sim 0.3$) of the dominant signal power in the correlation matrix of the temporal and spatial data vector, respectively [82]. In practice, a convenient estimate of the dominant signal power is the largest eigenvalue of the corresponding correlation matrices.

6.2   Partially Adaptive Implementation

Partially adaptive filter only uses a portion of the degree of freedom available in the weight adaptation process [40, 55]. It speeds the convergence and improves the transient performance of the filtering process. Unfortunately, reducing the adaptive degree of freedom leads to poorer interference cancellation capability. As a consequence, a primary concern in the design of partially adaptive filter is to minimize the performance degradation due to a reduced degree of freedom [53]. To construct the partially adaptive filter, we introduce a rank-reducing transformation $\mathbf{U}$. The transformation can be done on the input data vector or the blocking matrix, if the GSC scheme is to be employed [92]. Two techniques of partially adaptive filtering are noted: (1) method 1: reduced-size input data (RZ-ID), (2) method 2: reduced-size blocking matrix of GSC (RZ-BM). The diagrams of RZ-ID and RZ-BM are shown in Figure 6.1(a) and 6.1(b), respectively.

6.2.1   Method 1: Reduced-Size Input Data

To reduce the number of adaptive filter taps, we introduce a rank-reducing transformation matrix $\mathbf{U}$ of size $P \times P'$, where P is the tap number of full adaptation and P' is tap number of partial adaptation. For the cases of the adaptive correlators mentioned in the previous chapters, the tap number of a fully adaptive filter is $P = N + L - 1$, and P' is chosen to be $P' \leq N - 1$. The received input data vector is pre-multiplied by $\mathbf{U}^H$, which produces an P'-dim vector. We will always assume $\mathbf{U}$ to be full rank.

We denote the reduced-dimension received data vector as $\mathbf{x}_u(i) = \mathbf{U}^H\mathbf{x}(i)$. Here $\mathbf{x}(i)$ could be $\mathbf{x}_{c-ST}$ or $\mathbf{x}_{c-BT}$, if the partially adaptive algorithm is employed in the time domain. The reduced-dimension MMSE receiver vector $\mathbf{s}_u$ is found as the solution to the Wiener-Hopf

quation $\mathbf{R}_{\mathbf{x}_u}\mathbf{s}_u = \mathbf{r}_u$, where $\mathbf{R}_{\mathbf{x}_u} = E\{\mathbf{x}_u(i)\mathbf{x}_u(i)^H\}$ and $\mathbf{r}_u = E\{\mathbf{x}_u(i)b_1^*(i)\}$. Then the error probability from (3.54) is given by

$$P_1 = \frac{1}{2^{K-1}} \sum_{\bar{\mathbf{b}} \in \{-1,1\}^{K-1}, b_1=-1} Q\left(\frac{\mathcal{R}\left\{\mathbf{s}_u^H \mathbf{U}^H \bar{\bar{\mathbf{H}}}\mathbf{b}\right\}}{\sigma_n \left(\mathbf{s}_u^H \mathbf{U}^H \mathbf{U}\mathbf{s}_u\right)^{1/2}}\right) \tag{6.5}$$

where $\bar{\bar{\mathbf{H}}} = [\tilde{\mathbf{h}}_1, \tilde{\mathbf{h}}_2, \ldots, \tilde{\mathbf{h}}_K]$, $\tilde{\mathbf{h}}_k$ is the cascade Pre-ST or Pre-BT CSV of user k, and $\bar{\mathbf{b}}$ is the transmitted data symbol sequence of all but the desired user.

Optimum Dimension Reduction

The optimum transformation is defined as the transformation that conserves the error probability, i.e., the transformation $\mathbf{U}$ for which the MMSE receiver based on the reduced-size input data vector $\mathbf{U}^H\mathbf{x}(i)$ has the same error probability as the MMSE receiver based on original input data vector $\mathbf{x}(i)$. In [39], it was proved that, if $\mathbf{U}$ is such that $\Re\{\bar{\bar{\mathbf{H}}}\} \subseteq \Re\{\mathbf{U}\}$, $\Re\{\cdot\}$ means range of $\{\cdot\}$, and $\mathbf{U}^H\mathbf{U} = \mathbf{I}_{P'}$, the MMSE receiver with reduced-size transformation $\mathbf{U}$ will have the same probability as the MMSE receiver without dimension reduction. The optimum dimension reduction is not unique and requires knowledge of the subspace $\Re\{\bar{\bar{\mathbf{H}}}\}$.
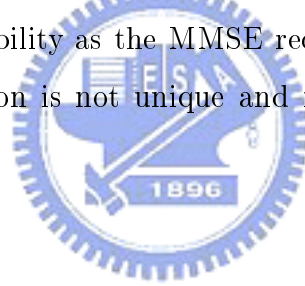
Eigenvector Identification

The signal space is spanned by the CSVs of active users, i.e, the column vectors of $\bar{\bar{\mathbf{H}}}$. It is assumed that the columns of $\mathbf{E}_s$ are the eigenvectors corresponding to the P' largest eigenvalues of the autocorrelation matrix $\mathbf{R} = E\{\mathbf{x}(i)\mathbf{x}^H(i)\}$. It is easy to understand that $\Re\{\bar{\bar{\mathbf{H}}}\} = \Re\{\mathbf{E}_s\}$. The optimal selection of the reduced-size transformation is to satisfy the condition $\mathbf{U} = \mathbf{E}_s$ [92]. An estimate $\hat{\mathbf{E}}_s$ is found from the EVD of the sample correlation matrix $\hat{\mathbf{R}}$:

$$\hat{\mathbf{R}} = \frac{1}{N_s} \sum_{i=1}^{N_s} \mathbf{x}(i)\mathbf{x}^H(i) = \hat{\mathbf{E}}_s\hat{\Lambda}_s\hat{\mathbf{E}}_s + \hat{\mathbf{E}}_n\hat{\Lambda}_n\hat{\mathbf{E}}_n \tag{6.6}$$

The matrix $\mathbf{U} = \hat{\mathbf{E}}_s$ is called the eigenvector reduced-size transformation.

Cyclically Shifted Filter Bank (CFSB)

In [15, 94], the columns of $\mathbf{U}$ are found as a bank of P' matched filters, where each filter is matched to the multipath signature sequences of desired user cyclically shifted with $\Delta = P/P'$ steps. We assume for convenience, that Δ is integer. The CFSB reduced-size transformation is $\mathbf{U} = [\mathbf{c}_{1,l}, \mathbf{c}_{1,l}^{\Delta}, \ldots, \mathbf{c}_{1,l}^{(P'-1)\Delta}]$ when the lth finger of adaptive correlators are being processed, where $\mathbf{c}_{1,l}^{\Delta}$ denotes $\mathbf{c}_{1,l}$ cyclically shifted Δ by steps.

Symmetrically Dimension Reduction (SDR)

The SDR transformation forms the elements of the reduced received vector as partial sums of the matched filter output. The reduced-size transformation $\mathbf{U}$ is found as

$$\mathbf{U} = [\mathbf{c}_{1,l_{\{0:\Delta-1\}}}, \mathbf{c}_{1,l_{\{\Delta:2\Delta-1\}}}, \ldots, \mathbf{c}_{1,l_{\{(P'-1)\Delta:P\}}}] \tag{6.7}$$

for the lth finger, where the partially despread vector is given by

$$\mathbf{c}_{1,l_{\{k\Delta:(k+1)\Delta-1\}}} = \left[0, \ldots, 0, \mathbf{c}_{1,l}[k\Delta : (k+1)\Delta-1]^T, 0, \ldots, 0\right]^T \tag{6.8}$$

where $\mathbf{c}_{1,l_{\{k\Delta:(k+1)\Delta-1\}}}$ is a P-dim vector with nonzero values of entries only within the region $\{k\Delta, (k+1)\Delta - 1\}$.

6.2.2 Method 2: Reduced-Size Blocking Matrix

The reduced-size transformation $\mathbf{U}$, being a full column rank matrix, can be incorporated with the blocking matrix $\mathbf{B}$, resulting in a new equivalent GSC structure. The GSC weight vector can be written as

$$\mathbf{s} = \mathbf{s}_c - \mathbf{B}\mathbf{U}\mathbf{s}_a \tag{6.9}$$

where $\mathbf{s}_c$ is the nonadaptive weight vector, which can be a signature sequence in the time domain, or a steering vector in the space domain, and $\mathbf{s}_a$ is the associated adaptive weight vector. The vector $\mathbf{s}_a$ is found as the solution to the unconstrained optimization problem:

$$\min_{\mathbf{s_a}} (\mathbf{s}_c - \mathbf{B}\mathbf{U}\mathbf{s}_a)^H \mathbf{R}(\mathbf{s}_c - \mathbf{B}\mathbf{U}\mathbf{s}_a) \tag{6.10}$$

This minimization results in

$$\mathbf{s}_a = \left(\mathbf{U}^H \mathbf{B}^H \mathbf{R} \mathbf{B} \mathbf{U} \right)^{-1} \mathbf{U}^H \mathbf{B}^H \mathbf{R} \mathbf{s}_c \tag{6.11}$$

Using (6.9) and (6.10), the overall GSC weight vector is then given by

$$\mathbf{s} = \left(\mathbf{I} - \mathbf{B} \mathbf{U} (\mathbf{U}^H \mathbf{B}^H \mathbf{R} \mathbf{B} \mathbf{U})^{-1} \mathbf{U}^H \mathbf{B}^H \mathbf{R} \right) \mathbf{s}_c \tag{6.12}$$

It can be shown that the output SINR is given by

$$\text{SINR}_o = \left(\mathbf{s}_c^H \mathbf{R} \mathbf{s}_c - \mathbf{s}_c^H \mathbf{R} \mathbf{B} \mathbf{U} (\mathbf{U}^H \mathbf{B}^H \mathbf{R} \mathbf{B} \mathbf{U})^{-1} \mathbf{U}^H \mathbf{B}^H \mathbf{R} \mathbf{s}_c \right)^{-1} \tag{6.13}$$

There are a variety of criteria for choosing the reduced-size transformation matrix $\mathbf{U}$ for the reduced-size GSC. We will discuss these criteria in the following.

Maximum Output SINR

In this criterion, the goal is to maximize the output SINR in (6.13). Since the first term $\mathbf{s}_c^H \mathbf{R} \mathbf{s}_c$ is fixed, the minimization is achieved by maximizing the latter term. The cost function is obtained as

$$J_{gsc} = \mathbf{s}_c^H \mathbf{R} \mathbf{B} \mathbf{U} (\mathbf{U}^H \mathbf{B}^H \mathbf{R} \mathbf{B} \mathbf{U})^{-1} \mathbf{U}^H \mathbf{B}^H \mathbf{R} \mathbf{s}_c \tag{6.14}$$

For a given reduced-size P', one way the J_{gsc} may be optimized is to choose a transformation matrix $\mathbf{U}$ satisfying

$$\mathbf{B} \mathbf{U} = \mathbf{E}_s \tag{6.15}$$

where $\mathbf{E}_s$ consists of the P' principal eigenvectors of $\mathbf{R}$. The $\mathbf{U}$ can be obtained by solving the least squares problem in (6.15). It is easy to show that with this optimal choice of $\mathbf{U}$, the optimal output SINR is given by

$$\begin{aligned} \text{SINR}_o &= \left(\mathbf{s}_c^H \mathbf{R} \mathbf{s}_c - \mathbf{s}_c^H \mathbf{E}_s \mathbf{\Lambda}_s \mathbf{E}_s^H \mathbf{s}_c \right)^{-1} \\ &= \left(\mathbf{s}_c^H \mathbf{E}_n \mathbf{\Lambda}_n \mathbf{E}_n^H \mathbf{s}_c \right)^{-1} \end{aligned} \tag{6.16}$$

where $\mathbf{R} = \mathbf{E}_s \mathbf{\Lambda}_s \mathbf{E}_s + \mathbf{E}_n \mathbf{\Lambda}_n \mathbf{E}_n$ and $\mathbf{E}_n$ consists of the other eigenvectors of $\mathbf{R}$ with the smallest eigenvalue.

To avoid the complexity of solving a least squares problem, let the matrix $\mathbf{U}$ be restricted to consist of P' of the P eigenvectors of $\mathbf{R}_a = \mathbf{B}^H \mathbf{R} \mathbf{B}$, where $\mathbf{R}_a = \bar{\mathbf{E}}_s \bar{\mathbf{\Lambda}}_s \bar{\mathbf{E}}_s^H + \bar{\mathbf{E}}_n \bar{\mathbf{\Lambda}}_n \bar{\mathbf{E}}_n^H$, and $\text{rank}\{\bar{\mathbf{E}}_s\} = P'$. A natural choice would be let the reduced-size transformation consist of the P' principal eigenvectors of $\mathbf{R}_a$, i.e., $\mathbf{U} = \bar{\mathbf{E}}_s$.

Cross Spectral Metric (CSM)

For a known covariance matrix $\mathbf{R}$ and a given reduced-size dimension P', the optimal approach that maximizes the output SINR is suggested in [38, 95], in which $\mathbf{U}$ is constructed from the P' eigenvectors of $\mathbf{R}_a = \mathbf{B}^H \mathbf{R} \mathbf{B}$ that maximizes the quantity:

$$\frac{|\bar{\mathbf{e}}_i^H \mathbf{B} \mathbf{R} \mathbf{s}_c|}{\bar{\lambda}_i} \tag{6.17}$$

where $\bar{\mathbf{e}}_i$ and $\bar{\lambda}_i$ are, respectively, eigenvectors and eigenvalues of $\mathbf{R}_a$. This method is referred as the cross spectral metric (CSM) method.

Unitary Transformation

Since the motivation for reducing the rank of adaptive problems is to decrease the overall computational complexity, it does not seem appropriate to perform an EVD on the lower branch of correlation matrix. In this regard, other unitary transformations should be used in place of EVD. The appropriate transformation to use depends on the nature of the lower branch. For example, the discrete cosine transformation (DCT) is well known to approximate the EVD for correlated data when the amount of data approaches infinity [96]. The DCT matrix will therefore be used as a substitute for the eigenfilters in (6.17). For DCT reduced-size transformation matrix, $\mathbf{U}$ is defined to be those P' columns of the DCT matrix $\mathbf{Q}$ which maximize the following metric:

$$\max_i \frac{\left| \mathbf{q}_i^H \mathbf{B}^H \mathbf{R} \mathbf{s}_c \right|}{\sigma_{q_i}} \tag{6.18}$$

where $\mathbf{q}_i$ is the ith column of the DCT matrix $\mathbf{Q}$ and $\sigma_{q_i} = \left| \mathbf{q}_i^H \mathbf{B}^H \mathbf{x} \right|^2$ is the associated filter output.

6.3 Partially Adaptive Implementation for Multiuser Scenario

In previous chapters, we have introduced a set of adaptive correlators to perform despreading and MAI's suppression. They are realized in the form of GSC, and require no pilot symbols assisted channel estimation. As described in the previous sections, the partially adaptive methods work with a reduced-dimension P' adaptive weights through the use of a $P \times P'$ linear transformation $\mathbf{U}$. In the case of adaptive correlators based on the modified GSC techniques as in the proposed receivers, the blocking matrix $\mathbf{B}_c$ of size $(N+L-1) \times (N-1)$ is modified into a smaller one of size $(N+L-1) \times P'$, where $P' < (N-1)$. The criteria for the selection of $\mathbf{U}$ include: (1) P' should be as small as possible (2) MAI should be retained as much as possible in the lower branch. Criterion (1) is for complexity reduction and (2) is for optimal mutual cancellation of MAI in the upper and lower branches of GSC schemes in [97].

To develop the partially adaptive GSC for multiuser scenarios, we rewrite the MMSE criterion as

$$\min_{\mathbf{g}_l} \quad E\left\{\left|\mathbf{c}_{1,l}^H\mathbf{x}(i) - \mathbf{g}_l^H\mathbf{B}_c^H\mathbf{x}(i)\right|\right\} \equiv \left\|\mathbf{R}^{1/2}\mathbf{B}_c\mathbf{g}_l - \mathbf{R}^{1/2}\mathbf{c}_{1,l}\right\|^2 \tag{6.19}$$

Note from (6.19) that the optimal GSC weight vector $\mathbf{g}_l$ is the one lying in the subspace $\Re\left\{\mathbf{R}^{1/2}\mathbf{B}_c\right\}$ that is closest to $\mathbf{R}^{1/2}\mathbf{c}_{1,l}$. In other words, $\mathbf{R}^{1/2}\mathbf{B}_c\mathbf{g}_l$ should be in the direction that exhibits maximum "correlation" with $\mathbf{R}^{1/2}\mathbf{c}_{1,l}$. It is therefore desired that the blocking matrix $\mathbf{B}_c$ be chosen such that the crosscorrelation of the upper and the lower branch outputs, $\rho = \left|\mathbf{c}_{1,l}^H\mathbf{R}\mathbf{B}_c\mathbf{g}_l\right|$, is large. Since $\mathbf{B}_c^H\mathbf{C}_1 = \mathbf{0}$, the only way to maximize ρ is to retain as much MAI as possible. Therefore, an essential criterion for choosing a reduced-size blocking matrix for implementation is such that the upper and the lower branch outputs of the GSC have a large crosscorrelation [97]. Since the lower branch contains no signal, the only way to maximize the crosscorrelation is to retain as much MAI as possible. By doing so, a maximum mutual cancellation of interference can be achieved between the upper and lower branch.

Based on criterion (2), a simple partially adaptive scheme is suggested for a multiuser scenario in which P' MAI's are present in the system, and their composite signature vector's

can be obtained by pilot symbols assisted channel estimation. From (3.24), the estimated $(N + L - 1) \times 1$ CSV of user k can be expressed as

$$\hat{\mathbf{h}}_k = \sum_{l=1}^{L} \hat{\alpha}_{k,l} \mathbf{c}_{k,l} \tag{6.20}$$

for $k = 2, \ldots, K$, where $\hat{\alpha}_{k,l}$ is the channel gain estimate at the lth finger. Given these CSV estimates, a reduced-size blocking matrix $\mathbf{B}_{P'}$ retaining the maximum MAI can be constructed by projecting onto the column space of $\mathbf{B}_c$ the set of vectors $\left\{ \hat{\mathbf{h}}_k \right\}$:

$$\mathbf{B}_{P'} = \mathbf{B}_c \mathbf{B}_c^H \left[\hat{\mathbf{h}}_2 \cdots \hat{\mathbf{h}}_K \right] \tag{6.21}$$

where we assume orthonormal columns of $\mathbf{B}_c$ such that $\mathbf{B}_c^H \mathbf{B}_c = \mathbf{I}$. So the linear transformation $\mathbf{U}$ following $\mathbf{B}_c$ is

$$\mathbf{U} = \mathbf{B}_c^H \left[\hat{\mathbf{h}}_2 \cdots \hat{\mathbf{h}}_K \right] \tag{6.22}$$

Simple algebra shows that $\mathbf{B}_{P'}$ is an $(N + L - 1) \times (K - 1)$ matrix, the reduced-size P' equals to the number of interferers, which removes the signal and retains as much MAI as possible in the sense of maximum crosscorrelation. Partially adaptative realization via (6.21) is simple and proves robust to errors in MAI's channel estimates. In particular, errors in $\hat{\mathbf{h}}_k$'s tend to decrease the crosscorrelation between the upper and lower branches, and results in only slight performance degradation. When viewed as a multiuser detector, the partially adaptive receiver is much more robust than the conventional ones, which detect and subtract the MAI [98]. In conventional multiuser interference cancellers, a small error in the MAI's channel estimate can result in an enhanced MAI power and possible error propagation.

Note that $\mathbf{B}_{P'}$ can be regarded as the "smallest" blocking matrix with the number of columns (degree of freedom for MAI suppression) equal to the number of detected MAI. If the partially adaptive receiver performs $(K-1)$-dim processing, where $K \leq N$, then at most $K - 1$ MAI's can be suppressed. By doing so, the GSC can concentrate on those dominant MAI's with the smallest possible degree of freedom, leading to lower complexity and better convergence.

6.4 Iterative Maximum SINR Receiver via Decision Aided Signal Reconstruction

The GSC correlators are a variation of the LCMV combiner and share the same characteristics of the latter, e.g., good interference cancellation and poor convergence. By poor convergence is meant that there is usually a certain performance degradation due to finite data samples. In [40], an analysis of the LCMV beamformer reveals that the main cause of its poor convergence is the presence of a non-zero crosscorrelation between the signal and interference-plus-noise due to finite samples. The crosscorrelation term induces a perturbation on the beamformer weight vector, which in turn cause a drop in output SINR. With the increase of data sample size, this crosscorrelation gradually vanished and the LCMV beamformer approaches the optimal MSINR correlator. The same statements apply to GSC correlator's. Define a general form of input data matrix $\bar{\mathbf{X}} = [\mathbf{x}(1), \mathbf{x}(2), \cdots, \mathbf{x}(N_s)]$ and let $\bar{\mathbf{X}} = \bar{\mathbf{X}}_s + \bar{\mathbf{X}}_{in}$, where $\bar{\mathbf{X}}_s$ is the input data matrix due to the desired signal and $\bar{\mathbf{X}}_{in}$ is the input data matrix due to the interference-plus-noise. Then, the sample correlation matrix can be estimated via input data samples. For a total of N_s samples, the autocorrelation matrix is given by

$$
\begin{aligned}
\hat{\mathbf{R}} &= \frac{1}{N_s} \bar{\mathbf{X}} \bar{\mathbf{X}}^H \\
&= \frac{1}{N_s} \left(\bar{\mathbf{X}}_s \bar{\mathbf{X}}_s^H + \bar{\mathbf{X}}_s \bar{\mathbf{X}}_{in}^H + \bar{\mathbf{X}}_{in} \bar{\mathbf{X}}_s^H + \bar{\mathbf{X}}_{in} \bar{\mathbf{X}}_{in}^H \right) \\
&= \hat{\mathbf{R}}_s + \hat{\mathbf{R}}_{in} + \hat{\mathbf{R}}_{s,in}
\end{aligned}
\tag{6.23}
$$

where $\hat{\mathbf{R}}_s$, $\hat{\mathbf{R}}_{in}$ and $\hat{\mathbf{R}}_{s,in}$ are the sample signal correlation matrix, interference-plus-noise correlation matrix, and crosscorrelation matrix between signal and interference-plus-noise, respectively. Using the fact $\mathbf{B}_c^H \hat{\mathbf{R}}_s \simeq \mathbf{0}$, we have the optimal weights of GSC

$$
\mathbf{s}_{1,l} = \left[\mathbf{I} - \mathbf{B}_c (\mathbf{B}_c^H \hat{\mathbf{R}}_{in} \mathbf{B}_c)^{-1} \mathbf{B}_c^H \hat{\mathbf{R}}_{in} \right] \mathbf{c}_{1,l} - \mathbf{B}_c (\mathbf{B}_c^H \hat{\mathbf{R}}_{in} \mathbf{B}_c)^{-1} \mathbf{B}_c^H \hat{\mathbf{R}}_{s,in} \mathbf{c}_{1,l}
\tag{6.24}
$$

Note that the first term on the right-hand side of (6.24) represents the "optimal" maximum SINR weight vector, and the second term represents the perturbation leading to poor convergence [40]. A natural way to remedy this is then by removing the perturbation term, which can be achieved by removing the desired signal component from the input data vector $\mathbf{x}(i)$

154

such that $\hat{\mathbf{R}}_{s,in} = \mathbf{0}$. This suggests an iterative procedure in which the signal is estimated, reconstructed at the jth iteration, and subtracted from $\mathbf{x}(i)$ at the $(j+1)$th iteration.

With the MAI is removed, channel estimation ($\hat{\alpha}'_{1,l}s$) for the desired user can be done accurately, leading to improved performance as compared to the conventional RAKE receiver. However, the GSC is blind in nature and usually exhibits slow convergence due to the residual signal effect. To remedy this, a decision aided scheme is introduced in which the signal is estimated and then subtracted from the input data before the computation of optimal weight vector of GSC scheme. First, assume that at the jth iteration, the received data $\mathbf{x}(i)$ is available and despread into

$$\mathbf{y}_{1,l}^{(j)}(i) = \mathbf{s}_{1,l}^{(j)}{}^{H} \mathbf{x}(i) \tag{6.25}$$

where $\mathbf{s}_{1,1}^{(j)}$ is estimated by (6.24) using the "signal-substracted" data $\mathbf{x}_{in}^{(j)}$ as the GSC input:

$$\mathbf{s}_{1,l}^{(j)} = \left[\mathbf{I} - \mathbf{B}_c (\mathbf{B}_c^H \mathbf{R}_{in}^{(j)} \mathbf{B}_c)^{-1} \mathbf{B}_c^H \mathbf{R}_{in}^{(j)} \right] \mathbf{c}_{1,l} \tag{6.26}$$

where $\mathbf{R}_{in}^{(j)} = E\left\{ \mathbf{x}_{in}^{(j)}(i)\mathbf{x}_{in}^{(j)}{}^{H}(i) \right\}$. With $\mathbf{y}_{1,l}^{(j)}(i)$ available, we can obtain the channel estimate using a sequence of N_p pilot symbols:

$$\hat{\alpha}_{1,l}^{(j)} = \frac{1}{N_p} \sum_{i=1}^{N_p} y_{1,l}^{(j)}(i) \tag{6.27}$$

Using this channel estimate, the random phase of the lth finger output $y_{1,l}^{(j)}$ is removed and coherent RAKE combining is achieved by

$$y_1^{(j)}(i) = \sum_{l=1}^{L} \hat{\alpha}_{1,l}^{(j)*} y_{1,l}^{(j)}(i) \tag{6.28}$$

which is then sent to the data decision device:

$$\hat{b}_1^{(j)}(i) = \text{sign}\left(\left\{ \hat{y}_1^{(j)}(i) \right\} \right) \tag{6.29}$$

Second, signal reconstruction is done by exploiting the channel estimate $\hat{\alpha}_{1,l}^{(j)}$, the desired user's signature $\mathbf{c}_{1,l}$ and estimated data bit $\hat{b}_1^{(j)}(i)$ as follows:

$$\hat{\mathbf{x}}_s^{(j)}(i) = \hat{b}_1^{(j)}(i) \sum_{l=1}^{L} \hat{\alpha}_{1,l}^{(j)} \mathbf{c}_{1,l} \tag{6.30}$$

155

where $\hat{\mathbf{x}}_s^{(j)}(i)$ is the desired signal estimated at jth iteration. Note that $\hat{\alpha}_{1,l}^{(j)}$'s are used for both signal reconstruction and signal symbol detection. Finally, the reconstructed signal is subtracted from the data sent to the $(j+1)$th iteration, which yields

$$\mathbf{x}_{in}^{(j+1)}(i) = \mathbf{x}(i) - \hat{\mathbf{x}}_s^{(j)}(i) \tag{6.31}$$

By using $\mathbf{x}_{in}^{(j+1)}(i)$ as the GSC input, the adverse slow convergence can be effectively improved, and the performance can be achieved nearly the optimal MMSE with a moderate size of pilot symbols. Due to signal subtraction, the receiver will act like the optimal MSINR receiver operating on $\mathbf{R}_{in}$, which offers the best comprise between MAI plus noise suppression and signal reception. The above described procedure can be iterated several times, if necessary, to gain further improvement. The overall scheme of iteration MSINR is depicted in Figure 6.2.

Performance Analysis:

The output SINR at the jth is denoted as SINR_o:

$$\begin{aligned} \text{SINR}_o &= \frac{\text{desired signal output power}}{\text{MAI + noise output power}} \\ &= \frac{\mathbf{s}_{1,l}^{(j)^H} \mathbf{R}_s \mathbf{s}_{1,l}^{(j)}}{\mathbf{s}_{1,l}^{(j)^H} \mathbf{R}_{in} \mathbf{s}_{1,l}^{(j)}} \end{aligned} \tag{6.32}$$

The corresponding BER can be calculated using the well known approximation [45]:

$$P_e \approx Q\left(\sqrt{\text{SINR}_o}\right) \tag{6.33}$$

For the purpose of simplifying notation, the weight vector is denoted as $\mathbf{s}_l = \mathbf{s}_{1,l}^{(j)}$ without reference to iteration and subscript. The optimal weight vector of the GSC receiver can be expressed as

$$\mathbf{s}_l = \left[\mathbf{I} - \mathbf{B}_c (\mathbf{B}_c^H \mathbf{R} \mathbf{B}_c)^{-1} \mathbf{B}_c^H \mathbf{R}\right] \mathbf{c}_{1,l} \tag{6.34}$$

where $\mathbf{c}_{1,l}$ is the lth signature vector of user 1. The output power of GSC can be expressed as

$$P_o = \mathbf{s}_l^H \mathbf{R} \mathbf{s}_l = \mathbf{c}_{1,l}^H \mathbf{R} \mathbf{c}_{1,l} - \mathbf{c}_{1,l}^H \mathbf{R} \mathbf{B}_c (\mathbf{B}_c^H \mathbf{R} \mathbf{B}_c)^{-1} \mathbf{B}_c^H \mathbf{R} \mathbf{c}_{1,l} \tag{6.35}$$

156

In the ideal case that the signal and noise are uncorrelated, $\mathbf{R} = \mathbf{R}_s + \mathbf{R}_{in}$, and $\mathbf{B}_c^H \mathbf{R}_s = \mathbf{0}$:

$$P_s = \mathbf{c}_{1,l}^H \mathbf{R}_s \mathbf{c}_{1,l} \tag{6.36}$$

and

$$P_{in} = \mathbf{c}_{1,l}^H \mathbf{R}_{in} \mathbf{c}_{1,l} - \mathbf{c}_{1,l}^H \mathbf{R}_{in} \mathbf{B}_c (\mathbf{B}_c^H \mathbf{R}_{in} \mathbf{B}_c)^{-1} \mathbf{B}_c^H \mathbf{R}_{in} \mathbf{c}_{1,l} \tag{6.37}$$

Thus, the output SINR of GSC receiver can be expressed as

$$
\begin{aligned}
\mathrm{SINR}_{GSC} &= \frac{P_s}{P_{in}} = \frac{\mathbf{c}_{1,l}^H \mathbf{R}_s \mathbf{c}_{1,l}}{\mathbf{c}_{1,l}^H \mathbf{R}_{in} \mathbf{c}_{1,l} - \mathbf{c}_{1,l}^H \mathbf{R}_{in} \mathbf{B}_c (\mathbf{B}_c^H \mathbf{R}_{in} \mathbf{B}_c)^{-1} \mathbf{B}_c^H \mathbf{R}_{in} \mathbf{c}_{1,l}} \\
&= \frac{1}{\frac{P_o}{P_s} - 1}
\end{aligned}
\tag{6.38}
$$

The equation of (6.38) and SINR of MOE are identical [21]. On the other hands, comparing the output SINR of MOE with that of MMSE shows that they tend to be close to each other at high SNR [21]:

$$\mathrm{SINR}_{GSC} = \mathrm{SINR}_{MOE} \approx \mathrm{SINR}_{MMSE} \tag{6.39}$$

The corresponding approximate BER is (6.33)

$$P_e^{GSC} = P_e^{MOE} \approx P_e^{MMSE} \tag{6.40}$$

For the output SINR of the MSINR receiver, the analysis of performance is the same as the GSC receiver except that the desired signal is subtracted before going through the GSC scheme.

6.5 Dynamic Sector Synthesis and Narrowband Interference Cancellation

In addition to multipath fading effects and MAI, a CDMA system can also be subject to limiting factors such as narrowband interference (NBI). There are three basic types of NBI: (1) tonal signals; (2) narrowband digital communication signals; (3) entropic narrowband stochastic processes. Tonal signals are those which consist of sum of pure sinusoidal signals.

These signals are useful for modeling tone jammers and other harmonic interference phenomena. Narrowband digital communication signals generalize tonal signals to include digitally modulated carriers. This leads to signals with nonzero-bandwidth components, and the digital signaling structure can be exploited to improve the NBI suppression capability. Less structure can be assumed by modeling the NBI as entropic narrowband stochastic processes, such as narrowband autoregressions.

Process in the area of NBI suppression for DS/CDMA system up until the late 1980s is reviewed by [99]. The principle techniques of that era were frequency-domain and predictive or interpolative techniques based on linear predictors/interpolators. In the past decade, there have been a new techniques which make use of linear code-aided methods for suppression of NBI both individually and jointly with MAI. However, the statistical characteristics of NBI look like a nonstationary signal, except when the processing window is spanned over a long enough observation interval [100]. This would be impractical for real-time implementation. It is thus desirable to use an antenna array for suppressing the NBI since the spatial statistics of NBI is relatively stationary in most cases. Here we present a scheme in which a set of diversity beams is constructed with NBI suppression capability, and we also present a way of dynamic beam synthesis to adapt to the traffic of the system.

6.5.1 NBI Suppression by Diversity Beamformers

To suppress the NBI via an antenna array, we first estimate the AOA's of the NBI. By removing all the CDMA signals from the received signals and keeping the spatial signature of NBI unchanged, we can estimate the AOA's of the NBI accurately via well established AOA estimation techniques. This can be done by despreading the received signal $\mathbf{X}(i)$ in (3.25) with a specificallt designed signature vector $\mathbf{s}_p$ which is obtained by

$$\min_{\mathbf{s}_p} \quad \left\| \mathbf{s}_p{}^H \mathbf{C} \right\|^2$$

$$\text{subject to: } \mathbf{s}_p{}^H \mathbf{s}_p = 1 \tag{6.41}$$

where $\mathbf{C} = [\mathbf{C}_1, \mathbf{C}_2, \cdots, \mathbf{C}_K]$ is the signature matrix of the active users, with $\mathbf{C}_k = [\mathbf{c}_{k,1}, \mathbf{c}_{k,2}, \cdots, \mathbf{c}_{k,L}]$ being the kth users' multipath signature matrix, as defined in (2.11). The solution to (6.41)

is the minimum eigenvector, denoted as $\mathbf{s}_{p,o}$, of the correlation matrix $\mathbf{R}_c = E\left\{\mathbf{C}\mathbf{C}^H\right\}$. The despread data vector is then obtained as

$$\mathbf{x}_p(i) = \mathbf{X}(i)\mathbf{s}_{p,o}^* \tag{6.42}$$

We refer to $\mathbf{s}_{p,o}$ as the complemental despreading vector since it performs the complementary despreading function of for CDMA signals. After complementary despreading, all CDMA signals will be attenuated to a great extent, and the remaining components include only NBI and noise. In this case, AOA estimation techniques can be employed on $\mathbf{x}_p(i)$ to locate the NBI. A promising technique for AOA estimation is based on Capon's minimum variance technique [21] which improves the poor resolution of classical methods and is less complex than the subspace or maximum likelihood methods. This technique minimizes the contribution of the undesired interference by minimizing the power while maintaining the gain along the look direction to be unity. That is

$$\min_{\mathbf{w}} \quad P \equiv \mathbf{w}^H \mathbf{R}_p \mathbf{w}$$

$$\text{subject to: } \mathbf{w}^H \mathbf{a}(\theta) = 1 \tag{6.43}$$

where $\mathbf{R}_p = E\left\{\mathbf{x}_p(i)\mathbf{x}_p^H(i)\right\}$. By using the Lagrange multiplier technique, the solution to (6.43) can be shown to be [21]

$$\mathbf{w}_o = \frac{\mathbf{R}_p^{-1}\mathbf{a}(\theta)}{\mathbf{a}^H(\theta)\mathbf{R}_p^{-1}\mathbf{a}(\theta)} \tag{6.44}$$

Now the output spatial power spectrum of the beamformer as a function of the AOA is given by

$$P(\theta) = \frac{1}{\mathbf{a}^H(\theta)\mathbf{R}_p^{-1}\mathbf{a}(\theta)} \tag{6.45}$$

By computing the spectrum for θ over the entire range of field-of-view, AOA's of the NBI can be estimated by locating the peaks in the spectrum.

6.5.2 Dynamic Sector Synthesis by Diversity Beamformers Selection

Cell sectorization has been widely proposed for improving system capacity in cellular systems [101]. In a sectored system, every cell is divided into multiple sectors, and each

159

sector is served by a dedicated antenna array. Through dynamic sector synthesis, the network operator can customize the azimuth anglular coverage of each sector. This allows the operator to balance the traffic loading across sectors, to manage handoff overhead, and to control the interference. According to the distribution of users and strong NBI, the entire field-of-view is divided into several dynamic sectors. Each dynamic sector is covered by a set of M diversity beamformers with NBI suppressing constraints and each responsible for a subset of users. These diversity beamformers suppress the NBI and enhance the SINR of a subset of CDMA users in the associated dynamic sector denoted as Θ_s. Let θ_m, $m = 1, \ldots, M$, be the set of angles well representing Θ_s and denote as $\mathbf{a}_m = \mathbf{a}(\theta_m)$. Assume that the AOA's of NBI have been estimated and denoted as $\hat{\phi}_n$, $n = 1, \ldots, \mathcal{N}$. In order to retain the CDMA signals while rejecting the NBI, we consider the following multiply constrained minimum variance problem:

$$\min_{\mathbf{w}_m} \quad \mathbf{w}_m^H \mathbf{Q}_a \mathbf{w}_m$$

$$\text{subject to: } \mathbf{w}_m^H \mathbf{a}_m = 1 \tag{6.46}$$

where $\mathbf{Q}_a = \left[\mathbf{a}(\hat{\phi}_1), \cdots, \mathbf{a}(\hat{\phi}_\mathcal{N}) \right] \left[\mathbf{a}(\hat{\phi}_1), \cdots, \mathbf{a}(\hat{\phi}_\mathcal{N}) \right]^H$ is the spatial signature correlation matrix of the NBI. The solution to (6.46) is given by

$$\mathbf{s}_{m,o} = \frac{\mathbf{Q}_a^{-1} \mathbf{a}_m}{\mathbf{a}_m^H \mathbf{Q}_a^{-1} \mathbf{a}_m} \tag{6.47}$$

The beamforming matrix $\mathbf{W} = [\mathbf{w}_{1,o}, \mathbf{w}_{2,o}, \cdots, \mathbf{w}_{M,o}]$ are applied to convert the space-time data matrix $\mathbf{X}(i)$ with dimension $D \times (N + L - 1)$ into beamspace-time data matrix $\mathbf{Y}(i)$ with dimension $M \times (N + L - 1)$, such that

$$\begin{aligned} \mathbf{Y}(i) &= [\mathbf{w}_{1,o}, \mathbf{w}_{2,o}, \cdots, \mathbf{w}_{M,o}]^H \mathbf{X}(i) \\ &= \mathbf{W}_o^H \mathbf{X}(i) \\ &= \left[\mathbf{y}_1^T(i), \mathbf{y}_2^T(i), \cdots, \mathbf{y}_M^T(i) \right]^T \end{aligned} \tag{6.48}$$

The vectors $\mathbf{y}_m(i)$, $m = 1, \ldots, M$, are the chip-sampled data vectors at the mth beam. In summary, the look angles are chosen such that the M beams cover a dynamic sector Θ_s, and the dynamic sector is adapted to balance the traffic load, to reduce the handoff overhead, and to control the interference, especially for strong NBI.

160

6.6   Simulation Results

Computer simulations are conducted to demonstrate the effectiveness of the schemes developed in this chapter. The receiver output SINR is used as the evaluation index. Also, the input SNR is defined as $\mathrm{SNR}_i = \sigma_1^2/\sigma_n^2$, and the near-far-ratio is defined as $\mathrm{NFR} = \sigma_k^2/\sigma_1^2$, $k = 2, \ldots, K$, where we assume equal power MAI for convenience. The path gains $\alpha_{k,j}$'s are assumed independent, identically distributed unit variance complex Gaussian random variables, the path delays $\tau_{k,j}$'s are assumed uniform over $\{0, 3T_c\}$, and the number of fingers of the receiver is $L = 4$. All CDMA signals are generated with BPSK data modulation and Gold codes of length 31 are used as the spreading codes. For each simulation trial, N_s symbols (including data and pilot) are used to obtain the sample estimate of correlation matrix and N_p pilot symbols are used to obtain the $\hat{\alpha}_{1,l}^{(j)}$'s. Unless otherwise mentioned, the following standard parameters are assumed: $K = 10$, $\mathrm{SNR}_i = 0$ dB, $\mathrm{NFR} = 10$ dB, $N_s = 500$, $N_p = 50$, the number of iterations is $J = 3$, and the number of antenna element $D = 1$. Each simulation result is obtained by 100 independent trials, with each trial using a different set of $\alpha_{k,l}$'s and data/noise sequence.

In the first set of simulations, the superiority of the robust GSC receiver, with diagonal loading of 0.3 of the dominant eigenvalue of the correlation matrix, is evaluated in the presence of modelling errors. For comparison, the non-robust receiver is also included. Without loss of generality, it is assumed a single antenna element is used. Figure 6.3(a) shows the output SINR for different numbers of symbols N_s. The results show that the output SINR curve of the non-robust GSC receiver is oscillated during startup. In Figure 6.3(b), modeling errors are generated by adding a Gaussian random vector with the variance 10^{-2} to the CSV of the desired user. The simulaiton results show the output SINR of non-robust GSC is worse than the robust GSC, as expected, due to its higher sensitivity to modeling errors.

In the second set of simulations, we compare the output SINR performance of different reduced-dimension GSC receivers. The system capacity is evaluated with $\mathrm{NFR} = 10$ dB in Figure 6.4 for (a) $P' = 11$ and (b) $P' = 21$. In particular, GSC_F, GSC_{P1}, GSC_{P2} and GSC_{P3} respresent, respectively, the fully adaptive, multiuser partially adaptive receiver described by (6.22), EVD based partially adaptive receiver described by (6.15), and unitary

transformation partially adaptive receiver described by (6.18). For comparison, we also include the results of the PST-RAKE receiver described by (3.49) and CST-RAKE receiver in (3.60). As expected, the PST-RAKE receiver gives the best performance, and the fully adaptive GSC receiver has nearly the same performance of the PST-RAKE for a wide range of user number K. The conventional CST-RAKE receiver totally fails due to the lack of interference suppression. Note that the partially adaptive receivers GSC_{P1}, GSC_{P2} and GSC_{P3} degrade quickly with $K > P'$ due to the exhaustion of degree of freedom for MAI suppression. For the user number $K < P'$, the performance of both the multiuser GSC_{P3} and EVD GSC_{P1} partially adaptive receivers approaches the fully adaptive GSC receiver, but the unitary transformation exhibits a larger performance loss compared to the other two partially adaptive receivers. This is due to the approximation errors incurred with the transformation.

In the third simulation, the output SINR performance of the proposed GSC receiver versus the number of symbols is evaluated with $K = 5$, $P' = 11$ and NFR = 10 dB as a function of iteration number J. Included are the fully adaptive receiver GSC_F, multiuser partially adaptive receiver GSC_{P1} and EVD based partially adaptive receiver GSC_{P2}. For channel estimation, $N_p = N_s/10$ pilot symbols are used. For the partially adaptive receivers, true channel vectors are assumed for the MAI, i.e., $\hat{\mathbf{h}}_k = \mathbf{h}_k$, $k = 2, \ldots, K$. The results in Figure 6.5 show that the proposed three receivers successively approach the optimal receiver after three iterations. After convergence, the two partially adaptive receivers have almost the same performance of the fully adaptive receiver, confirming that the reduced-dimension transformation in (6.21) retains the full interference suppression capability of the fullly adaptive receiver.

The fourth simulation compares the convergence behaviors of the proposed receiver with the MMSE and the proposed MSINR receivers described in Section 6.4. The proposed receiver uses $N_p = N_s/10$ pilot symbols, and the MMSE receiver uses either $N_p = N_s/10$ or $N_p = N_s$ (full) pilot symbols. The MSINR receiver is considered as blind with $N_p = 0$. The results given in Figure 6.6 show that the proposed receiver with 1/10 pilot symbols converges in about 200 data symbols and is only 1 dB away from the full pilot MMSE receiver. On the other hand, the MMSE receiver using full pilot symbols offers the best performance, but

degrades significantly if only 1/10 pilot symbols are available. The reasons for the significant discrepancy between the proposed and MMSE receivers with a low pilot symbol ratio is that the proposed receiver cancels the MAI before channel estimation whereas the MMSE receiver estimates the channel in the presence of strong MAI. The MSINR receiver is better than the MMSE receiver with 1/10 pilot symbols for a small N_s, but is inferior to the proposed receiver by about 9 dB. Although the MSINR receiver is known to approach the MMSE receiver under good conditions such as high SNR and moderate multipath fading and MAI, it is unable to maintain the same performance under the severe conditions assumed in the simulation. A close investigation of the simulation results reveals that the MOE receiver successfully cancels the MAI, but gives a low gain for the desired signal due to channel mismatch. Note that pilot symbols can be used for the MSINR receiver to obtain the channel phase, but this does not make any difference to its output SINR performance.

In the final simulation, we consider the complementary despreading technique for dynamic sector synthesis and NBI suppression. In this case, an antenna array of $D = 9$ elements is used. In addition to the MAI, there are two equal power BPSK NBI arriving from $30°$ and $-45°$, with bit rate being 0.8 times that of the CDMA signal. The NBI-to-signal ratio (NSR), which is the ratio of the NBI power to SOI power before spreading, is 20 dB. To demostrate the efficacy of complementary spreading and AOA estimation of NBI, the spatial spectrum is computed for the field-of-view $[-60°, 60°]$ and plotted in Figure 6.7. The peak in the plot gives the AOA estimates of the NBI which is close to the real AOA's of the two NBI's. $M = 7$ diversity beams are then formed at look directions $\{-35°, -20°, -10°, 0°, 15°, 45°, 55°\}$ to cover the field-of-view, skipping the NBI purposedly. In Figure 6.8, the patterns of diversity beams are plotted for the case $K = 5$ users and NFR $= 0$ dB. The mainlobes and deep nulls confirm that the diversity beamformer can indeed effectively collect the SOI and suppress the strong NBI.

6.7 Summary

In this chapter, solutions have been proposed to (1) facilitate real-time implementation for CDMA receivers (2) avoid system unstability (3) speed up convergence, and reduce per-

formance degradation due to finite data samples. For low-complexity implementation, a partially adaptive realization of the GSC matched filters based on multiuser information is presented as an alternative to conventional multiuser receivers. This method is shown to be robust to multiuser estimation errors, and offer nearly the same performance of fully adaptive methods. For system stability, a simple yet effective dagonal loading method is suggested which offer significant improvement especially when a few strong signals are present. For better convergence behaviors of the GSC based receivers, an iterative maximum SINR receiver based on the decision aided scheme is proposed. In this scheme, the signal waveform is first constructed, and then subtracted from the input data sent to the next iteration. With signal subtraction, the proposed GSC CDMA receivers can achieve nearly the performance of ideal MSINR receiver within a few iterations.

A major issue in spread spectrum communications is the NBI. The NBI acts like a non-stationary signal for temporal processing, and requires a large degree of freedom for effective suppression. An effective remedy for NBI is through the use of antenna array processing to suppress the NBI in the spatial domain. This is because that the NBI is relatively stationary in the space domain. We introduce a new method in which a complementary despreading scheme is employed to remove the CDMA signals first, and the AOA of NBI is estimated. By using a set of diversity beamformers with null constraints set at the estimated NBI AOA's, a dynamic sector is synthesized. With dynamic sector synthesis, the network operator can customize azimuth angular region partition. This allows the operator to balance the traffic loading across sctors, to manage handoff overhead, and to control the interference in the sector.
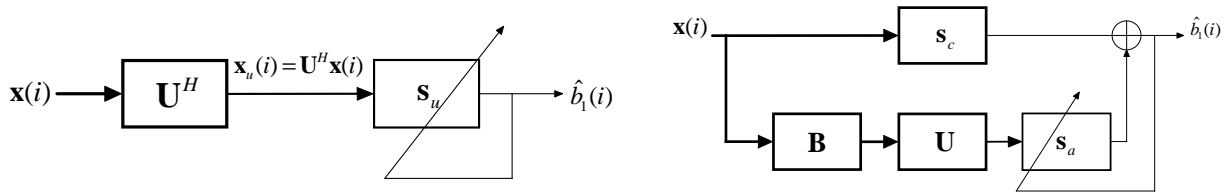
Figure 6.1: Structures of partially adaptive methods for (a) RZ-ID (b) RZ-BM.
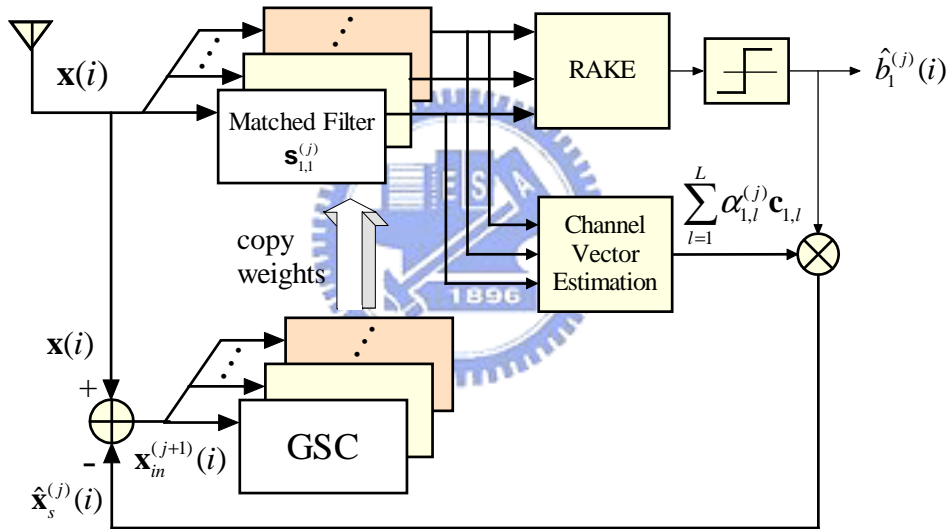

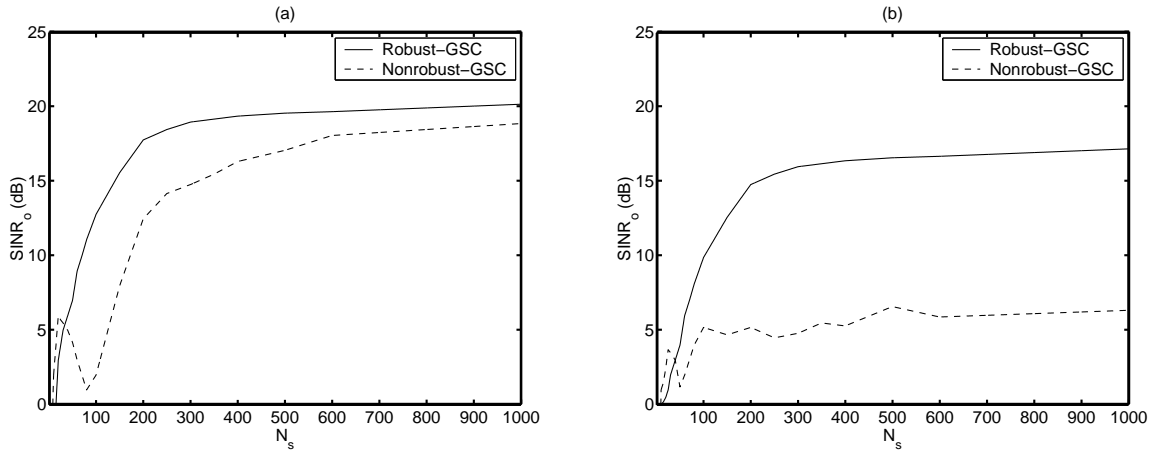Figure 6.2: Structure of iterative MSINR receiver

Figure 6.3: Evaluation of numerical stability of adaptive GSC with (a) diagonal loading and (b) modeling errors.
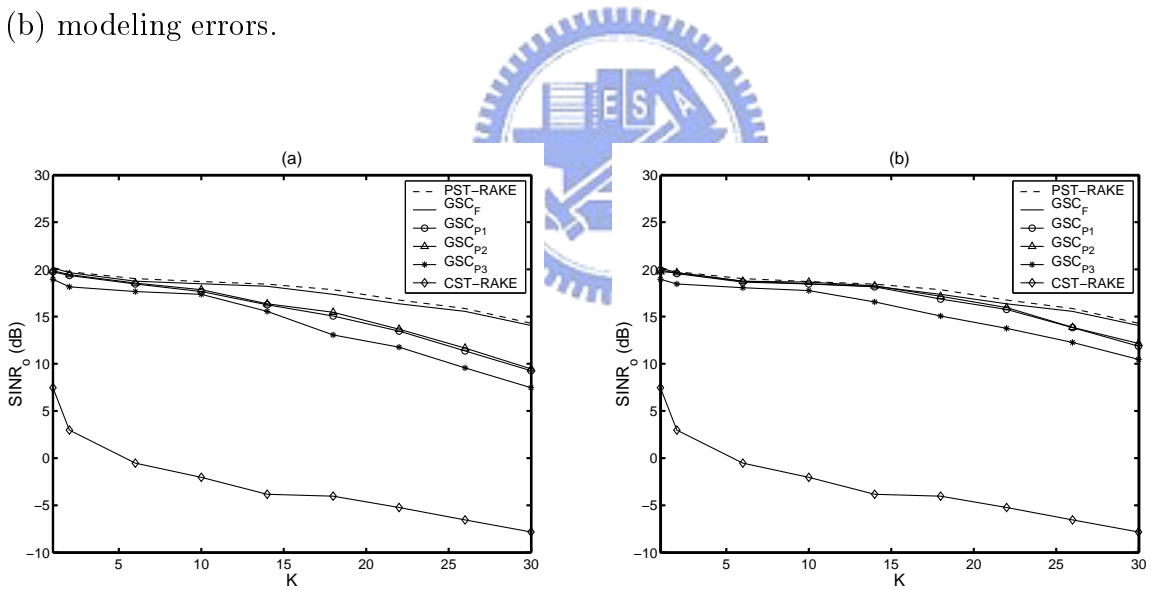

Figure 6.4: Output SINR obtained with partially adaptive algorithm with (a) $P' = 11$ and (b) $P' = 21$.
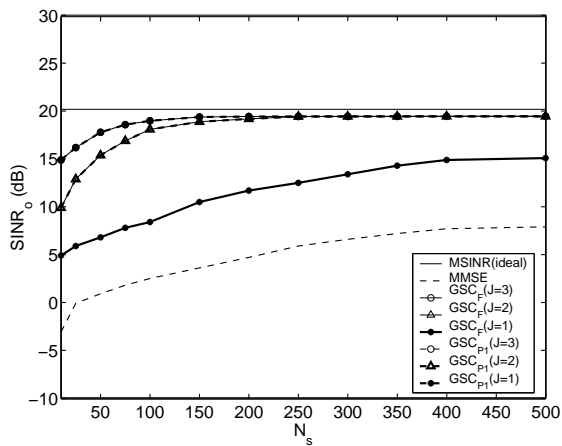
Figure 6.5: Output SINR versus number of symbols for MSINR receivers at different iterations.
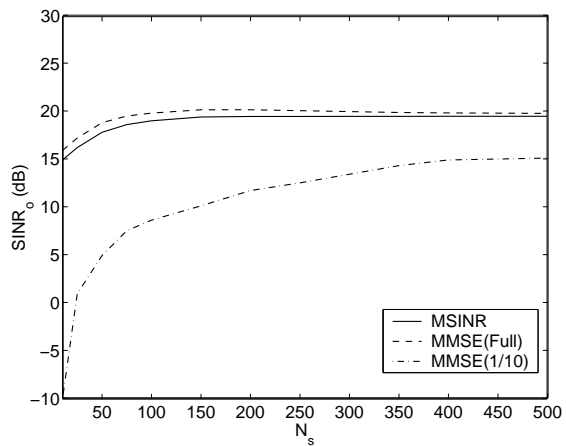
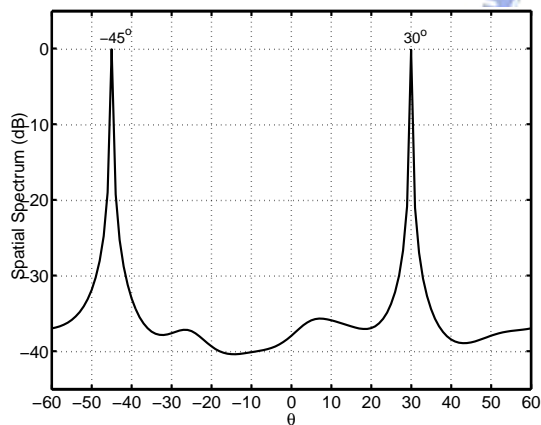Figure 6.6: Convergence behavior of MSINR receiver with 1/10 pilot symbols of MMSE receivers.

Figure 6.7: AOA estimation of NBI via complementary despreading with $D = 9$ antenna elements.
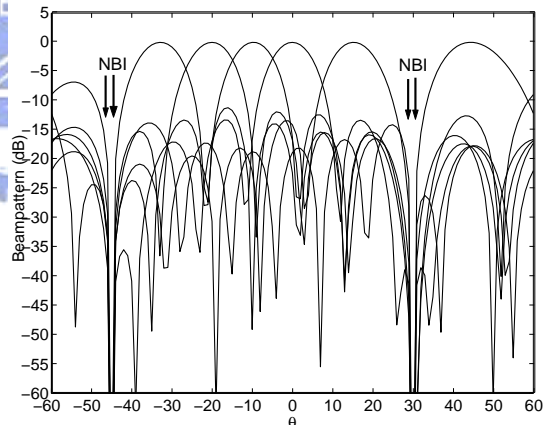
Figure 6.8: Patterns of diversity beamformers for NBI suppression in dynamic sector synthesis, with $D = 9$ and $M = 7$.

167

Chapter 7

Conclusions

7.1 Summary of Thesis

Advanced space-time 2-D RAKE receivers capable of suppressing MAI and NBI in CDMA systems and operating in frequency selective fading channels were considered in this thesis. The introductory Chapter included a literature review related to the topics under consideration. In Chapter 2, the DS/CDMA system model has been introduced. As a motivation for the rest of the thesis, some of the weak points of conventional RAKE receivers have been pointed out. And, as condidate techniques for increasing the system capacity and enhancing near-far resistance, the multiuser detection and linear single user detection techniques have been derived. In order to compare the performance of various forms of CDMA detectors, three performance measures were defined.

One advanced approach to improving signal processing is the space-time processing, which operates simultaneously on multiple antennas and multiple taps. In Chapter 3, we have developed various models of space-time 2-D RAKE receivers, including Post-ST, Post-BT, Pre-ST and Pre-BT 2-D RAKE receivers. In addition to various linear space-time multiuser detectors, the parallel interference cancellation (PIC) and successive interference cancellation (SIC) CDMA receivers also have been discussed in the Chapter. A blind space-time CDMA receiver based on the GSC technique has been introduced. To avoid signal cancellation, we

have proposed a novel method for constructing the blocking matrix in the lower branch of the GSC. For spatial processing, we removed the desired signal coming from the working sector in the lower branch of the spatial GSC by judiciously designing the spatial blocking matrix. And for temporal processing, we removed the signal coming within the delay spread in the lower branch of the temporal GSC by judiciously designing the temporal blocking matrix. The simulation results have shown that the performance of the proposed CDMA receiver approached the performance of the MMSE receiver.

Chapter 4 proposed three novel beamspace-time 2-D RAKE receivers for sectored CDMA systems. In a sectored cellular system, the entire field-of-view is divided into several working sectors, with each sector responsible for a distinctive set of users. With an antenna array incorporated, sectorization can be done adaptively to meet two major requirements. First, multiple beams are formed to collect multipath components of desired signal. Second, strong MAI outside the sector is suppressed in the sidelobe of these beams. The outputs of the beamformers are processed by a bank of adaptive correlators, which are formed by a set of modified GSC to collect the multipath components of desired signals and to suppress the in-sector MAI. Adaptive implementation of these 2-D RAKE receivers has also been introduced and simulation results presented to confirm their effectiveness.

In Chapter 5, various types of adaptive CDMA receivers were introduced. The adaptive algorithms can avoid matrix inversion for reduced complexity complexity, which is most efficient especially repeated matrix inversion is necessary when the channel was nonstationary. The adaptive algorithms were implemented in a sequential time-recursive fashion, such as the popular LMS and RLS algorithms. The LMS algorithm has a low computational complexity but can be slow in convergence. The RLS algorithm is faster in convergence, but needs more computations at each iteration. We have also introduced a constrained LMS algorithm for the GSC architecture. Moreover, we have proposed robust adaptive techniques that are shown to substaintially improve the system performance with signature errors present. Furthermore, the maximal ratio combining was also realized with an adaptive algorithm in order to track the principal component eigenvector efficiently.

Miscellaneous implementation issues have been discussed in Chapter 6. The diagonal loading method has been used to enhance the robustness of adaptive algorithms. Some

partially adaptive methods have been introduced to increase the speed of convergence of the receivers, without sacrificing their performance. In particular, a partially adaptive GSC algorithm was proposed for multiuser scenarios. The criterion for partially adaptive GSC was to keep the MAI on both the upper and lower branches and to remove the desired signal on the lower branch. Simulation results showed that the performance of the proposed partially adaptive receivers approached that of the the fully adaptive versions. Also, the results showed that improved performance could be achieved via iterative adaptations. We also found that an even more effective way to improve the GSC convergence and to maximize the putput SINR is to remove the desired signal before doing GSC. An analysis of LCMV beamformer revealed that the main cause of its poor convergence is the presence of a non-zero crosscorrelation between the signal and interference-plus-noise due to finite samples. The same statements apply to GSC receivers. This suggests an iterative procedure in which the signal is estimated, reconstructed, and subtracted the signal from the next input signal of GSC at the next iteration. The NBI acts like a nonstationary signals within the processing window of the adaptive receiver, so it is desirable to use the antenna array to suppress the NBI in the spatial domain since the spatial feature of the NBI is relatively stationary. We have presented a diversity beamforming scheme to suppress the NBI and a method of dynamic sector synthesis for adapting to the traffic of CDMA systems. The dynamic sector synthesis technique can offer customized azimuthal coverage. This allows the operator to balance the traffic loading across sectors, to manage handoff overhead, and to control the interference.

7.2 Future Work

Although the research studies presented in this thesis have thoroughly discussed receiver design on space-time processing for CDMA systems, there are several other topics which remain to be addressed:

- Forward Link Processing

  In general, the forward link of CDMA systems provides better performance than the reverse link, because the interference observed at each mobile can be controlled in a

much easier way. However, since the forward and reverse links use different frequency bands and, therefore, the multipath vector channels for both links are quite different, the basestation cannot use the receiver weights operating on the reverse link for the forward link. Hence, forward link beamforming requires special treatment, and represents an interesting and important research topic for further study.

- Space-Time Coding

  The performance analysis of the proposed CDMA receivers did not include the effects of channel coding. To fully exploit the system capacity, we are interested in investigating joint transmitter/receiver design by using effective space-time codes at the transmitter. Extension of this performance analysis to include these effects will also be another future research direction.

- Long-Code Spreading Sequence

  The thesis considered only DS/CDMA systems employing periodic (short) spreading sequences. The case of aperiodic (long) spreading sequences should be studied as well. We remark that in the presence of aperiodic spreading sequences, only the "chip-level" channel can be considered time-invariant, not the symbol-level channel. In this case, a different data model is neede for the development of adaptive receivers. This represents an issue of further research in the design of the of DS/CDMA systems.

- Hardware Implementation

  The implementation of practical space-time CDMA receivers is an area of ongoing research. On one hand, one aims to improve the performance of receivers and to increase the system capacity. On the other hand, one looks for easy implementations in real world applications. With improved algorithm performance, there is typically a cost in increased computational complexity. However, there are practical limitations on current hardware technologies, such as linear amplifier and antenna calibration for antenna array, the sampling rate and finite precision for analogue to digital converters (ADCs) and implementation of adaptive algorithms with fixed-point DSP or FPGA. As technology progresses, looking for more robust and high performance real-time receiver architectures will continue to be a dynamic and interesting research field.

Bibliography

[1] T. S. Rappaport, *Wireless Communications: Principles and Practice*. Prentice Hall, NJ, 1996.

[2] K. Buchannan, "Imt2000: Service provider's perspective," *IEEE Personal Communi- caitons*, pp. 8–13, Aug 1997.

[3] E. Nikula, A. Toskala, E. Dahlman, L. Girard and A. Klein, "Frames multiple access for Umts and Imt-2000," *IEEE Personal Communications*, pp. 16–24, Apr. 1998.

[4] T. Ojanpera and R. Prasad, "An overview of third-generation wireless personal commu- nications: A european perspective," *IEEE Personal Communications*, pp. 59–65, Dec. 1998.

[5] T. Ojanpera and R. Prasad, *Wideband CDMA for Third Generation Mobile Communi- caitons*. Artech House, 2000.

[6] H. Holma and A. Toskala, *WCDMA for UMTS*. John Wiley, Sons. Ltd., 2000.

[7] A. J. Viterbi, *CDMA : Principles of Spread Spectrum Communication*. Addison-Wesley, 1995.

[8] P. Jung, P. W. Baier and A. Steil, "Advantages of CDMA and spread spectrum tech- niques over FDMA and TDMA in cellular mobile radio applications," *IEEE Trans. Veh. Technol.*, vol. 42, pp. 357–364, Aug. 1993.

[9] A. J. Viterbi, A. M. Viterbi, K. S. Gilhousen and E. Zehavi, "Soft handoff extends CDMA cell coverage and increase reverse link capacity," *IEEE J. Select. Areas Com- mun.*, vol. 12, pp. 1281–1288, Oct. 1994.

[10] P. F. Driessen and G. J. Foschini, "On the capacity formula for multiple input multiple output wireless channels: a geometric interpretation," ICC'99, vol. 3, pp. 1603–1607, 1999.

[11] S. Verdu, *Multiuser Detection*. New York: Cambridge Univ. Press, 1998.

[12] B. Sklar, "Rayleigh fading channels in mobile digital communication systems .ii. mitigation," *IEEE Communication Magazine*, vol. 35, pp. 102–109, Jul. 1997.

[13] R. Lupas and S. Verdu, "Near-far resistance of multiuser detectors in asynchronous channels," *IEEE Trans. Commun.*, vol. 38, Mar. 1990.

[14] R. Lupas and S. Verdu, "Linear multiuser detectors for synchronous code-division multiple-access channels," *IEEE Trans. Inform. Theory*, vol. 35, pp. 123–136, Jan. 1989.

[15] U. Madhow and M. Honig, "MMSE interference suppression for direct-sequence spread-spectrum CDMA," *IEEE Trans. Commun.*, vol. 42, pp. 3178–3188, Dec. 1994.

[16] S. E. Bensley and B. Aazhang, "Subspace-based channel estimation for code division multiple access communication system," *IEEE Trans. Commun.*, vol. 44, pp. 1009–1020, Aug. 1996.

[17] X. Wang and H. V. Poor, "Blind adaptive multiuser detection in multipath CDMA channels based on subspace tracking," *IEEE Trans. Signal Processing*, vol. 46, pp. 3030–3044, Nov. 1998.

[18] M. Honig and S. Verdu, "Blind adaptive multiuser detection," *IEEE Trans. Inform. Theory*, vol. 41, pp. 944–960, Jul. 1995.

[19] J. B. Schodorf and D. B. Williams, "A constrained optimization approach to multiuser detection," *IEEE Trans. Signal Processing*, vol. 45, pp. 258–262, Jan. 1997.

[20] M. K. Tsatsanis, "Inverse filtering criteria for CDMA systems," *IEEE Trans. Signal Processing*, vol. 45, pp. 102–112, Jan. 1997.

[21] D. H. Johnson and D. E. Dudgeon, *Array Signal Processing: Concepts and Techniques*. New Jersey: Prentice Hall, 1993.

[22] Z. Tian and H. L. Van Trees, "A quadratically constrained decision feedback equalizer for DS-CDMA communication systems," *SPAWC'99*, May 1999.

[23] M. K. Tsatsanis and Z. Wu, "Performance analysis of minimum variance CDMA receivers," *IEEE Trans. Signal Processing*, vol. 46, pp. 3014–3022, Nov. 1998.

[24] T. S. Lee, T. C. Tsai and C. C. Chen, "A beamsapce-time blind rake receiver for sectored CDMA systems," *Wireless Personal Communications*, vol. 17, pp. 65–83, 2001.

[25] A. F. Naguib and T. Kailath, "Capacity improvement with base-station antenna arrays in cellular CDMA," *IEEE. Trans. Veh. Technol.*, vol. 43, pp. 691–698, Aug. 1994.

[26] S. Kandala, E. S. Sousa and S. Pasupathy, "Multi-user multi-sensor detectors for CDMA networks," *IEEE Trans. Commun.*, vol. 43, pp. 946–957, Apr. 1994.

[27] S. Miller and S. Schwartz, "Integrated spatial-temporal detectors for asynchronous Gaussian multiple-access channels," *IEEE Trans. Commun.*, vol. 43, pp. 396–411, 1995.

[28] X. Wang and H. V. Poor, "Space-time multiuser detection in multipath CDMA channels," *IEEE Trans. Signal Processing*, vol. 47, pp. 2356–2374, Sep. 1999.

[29] X. Bernstein and A. M. Haimovich, "Space-time optimum combining for CDMA communications," *Wireless Personal Communications*, vol. 3, pp. 73–89, 1996.

[30] A. F. Naguib and A. Paulraj, "Performance of wireless CDMA with M-ary orthogonal modulation and cell site antenna arrays," *IEEE J. Select. Areas Commun.*, vol. 14, pp. 1770–1783, Dec. 1996.

[31] H. Liu and M. D. Zoltowski, "Blind equalization in antenna array CDMA systems," *IEEE Trans. Signal Processing*, vol. 45, pp. 161–172, Jan. 1997.

[32] T. F. Wong, T. M. Lok, J. S. Lehnert and M. D. Zoltowski, "A linear receiver for direct-sequence spread spectrum multiple-access system with antenna arrays and blind adaptation," *IEEE Trans. Inform. Theory*, vol. 44, pp. 659–676, Mar. 1998.

[33] G. Woodward and B. S. Vucetic, "Adaptive detection for DS-CDMA," *Proc. IEEE*, vol. 86, pp. 1413–1434, Jul. 1998.

[34] Z. Tian, K. L. Bell and H. L. Van Trees, "Robust constrained linear receivers for CDMA wireless systems," *IEEE Trans. Signal Processing*, vol. 49, pp. 1510–1522, Jul. 2001.

[35] T. S. Lee and T. C. Tsai, "A beamspace-time interference cancelling CDMA receiver for sectored communications in a multipath environment," *IEEE J. Sel. Areas Commun.*, vol. 19, pp. 1374–1384, Jul. 2001.

[36] X. Wang and H. V. Poor, "Blind multiuser detection: a subspace approach," *IEEE Trans. Inform. Theory*, vol. 44, pp. 677–690, Mar. 1998.

[37] I. S. Reed, J. D. Mallett and L. E. Brennan, "Rapid convergence rate in adaptive arrays," *IEEE Trans. on Aerospace and Electronic Systems*, vol. 10, pp. 853–863, Nov. 1974.

[38] J. S. Goldstein and I. S. Reed, "Subspace selection for partially adaptive sensor array processing," *IEEE Trans. Aerospace and Electronic Systems*, vol. 33, pp. 539–544, Apr. 1997.

[39] E. G. Strom and S. L. Miller, "Properties of the single-bit single-user MMSE receiver for DS-CDMA systems," *IEEE Trans. Commun.*, vol. 47, pp. 416–425, Mar. 1999.

[40] B. V. Veen, *Adaptive Radar Detection and Estimation*, ch. Minimum Variance Beamforming. New York, Wiley, 1992.

[41] S. Verdu, "Minimum probability of error for asynchronous Gaussian multiple-access channels," *IEEE Trans. Inform. Theory*, vol. 32, no. 1, pp. 85–96, 1986.

[42] A. Duel-Hallen, J. Holtzman and Z. Zvonar, "Multiuser detection for CDMA system," *IEEE Personal Communications*, pp. 46–58, Apr. 1995.

[43] R. Price and Jr. P. E. Green, "A communication technique for multipath channels," *Proc. IRE*, vol. 45, pp. 555–570, Mar. 1958.

[44] E. Berlekamp, R. E. Pelle and S. P. Pope, "The application of error control to communications," *IEEE Communication Magazine*, vol. 25, pp. 44–57, Apr. 1987.

[45] J. Proakis, *Digital Communications*. New York: McGraw-Hill, 1989.

[46] S. Vedu, "Advanced in statistical signal processing - multiuser detection," *JAI Press*, vol. 2, pp. 369–409, 1993.

[47] Z. Xie, R. T. Short and C. K. Rushforth, "A family of suboptimum detectors for coherent multiuser communications," *IEEE J. Select. Areas Commun.*, vol. 8, pp. 683–690, May 1990.

[48] S. M. Kay, *Fundamentals of Statistical Signal Processing*. New Jersey: Prentice Hall, 1993.

[49] F. C. Chneg and J. M. Holtzman, "Effect of tracking error on DS/CDMA successive interference cancellation," *Proc. IEEE GLOBECOM*, pp. 166–170, 1994.

[50] R. M. Buehrer, A. Kaul, S. Striglis and B. D. Woerner, "Analysis of DS-CDMA parallel interference cancellation with phase and timing errors," *IEEE J. Select. Areas Commun.*, vol. 14, pp. 1522–1535, Oct. 1996.

[51] H. V. Poor and G. W. Wornell, eds., *Wireless Communications: Signal Processing Perspectives*. New Jersey: Prentice Hall, 1998.

[52] X. Zhang, D. Brady, "Asymptotic multiuser efficiencies for decision-directed multiuser detectors," *IEEE Trans. Inform. Theory*, vol. 44, pp. 502–515, Mar. 1998.

[53] S. Haykin, *Adaptive Filter Theory*. New Jersey: Prentice Hall, 1996.

[54] N. B. Mandayam and S. Verdu, "Analysis of an approximation decorrelating detector," in *Proc. of Annual Allerton Conference on Communication, Control and Computing*, (Monticello, IL), pp. 1043–1052, Oct. 1995.

[55] B. D. Van Veen and K. M. Buckley, "Beamforming: a versatile approach to spatial filtering," *IEEE Acoust. Speech Signal Processing Magazine*, vol. 42, pp. 4–24, Apr. 1988.

[56] T. F. Wong, T. M. Lok, J. S. Lehnert and M. D. Zoltowski, "A linear receiver for direct-sequence spread-spectrum multiple-access systems with antenna arrays and blind adaptation," *IEEE Trans. Inform. Theory*, vol. 44, pp. 659–676, Mar. 1998.

[57] F. D. Garber and M. B. Pursley, "Optimal phases of maximal sequences for asynchronous spread-spectrum multiplexing," *IEE Electron. Let.*, vol. 16, no. 19, pp. 756–757, 1980.

[58] H. Krim and M. Viberg, "Two decades of array signal processing research," *IEEE Signal Processing Magazine*, pp. 67–94, Jul. 1996.

[59] L. C. Godara, "Applications of antenna arrays to mobile communications, part i: performance improvement, feasibility and system considerations," *Proc. IEEE*, vol. 85, pp. 1031–1195, Jul. 1997.

[60] L. C. Gordara, "Applications of antenna arrays to mobile communications part ii: beamforming and direction-of-arrival considerations," *Proc. IEEE*, vol. 85, pp. 1195–1245, Aug. 1997.

[61] G. Tsoulos, M. Beach and J. McGeehan, "Wireless personal communication for the 21st century : European technological advances in adaptive antennas," *IEEE Communications Magazine*, vol. 35, pp. 102–109, Sep. 1997.

[62] A. J. Paulraj and C. B. Papadias, "Space-time processing for wireless communications," *IEEE Signal Processing Magazine*, vol. 14, pp. 49–83, Nov. 1997.

[63] H. Liu and M. D. Zoltowski, "Blind equalization in antenna array CDMA systems," *IEEE Trans. Signal Processing*, vol. 45, pp. 161–172, Jan. 1997.

[64] J. C. Liberti and T. S. Rappaport, *Smart Antennas for Wireless Communications: IS-95 and Third Generation CDMA Applications.* New Jersey: Prentice Hall, 1999.

[65] C. Y. Lee, *Mobile Communications Design Fundamentals.* New York, Wiley, 2nd ed., 1993.

[66] J. H. Winters, "Smart antennas for wireless systems," *IEEE Personal Communications*, pp. 23–27, Feb. 1998.

[67] X. Wang and V. Poor, "Space-time multi-user detection in multipath CDMA channels," *IEEE Trans. Signal Processing*, vol. 47, pp. 2356–2374, Sept. 1999.

[68] B. Yang, "Projection approximation subspace tracking," *IEEE Trans. Signal Processing*, vol. 44, pp. 95–107, Jan. 1995.

[69] C. B. Papadias and H. Huang, "Linear space-time multiuser detection for multipath CDMA channels," *IEEE J. Select. Areas Commun.*, vol. 19, pp. 254–264, Feb. 2001.

[70] D. G. Manolakis, V. K. Ingle and S. M. Kogan, *Statistical and Adaptive Signal Processing*. McGraw Hill, 2000.

[71] B. Young, *Iterative Solution of Large Linear System*. New York Academic, 1971.

[72] L. A. Hageman and D. M. Young, *Applied Iterative Methods*. Academic Press, 1981.

[73] D. Divsalar, M. Simon and D. Raphaeli, "Improved parallel interference cancellation for CDMA," *IEEE Trans. Commun.*, vol. 46, pp. 258–268, Feb. 1998.

[74] P. V. Rooyen, M. Lotter and D. V. WYK, *Space-Time processing for CDMA mobile communications*. Kluwer Academic Publishers, 2000.

[75] G.H. Goloub and C. F. V. Loan , *Matrix Computations*. John Hopkins Univ. Press, 2nd ed., 1989.

[76] O. L. Frost, "An algorithm for linearly constrained adaptive array processing," *Proc. IEEE*, vol. 60, pp. 926–935, Aug. 1972.

[77] B. Yang, "An extension of the PASTd algorithm to both rank and subspace tracking," *IEEE Signal Processing Let.*, vol. 2, pp. 179–182, 1995.

[78] B. Yang, "Asymptotic convergence analysis of the projection approximation subspace tracking algorithms," *Signal Processing*, vol. 50, pp. 123–136, 1996.

[79] P. B. Rapajic and B. Vucetic, "Adaptive receiver structures for asynchronous CDMA systems," *IEEE J. Select. Areas Commun.*, vol. 12, pp. 685–697, May 1994.

[80] J. N. Maksym, "A robust formulation of an optimum cross-spectral beamformer for linear arrays," *J. Acoust. Soc. Am.*, vol. 65, pp. 971–975, Apr. 1979.

[81] B. D. Carlson, "Covariance matrix estimation errors and diagonal loading in adaptive arrays," *IEEE Trans. Aerospace and Electronic Systems*, vol. 24, pp. 397–401, Jul. 1988.

[82] T. S. Lee and Z. S. Lee, "A setorized beamspace adaptive diversity combiner for multi-path environments," *IEEE Trans. Veh. Technol.*, vol. 48, pp. 1503–1510, Sep. 1999.

[83] B. Widrow, K. M. Duvall, R. P. Gooch and W. C. man, "Signal cancellation phenomena in adaptive antennas: causes and cures," *IEEE Trans. Antennas and Propagation*, vol. 30, pp. 469–478, May 1982.

[84] K. M. Buckley, "Spatial/spectral filtering with linearly constrained minimum variance beamformers," *IEEE Trans. Acoust. Speech Signal Processing*, vol. 35, pp. 249–266, Mar. 1987.

[85] S. Sakagami, S. Aoyama, K. Kuboi, S. Shirota and A. Akeyama, "Vehicle position esti-mates by multibeam antennas in multipath environment," *IEEE Trans. Veh. Technol.*, vol. 41, no. 1, pp. 63–68, Feb. 1992.

[86] T. M. Lok, T. F. Wong and J. S. Lehnert, "Blind adaptive signal reception for MC-CDMA systems in Rayleigh fading channels," *IEEE Trans. Commun.*, vol. 47, pp. 464–471, Mar. 1999.

[87] S. Kapoor, S. Gollamundi, S. Nagaraj and Y. F. Huang, "Adaptive multiuser detection and beamforming for interference suppression in CDMA mobile radio systems," *IEEE Trans. Veh. Technol.*, vol. 48, pp. 1341–1355, Sep. 1999.

[88] I. Parra, G. Xu and H. Liu, "A least squares projection constant modulus approach," *PIMRC*, vol. 2, pp. 673–676, 1995.

[89] J. Capon, "High-resolution frequency-wavenumber spectrum analysis," *Proc. IEEE*, vol. 57, pp. 1408–1418, Aug. 1969.

[90] D. A. Pados and S. N. Batalama, "Joint space-time auxiliary-vector filtering for DS/CDMA systems with antenna array," *IEEE Trans. Commun.*, vol. 47, pp. 1406–1415, Sep. 1999.

[91] M. C. Doğan and J. M. Mendel, "Cumulant-based blind optimum beamforming," *IEEE Trans. Aerospace and Electronic Systems*, vol. 44, pp. 722–741, Jul. 1994.

[92] C. D. Peckman, A. M. Haimovich, T. F. Ayoub, J. S. Goldstein and L. S. Reed, "Reduced-rank STAP performance analysis," *IEEE Trans. on Aerospace and Electronic Systems*, vol. 36, pp. 664–676, Apr. 2000.

[93] E. G. Strom, S. Parkvall, S. L. Miller and B. E. Ottersten, "Propagation delay estimation in asynchronous direct-sequence code division multiple access systems," *IEEE Trans. Commun.*, vol. 44, pp. 84–93, Jan. 1996.

[94] U. Madhow and M. L. Honig, "Error probability and near-far resistance of minimum mean square error interference suppression schemes for CDMA," *IEEE Global Telecommun. Conf.*, pp. 1339–1343, 1992.

[95] J. S. Goldstein and I. Reed, "Reduced-rank adaptive filtering," *IEEE Trans. Signal Processing*, vol. 45, pp. 492–296, Feb. 1997.

[96] J. Schodorf and D. Williams, "Partially adaptive multiuser detection," *ICASSP'96*, pp. 367–371, 1996.

[97] M. Wax and Y. Anu., "Performance analysis of the minimum variance beamformer," *IEEE Trans. Signal Processing*, vol. 44, pp. 928–937, Apr. 1996.

[98] S. Moshavi, "Multi-user detection for DS-CDMA communications," *IEEE Communications Magazine*, pp. 124–135, Oct. 1996.

[99] L. B. Milstein, "Interference rejection techniques in spread spectrum communications," *Proc. IEEE*, vol. 76, pp. 657–671, June 1988.

[100] H. V. Poor and X. Wang, "Blind adaptive suppression of narrowband digital interfer-
ers," *Wireless Personal Communications*, vol. 6, pp. 69–96, 1998.

[101] G. K. Chan, "Effects of sectorization on the spectrum efficiency of cellular radio sys-
tems," *IEEE Trans. Veh. Technol.*, vol. 41, pp. 217–225, Aug. 1992.